Improving Arsenic Tolerance in Plants

Emma Rebecca Lindsay

PhD

University of York

Biology

September 2016

Abstract

Arsenic is a toxic metalloid contaminating soil and water supplies in many regions worldwide, and its entry into the food chain poses a serious health risk to millions of people [1]. Arsenic is toxic to plants, lowering the rate of photosynthesis and inhibiting growth, resulting in a reduction in crop yields [2]. Therefore, there is a pressing need to improve arsenic tolerance in plants and reduce accumulation of arsenic in crops. To this end, an arsenite efflux transporter from yeast was heterologously expressed in rice plants under the control of tissue specific promoters. Expression in different tissues led to altered arsenic tolerance and tissue distribution, indicating that this is a promising strategy for the future development of arsenic tolerant varieties.

The role of NIP aquaporins in arsenic transport and tolerance in the model plant *Arabidopsis* was explored in Chapter 3. AtNIP6;1 and AtNIP7;1 were identified as relevant targets for engineering arsenic tolerance and reducing seed/grain arsenic accumulation in crops. Loss of function mutations in both genes resulted in increased tolerance to arsenate and reduced accumulation of arsenic in the seed by up to 55%.

Further targets for engineering arsenic tolerance were identified from a collection of T-DNA insertion mutants of *Arabidopsis* using forward and reverse genetic screening approaches. Two of these were further characterised for their role in arsenic tolerance and accumulation. AtLsi2 was found to be involved in the root to shoot translocation of arsenic and may be involved in boron homeostasis while AtWRKY59 was identified as a potential regulator of the arsenic response. Disruption of the *AtWRKY59* gene resulted in increased tolerance and reduced uptake of arsenic.

Table of Contents

List of Figures

List of Tables

Acknowledgements

I would like to take this opportunity to thank everyone who has helped and supported me throughout the past four years, not least the BBSRC for funding this research with a DTP studentship. Thanks to my supervisor Frans Maathuis for the opportunity to undertake this research in his group, for his ideas, advice and encouragement. Also to my co-supervisor Kelly Redeker and TAP members Neil Bruce and Sue Hartley for taking the time to provide useful feedback and ideas throughout and to Steve McGrath for agreeing to act as my external examiner.

I would also like to thank Mark Hodson for access to the ICP-OES, and Rebecca Sutton for providing instruction and a friendly face whenever I found myself in the Environment Department. I'd also like to thank Darren Phillips at the BDC for access to the ICP-MS.

Huge thanks to everyone on L2 for their help and company both in the lab and out, special mention to the coffee club members who have happily enabled my caffeine addiction and helped keep me motivated for four long years. York has been a fantastic place to work and live, and this thesis would not have been possible without the support and patience of all my friends and family.

Authors Declaration

I declare that I am the sole author of this work and that it is original except where indicated by reference in the text. No part of this work has been previously presented for examination for any other degree at this or any other institution.

Publications arising from this work:

Lindsay, E. R. & Maathuis, F. J. M. (2016) *Arabidopsis thaliana* NIP7;1 is involved in tissue arsenic distribution and tolerance in response to arsenate, *FEBS Letters.* **590**, 779-786.

Chapter 1: Introduction

Arsenic (As) is a toxic metalloid that is found ubiquitously in the environment. It is the 20th most abundant element in the earth's crust and is present as a component of more than 245 different minerals [3]. Sources of As in the environment are both naturally occurring and anthropogenic in nature. Arsenic has historically been used extensively in agriculture as a component of insecticides and herbicides [3] and is a contaminant of phosphate fertilisers [4]. Arsenic is also an industrial waste product; it is used as a desiccant and wood preservative and is a by-product of mining, smelting and combustion of fossil fuels [3, 5].

Despite its use as a therapeutic agent for the treatment of acute promyelocytic leukaemia and trypanosomiasis [6], As is toxic to all living organisms and has been categorised as a Class 1 carcinogen by the WHO and International Agency for Research on Cancer [7]. Acute As poisoning is relatively rare, mostly arising from accidental ingestion of arsenical pesticides or insecticides. A lethal dose of 100-300 mg inorganic As leads to vomiting and diarrhoea and ultimately death within around 24-96 hours as a result of massive fluid loss and severe dehydration [8]. Chronic As poisoning is significantly more widespread and so presents much more of a cause for concern. Prolonged exposure to even very low concentrations of As can lead to arsenicosis, which can result in various effects on health ranging from skin lesions to gastrointestinal, cardiovascular, neurological and respiratory diseases and malignancies [8]. Human exposure to As predominantly occurs through intake of contaminated drinking water and its entry into the food chain through uptake and accumulation in crop plants [9]. There is no known cure or effective treatment for acute or chronic As poisoning [8] and so there is an urgent need to reduce exposure by providing safe food and drinking water.

1.1 Arsenic Speciation, Bioavailability and Contamination

There are various species of organic and inorganic As found in the environment. Inorganic As has four oxidation states; -III, 0, III and V. Of these, arsenite (AsIII) and arsenate (AsV) are by far the most common in the terrestrial environment. There are numerous organic forms of As found in nature, some of which have been detected in plant tissues including methylated As species, arsenosugars and arsenobetaine (Figure 1.1) [10]. The speciation of As in the soil is dependent on many different factors, including pH, redox potential and the presence of microbes with the ability to transform As species. Inorganic AsIII can be oxidised to AsV which in turn can be reduced to AsIII through both biotic and abiotic processes under the correct conditions. Inorganic As can also undergo biomethylation and subsequent demethylation through microbial activity [11]. Thus, the more complex As species, such as arsenobetaine and

arsenosugars, are degraded in the soil to release dimethylarsinic acid (DMA) and inorganic As [1]. The most abundant species of As in soil solutions are AsIII, AsV, monomethylarsonic acid (MMA) and DMA with AsV being the predominant species in aerobic soils whereas in anaerobic soils AsIII predominates [1].

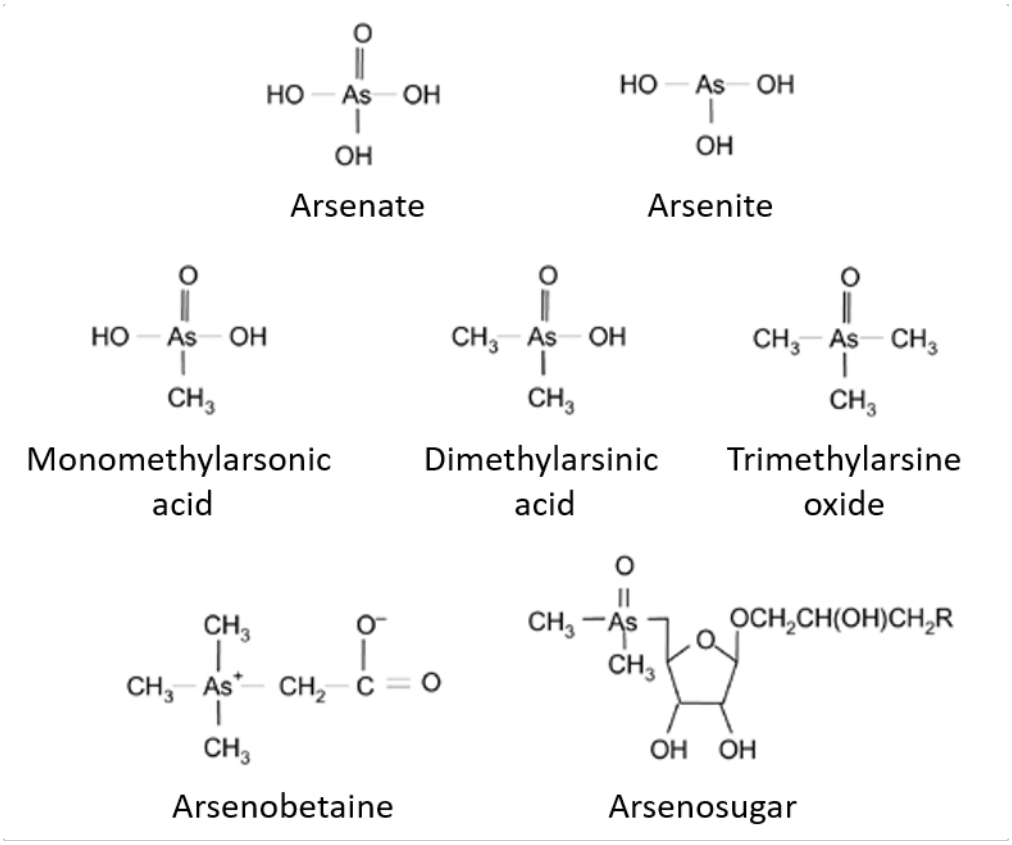

Figure 1.1 Arsenic species in plants
The figure shows the chemical structure of some of the As species detected in plants. The figure has been adapted from Meharg, A.A. and Hartley-Whitaker, J. [10]

The speciation of As impacts greatly on its bioavailability and consequently on its uptake and accumulation in plants. The dynamics of As speciation and mobility in the soil solution are complex and influenced by many factors including geochemical processes, microbe mediated reactions, site specific soil composition and agricultural practices such as fertiliser application and irrigation cycles [12]. The bioavailability of AsV is generally low, since it is strongly adsorbed by iron and aluminium oxides and hydroxides, whereas AsIII is mobilised into the soil solution under anaerobic conditions where it is more bioavailable [13].

The average concentration of As in most rocks ranges from 0.5 to 2.5 ppm, although concentrations as high as 3000 ppm have been reported for some recent marine sediments [3]. The As concentration of soil tends to be higher than that of rocks, and varies considerably among geographic regions. The average soil As concentration

globally is predicted to be around 5 ppm, however the concentration can reach up to hundreds or thousands of ppm in contaminated areas [7]. In drinking water, recommended guidelines set by the WHO state that As levels should not exceed 0.01 ppm while the maximum concentration permitted is 0.05 ppm. However, As contamination of groundwater is widespread and reported concentrations range from 0.0005 to 5 ppm across more than 70 countries worldwide [5]. For example, the drilling of tubewells in South-East Asia to provide disease free drinking water inadvertently resulted in chronic As poisoning of millions of people, as much of the water from these wells is contaminated with naturally occurring inorganic As [14]. In Bangladesh alone, a population of 57 million people is estimated to be at risk of exposure to drinking water contaminated with dangerous levels of As, and more than 100 million people are at risk worldwide [15].

In many regions, As contaminated groundwater is also used for crop irrigation, leading to an increased build-up of As in the soil and enhanced entry of As into the food chain through its accumulation in crops. This is particularly concerning in the case of rice, which is the largest dietary source of arsenic exposure in populations not exposed through contaminated drinking water. Even in areas with elevated As levels in the water, rice is a major contributor to As exposure - a problem that affects millions of people worldwide who rely on rice as a major dietary staple [16, 17]. Compared to other crops, rice takes up arsenic very efficiently, with grain concentrations up to ten times that of other cereals [1, 18]. This is due to a combination of anthropological, environmental and physiological factors. Contamination of paddy field soil can occur through previous treatment with arsenical pesticides and from mining or other industrial activities. Irrigation of paddy fields with arsenic laden groundwater contributes to elevated grain As levels [19], and this is exacerbated by the anaerobic conditions of flooded paddy fields which result in increased AsIII mobility and bioavailability [20]. The concentration of As in contaminated paddy fields varies significantly between the soil, irrigation water, standing water and soil pore water, however it is the pool of As in the soil pore water that is considered to be most readily accessible for plant uptake [21]. Concentrations of As in soil pore water of paddy fields irrigated with As contaminated water have been reported to range from 0.01 ppm to as much as 10 ppm in extreme cases [21-24].

Contamination of agricultural soil and irrigation water results in increased As levels in several crops including rice, maize and some vegetables, however consumption of contaminated rice provides the largest contribution to dietary inorganic As intake [1, 16]. A ‘normal range’ of 0.08 to 0.2 ppm has been estimated for rice from non-As contaminated areas [25]. Recently revised regulations pertaining to the maximum

acceptable levels of inorganic As in rice based products in the EU (0.2 ppm, or 0.1 ppm for rice used to produce food for infants) [26] and China (0.2 ppm) [27] suggest that most rice grown in non-As contaminated regions should be relatively safe to eat. However, rice grain concentrations as high as 2 ppm have been reported from contaminated areas [16, 25, 28]. This poses a serious health risk for populations with a rice based subsistence diet and therefore reducing As accumulation in rice is a major focus of research to mitigate human As exposure.

1.2 Arsenic Toxicity in Plants

Arsenic is a non-essential metalloid and is toxic to plants. The toxicity of As is dependent on the speciation, with inorganic forms generally considered to be more toxic than organic ones [2]. However, this conclusion is largely based on animal toxicity and does not appear to be consistently the case in plants, with many studies reporting different orders of phytoxicity between As species. In two *Spartina* species, the order of phytotoxicity was DMAV = MMAV > AsIII = AsV [29], whereas in rice the order was MMAV > AsIII > AsV = DMAV [30] and in maize the order was AsV > AsIII > DMAV [31]. A recent study in *Arabidopsis* determined that the methylated As species DMAV and MMAV are more phytotoxic than inorganic AsV [32] while transgenic *Arabidopsis* expressing an algal *arsM* (S-adenosylmethyltransferase) gene was able to convert inorganic AsIII to DMAV in the shoot, resulting in increased sensitivity to AsIII treatment suggesting DMAV is more phytotoxic than AsIII [33].

The mode of toxicity at the molecular level is dependent on the speciation of As. AsV is a phosphate analogue and as such can substitute for phosphate in biochemical reactions, thereby disrupting essential cellular processes such as oxidative phosphorylation, glycolysis, phospholipid metabolism, DNA and RNA synthesis and repair and protein phosphorylation [34]. Uncoupling of electron transport in mitochondria and chloroplasts due to futile cycling of ADP, AsV and ADP-AsV as a result of the unstable AsV-ester bond, could severely impact on cellular energy status [35].

AsIII is highly reactive toward thiol groups, binding them with a high affinity and so is able to disrupt protein structure and function. Proteins known to be bound by AsIII include transcription factors, redox regulatory enzymes, metabolic enzymes and proteins involved in proteolysis and signal transduction. Methylated forms of AsIII, including MMAIII and DMAIII are also reactive with sulfhydryl groups and are reported to be even more potent inhibitors of enzyme function than inorganic AsIII [34].

Inorganic As exposure induces the production of reactive oxygen species (ROS) in plants, including superoxide, peroxide and the hydroxyl radicle [36]. The generation of excessive ROS upon As exposure leads to oxidative stress which can cause lipid peroxidation and cellular damage, and is thought to be the main driver of As toxicity in plants [34]. Arsenic exposure damages the chloroplast membrane leading to a reduction in the level of CO_2 fixation and a reduced rate of photosynthesis. It may also impact on the uptake of micro and macronutrients through competition for transport and as a result of membrane damage [2]. Ultimately, As exposure leads to impaired plant growth, reduced biomass accumulation and reduced crop yields [2, 22]. Rice yields measured from an area of Bangladesh irrigated with As contaminated water (resulting in a gradient of soil As concentration from 10 to 70 ppm) fell dramatically from 7-9 tonnes per hectare to 2-3 tonnes per hectare [22]. Therefore, it is not only important to reduce accumulation of As in crops to limit human exposure but also to improve tolerance to As in order to limit yield loss.

1.3 Arsenic Transport in Plants

1.3.1 Arsenate Transport in Plants

AsV is a chemical and structural analogue of phosphate (P) and so is taken up through the P transport pathway in plants. In *Arabidopsis*, several members of the high-affinity P transporter family have been implicated in AsV transport. *AtPht1;1* and *AtPht1;4* were identified as the highest expressed in root tissues, where they contribute to P uptake in both low and high external concentrations [37]. Loss of function mutants in *Atpht1;1* were more tolerant to AsV exposure, and a double knockout in *pht1;1pht1;4* displayed enhanced tolerance relative to the single knockout and WT plants [37]. Similarly, loss of function mutants in *Atpht1;9* and *pht1;9pht1;8* were more tolerant to AsV and were deficient in both P and As uptake [38]. *AtPht1;5* is expressed in root and shoot tissue and is suggested to be involved in the source to sink mobilisation of P [39]. Loss of function in *Atpht1;5* resulted in increased sensitivity to P deficiency and increased tolerance to AsV [39]. Overexpression of *AtPht1;1, Pht1;7* and *Pht1;9* in *Arabidopsis* increased the sensitivity of the plants to AsV exposure and increased As uptake [38, 40].

In addition to the Pht1 family of P influx transporters, a P efflux transporter has been identified in *Arabidopsis* (*AtPHO1*) which is involved in long distance transport of P from the root to shoot presumably by loading of P into the xylem in roots [41, 42]. Although loss of function mutations in *pho1* resulted in reduced translocation of P to the shoot, this was not the case for As [43]. Conversely, loss of function in *pho2* (a

ubiquitin-conjugating E2 enzyme required for degradation of *PHO1* [44]) resulted in increased translocation of P, and to a much lesser extent As, to the shoot [43]. This suggests that the contribution of *PHO1* to long distance transport of AsV in *Arabidopsis* is relatively minor. In both WT and *pho2* plants, the majority of As in the shoots was AsIII rather than AsV, suggesting that it is AsIII and not AsV that is the main species translocated from root to shoot in *Arabidopsis* [43]. There are 10 putative homologues of *PHO1* in *Arabidopsis* which have yet to be characterised for their P and AsV transport capabilities [41]. They are expressed in a diverse range of plant tissues but many are localised to the vascular tissues [45], marking them as interesting candidates for future investigations into long distance AsV transport.

There are 13 members of the Pht1 family in rice, two of which have been implicated in AsV transport so far. Overexpression of *OsPht1;8* resulted in increased AsV uptake and translocation to the shoot through the xylem when exposed to AsV in hydroponics [46]. The K_m values of OsPht1;8 for AsV and P were found to be similar, although the V_{max} for P was two to three times larger than for AsV and AsV uptake was competitively inhibited in the presence of P [46]. Overexpression of the constitutively expressed *OsPht1;1* similarly increased AsV uptake and translocation to the shoot when grown in hydroponics [47]. The physiological relevance of AsV uptake and accumulation through P transporters in rice may be negligible when grown in flooded soil, as AsIII is the predominant species available for uptake in anaerobic conditions. Indeed, when *OsPht1;8* overexpressing plants were exposed to AsV in flooded soil there was an increase in the P, but not in the As concentration, of rice straw and grain tissue [46].

Recently, three members of the Pht1 family have been identified in the As hyperaccumulating fern *Pteris vittata* [48]. One of these, *PvPht1;3* was characterised for P and AsV transport capability. Yeast cells heterologously expressing *PvPht1;3* showed enhanced sensitivity to AsV and accumulated higher concentrations of As compared with empty vector controls and *AtPht1;5* expressing cells. Uptake of P was moderately inhibited by the presence of AsV in *AtPht1;5* expressing cells, indicating that AtPht1;5 exhibits a preference for P uptake over AsV, consistent with reports of other Pht1 transporters [48, 49]. However, P uptake in *PvPht1;3* expressing yeast was strongly inhibited by AsV and the affinity of PvPht1;3 was predicted to be similar for P and AsV. Species in the *Pteris* genus that hyperaccumulate As have been reported to have a lower K_m value for AsV uptake than non-accumulating species [48], suggesting there may be a P transporter with relatively high affinity for AsV in this species. It was suggested that this could be attributed to PtPht1;3, which has a higher affinity for AsV compared to Pht transporters characterised in other species. This may contribute to the enhanced As uptake and accumulation observed in this species [48, 50].

1.3.2 Arsenite Transport in Plants

AsIII is the predominant As species in anaerobic environments such as flooded paddy fields, where it is present in the soil solution as an undissociated neutral molecule at pH < 8 [51]. Knowledge of AsIII transport in plants has stemmed from research in microbial systems including *E. coli* and yeast, where it was discovered that some aquaglyceroporins are permeable to AsIII [52]. Aquaglyceroporins are a subfamily of the aquaporins and are characterised by a larger pore size and permeability to neutral molecules such as glycerol. Plant aquaglyceroporins can be broadly separated into four subgroups based on sequence homology. Two subgroups of which (nodulin-26-like intrinsic proteins (NIPs) and plasma membrane intrinsic proteins (PIPs)) contain members which have been shown to facilitate AsIII transport in plants in addition to transporting essential nutrients such as silicon and boron [53-59]. Out of nine members of the NIP subfamily in *Arabidopsis*, six have been shown to have AsIII transport capability so far. Of these, loss-of-function mutations in five (*nip1;1, nip1;2, nip3;1, nip5;1* and *nip7;1*) resulted in reduced plant As levels, while three showed increased tolerance to AsIII exposure (*nip1;1, nip3;1* and *nip7;1*) [58-60]. *Arabidopsis* NIPs have different temporal and spatial expression patterns which may contribute to their perceived role in As uptake and translocation throughout the plant, something which remains to be fully investigated.

AsIII uptake is particularly relevant for plants such as rice which are often grown in the reducing, anaerobic environment of a flooded paddy field. Rice is a silicon (Si) accumulator, and its highly efficient silicon uptake and transport pathway may be one of the reasons for its relatively elevated AsIII intake [56]. The majority of AsIII and silicic acid is taken up into the root through the NIP OsNIP2;1/Lsi1 [53, 56]. Lsi1 is strongly expressed in the root where it localises to the plasma membrane on the distal side of the exo- and endodermal cells [53, 56]. Five other rice NIPs have been shown to have AsIII transport capability: OsNIP2;2/Lsi6, OsNIP1;1, OsNIP3;1, OsNIP3;2 and OsNIP3;3 [56, 57, 61]. Compared to Lsi1, the other AsIII transporting NIPs are expressed at relatively low levels in the root and so probably do not contribute greatly to AsIII uptake [51]. The expression *of Lsi6, OsNIP3;1* and *OsNIP3;2* is highest in the root while *OsNIP1;*1 and *OsNIP3;3* are most highly expressed in the reproductive tissues [62]. *Lsi6* is also expressed in the leaf sheaths and leaf blades where it localises to the adaxial side of xylem parenchyma cells [63] suggesting it may be involved in Si/AsIII distribution rather than uptake.

AsIII uptake through the NIP Lsi1 is assumed to be passive and driven by the concentration gradient, based on many studies showing aquaporins facilitate diffusion

across the membrane [64]. Efficient uptake is sustained by the active efflux of AsIII towards the stele through the efflux transporter Lsi2, which is localised to the proximal side of the exo- and endodermal cells in the root where Lsi1 is located on the distal side. This coupling of influx and efflux transporters in the same cell helps maintain the concentration gradient in the root, leading to efficient transport of silicon (and to a lesser extent AsIII) across the cells [65]. Loss of function of either Lsi1 or Lsi2 results in markedly reduced uptake and translocation of both silicon and AsIII to the shoot and, in the case of *lsi2,* the grain [56].

Lsi2 is also highly expressed in the nodes where it is localised to the distal side of bundle sheath cells of the enlarged vascular bundle [66, 67]. The node has been identified as a critical hub for the distribution of essential nutrients in monocots and appears to be equally important in controlling the distribution of As in rice [67]. In *lsi2* knockout rice plants, excised panicles cut below the first node and fed with AsIII accumulated significantly more AsIII in the node and flag leaf but less AsIII in the first internode and grain [67].

Recent studies into the role of NIPs and Lsi2-like transporters in Si distribution in rice have revealed the contribution of Lsi2, Lsi3 (an Lsi2-like efflux transporter) and Lsi6 (a NIP) to intervascular transfer of Si in the node which is essential for the preferential distribution of Si to the husk [66]. In rice, large and small vascular bundles run from the lower nodes and connect to the flag leaf, becoming enlarged at the nodes. Diffuse vascular bundles run parallel to and surround the enlarged large vascular bundles in the node and connect to the panicle in the uppermost internode [68]. Therefore, transfer between enlarged and diffuse vascular bundles at the nodes is necessary in order to deliver nutrients such as Si from the roots to the developing seeds. Enlarged and diffuse vascular bundles are separated by the parenchyma cell bridge; Si is transported out of the xylem of the enlarged vascular bundle by Lsi6 which is localised to the proximal side of xylem transfer cells [68]. Si then moves symplastically through plasmodesmata to the bundle sheath cells of the enlarged vascular bundle, where Lsi2 is polarly localised to the distal side of the cell [66]. A proportion of Si is effluxed from the bundle sheath cells by Lsi2 into the apoplast of the parenchyma cell bridge and transported to the diffuse vascular bundle. The remaining Si is transferred to the parenchyma cell bridge and reloaded to the diffuse vascular bundle by Lsi3 which is localised in a non-polar fashion in the parenchyma cells between the bundle sheath and diffuse vascular bundle [66]. Loss of function mutation in either *Lsi2, Lsi3* or *Lsi6* resulted in reduced Si in the panicles but increased distribution of Si to the flag leaf [66, 68] implying that all three transporters are required for efficient accumulation of Si in the husk. This efficient Si transport pathway could also prove to be important in

determining As distribution between tissues, including the grain, and may be an interesting target for engineering As free rice grain in the future.

A member of the natural resistance-associated macrophage protein (NRAMP) transporter family in rice has been identified as an AsIII transporter. When heterologously expressed in *Arabidopsis, OsNRAMP1* localised to the endodermis and pericycle cells of the root [69]. Expression of *OsNRAMP1* resulted in increased As uptake, accumulation and tolerance, although its role in AsIII transport in rice is unclear. More recently, another class of transporter was found to facilitate AsIII transport in *Arabidopsis*. *AtINT2* and *AtINT4* are plasma membrane, H^+-coupled, inositol transporters that are expressed in phloem companion cells where they have a role in the delivery of inositol to the reproductive tissues through uploading of inositol into the phloem [70]. Loss of function mutations in either *AtINT2* or *AtINT4* resulted in reduced As loading of the phloem and reduced As concentration in shoot tissue, empty siliques and seeds [70], indicating that phloem As transport is a key component of the pathway leading to As accumulation in seeds.

1.3.3 Transport of Organic Arsenic Species in Plants

Compared with inorganic As, methylated As species are generally taken up much less efficiently by plants, with AsV being taken up 2.5 and 5 times more efficiently than MMA and DMA [71]. MMA and DMA can be taken up through the NIP transporter *Lsi1* in rice plants; loss of function in *lsi1* reduced uptake by 80% and 50% respectively [72]. The latter suggests there are additional routes for organic As uptake which have yet to be identified.

1.3.4 Long Distance Transport of Arsenic in Plants

In contrast to the relatively inefficient uptake of methylated As, organic As is much more readily translocated from root to shoot than inorganic As. Inorganic As generally shows low mobility in terms of root to shoot translocation in plants, with the exception of hyperaccumulators such as *Pteris vittata* which can accumulate As to >2% dry weight in the shoots [73]. In most cases studied so far, the majority of As in xylem sap is in the form of AsIII, with AsV making up a relatively small proportion even when plants are fed with AsV [51]. The mobility of As in the xylem varies between plant species but most plants have low xylem:external-medium As concentrations, with values generally lower than 1 except in the case of As hyperaccumulators [51].

In rice, DMA is translocated to the grain through both the xylem and phloem around 10 times more efficiently than AsIII which is mostly translocated through the phloem [74].

The majority of inorganic As taken up into the plant remains in the root tissue, a proportion is translocated to the shoot where it accumulates in the stems and leaves and only a very small proportion in the grain, whereas the proportion of DMA in reproductive tissues is much higher than in the vegetative tissue [74, 75]. DMA is also more mobile within the grain compared to inorganic As which accumulates in the ovular vascular traces on the surface of the grain while DMA permeates readily into the endosperm [76].

1.4 Arsenic Detoxification Mechanisms

There are common mechanisms for dealing with As toxicity found in prokaryotes and unicellular eukaryotes. In bacteria, As resistance is conferred by the *ars* operon which usually consists of three genes; *ArsR, ArsB* and *ArsC*. The first of these, *ArsR,* encodes a repressor that is inactivated in the presence of As, initiating the transcription of *ArsB* and *ArsC*. *ArsC* encodes an AsV reductase which reduces AsV to AsIII and *ArsB* encodes an AsIII/H^+ antiporter for efflux of AsIII from the cell [77]. In yeast, a similar detoxification mechanism is provided by the gene cluster of *ACR1, ACR2* and *ACR3*. *ACR1* is a transcription factor regulating expression of *ACR2* and *ACR3* which encode an arsenate reductase and a plasma membrane AsIII/H^+ efflux transporter respectively [78, 79]. In both systems, AsV is reduced to AsIII prior to efflux from the cell. Yeast has an additional mechanism for detoxification of AsIII; complexation with glutathione (GSH) and sequestration in the vacuole through the ABC transporter YCF1 [80].

1.4.1 Arsenate Reduction in Plants

Numerous speciation analyses of As in plant tissues have revealed that generally, the majority of As is present as AsIII even when plants are exposed solely to AsV. Following exposure to AsV, AsIII accounted for more than 90% of As present in the root and shoot tissue of *Brassica juncea* (Indian mustard) [81], roots of tomato and rice plants [82] and shoot tissue of *Arabidopsis* [83]. This suggests that plants have a high capacity for AsV reduction. Arsenate can be reduced non-enzymatically by GSH via an AsIII-*tris*-glutathione intermediate resulting in AsIII and the oxidised disulphide form of glutathione (GSSG) [84]. However, this reaction alone is likely to be too slow and inefficient to account for the volume of AsV reduction observed in plant tissues. In the AsV tolerant grass *Holcus lanatus* at least 90% of the reductase capability of root protein extracts was found to be enzymatic suggesting the presence of arsenate reductase enzymes in plants [85].

Homologues of the yeast *ACR2* arsenate reductase gene, which uses glutaredoxin (Grx) and GSH as reductants, have been identified in *Arabidopsis* [86-88], *H. lanatus* [85], *P. vittata* [89] and rice [90]. Plant *ACR2* genes are members of the protein tyrosine phosphatase superfamily, which includes the human *CDC25* (cell cycle dual-specificity phosphatase) genes. With the exception of *PvACR2*, the plant *CDC25*-like *ACR2* genes have both phosphatase and arsenate reductase activity [90, 91]. Although all plant ACR2 reductases identified so far have arsenate reductase activity *in vitro,* it seems not all function as arsenate reductases *in planta;* loss of function mutation in *AtACR2* did not result in reduced reductase activity in *Arabidopsis* roots and had no effect on AsV tolerance, accumulation or efflux [92].

A functioning arsenate reductase in *Arabidopsis* has since been described; *ATQ1/HAC1* is expressed primarily in the root hairs, epidermal cells and pericycle cells of the stele in the roots where it reduces AsV to AsIII [88]. Knockout mutations in *ATQ1/HAC1* resulted in increased sensitivity to AsV but not AsIII exposure and significantly reduced the ratio of AsIII/AsV in plant tissues [87]. In addition, *atq1/hac1* knockouts lose the ability to efflux AsIII from the roots and instead show increased loading of As into the vasculature resulting in increased root to shoot As translocation [88]. This suggests that reduction of AsV to AsIII is a crucial step in AsV detoxification that is required for efflux of As from the roots and for exclusion of As from the above ground tissues in *Arabidopsis*. Reduction of AsV is probably important for restricting root to shoot translocation due to the reactivity of AsIII with thiol containing peptides; complexation of AsIII in the roots is known to reduce its mobility through the xylem [93].

1.4.2 Complexation and Sequestration of Arsenic in Plants

AsIII can be detoxified in plants by complexation with thiol-rich peptides such as GSH and phytochelatins (PCs) and subsequent sequestration in the vacuole. PCs are GSH derived metal-binding peptides whose structure is $(\gamma\text{-Glu-Cys})_n$-Gly where *n* is typically between 2 and 5 [94]. PCs are unique to plants and their synthesis is induced by As and other toxic metals/metalloids. In rice plants, a number of genes related to GSH and PC synthesis, metabolism and transport are upregulated following As exposure [51, 95]. A number of different As-PC complexes have been detected in plant tissues. The predominant form in sunflower plants was GSH-AsIII-PC_2 after one hour of exposure and AsIII-PC_3 after three hours of exposure [96]. AsIII-PC_3 also dominated in *Holcus lanatus* plants [97] while AsIII-PC_3, AsIII-PC_4 and others dominated in rice [98]. The amount of As complexed with thiols has been found to differ between species; almost all As in roots and shoots of *B. juncea* was bound to thiol groups [81], in *Arabidopsis*

roots 69% of As was complexed with PCs [93] while in rice root tissue up to 45% of As detected was complexed with PCs [98].

Complexation of AsIII with thiol-rich peptides is an important component of the As detoxification machinery. The *Arabidopsis cad1-2* and *cad1-3* mutants are deficient in GSH and PC synthesis respectively and are both around 20 times more sensitive to AsV compared to WT plants [93]. The two mutants also showed greater As mobility with a significantly higher shoot to root ratio of As compared to WT as well as enhanced efflux of AsIII from the roots [93].

The increased mobility of As observed in plants lacking GSH and PCs may be due to reduced sequestration of complexed As in the root vacuoles. In yeast, the ABC-type transporter Ycf1p confers resistance to AsIII by transporting AsIII-GSH_3 complexes into the vacuole [80]. In plants, some ABC transporters have been identified which transport AsIII-PC complexes across the tonoplast. In *Arabidopsis, AtABCC1* and *AtABCC2* are responsible for the vast majority of AsIII-PC sequestration in the vacuole. Transport of AsIII-PC_2 complexes was reduced by 85% in vacuoles isolated from *abcc1/abcc2* double knockouts compared to WT [99]. The double knockout plants were also significantly more sensitive to AsV exposure than WT or single mutant plants [99]. In rice, *OsABCC1* is expressed in the roots, leaves, nodes, peduncle and rachis where it localises to the tonoplast and is thought to be involved in sequestration of AsIII-PCs [100]. *OsABCC1* was able to rescue the AsV sensitivity phenotype of *abcc1/abcc2* double mutants in *Arabidopsis,* suggesting it functions in a similar way. In rice, *OsABCCC1* localises to the phloem region of vascular bundles in the nodes, where it is proposed to restrict As transport to the grains by sequestration in the vacuole. In *OsABCC1* knockout plants, the As concentration of the grain was increased while concentration of As in the nodes was reduced [100].

Hyperaccumulators of As such as *Pteris vittata* do not require chelation with PCs for detoxification of AsIII, since only 1-3% of the total plant As is complexed with PCs in these plants [101]. Instead, hyperaccumulators appear to sequester AsIII directly in the vacuoles. An AsIII/H^+ antiporter that localises to the tonoplast in *Pteris vittata* has been identified; *PvACR3* and *PvACR3.1* are related to the AsIII efflux transporter *ScACR3* found in yeast [102]. Knocking down the expression of *PvACR3* (but not *PvACR3.1*) conferred As sensitivity on *P. vittata* gametophytes. *PvACR3* was also able to rescue the As sensitive phenotype of Δ*acr3* yeast suggesting that it performs an analogous function [102]. Other *ACR3* homologues have been found in mosses, ferns, lycophytes and gymnosperms, however none have been identified in flowering plants [102].

1.4.3 Efflux of Arsenic from Plant Roots

There is evidence of both AsIII and AsV efflux from plant roots, although the mechanism by which this occurs is not fully understood. AsIII efflux from tomato plant roots was inhibited by CCCP but not vanadate, suggesting that AsIII efflux is an energy dependent process but is not mediated by a P-type ATPase [82]. On the other hand, AsV efflux was not inhibited by CCCP and appears to be passive [82].

The expression of several plant NIP aquaglyceroporins in yeast conferred enhanced tolerance to AsV, indicating that they are bi-directional AsIII channels and may be involved in AsIII efflux from plants [57]. Indeed, AsIII efflux activity has been demonstrated for OsNIP2;1/Lsi1 from rice roots. Loss of function *lsi1* plants had reduced As efflux capability, with the mutants plants exuding 15-20% less As compared to WT plants [103]. Transporters responsible for the remaining 80% of the As efflux capacity of rice roots remain to be identified.

1.4.4 Regulation of Arsenic Detoxification Mechanisms in Plants

The regulatory mechanisms controlling plant responses to As are not well understood. Thus far, only one As-responsive transcription factor has been characterised in plants to my knowledge; *AtWRKY6.* Upon exposure to AsV, the phosphate transporter *AtPht1;1* is transcriptionally downregulated and delocalised from the plasma membrane, resulting in reduced AsV uptake [104]. When AsV was removed, the expression and membrane localisation of *Pht1;1* was quickly restored, and the response to AsV was more rapid than the response to P starvation or resupply [104]. Expression of *WRKY6* is upregulated in response to AsV and has been shown to be required for the AsV-specific repression of *Pht1;1* [104].

Sung, D. *et al.* [105] identified *PAF1* as the causal gene in an AsIII and AsV tolerant mutant through a genetic screen and mapping. *PAF1* (proteasome α subunit F1) is a subunit of the 26S proteasome complex which has been implicated in the regulation of plant responses to environmental stimuli including oxidative stress [106]. *PAF1* negatively regulates the As induced expression of key genes involved in the synthesis of thiol biosynthesis. In *paf1* loss of function mutants, there was a higher level of thiol containing compounds including GSH and PCs compared to WT, resulting in increased As accumulation and tolerance in the mutant plants [105].

Recently, Mohan, T.C. *et al.* [107] identified the phytohormone cytokinin as a negative regulator of As tolerance mechanisms in *Arabidopsis*. Exposure of WT plants to AsV led to a depletion in plant cytokinin levels caused by downregulation of genes involved

in cytokinin synthesis and metabolism. Mutant plants deficient in cytokinin signalling and biosynthesis were more tolerant to AsV which was attributed to an increase in the level of thiol containing compounds including GSH and PCs [107]. Cytokinin deficient *Arabidopsis* and tobacco plants were more tolerant to AsV and accumulated higher levels of As. This is analogous to the As tolerance mechanism observed in *paf1* mutants, suggesting they may be involved in the same regulatory pathway.

Transcriptomic studies of rice and *Arabidopsis* plants exposed to As have implicated the phytohormones jasmonic acid and ethylene in the As response [108, 109]. In addition, numerous transcription factors and miRNAs are differentially expressed in response to As in plant tissues [109, 110]. These studies provide a foundation for future research into the function of these differentially expressed regulatory genes, which may provide a clearer and more detailed picture of the signalling and regulation of the As detoxification mechanisms in plants.

1.5 Improving Arsenic Tolerance in Plants

There is an urgent need to improve As tolerance and reduce As accumulation in crop plants in order to limit the entry of As into the food chain. There are many potential strategies for mitigation of As contamination in water, soil and crops. These include agricultural strategies, such as growing rice in aerobic rather than anaerobic conditions, for at least part of the growing season, or through fertilisation with Si to limit AsIII accumulation through competitive uptake [111]. Another strategy to reduce As in rice is to find novel ways of preparing the grain, for example by rinsing and cooking in a large volume of water, which can remove some of the inorganic As from the cooked rice [112].

Ideally, the problem of As contamination would be resolved at the source, through soil remediation and use of non-contaminated irrigation and drinking water. Soil remediation could potentially be achieved through phytoremediation utilising As hyperaccumulating plant species such as *P. vittata.* However, in order to be utilised over large areas, the process must be highly efficient and cost effective. Most known As hyperaccumulating species are adapted to tropical and sub-tropical conditions and as such may not be suitable for cooler regions [1]. Other long term measures include identification of the sources of As contamination with the aim of minimising As input to the agricultural systems and breeding of crop cultivars with low As uptake capacity [1]. It is likely that multiple strategies will be required in order to fully minimise the entry of As into the food chain. Strategies to reduce As uptake and accumulation in the edible portions of crop plants and to improve tolerance to As can take advantage of recent

advances in biotechnology and knowledge of As uptake and detoxification mechanisms in plants.

Transgenic approaches to improving As tolerance in plants have seen some success in both model and crop species. One strategy is to reduce As uptake through loss of function mutation in As permeable transporters. However, this can lead to detrimental effects on plant nutrition due to the shared uptake pathways of As and essential or beneficial nutrients. For example, loss of function in *OsLsi1* or *OsLsi2* reduces As uptake but also leads to detrimental effects on plant growth such as increased risk of biotic stress, reduced fertility and yield loss, caused by reduced silicon uptake [53, 65]. In future, it may be possible to generate variants of As uptake transporters with increased selectivity for their native substrates while excluding As.

Alternative strategies aim to improve AsV reduction and generate more efficient detoxification of AsIII through complexation and sequestration in the vacuole. Overexpression of the *Arabidopsis Phytochelatin synthase* gene (*AtPCS1*), which catalyses the final step in PC biosynthesis, led to enhanced levels of thiol peptides in root and shoot tissue and a significant increase in tolerance to AsV in *Arabidopsis* plants [113]. Heterologous expression of *AtPCS1* in *B. juncea* also increased tolerance to AsV compared to WT plants and did not alter levels of As accumulation [114]. Overexpression of a bacterial *γ-glutamylcysteine synthetase* (*γ-ECS*) gene, which catalyses the first step in PC biosynthesis, had a similar effect on *Arabidopsis* plants; increased tissue thiol concentration and enhanced tolerance to AsV with no change in the As accumulation in the above ground tissues [115]. However, *Arabidopsis* plants overexpressing *γ-ECS* were hypersensitive to cadmium (Cd) exposure and even trace amounts of Cd inhibited AsV tolerance [115] which could limit the effectiveness of this strategy in soils contaminated with both As and Cd. In contrast, when bacterial *γ-ECS* or *Glutathione synthetase* (*GSH*) genes were expressed in *B. juncea*, transgenic plants were more tolerant to both Cd and As stress [116].

Combining expression of a bacterial arsenate reductase (*ArsC*) in the shoots of *Arabidopsis* with constitutive expression of bacterial *γ-ECS* further enhanced tolerance to AsV and also increased accumulation of As by 2-3 fold [83]. Similarly, combining expression of *PCS1* and *GSH1* genes (derived from garlic and yeast respectively) enhanced tolerance of *Arabidopsis* plants to both Cd and As to a greater extent than single transformants and increased heavy metal accumulation [117]. In both studies, plants were designed to be more tolerant to As stress and to accumulate higher levels of As than WT for phytoremediation purposes. Nonetheless, a similar approach may be useful for crop plants if accumulation of As could be restricted to the root tissue (or to

the inedible portions of the plants), perhaps by restricting the expression pattern of the transgenes. For example, heterologous expression of the fission yeast PC-Cd transporter (*SpHMT1*) in *Arabidopsis* increased the sequestration capacity of transgenic plants. SpHMT1 localised to the tonoplast and significantly increased tolerance to, and accumulation of, Cd and As [118]. When the expression of *SpHMT1* was restricted to the roots of *Arabidopsis*, As accumulation was increased in root tissue compared to WT plants but significantly reduced in the shoot and in the seed [118].

Heterologous expression of glutaredoxins from *Pteris vittata* and rice in *Arabidopsis* resulted in increased tolerance to AsIII and AsV and significantly reduced As accumulation [119, 120]. Glutaredoxins are GSH dependent oxidoreductases with roles in the protection against oxidative stress, regulating iron homeostasis and redox signalling pathways [121]. Arsenic regulated glutaredoxins from rice (*OsGrx-C7* and *OsGrx-C2.1*) have been shown to have glutathione reductase and AsV reductase activities *in vitro* [122]. Overexpression of *OsGrx-C7* and *OsGrx-C2.1* in *Arabidopsis* increased the GSH tissue concentration and reduced tissue As accumulation [120]. This suggests that some plant glutaredoxins may be involved in As detoxification, either directly through AsV reduction or indirectly through cellular redox homeostasis. They have also been suggested to increase As efflux through the transcriptional regulation of aquaporins [120, 122]. Further investigation will be required to uncover the precise role of these glutaredoxins in As metabolism and detoxification, but they are nonetheless interesting and promising candidates for generating As tolerant and As excluding crops in the future.

Another potential strategy is to engineer plants with As methylation capability such that volatile trimethylarsine gas is generated and released to the atmosphere. This has been attempted with some success in rice plants expressing a bacterial S-adenosylmethyltransferase (arsM) enzyme [123]. Rice plants expressing *arsM* did not grow differently than WT plants after long term As exposure but did accumulate less As in the root and had an increased proportion of methylated As species in the shoot. *ArsM* expressing rice were able to produce volatile arsenicals, releasing the equivalent of 0.06% of total plant As to the atmosphere [123]. As a proof of concept, this study is promising and suggests that with an optimal *arsM* gene plants could be engineered with the ability to release volatile As. More recently, an *arsM* gene from a fungus isolated from an As contaminated area of West Bengal (*WaarsM)* has been expressed in *Arabidopsis* [124]. Plants expressing *WaarsM* were more tolerant to AsIII and AsV exposure and accumulated significantly less As in the shoot and in the seed compared to WT. The authors describe *WaarsM* expressing plants as releasing high amounts of volatile As (although the amount relative to total plant As is not provided) which

suggests that *WaarsM* is an interesting candidate for expression in crop plants. If the effect on *Arabidopsis* could be replicated in crop plants, they would be more tolerant and accumulate less As in the grain whilst also providing a phytoremediation service by taking up As from the soil and releasing volatile As to the atmosphere [124].

An alternative approach, which could potentially improve tolerance and reduce As accumulation simultaneously, is to increase efflux of As from the plant. Although plant roots have been shown to release both AsIII and AsV to the external medium, no dedicated plant As efflux pathway has yet been identified [82] which suggests there is scope to enhance this function. In contrast to plants, prokaryotes and unicellular eukaryotes possess dedicated As efflux systems. In bacteria, the ArsAB operon coordinates removal of arsenic through AsIII translocating ATPases [125] while in yeast, cytoplasmic AsIII is effluxed to the external medium via the $AsIII/H^+$ Antiporter ScACR3p [126]. Heterologous expression of *ScACR3* in both *Arabidopsis* and rice successfully increased AsIII efflux from the roots [127, 128]. In *Arabidopsis*, *ScACR3p* expression improved tolerance to As but also increased root to shoot As translocation [127]. While in rice, *ScACR3p* expression reduced As accumulation in the grain and did not affect root to shoot As translocation [128]. A homologue of *ScACR3p* from the As hyperaccumulator *Pteris vittata* was expressed in *Arabidopsis* where it localised to the plasma membrane and increased As efflux from the roots [129]. *PvACR3* expressing plants were significantly more tolerant to both AsIII and AsV exposure and accumulated less As in the roots, but had increased root to shoot As translocation, accumulating around 7 fold more As in the shoot than WT plants [129].

1.6 Aims

Many efforts to improve As tolerance in plants have also resulted in increased accumulation of As or increased root to shoot translocation. Nevertheless, some successful and promising strategies have been reported, a selection of which is described above. In order to improve upon these in the future, it will be necessary to further our understanding of As transport, metabolism and detoxification mechanisms in plants.

The main aim of this thesis is to contribute knowledge which will aid in the improvement of As tolerance in plants while simultaneously reducing As accumulation, thereby mitigating the entry of As into the food chain. The first chapter aims to improve upon previous studies by heterologous expression of *ScACR3p* in rice using tissue specific promoters to maximise As efflux from the roots and reduce translocation to the shoot. The second chapter focuses on the role of NIP aquaglyceroporins in As transport and

tolerance in the model plant *Arabidopsis* while the third chapter uses forward and reverse genetic screening techniques to identify new components of the As response in *Arabidopsis* and describes their potential as new candidates for improving As tolerance in plants.

Chapter 2: Heterologous Expression of *ScACR3p* Alters Arsenic Tolerance and Accumulation in Rice

2.1 Introduction

ScACR3p was first characterised as an AsIII transporter by Wysocki, R. *et al.* [79]. The protein has 10 putative transmembrane spanning domains (Figure 2.1) and a sub-cellular localisation to the plasma membrane [79, 130]. The 45.8-kDa protein comprises 404 amino acids and is predicted to contain 3 *N*-glycosylation sites and 8 potential phosphorylation sites (4 each for protein kinase C and casein kinase II) [79]. ACR3 is a low affinity AsIII/H^+ transporter with an apparent K_m of 2mM for AsIII [126]. A potential model of AsIII transport through ACR3 discussed by Markowska, K. *et al.* [131] suggests a similar mechanism to that of a bacterial bile acid sodium transporter (ASBT) involving the interaction of AsIII with thiol groups and other polar/charged and aromatic residues, particularly in transmembrane domains 4, 9 and 10 [131, 132].

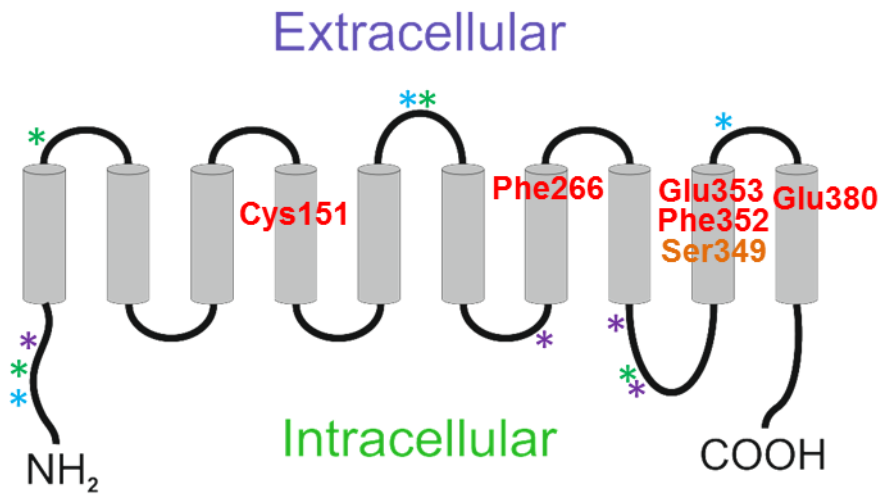

Figure 2.1 Predicted topology of the ScACR3 protein
Predicted topology of the ScACR3 protein showing ten transmembrane domains. Blue, green and purple asterisks indicate the sites of predicted *N*-glycosylation, phosphorylation by protein kinase C and phosphorylation by casein kinase II respectively. Residues highlighted in red text are essential for AsIII efflux activity while mutation of residues in orange results in reduced AsIII/H^+ exchange.

Homologues of ACR3 have been identified in gymnosperms (such as the tonoplast localised *PvACR3* in the As hyperaccumulator *Pteris vittata* [102]), however, there are no closely related genes found in angiosperms, including rice. Therefore, in order to enhance As efflux from roots in plants, *ScACR3p* has been heterologously expressed in both rice and the model plant *Arabidopsis* [127, 128]. In both cases, ACR3 was expressed under the control of the constitutive CaMV 35S promoter. In *Arabidopsis*, ACR3 localised to the plasma membrane and conferred increased tolerance to both AsIII and AsV at the cellular and whole plant level. However, in addition to increasing AsIII efflux from the roots, expression of *ACR3* also led to increased translocation of As

to the shoot [127]. In rice, expression of *ACR3* resulted in decreased tissue As concentrations (including shoot, root and grain, with reductions of up to around 30%) and increased efflux from the root compared to WT [128]. However, Duan, G. *et al.* [128] give no details of the effect of *ACR3* expression on rice plant growth in response to As. When *ACR3* was expressed in rice under the control of the 35S promoter by Waqar Ali (a previous PhD student in the Maathuis lab [133]), no difference in As tolerance was observed between the transgenic and WT lines exposed to either AsIII or AsV in hydroponics. Similarly to Duan, G. *et al*. [128], Waqar observed increased As efflux from the roots and decreased As concentrations in the roots and grain [133]. However, he also reported potentially detrimental effects such as an increase in As concentration in the xylem and an increased shoot to root As ratio which could explain the lack of improved As tolerance in these transgenic lines.

Heterologous expression of *ScACR3p* in specific plant tissues could impact on tissue As distribution and plant As tolerance, a hypothesis that was explored in this chapter by expressing *ScACR3p* in rice under the control of two different root specific promoters – namely the rice *CatalaseB* and *Lsi1/NIP2;1* promoters.

OsCatB encodes one of three differentially expressed catalase enzymes in rice which catalyse the breakdown of hydrogen peroxide to water and oxygen, offering protection from oxidative stress caused by excess reactive oxygen species. *CatB* is reported to be strongly expressed in root tissues of seedlings, while expression in mature plants is weaker and more widespread (detected in leaf blade and sheath, root and flower) [134]. Expression of *CatB* is induced in leaf tissue by drought and salinity stresses and is also upregulated by the stress hormone ABA [135-137]. This suggests that *CatB* is induced by abiotic stresses associated with oxidative stress, and so could potentially be upregulated upon exposure to As, a strong inducer of oxidative stress. Treatment of rice seedlings with AsV results in higher levels of reactive oxygen species as well as higher levels of peroxide in the roots [138].

The promoter region of the rice *CatalaseB* gene has been characterised previously by other research groups. Iwamoto, M. *et al.* [134] made progressively larger deletions from the 5' end of the 1066bp full length promoter fused to the GUS (β-Glucuronidase) reporter gene and transiently expressed the constructs in rice protoplasts. The full length *CatB* promoter showed levels of GUS expression around 20 times higher than the CaMV 35S promoter while the shortest *CatB* promoter fragment examined (-56 to +298bp, where 0 is the start of *CatB* cDNA) still showed levels of expression around 10 times higher than with 35S [134]. A similar experiment performed by Mondal, P. *et al.* [139] identified the promoter region from -121 to +56bp as the minimal core promoter

fragment. This fragment drove expression of the GUS gene at levels 6 to 8 times stronger than 35S in rice protoplasts . This strong expression profile and potential response to oxidative stress caused by arsenic treatment make the *OsCatB* promoter an interesting candidate to drive expression of *ACR3* in rice.

While *CatB* is reported to be preferentially and strongly expressed in the roots of rice seedlings, in mature rice plants (3 months old) *CatB* is weakly expressed in leaf, root and flower tissues [140]. Therefore, an additional root specific promoter (of *OsLsi1*) was identified. *Lsi1* is expressed strongly and constitutively in the roots but not in the leaves or panicles. A comparison of *CatB* and *Lsi1* expression patterns is shown in Figure 2.2.

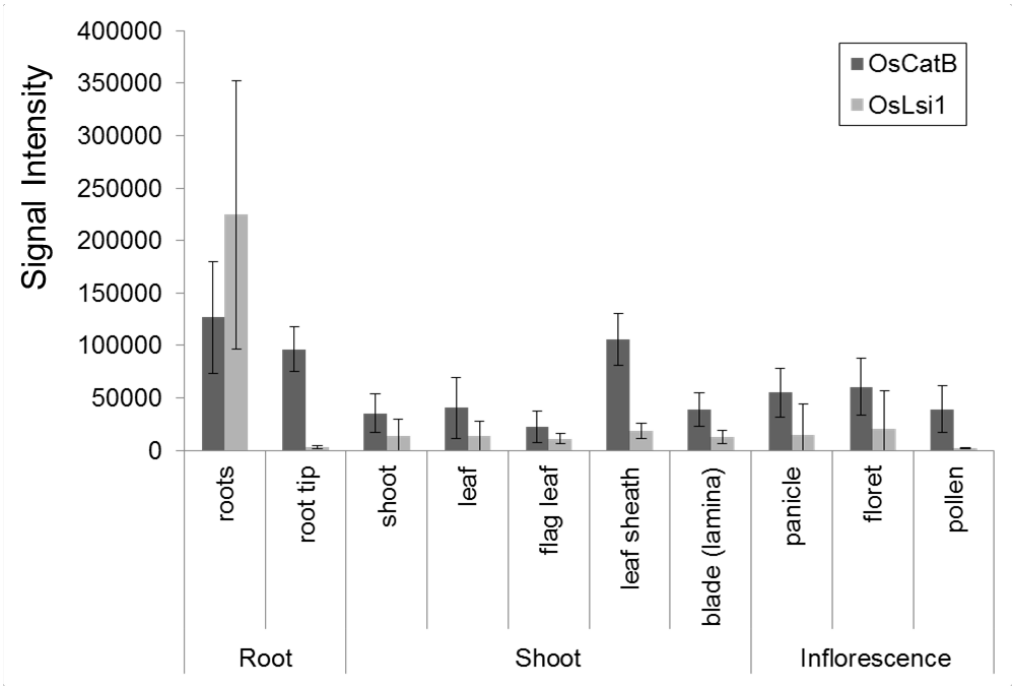

Figure 2.2 Expression patterns of *OsCatB* and *OsLsi1*
Graph showing the relative expression level of *OsCatB* and *OsLsi1* in different rice tissues. Data were obtained from the Genevestigator database [141]. Values are means ± SEs of signal intensities on the Affymetrix Rice Genome Array, plotted on a linear scale.

In the roots, Lsi1 localises to the distal side of the exodermis and endodermis of seminal, lateral and crown roots [142]. *Lsi1* expression levels remain constant throughout plant development except for a peak around the time of heading [142]. Expression of *Lsi1* is not affected by low concentrations of AsIII [56], but is induced by higher concentrations (25μM) and reduced by AsV [143]. A 2kb long region of the *OsLsi1* promoter has previously been used to drive expression of an *OsLsi1-GFP* fusion protein in rice [53, 142], and a 1.6kb portion was used to express the barley orthologue of *Lsi1* in rice [144]. In both cases, the transgene displayed the same sub-cellular localisation as OsLsi1, and so it is expected that under the control of the

OsLsi1 promoter, *ACR3* expression will be restricted to the exodermis and endodermis of the roots.

The endogenous Lsi1/NIP2:1 protein in rice functions alongside the unrelated efflux transporter Lsi2 as part of the highly efficient silicon (and AsIII) transport pathway. Both *Lsi1* and *Lsi2* are expressed in the exodermis and endodermis where they localise to opposite sides of the plasma membrane. Lsi1 facilitates uptake of silicon from the external medium into the root cells while Lsi2 actively effluxes silicon out of the cell towards the stele [65]. The effect of expressing *ACR3* in these same cells could depend on the spatial distribution within the plasma membrane. Localisation of *ACR3* on the distal side of the cell (alongside *Lsi1*) would enable efflux of As towards the external medium and so help reduce net As uptake. On the other hand, localisation of *ACR3* on the proximal side of the cell could complement AsIII efflux through *Lsi2*, leading to enhanced translocation and accumulation.

In this chapter, the effect of tissue specific expression of *ACR3* in rice was investigated to determine if such a manipulation of As transport could lead to increased As tolerance and reduced As accumulation. Targeting *ACR3* expression to the roots could further enhance AsIII efflux to the external medium without the potentially negative effects described above and thus improve rice tolerance to growth under As contaminated conditions. Differences in As tolerance and distribution between transgenic and azygous plants were explored following treatment with AsIII and AsV.

2.2 Materials and Methods

2.2.1 Generation of Transgenic Rice

2.2.1.1 *CatB:ACR3* Expressing Rice

Three independently transformed rice lines containing the *CatB:ACR3* construct were generated by a previous PhD student (Waqar Ali) and visiting researcher (Haiou Wang) using the method described here. Waqar Ali cloned the *CatB:ACR3* construct and Haiou Wang carried out the rice transformations.

A 340bp fragment of the *CatalaseB* promoter region (-221 to +115, where 0 is the start of the *CatB* cDNA) was amplified from rice genomic DNA using primers CatRevXho and CatForStu (Table 2.1). The sequence of the *CatalaseB* promoter fragment can be found in the Appendix (Figure 6.1). The 35S promoter region was removed from the vector pART7 using the restriction enzymes *Xho*I and *Stu*I, and replaced with the CatB promoter. ACR3 was cloned from pART7-35S:ACR3 [127] using primers ACR3Xho and ACR3Sma (Table 2.1) and inserted into the *Xho*I and *Sma*I restriction sites of

pART7-CatB. The CatB:ACR3 containing fragment was subcloned into pGreen0179 using the *Not*I restriction sites.

Table 2.1 Primers used for cloning and genotyping

Primer Name	Sequence	Tm (°C)
CatRevXho	ACACTCGAGTGTTGTGGGAGAGATGAG	58
CatForStu	CAGGCCTGTCTTATCTCCTCGTGATCC	58
ACR3Xho	GCCTCGAGATGTCAGAAGATCAAAAAAGT	54
ACR3Sma	GCCCCGGGATTTCTATTGTTCCATATAT	54
LsiFor	TGCTCTTCAGATGATATGTCGATTTCTGGC	56
LsiRevXho	ACACTCGAGGAGCTACTTGTGCAGCAC	56
ACR3F	AAAAAGTGAAAATTCGGTACCTTC	47
ACR3R	CTCGCGACTATTGCCAAAAT	47
ACTF	TATCCTCCGGTTGGATCTTG	49
ACTR	AGCAATTCCAGGAAACATGG	49

The binary vectors pGreen-CatB:ACR3 and pSoup [145] were co-transformed into the *Agrobacterium* strain AgI1 by electroporation. Recombinant *Agrobacterium* culture was then used to transform mature seeds of rice subgroup japonica cv Nipponbare as described by Nishimura, A. *et al.* [146]. Plants used for the experiments described below were from the T_3 generation.

2.2.1.2 *Lsi1:ACR3* Expressing Rice

The *Lsi1* promoter region (1594bp) was amplified from rice genomic DNA using primers LsiFor and LsiRevXho (Table 2.1), similar to those used by Chiba, Y. *et al.* [144]. The CatB promoter was removed from pART7-CatB:ACR3 using the restriction enzymes *Xho*I and *Stu*I and replaced with the Lsi1 promoter (cut with *Pvu*II and *Xho*I). Lsi1:ACR3 was subcloned into pGreen0179 using the *Not*I restriction sites. pGreen-Lsi1:ACR3 and pSoup were co-transformed into *Agrobacterium* prior to rice transformation as described above.

The *E. coli* strain DH5α was used for the cloning procedures. Restriction digests and ligations (T4 DNA ligase, NEB) were carried out according to the manufacturer's instructions. DNA fragments were excised and purified from agarose gels using the Wizard® SV Gel and PCR Clean-Up System (Promega). Chemically competent DH5α cells were transformed using heat shock and transformants were selected on LB (Luria-Bertani) agar plates containing the relevant antibiotic selection. Plasmid DNA was purified from transformed colonies using the NucleoSpin® Plasmid kit (Machery-

Nagel) and successful cloning confirmed using restriction digest and DNA sequencing (3130 Genetic Analyser, Technology Facility, University of York).

2.2.2 Genotyping

Transformed plants were identified using ACR3 specific primers (Table 2.1). Actin specific primers (Table 2.1) were used as a positive control to identify azygous individuals. Genomic DNA was extracted from leaf tissue ground in liquid nitrogen using the method described by Edwards *et al*. [147]. PCR was performed using GoTaq G2 Flexi DNA Polymerase (Promega) using the reaction mix and thermal cycler conditions in Table 2.2.

Table 2.2 Thermal cycler conditions for PCR using GoTaq G2 Flexi DNA Polymerase

Step	Temp (°C)	Time (s)
1	94	120
2	94	15
3	Tm	30
4	72	60 per kb
Repeat steps 2-4 35-40 times		
5	72	300

For each reaction, 11µl of master mix was added to 0.5µl DNA and 0.25µl of each primer (10µM). PCR product was then run on a 1% agarose gel containing SYBR Safe DNA Gel Stain (Invitrogen) alongside a 2-Log DNA ladder (NEB) and visualised using Genesnap (Syngene). An example gel (Figure 2.3) shows the results obtained for transgenic and azygous individuals.

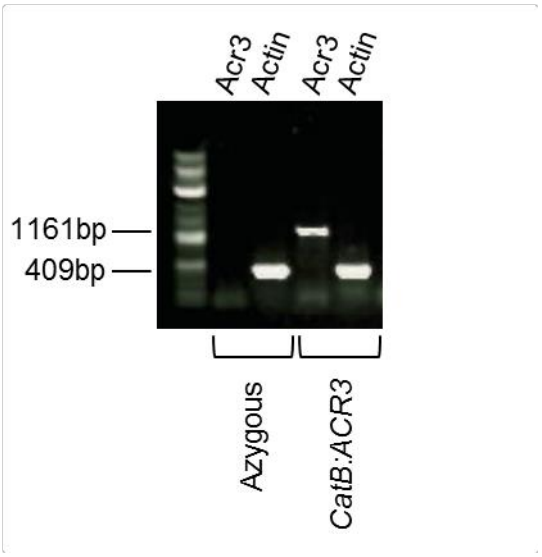

Figure 2.3 Agarose gel showing PCR products obtained from genotyping *CatB:ACR3* rice
PCR was performed on DNA from azygous and transgenic plants using ACR3 and Actin specific primers as indicated. The DNA fragment size is marked alongside the 2-Log DNA ladder run in the first lane.

2.2.3 Semiquantitative RT-PCR

RNA was extracted from transgenic rice tissues that were finely ground in liquid nitrogen using an E.Z.N.A Plant RNA Kit (Omega) according to the manufacturer's instructions. Remaining contaminating DNA was removed using RQ1 RNase-Free DNase (Promega). RNA was quantified using a Nanodrop and 1µg used in the cDNA synthesis reaction. cDNA was synthesised using the High-Capacity RNA-to-cDNA Kit (Applied Biosystems) according to the manufacturer's instructions. Negative control PCRs were performed prior to cDNA synthesis to confirm absence of contaminating DNA in the RNA samples using *OsAcr3* specific primers (Table 2.1, Figure 2.4). RT-PCR was performed using primers specific to *ACR3, CatB* and *Actin* (Table 2.3) using GoTaq G2 Flexi DNA Polymerase as described in section 2.2.2. Cycle numbers are as indicated in the text. For each condition, three biological and technical repeats were performed.

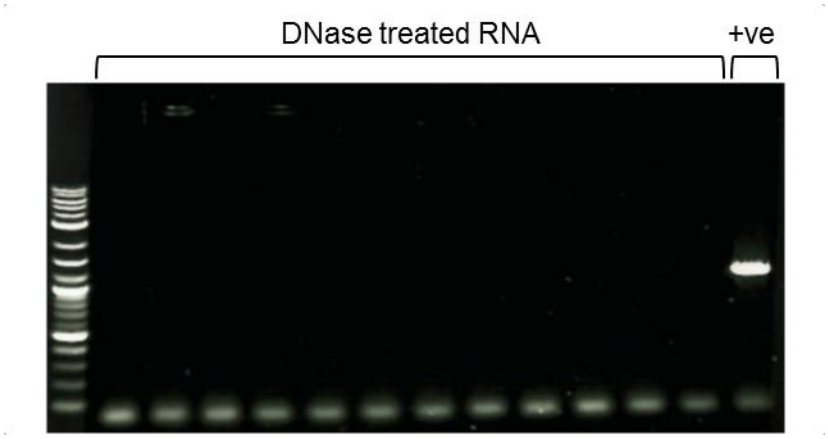

Figure 2.4 Agarose gel showing absence of contaminating DNA in RNA samples
PCR reactions were performed on DNase treated RNA samples using ACR3 specific primers to confirm the absence of contaminating DNA. A positive control using gDNA from *CatB:ACR3* rice is shown in the last lane of the gel.

Table 2.3 Primers used for RT-PCR on *CatB:ACR3* expressing rice

Primer Name	Sequence	Tm (°C)
RTACR3F	CTTTGTCCCATTGGTGCTTT	49
RTACR3R	TTCTTCCCCAGACCCTCTTT	49
RTCATBF	TTCGGTTCTCCACAGTCGTG	53
RTCATBR	TCAGTCAAGTCCTTCGTGGC	53
RTACTF	TATCCTCCGGTTGGATCTTG	49
RTACTR	AGCAATTCCAGGAAACATGG	49

2.2.4 Growth Conditions

Rice seeds were sown in boxes filled with terragreen flooded with water and germinated in the dark at 28°C for 5 days. Box lids were removed and seedlings placed in the glasshouse under the following conditions: 16hr light/8hr dark, night/day temperatures of 28°C/24°C and relative humidity around 60% with light radiation approx. 160W/m^2. Two week old (2wo) plants were transferred to hydroponics boxes containing Yoshida medium [148] supplemented with 276µM SiO_2. Medium was replenished weekly and supplemented with different concentrations of AsIII (as As_2O_3) or AsV (as KH_2AsO_4) as indicated.

2.2.5 Growth Experiments

Transgenic and azygous plants were grown as described in section 2.2.4. Three week old (3wo) plants were transferred to treatment conditions (Control, 10, 20, or 40µM

AsIII or 30, 40 or 50μM AsV). Plants were weighed and shoot length measured at the start of treatment and subsequently every four weeks until the plants were 15 weeks old (15wo). The number of live tillers was counted at the end of the experiment. Each experiment includes at least 6 plants of each genotype and the experiment was repeated four times. After completion of the growth experiment, a subset of the plants was returned to control medium (without As) until maturity. The number of grains produced was counted from at least three individuals of each genotype per experiment from plants that had been exposed to 20μM AsIII, 40 or 50μM AsV. Relative growth rates (RGR) were calculated according to Poorter, H *et al.* [149] using the equation below where W1 and W2 are plant fresh weight or height measured at time t1 and t2.

$$RGR = \frac{\ln W2 - \ln W1}{t2 - t1}$$

2.2.6 Arsenic Concentration Analysis

The total arsenic concentration of root and shoot tissue of transgenic and azygous plants was analysed after 4 and 12 weeks in treatment, corresponding to 7 week old (7wo) and 15 week old (15wo) plants, as was the As concentration of the grain. Root tissue was washed in ice cold desorption buffer (1mM K_2HPO_4, 0.5mM $Ca(NO_3)_2$ and 5mM MES-pH 5.6) for 15 minutes to remove apoplastic As and then rinsed thoroughly with dH_2O. Plant tissue was dried at 80°C for 24 hours and the dry weight of root and shoot tissues recorded. Tissue was cut into small (<1cm) pieces and a subsample taken for digestion (~50-100mg). Each sample contained material from three individual plants and each experiment was repeated three times. Samples were digested in HNO_3 at 70°C for 24 hours and diluted to 5% HNO_3 with ultrapure water (18.2 MΩ cm^{-1}) and filtered through filter paper (equivalent Whatman Grade 1). The As concentration of samples was determined using an ICP-OES (Thermo iCAP 7000 series).

2.2.7 Xylem Arsenic Concentration

The arsenic concentration of xylem sap was measured from transgenic and azygous rice lines. Three week old (3wo) plants were exposed to 50μM AsV in hydroponics for three days. The plants and medium were weighed at the beginning and end of treatment to enable calculation of transpiration rates. The stem of seedlings was cut 4cm above the root-shoot junction using a sharp blade. Seedlings were transferred to a pressure chamber (Digital Plant Water Potential Apparatus EL540-300) and xylem sap collected by applying pressure (~10 kiloPascal) for 20 minutes. Sap from five individual plants was bulked and made up to 2.2 ml using 5% HNO_3 and the As concentration analysed as above (Section 2.2.6).

2.2.8 Arsenic Efflux

Arsenic efflux was measured from 3wo plants following exposure to 250μM AsV for 24hrs in hydroponics. Three plants of each genotype were rinsed in dH_2O and placed in a 15ml plastic tube containing 13ml Yoshida medium and secured in place with a sponge. Separate tubes were set up for each time-point and samples taken after 1, 3, 6 and 24hours. The experiment was repeated three times. Root and shoot tissue samples were prepared for ICP-OES analysis as described in section 2.2.6. The Yoshida medium was filtered and made up to 5% HNO_3 for total As concentration analysis.

2.2.9 Statistical Analyses

Experiments were analysed in SPSS using a two-way ANOVA. The main effects and simple main effects were explored using Bonferroni adjusted pairwise comparisons. Alternatively, significant differences between genotypes were explored using unpaired *t*-tests or one-way ANOVA where appropriate and as indicated in the text. When a one-way ANOVA was used, significant differences between genotypes were explored using Tukey post-hoc analysis when there was homogeneity of variances (assessed by Levene's test of homogeneity of variances). When there was heterogeneity of variances, a one-way Welch ANOVA was used and the results interpreted using a Games-Howell post-hoc analysis.

2.3 Results

2.3.1 *Lsi1:ACR3* Expressing Rice

DNA sequencing of the pGreen-Lsi1:ACR3 plasmid revealed that only a short 226bp fragment (Figure 6.2 in the Appendix) of the Lsi1 promoter region had been inserted upstream of *ACR3* (henceforth referred to as Lsi1S). pGreen-Lsi1S:ACR3 was transformed into *Agrobacterium* and used to generate *Lsi1S:ACR3* expressing rice while the full length promoter was re-cloned.

Semiquantitative RT-PCR was performed on T_2 *Lsi1S:ACR3* expressing rice plants to determine if the Lsi1S promoter was sufficient to confer root specific expression. *ACR3* expression in the root, stem and leaf tissue of 3wo plants was investigated (Figure 2.5). Transcript was detected in all three tissues at similar levels in the transgenic plants, indicating that the Lsi1S promoter fragment is not sufficient to drive root specific expression in rice. No *ACR3* transcript was detected in cDNA from non-transgenic control plants (data not shown).

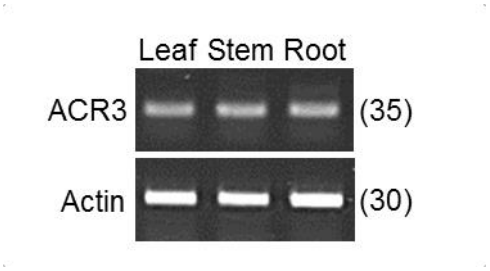

Figure 2.5 RT-PCR of *Lsi1S:ACR3* expressing rice
RT-PCR was performed on cDNA from leaf, stem and root tissue of *Lsi1S:ACR3* expressing rice using *ACR3* and *Actin* specific primers. Numbers in parenthesis indicate PCR cycle number.

Since the short Lsi1 promoter fragment failed to generate root specific expression, the full length Lsi1 promoter was re-cloned into pGreen0179 and used to transform rice calli. Putatively transformed plants were regenerated from 17 independent calli and tested for the presence of the transgene by PCR using *ACR3* specific primers. However, ACR3 could not be detected in any of the regenerated plants (data not shown) implying that the transformation was unsuccessful. When troubleshooting, it became apparent that there was a problem with the antibiotic selection – untransformed calli were resistant to hygromycin B. Therefore, fresh calli were induced from Nipponbare seed and the transformation procedure repeated. Unfortunately, no *Lsi1:ACR3* expressing plants could be successfully regenerated within the timeframe of this project.

2.3.2 RT-PCR Analysis of *CatB:ACR3* Expressing Rice

Three independently transformed *CatB:ACR3* expressing lines were obtained, however only two of these set seed (hereafter referred to as Line 1 and Line 2). RT-PCR was carried out on cDNA from root, stem and leaf tissue of 3wo plants using *ACR3* and *CatB* specific primers (Table 2.3) to compare the activity of the transgenic and endogenous *CatB* promoters (*Actin* specific primers were used as a loading control). A representative agarose gel for each line can be seen in Figure 2.6. No *ACR3* transcript was detected in cDNA from azygous control plants (data not shown).

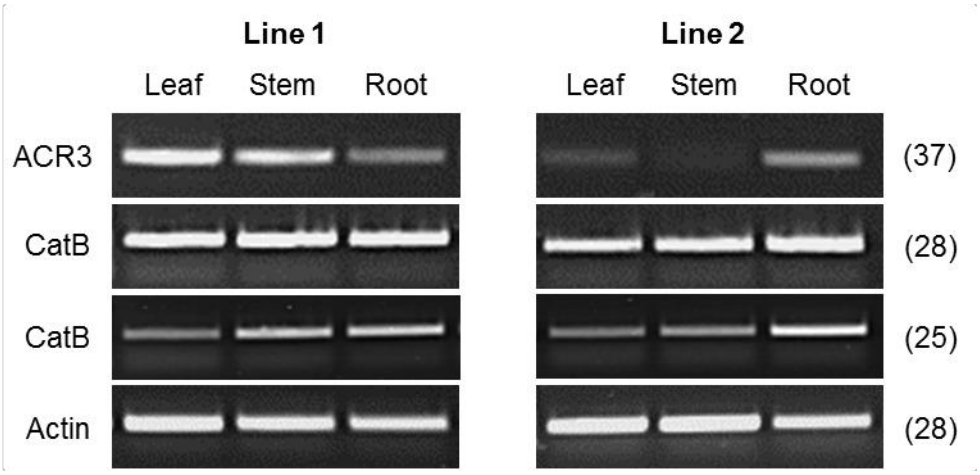

Figure 2.6 RT-PCR of 3wo *CatB:ACR3* expressing rice
RT-PCR was performed on leaf, stem and root tissue of three week old Line 1 and Line 2 plants using *ACR3*, *CatB* and *Actin* specific primers. Numbers in parenthesis indicate PCR cycle number.

The pattern of *ACR3* expression is different between the two lines. In Line 1, *ACR3* is expressed most strongly in the leaf and stem tissue while in Line 2 *ACR3* expression is strongest in the root and much weaker in the stem and leaf tissue. Compared to the expression level of *CatB*, the transgene is expressed at a relatively low level in both lines. Surprisingly, and contrary to previous reports [135, 137, 150], strong levels of *CatB* expression (similar to *Actin*) were detected in all three tissues. Although when fewer PCR cycles were performed, stronger expression of *CatB* in the root could be observed.

The effect of As exposure on *ACR3* and *CatB* expression was also investigated. RT-PCR was performed on leaf, stem and root tissue from 7wo plants after four weeks treatment in Control (0μM As), 20μM AsIII and 50μM AsV containing media. A representative agarose gel for each line can be seen in Figure 2.7.

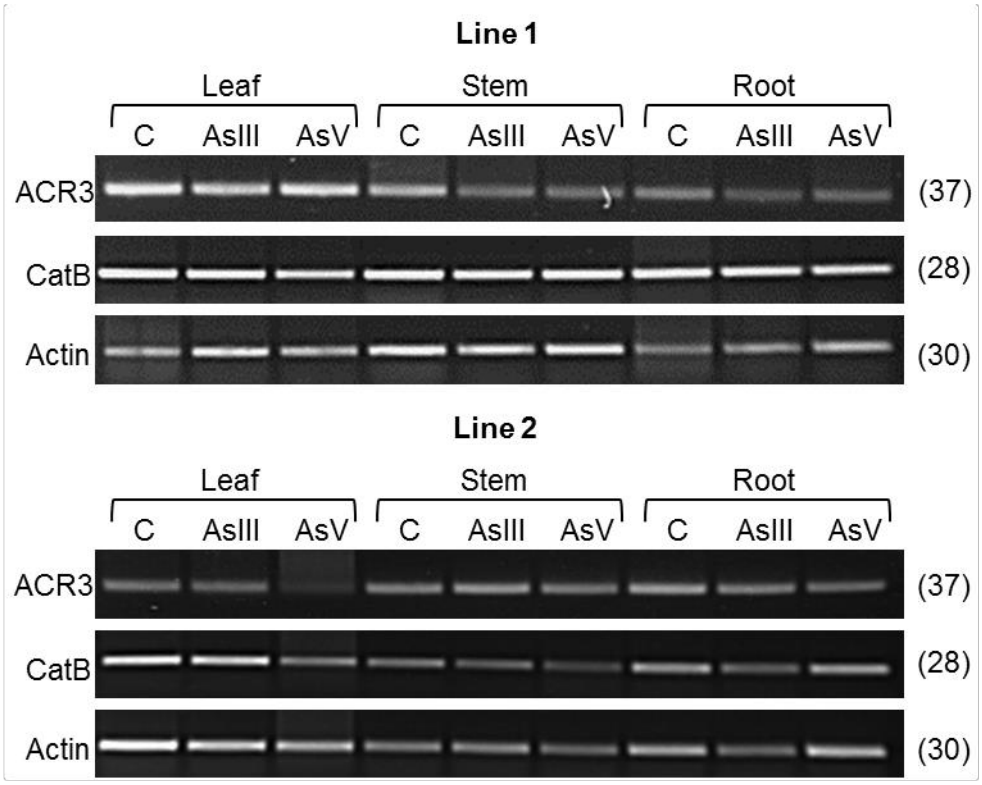

Figure 2.7 RT-PCR of 7wo *CatB:ACR3* expressing rice
RT-PCR was performed on leaf, stem and root tissue of seven week old Line 1 and Line 2 rice plants treated with control, 20μM AsIII or 50μM AsV hydroponic media for four weeks. Primers specific to *ACR3*, *CatB* and *Actin* were used. Numbers in parenthesis indicate PCR cycle number.

In control conditions, the expression pattern of *ACR3* in 7wo Line 1 plants is similar to that seen in 3wo plants, with higher expression in the leaf and stem than in the root tissue. In 7wo Line 2 plants, *ACR3* expression remains strongest in the roots, but is also detected in the stem and leaf tissues. *ACR3* expression appears to be downregulated after 4 weeks in As. In Line 1, this is most apparent in the stem and root tissues of plants treated with AsIII and AsV. In Line 2, *ACR3* expression appears reduced after As treatment in all three tissues, but most noticeably in the leaf. *CatB* expression was detected at similar levels in all three tissues of both Lines, and was not affected by As treatment.

2.3.3 Arsenic Tolerance of *CatB:ACR3* Expressing Rice

CatB:ACR3 expressing rice lines were exposed to a range of concentrations of AsIII and AsV over a 12 week period. Their fresh weight and shoot length was recorded every 4 weeks (at 3, 7, 11 and 15wo) and the number of tillers counted at the end of the treatment (15wo). Growth parameters were compared between transgenic and azygous lines to determine the effect of *CatB:ACR3* expression on As tolerance.

2.3.3.1 *CatB:ACR3* Expression Alters Shoot Length in Response to Arsenic

Figures 2.8 and 2.9 show the increase in shoot length of Line 1 and Line 2 transgenic and azygous rice over the course of the growth experiment. In control conditions, shoot lengths increased rapidly over the first four weeks of treatment and then continued to increase at a markedly reduced rate over the remaining 8 weeks (Figure 2.10). This suggests that under non-stressed conditions, the majority of shoot elongation occurs when the plants are 3 to 7 weeks old (consistent with field grown cultivars [151]). During this period, shoot elongation rate is hampered by the addition of AsIII or AsV to the medium with a reduction in shoot relative growth rate (RGR) which becomes more severe with increasing As concentration (Figure 2.11). For both Lines, azygous and transgenic plants responded similarly to As treatment. A two-way ANOVA was performed, and no significant interaction was found between genotype and treatment for each line, however there were some significant simple main effects (as indicated on Figure 2.11). Line 1 *CatB:ACR3* expressing plants increased in height at a slower rate than azygous plants in 40μM AsV and Line 2 transgenic shoot RGR was significantly lower than azygous RGR in 20μM AsIII. This suggests that *ACR3* expression may reduce tolerance to As, but this was not consistent across the range of concentrations tested.

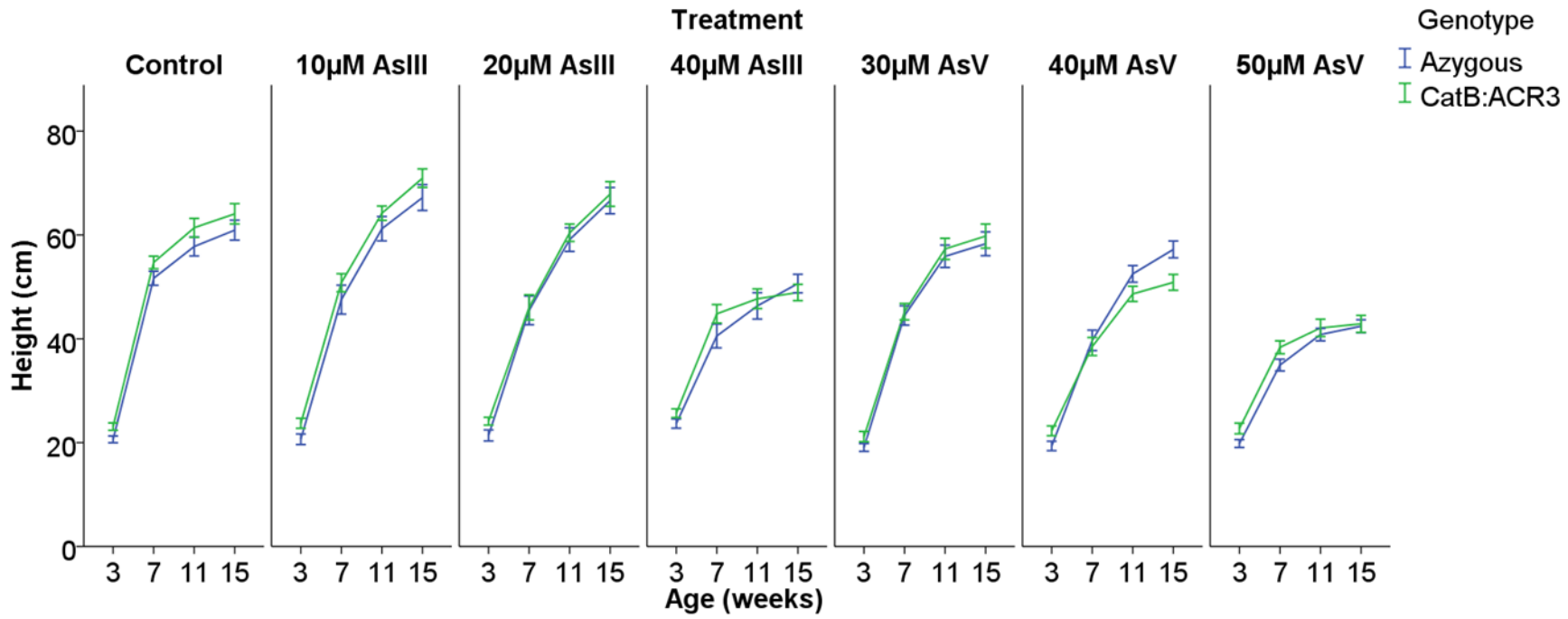

Figure 2.8 Heights of Line 1 *CatB:ACR3* expressing rice

Heights of Line 1 *CatB:ACR3* expressing and azygous plants from 3-15 weeks old. Plants were grown for 12 weeks in hydroponics and exposed to a range of AsIII and AsV treatments. Shoot lengths were measured every four weeks. Data are from four independent experiments and values are means ± SE.

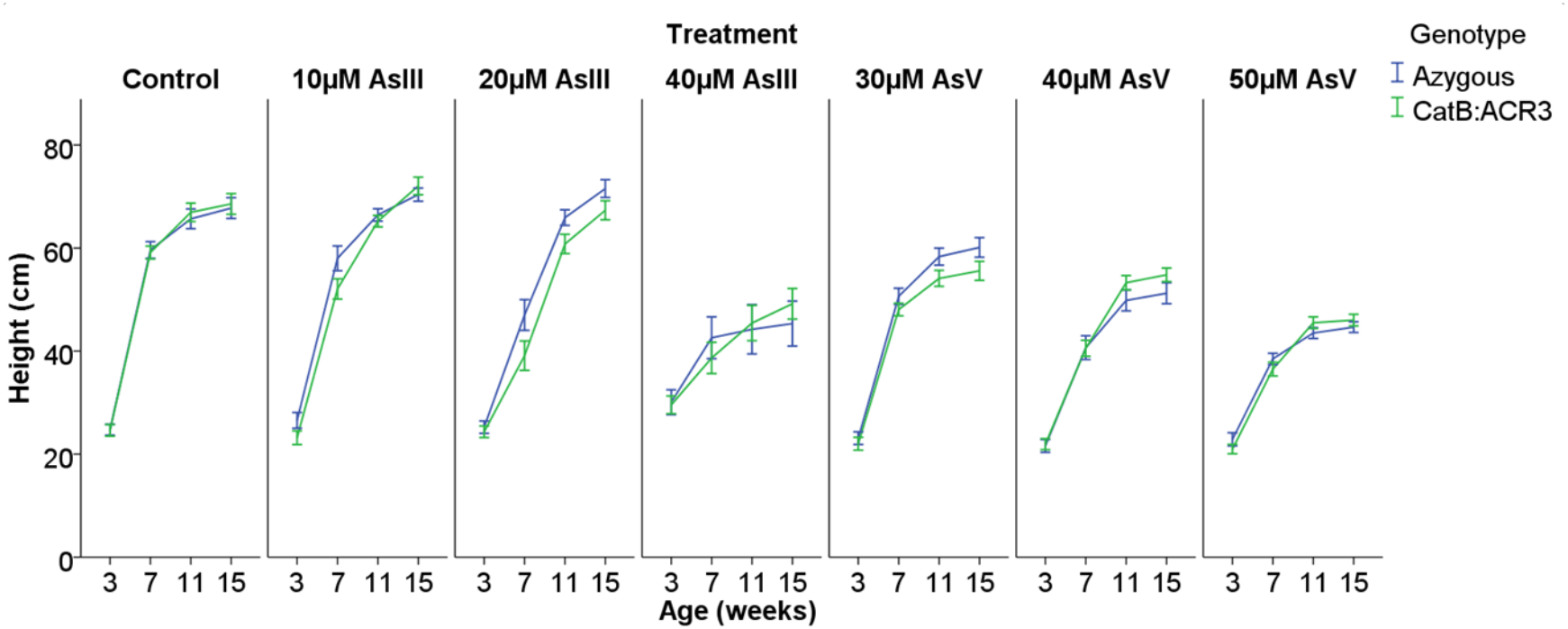

Figure 2.9 Heights of Line 2 *CatB:ACR3* expressing rice

Heights of Line 2 *CatB:ACR3* expressing and azygous plants from 3-15 weeks old. Plants were grown for 12 weeks in hydroponics and exposed to a range of AsIII and AsV treatments. Shoot lengths were measured every four weeks. Data are from four independent experiments and values are means ± SE.

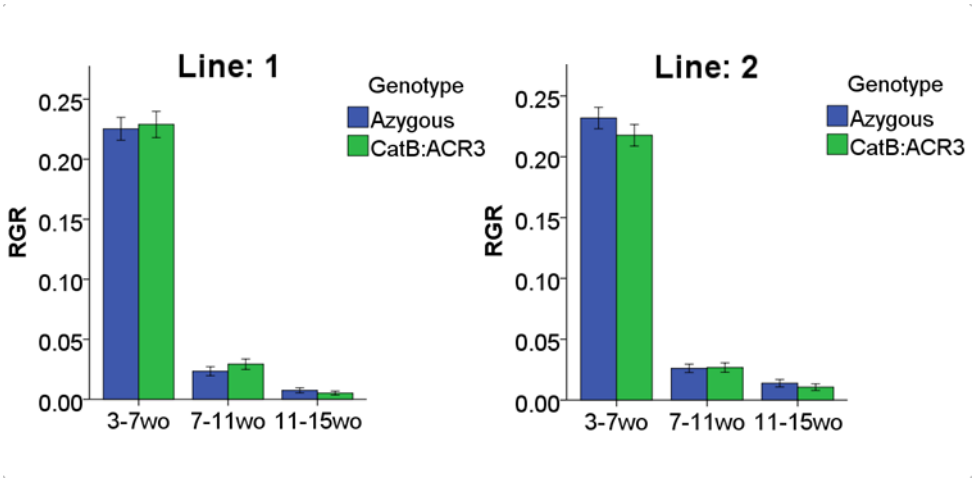

Figure 2.10 Shoot relative growth rates of Line 1 and Line 2 *CatB:ACR3* expressing rice
Graphs show the relative growth rate of shoot elongation over 4 week periods from 3 to 15 week old plants grown in control conditions. Data are from four independent experiments, values are means ± SE.

There is some evidence that Line 1 and Line 2 respond differently to As, as a significant interaction was found between Line and treatment on shoot RGR. Analysis of the simple main effects revealed Line 1 and 2 respond differently to 10 and 20μM AsIII and 50μM AsV treatments. This could be due to environmental effects, as some of the growth experiment repeats for each Line were conducted at different times, or it could be caused by somatic mutations introduced during the transformation procedure.

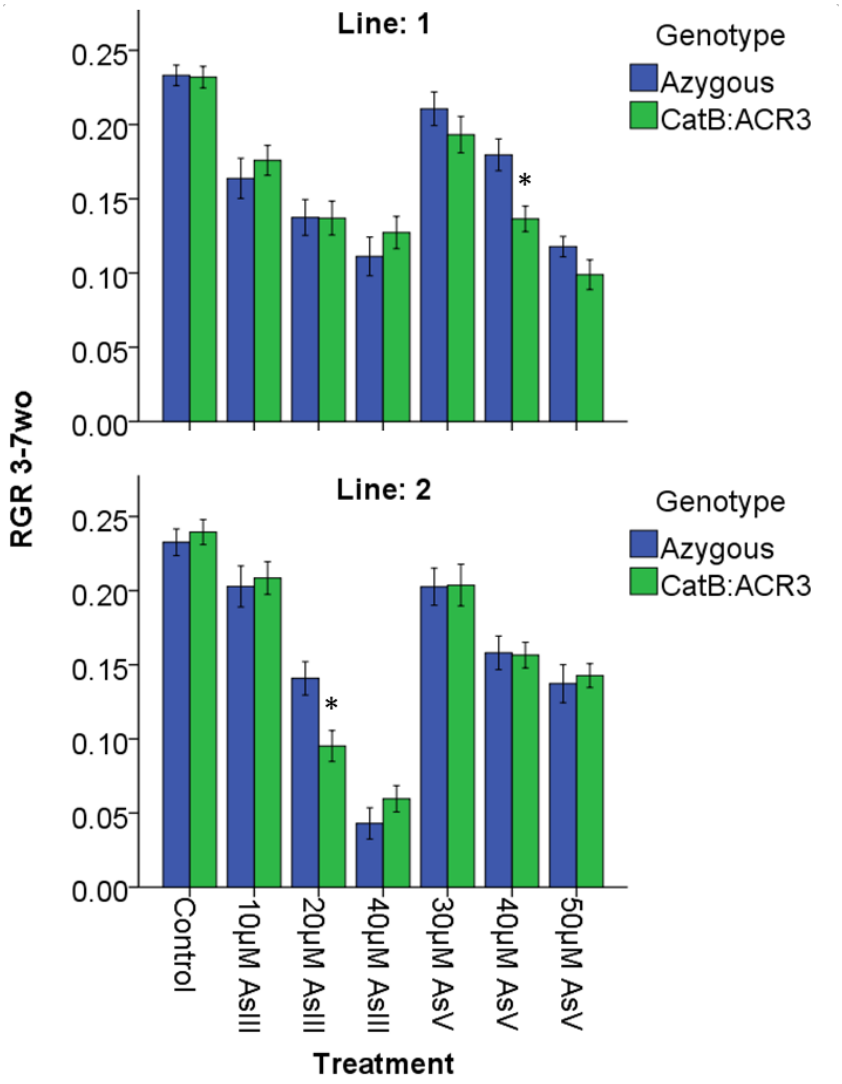

Figure 2.11 Shoot relative growth rates of 3-7wo *CatB:ACR3* expressing rice
Graphs show the rate of shoot elongation of Line 1 and Line 2 *CatB:ACR3* expressing rice over 4 weeks growth (from 3-7 weeks old) in different concentrations of AsIII or AsV. Data are from four independent experiments, values are means ± SE and asterisks indicate significant differences between genotypes at $P<0.05$.

Despite an initial reduction in shoot RGR during the first four weeks of treatment, plants in the lower concentrations of As tested were able to recover in the following 8 weeks and ended up as tall or even taller than plants in control conditions (Figures 2.8 and 2.9). This suggests that rice plants are able to compensate for reduced shoot growth during the initial four weeks of As exposure by increasing the rate of shoot elongation during long term exposure. To investigate this further, the shoot RGR of 7-15wo plants was examined (Figure 2.12).

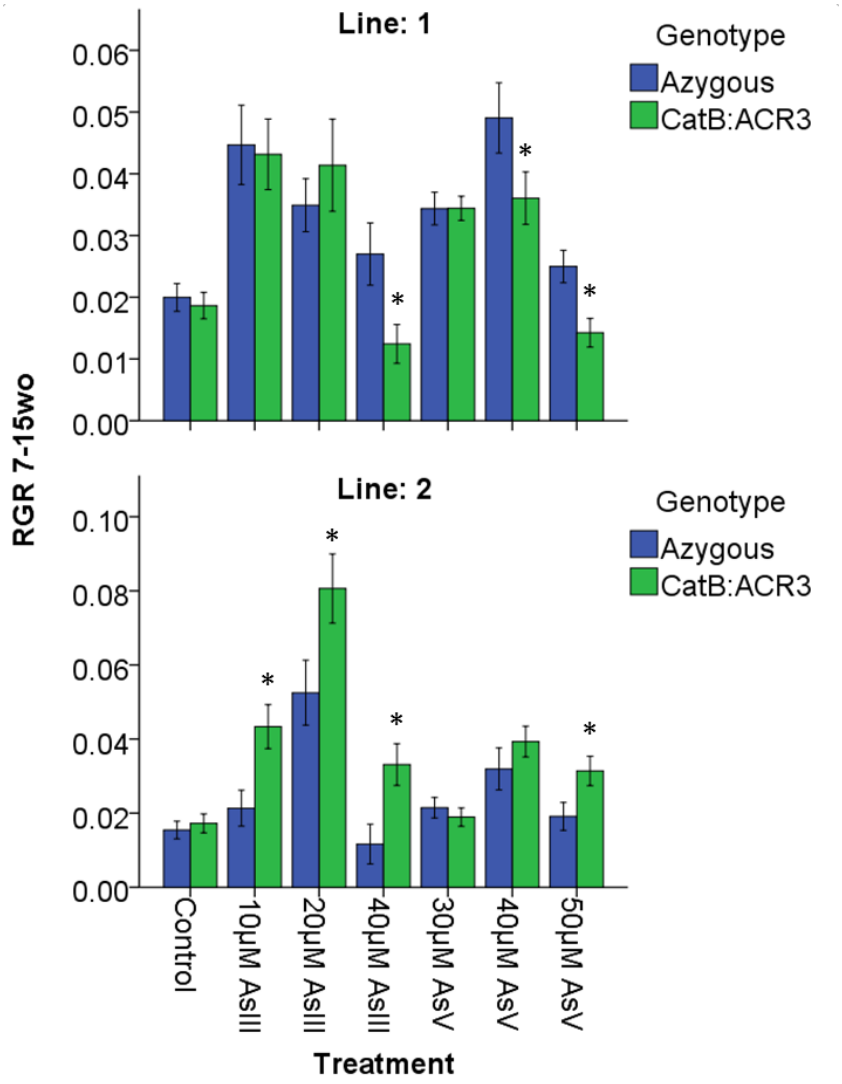

Figure 2.12 Shoot relative growth rates of 7-15wo *CatB:ACR3* expressing rice
Graphs show the rate of shoot elongation of Line 1 and Line 2 *CatB:ACR3* expressing rice over 8 weeks growth (from 7-15 weeks old) in different concentrations of AsIII or AsV. Data are from four independent experiments, values are means ± SE and asterisks indicate significant differences between genotypes at $P<0.05$.

Compared to growth in control conditions, rice plants exposed to As had an increased shoot RGR during the period when plants were 7-15wo (i.e. after 4 to 12 weeks of treatment). This increase in RGR was statistically significant for all but the highest concentrations of AsIII and AsV. The shoot RGR of azygous and *CatB:ACR3* expressing plants responded differently to As treatment. Line 1 transgenic plants had a significantly lower shoot RGR in 40μM AsIII and 40 and 50μM AsV compared to the azygous plants (Figure 2.12). Expression of *CatB:ACR3* had the opposite effect on Line 2, transgenic plants had a significantly higher shoot RGR than the azygous plants in 10, 20 and 40μM AsIII and 50μM AsV.

The average shoot RGR of plants over the course of the entire growth experiment (from 3wo to 15wo) was only significantly reduced compared to control conditions by

the highest concentrations of AsIII and AsV tested (Figure 2.13). This is probably because in the lower concentrations the plants were able to recover from the initial reduction in RGR (3-7wo, Figure 2.11) by increasing their shoot RGR compared to control conditions from 7-15wo (Figure 2.12) while in the higher concentrations (40μM AsIII and 50μM AsV) the RGR from 7-15wo was not increased compared to control conditions. The effect of *CatB:ACR3* expression on overall shoot RGR (3-15wo) was different between the two lines. Line 1 transgenic plants grew significantly slower than the azygous control in 40μM AsV while Line 2 transgenic plants grew faster than the azygous control in 50μM AsV (Figure 2.13).

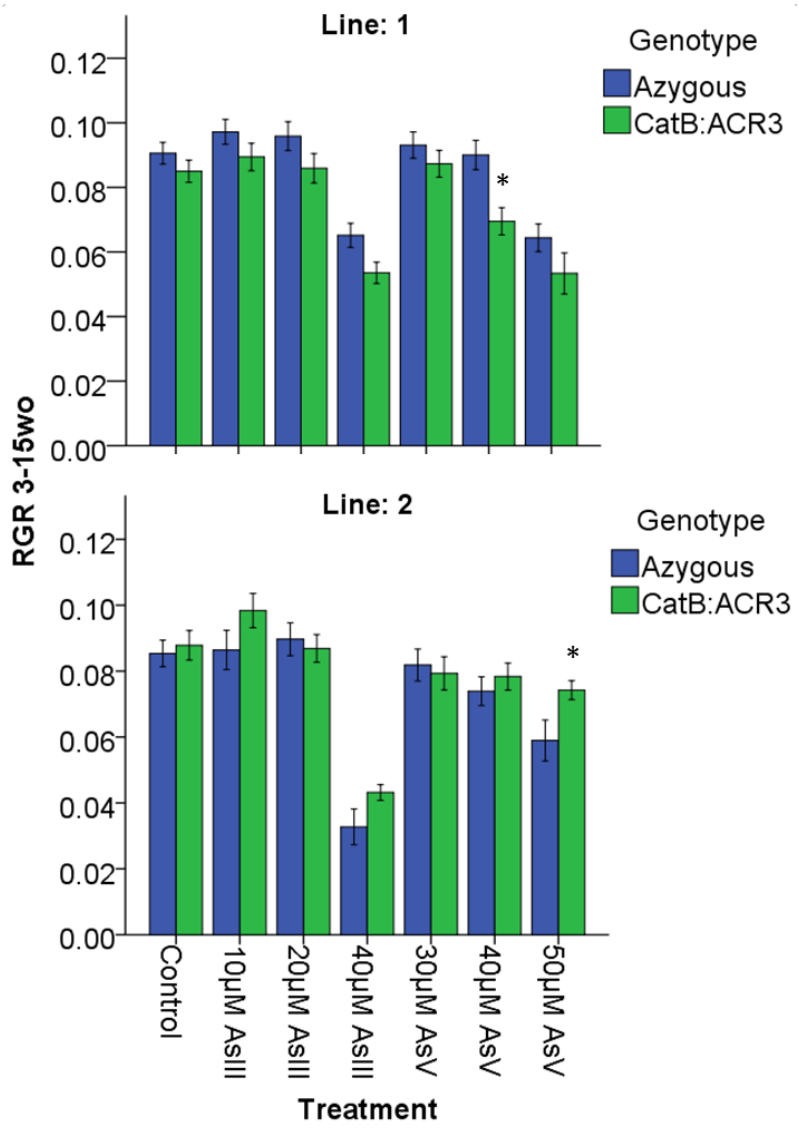

Figure 2.13 Shoot relative growth rates of 3-15wo *CatB:ACR3* expressing rice
Graphs show the rate of shoot elongation of Line 1 and Line 2 *CatB:ACR3* expressing rice over 12 weeks growth (from 3-15 weeks old) in different concentrations of AsIII or AsV. Data are from four independent experiments, values are means ± SE and asterisks indicate significant differences between genotypes at $P<0.05$.

Generally, the data suggest that *ACR3* expression in rice contributes to As tolerance and can have either a positive or a negative effect: Line 1 transgenic plants are less tolerant to As while Line 2 transgenic plants are more tolerant compared to the azygous control plants.

2.3.3.2 *CatB:ACR3* Expression Alters Fresh Biomass Accumulation in Response to As

The increase in weight of Line 1 and Line 2 plants over the course of the growth experiment (3-15wo) is shown in Figures 2.14 and 2.15 and the RGRs of 3-15wo plants are shown in Figure 2.16. The overall RGR of plants grown in 40μM AsIII and 30, 40 and 50μM AsV was reduced compared to growth in control conditions. There were no differences in RGR between Line 2 transgenic and azygous plants, however Line 1 *CatB:ACR3* expressing plants grew significantly slower than the azygous controls in 40μM AsIII and 40 and 50μM AsV (Figure 2.16) over the course of the experiment.

The weights of Line 1 azygous and transgenic plants were similar over the first four weeks of the experiment in all treatments. Over the remaining 8 weeks of the experiment, azygous Line 1 plants seemed to grow better than the transgenic plants in the higher concentrations of AsIII and AsV (Figure 2.14). This suggests that *CatB:ACR3* expression in Line 1 has an effect on growth after long term exposure to As. Line 2 *CatB:ACR3* expressing plants appear slightly less tolerant to short term As exposure (3-7wo) but more tolerant to long term (7-15wo) exposure at the higher concentrations tested (Figure 2.15). To investigate this further, the RGRs of Lines 1 and 2 during short and long term As exposure were compared.

Similar to shoot RGR, the rate of fresh weight accumulation (RGR) in control conditions is fastest when plants are 3-7wo and then decreases over time (Figure 2.17). When exposed to As, the RGR for 3-7wo plants is significantly reduced (Figure 2.18) in all concentrations tested (except Line 1 plants in 30μM AsV). There were no significant differences between the RGRs of Line 1 transgenic and azygous plants during short term As exposure. In contrast, Line 2 transgenic plants had a significantly lower RGR than azygous plants across treatments. Analysis of the simple main effects revealed Line 2 *CatB:ACR3* expressing plants grew significantly slower than azygous plants in 30μM AsV.

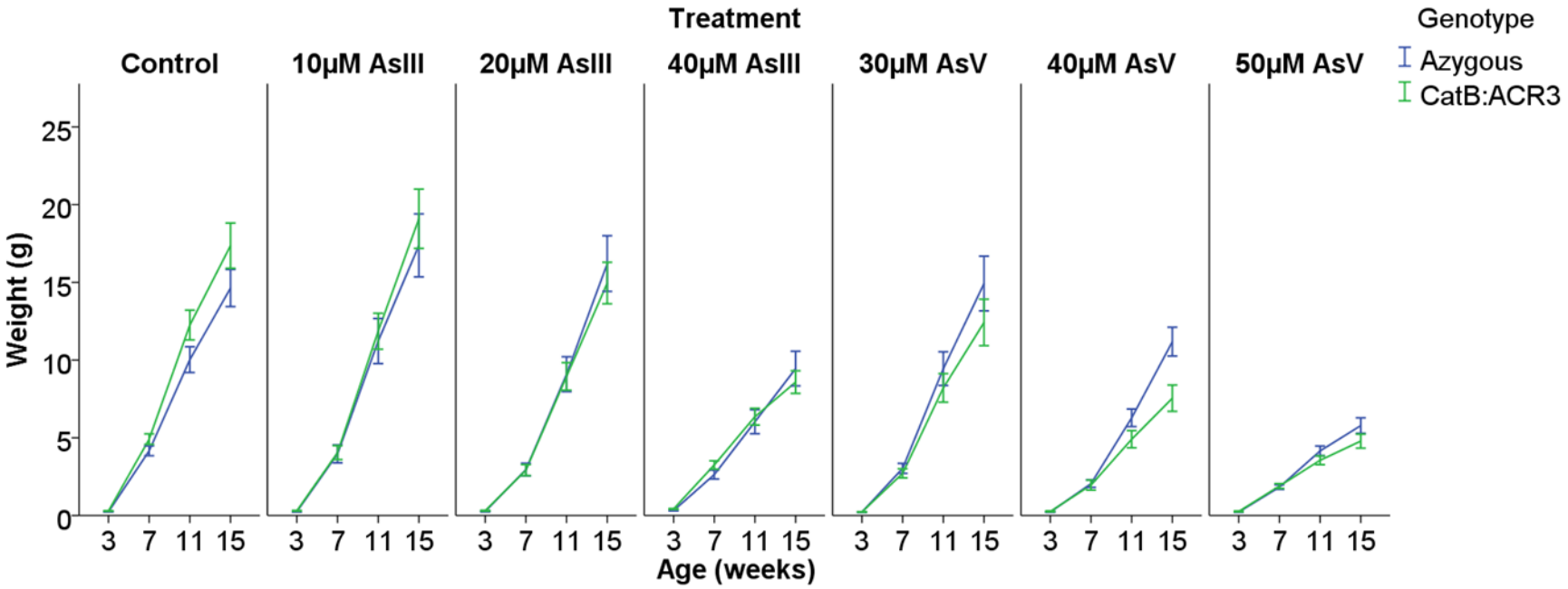

Figure 2.14 Weight of Line 1 *CatB:ACR3* expressing rice

Weights of Line 1 *CatB:ACR3* expressing and azygous plants from 3-15 weeks old. Plants were grown for 12 weeks in hydroponics and exposed to a range of AsIII and AsV treatments. Fresh weights were measured every four weeks. Data are from four independent experiments and values are means ± SE.

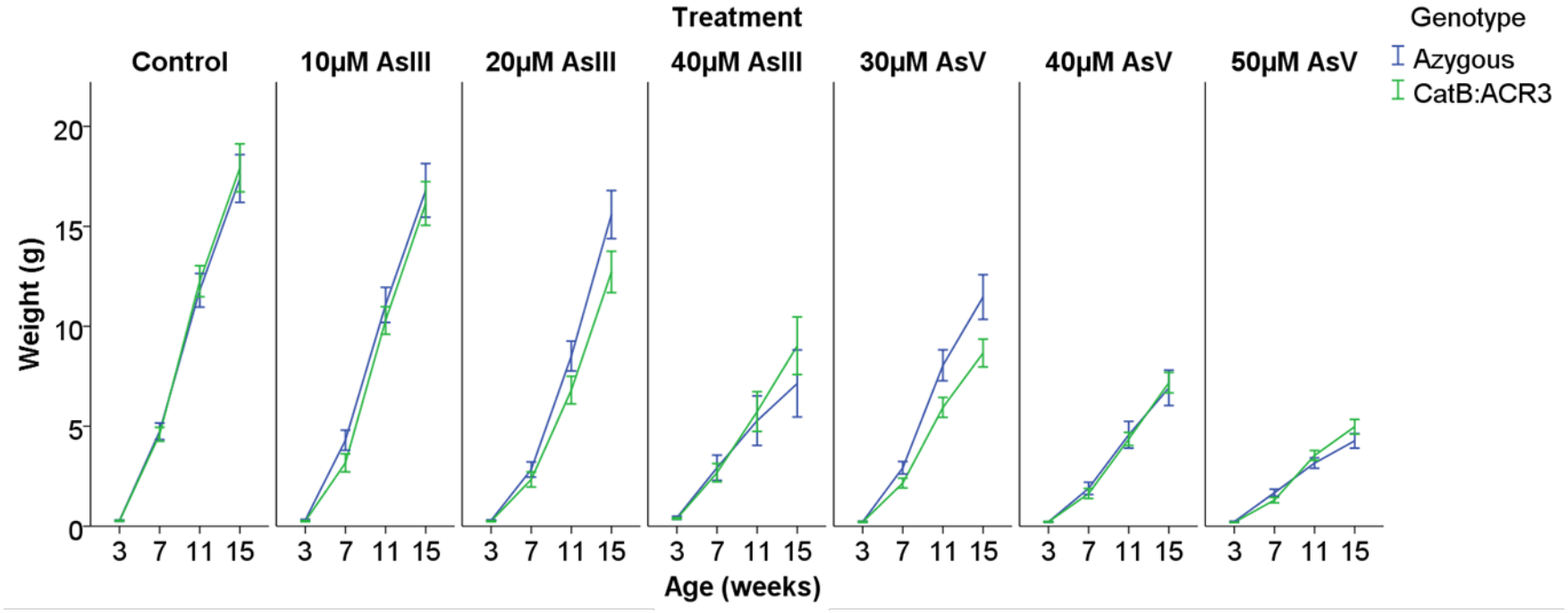

Figure 2.15 Weight of Line 2 *CatB:ACR3* expressing rice

Weights of Line 2 *CatB:ACR3* expressing and azygous plants from 3-15 weeks old. Plants were grown for 12 weeks in hydroponics and exposed to a range of AsIII and AsV treatments. Fresh weights were measured every four weeks. Data are from four independent experiments and values are means ± SE.

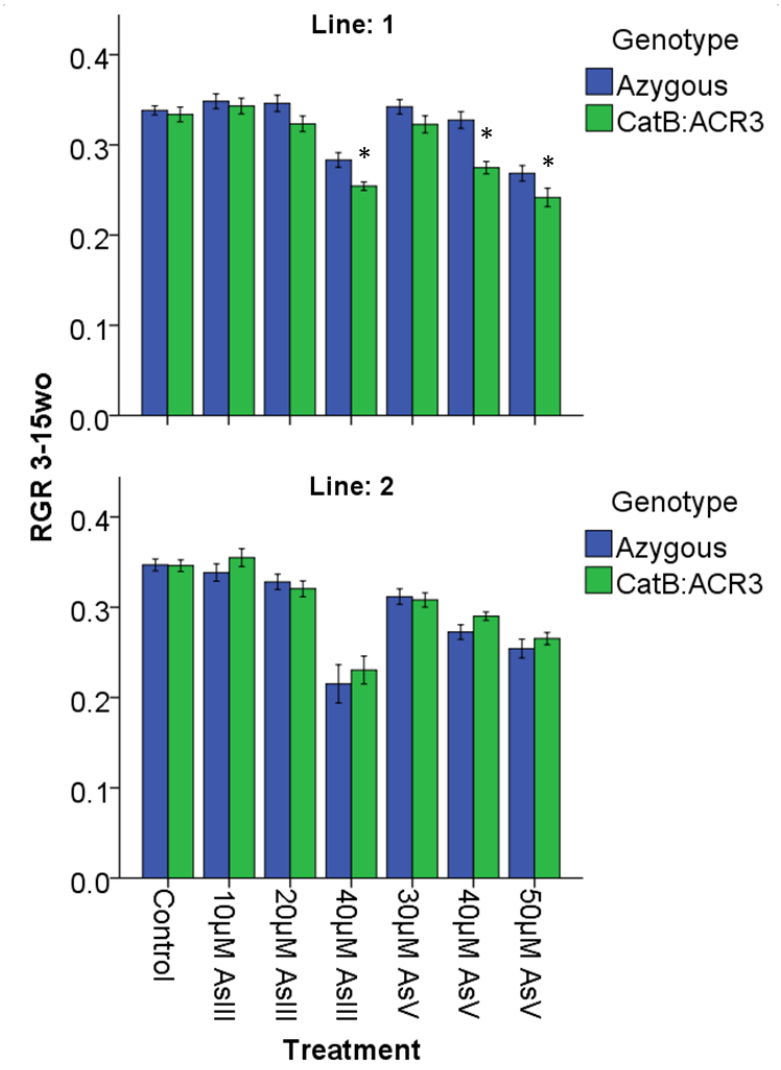

Figure 2.16 Relative growth rates of 3-15wo *CatB:ACR3* expressing rice
Graphs show the RGR of Line 1 and Line 2 *CatB:ACR3* expressing rice over 12 weeks growth (from 3-15 weeks old) in different concentrations of AsIII or AsV. Data are from four independent experiments, values are means ± SE and asterisks indicate significant differences between genotypes at $P<0.05$.

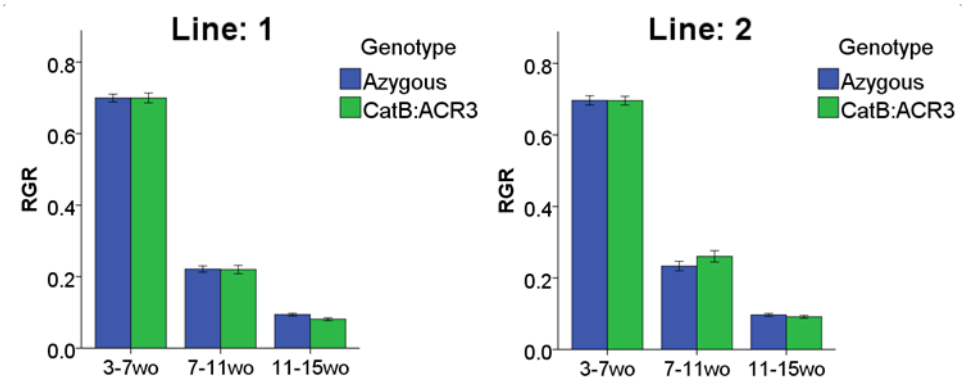

Figure 2.17 Relative growth rates of Line 1 and Line 2 *CatB:ACR3* expressing rice
Graphs show the rate of fresh weight accumulation over 4 week periods from 3 to 15 week old plants grown in control conditions. Data are from four independent experiments, values are means ± SE.

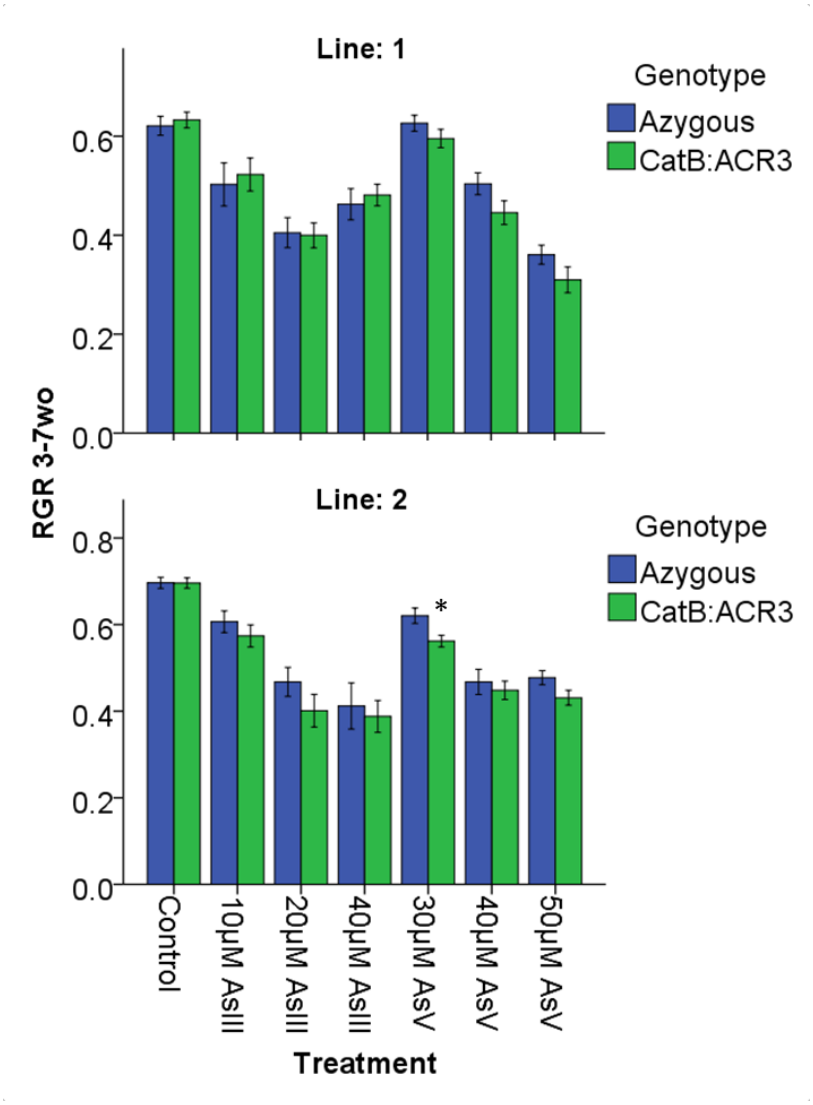

Figure 2.18 Relative growth rates of 3-7wo *CatB:ACR3* expressing rice
Graphs show the RGR of Line 1 and Line 2 *CatB:ACR3* expressing rice over 4 weeks growth (from 3-7 weeks old) in different concentrations of AsIII or AsV. Data are from four independent experiments, values are means ± SE and asterisks indicate significant differences between genotypes at $P<0.05$.

Long term As treatment had a similar effect on the rate of total biomass accumulation as observed for shoot elongation; the RGR of 7-15wo plants exposed to As was increased compared to control conditions in all but the highest concentrations of AsIII and AsV (Figure 2.19). The ability to increase RGR in response to long term As exposure differed between *CatB:ACR3* expressing and azygous control plants. The RGR of Line 1 transgenic plants was significantly lower than azygous while Line 2 transgenic plants grew significantly faster at the concentrations indicated in Figure 2.19. This suggests that *CatB:ACR3* expression alters the rate of fresh weight accumulation in response to long term As exposure. In Line 1, *ACR3* expression results in reduced tolerance to both AsIII and AsV. In Line 2, *ACR3* expression initially slightly reduced tolerance to As, but over long term exposure *ACR3* expression improved tolerance to As.

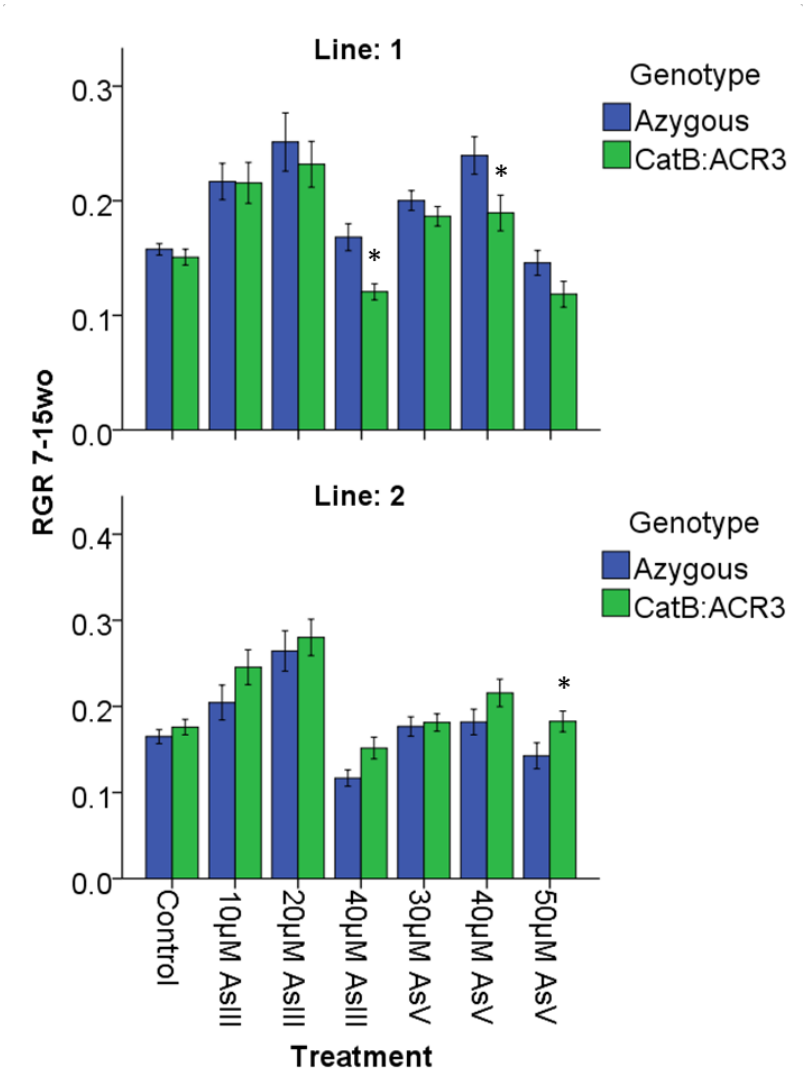

Figure 2.19 Relative growth rates of 7-15wo *CatB:ACR3* expressing rice
Graphs show the RGR of Line 1 and Line 2 *CatB:ACR3* expressing rice over 8 weeks growth (from 7-15 weeks old) in different concentrations of AsIII or AsV. Data are from four independent experiments, values are means ± SE and asterisks indicate significant differences between genotypes at $P<0.05$.

2.3.3.3 *CatB:ACR3* Expression Alters Tiller Number and Yield in Response to As

The tiller number was determined at the end of the growth experiment after 12 weeks of treatment. Figure 2.20 shows the average tiller number relative to the control conditions. Line 1 transgenic plants had fewer tillers on average than azygous plants in both 30 and 40μM AsV. Conversely, Line 2 transgenic plants had more tillers than azygous plants in 10μM AsIII and 50μM AsV.

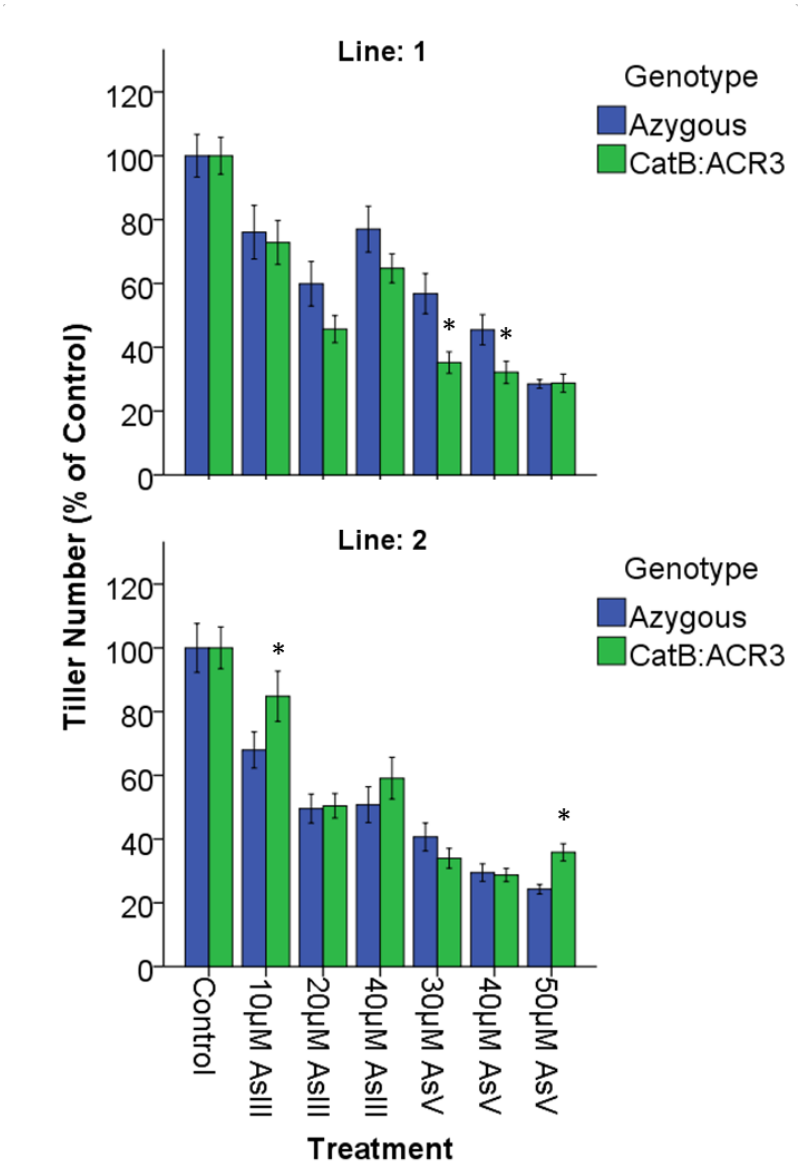

Figure 2.20 Tiller number
Graphs show the average tiller number of 15wo Line 1 and Line 2 plants expressed relative to the control conditions after 12 weeks growth in different concentrations of AsIII or AsV. Data are from four independent experiments, values are means ± SE and asterisks indicate significant differences between genotypes at $P<0.05$.

Plants were grown till maturity in As free medium and grain yields compared between genotypes (Figure 2.21). Plants exposed to 50μM AsV had a higher yield than those

exposed to 40µM AsV. This may be due to the relative developmental stage of the plants when returned to As free medium. Most plants had already reached the heading stage by 15wo, however those exposed to the higher concentrations of As tended to flower later and so grew for a longer period in As free medium before setting seed.

Line 1 *CatB:ACR3* expressing plants exposed to 40µM AsV had a significantly reduced grain yield compared to the azygous controls, while Line 2 *CatB:ACR3* expressing plants had increased grain yields compared to azygous plants after exposure to 50µM AsV. This pattern is consistent with the other growth parameters tested, and indicates that Line 1 *CatB:ACR3* expressing rice is more sensitive to arsenic while Line 2 *CatB:ACR3* expressing rice is more tolerant.

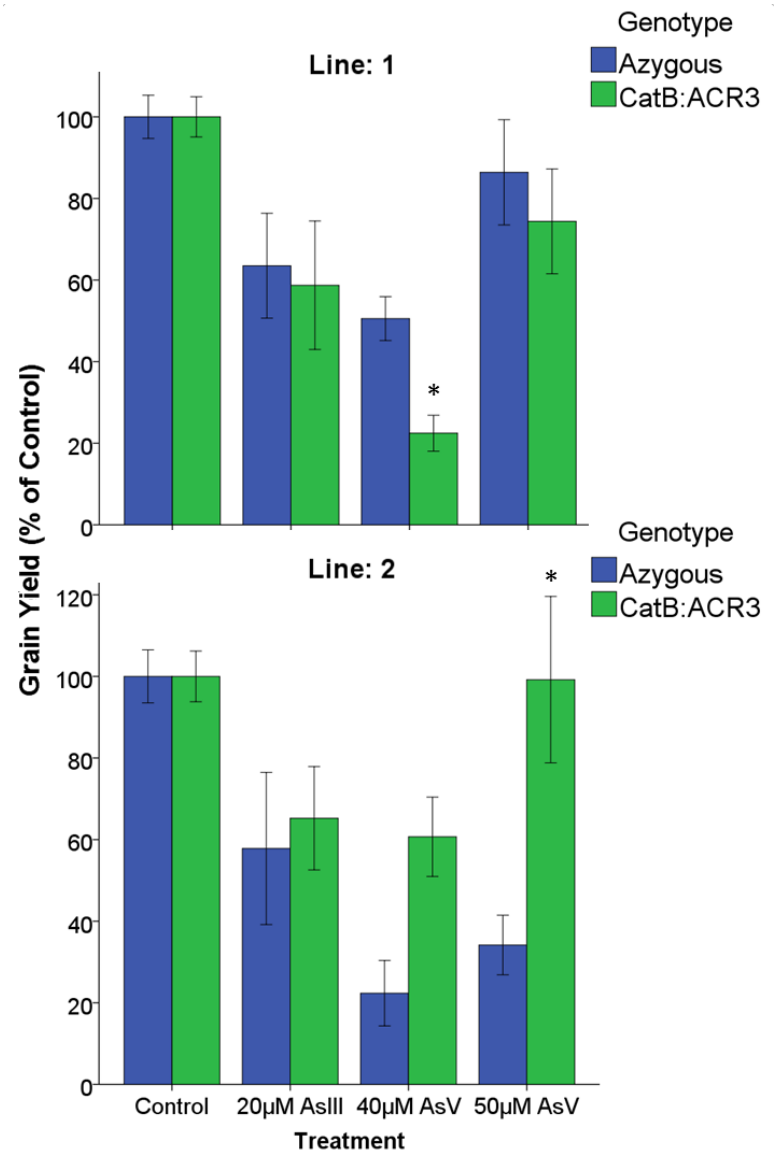

Figure 2.21 Grain yield
Graphs show the average grain yield of Line 1 and Line 2 plants after exposure to different concentrations of AsIII or AsV expressed as a percentage of yield in control conditions. Data are from four independent experiments, values are means ± SE and asterisks indicate significant differences between genotypes at $P<0.05$.

2.3.4 Arsenic Concentration of *CatB:ACR3* Expressing Rice

To investigate the effect of *CatB:ACR3* expression on As uptake, efflux and translocation within the plant, the total As concentration in different tissues of azygous and transgenic plants and the amount of As effluxed to the external medium was analysed and compared between transgenic and control lines.

2.3.4.1 Altered Arsenic Accumulation in *CatB:ACR3* Expressing Plants After Short Term Arsenic Exposure

The As concentration of root and shoot tissues of 7wo Line 1 plants was determined after four weeks in 40µM AsIII and 50µM AsV treatment (Figure 2.22). There were no differences in As concentration in the shoot, but transgenic plants had a lower concentration of As in the roots after 50µM AsV treatment. There were no significant differences in the total plant As accumulation or shoot:root partitioning of As between the azygous or *CatB:ACR3* expressing plants in either treatment.

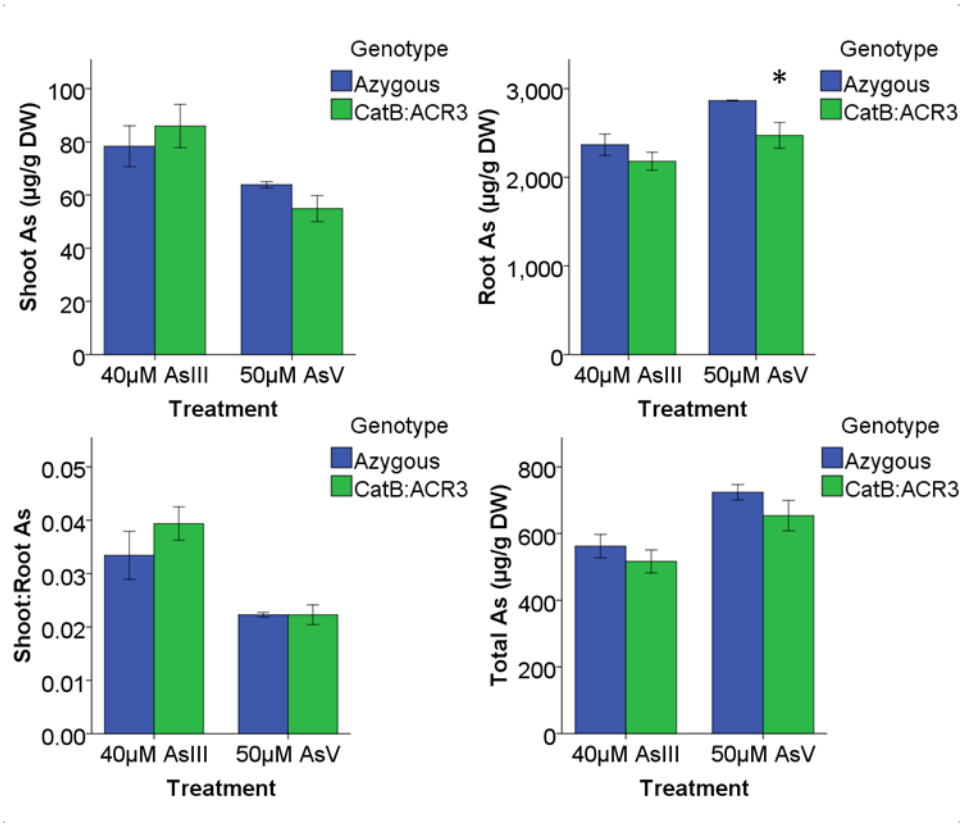

Figure 2.22 Arsenic concentration of 7wo Line 1 plants
Graphs show the total As concentration of 7wo Line 1 plants after four weeks exposure to 40µM AsIII or 50µM AsV. The top left and right panels show the average shoot and root As concentrations respectively. The bottom left panel shows the shoot:root As ratio and the bottom right panel shows the total plant As concentration. Data are from three independent experiments, values are means ±SEs and asterisks indicate significant differences between genotypes at $P<0.05$.

The results of the growth experiment suggest there may be a difference in how Line 2 *CatB:ACR3* plants respond to low and high concentrations of As. Line 2 transgenic plants were shorter and weighed less than azygous plants in 30μM AsV but were taller and weighed more in 50μM AsV (Figures 2.9 and 2.15). *CatB:ACR3* expression may affect As accumulation and translocation differently depending on the concentration of As exposure. To explore this further, the tissue As concentration of Line 2 plants was determined after 4 weeks exposure to 10 and 40μM AsIII and 30 and 50μM AsV (Figure 2.23).

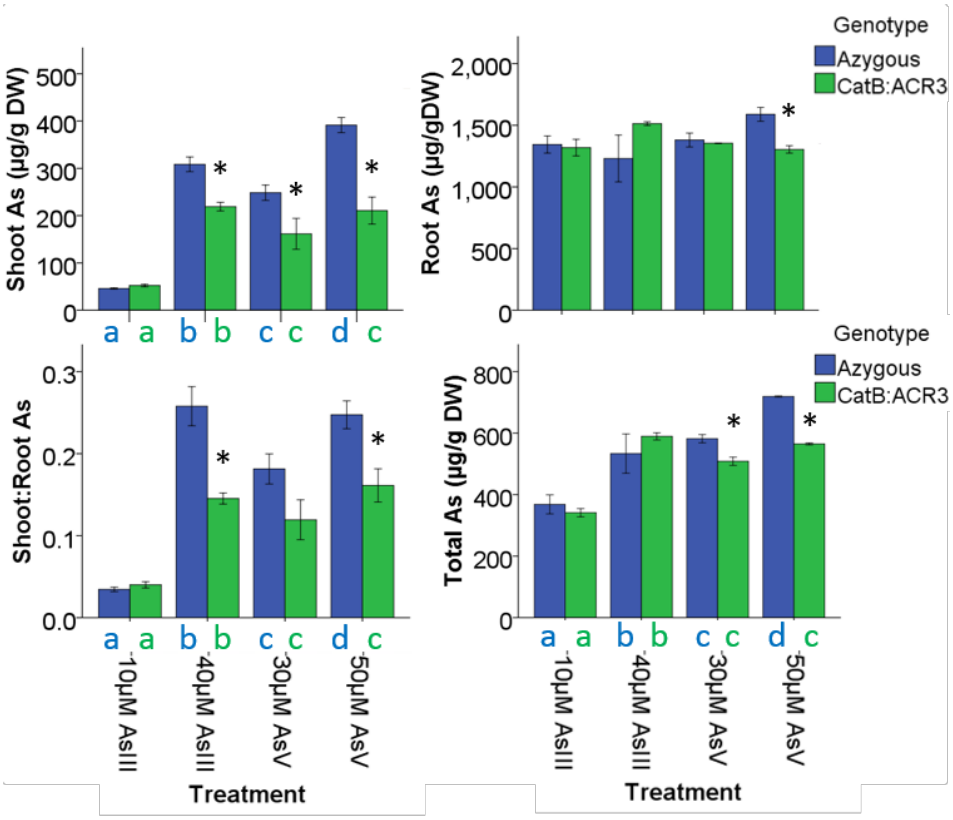

Figure 2.23 Arsenic concentration of 7wo Line 2 plants
Graphs show the total As concentration of 7wo Line 2 plants after four weeks exposure to different concentrations of AsIII or AsV. The top left and right panels show the average shoot and root As concentrations respectively. The bottom left panel shows the shoot:root As ratio and the bottom right panel shows the total plant As concentration. Data are from three independent experiments, values are means ±SEs asterisks indicate significant differences between genotypes and letters indicate significant differences between treatment at $P<0.05$.

Line 2 transgenic plants accumulated significantly less As in the shoot when exposed to 40μM AsIII and 30 and 50μM AsV. *CatB:ACR3* expressing plants also accumulated less As in the root tissues following exposure to 50μM AsV. In the higher As concentrations of 40μM AsIII and 50μM AsV, transgenic plants had significantly lower shoot:root As ratios than azygous plants. Transgenic plants had reduced total plant As concentrations after exposure to both 30 and 50μM AsV, although the difference

between transgenic and azygous plants was larger after treatment with the higher concentration of 50μM AsV.

Analysis of the main effect of treatment revealed that the concentration of As in the shoot increased with exposure to higher As concentrations, as did the shoot:root As ratio. However the concentration of As in root tissues was not different between the lower and higher As treatments. This suggests that upon exposure to higher concentrations of As, proportionally more As is translocated to the shoot. There was a significant interaction between genotype and treatment on shoot As, shoot:root As and total As concentration. Analysis of the simple main effects revealed that the shoot, total plant and shoot:root As concentration of azygous plants was significantly increased in plants exposed to the higher concentrations of both AsIII and AsV compared to the lower treatment. The same was true for *CatB:ACR3* expressing plants treated with AsIII however there was no significant difference between the shoot or shoot:root As concentrations of transgenic plants exposed to 30 or 50μM AsV.

Overall, Line 2 *CatB:ACR3* expressing plants appear to translocate less As to the shoots than non-transgenic plants. The difference between genotypes is most evident following treatment with higher concentrations of As, with *CatB:ACR3* plants grown in 50μM AsV accumulating less As in both root and shoot tissues suggesting a reduction in both the uptake and translocation of As compared to the azygous plants.

2.3.4.2 Altered Arsenic Accumulation in *CatB:ACR3* Expressing Plants After Long Term Arsenic Exposure

The root and shoot As concentration of 15wo Line 1 plants was analysed after 12 weeks of treatment with 40μM AsIII or 50μM AsV (Figure 2.24). There were no differences in As concentration between transgenic and azygous plants grown in 50μM AsV, however *CatB:ACR3* expressing plants had a significantly increased As concentration in the shoot after long term exposure to 40μM AsIII. Line 1 transgenic plants also had a significantly higher shoot:root ratio of As and a higher total plant As concentration than the azygous controls after long term exposure to 40μM AsIII.

The As concentration of 15wo Line 2 plants was analysed after 12 weeks of exposure to 10 and 40μM AsIII and 30 and 50μM AsV (Figure 2.25). The differences in As uptake and accumulation observed after short term treatment with the higher concentrations of 40μM AsIII and 50 μM AsV were no longer evident after long term exposure, in fact transgenic plants exposed to 40μM AsIII had a higher concentration of As in the shoot than the azygous controls. On the other hand, transgenic plants

exposed to 30µM AsV for 12 weeks had a significantly lower shoot As concentration as well as a reduced shoot:root As ratio compared to the non-*ACR3* expressing plants.

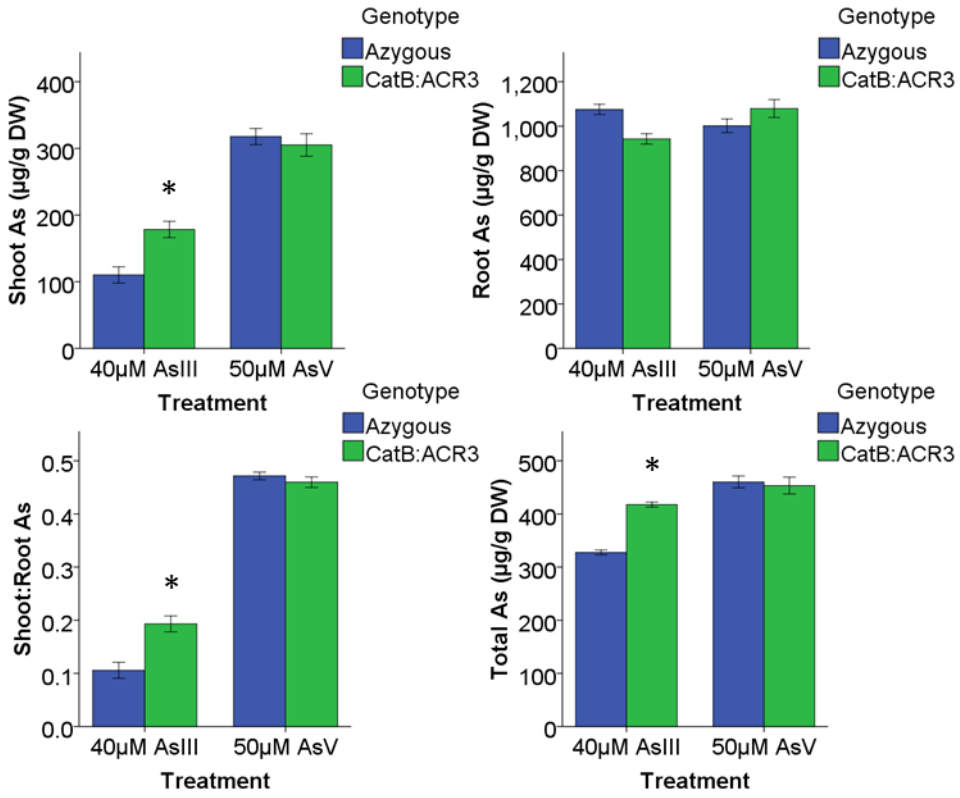

Figure 2.24 Arsenic concentration of 15wo Line 1 plants
Graphs show the total As contcentration of 15wo Line 1 plants after twelve weeks exposure to 40µM AsIII or 50µM AsV. The top left and right panels show the average shoot and root As concentrations respectively. The bottom left panel shows the shoot:root As ratio and the bottom right panel shows the total plant As concentration. Data are from three independent experiments, values are means ±SEs and asterisks indicate significant differences between genotypes at $P<0.05$.

Similar to what was seen after short term As exposure, long term exposure to the higher concentrations of AsIII and AsV resulted in increased shoot As concentrations and higher shoot:root As ratios compared to plants exposed to the lower As concentrations. However, the difference observed between azygous and transgenic plants in response to short term AsV treatment was no longer present after long term exposure, as both *CatB:ACR3* expressing and non-transgenic plants had increased shoot As concentrations (and shoot:root As ratios) after treatment with 50µM AsV compared to 30µM AsV.

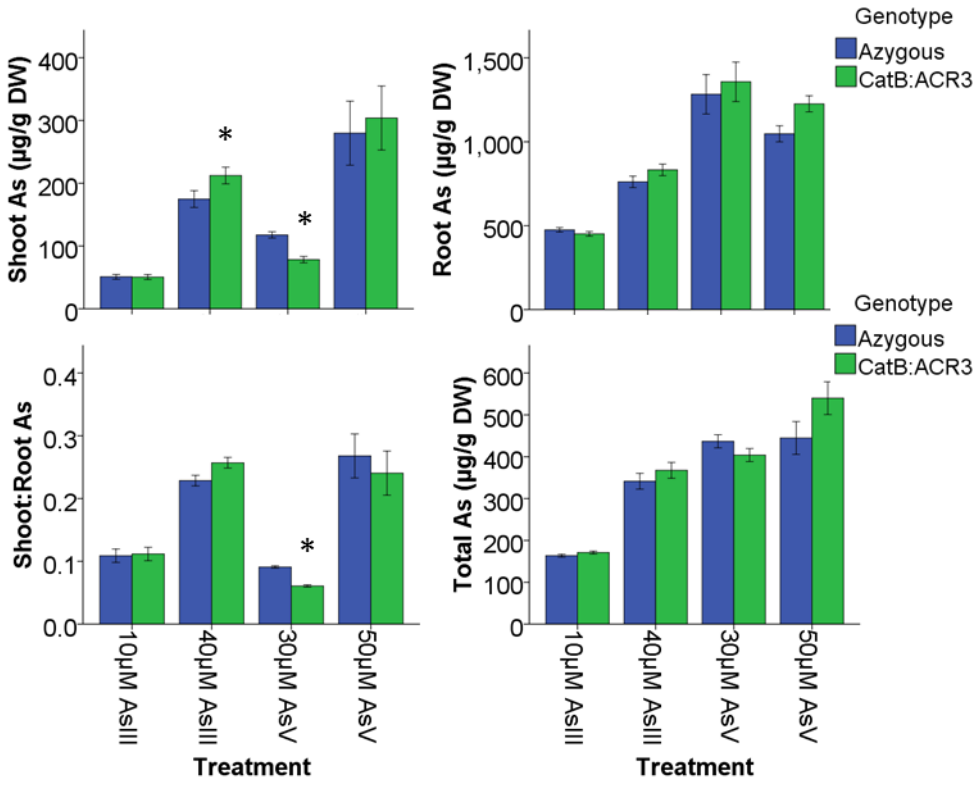

Figure 2.25 Arsenic concentration of 15wo Line 2 plants

Graphs show the total As concentration of 15wo Line 2 plants after twelve weeks exposure to different concentrations of AsIII or AsV. The top left and right panels show the average shoot and root As concentrations respectively. The bottom left panel shows the shoot:root As ratio and the bottom right panel shows the total plant As concentration. Data are from three independent experiments, values are means ±SEs and asterisks indicate significant differences between genotypes at $P<0.05$.

Root and total plant As concentrations were also higher in both *CatB:ACR3* expressing and azygous plants exposed to 40µM AsIII compared to 10µM AsIII, but not in plants exposed to 50µM AsV compared with 30µM AsV. Exposure to higher As concentrations led to increased translocation of As to the shoot, consistent with what was observed after short term As exposure (Section 2.3.4.1). In the case of AsIII treatment, long term exposure to the higher concentration also resulted in increased root and total plant As concentrations.

2.3.4.3 *CatB:ACR3* Expression Does Not Significantly Affect Grain Arsenic Levels

Line 1 and 2 *CatB:ACR3* expressing and azygous plants exposed to 20µM AsIII and 40µM AsV for 12 weeks in hydroponics were transferred to As free medium and grown to maturity. Rice grain was collected, dehusked and analysed for As concentration (Figure 2.26). There were no differences in grain As concentration between *CatB:ACR3* expressing and azygous plants in either treatment for Line 1 or Line 2.

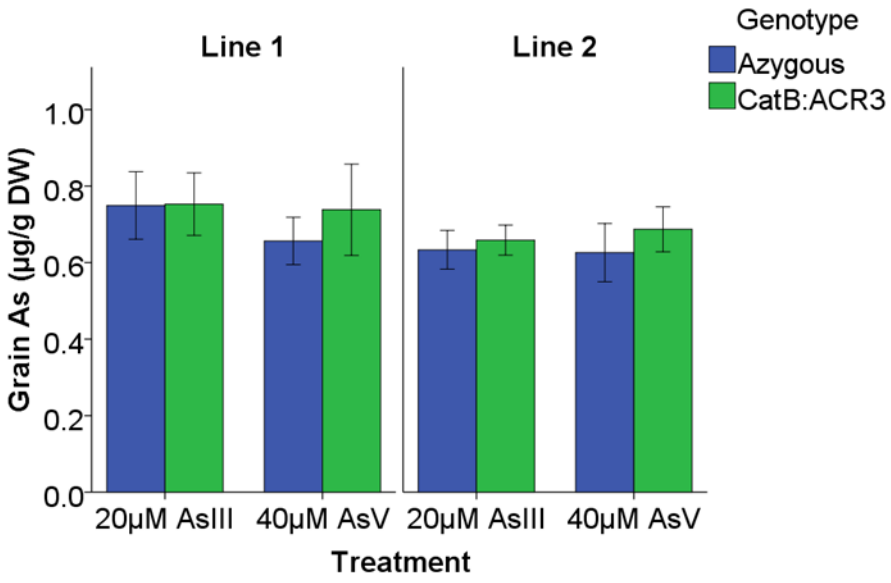

Figure 2.26 Grain As concentration
The graph shows the As concentration of Line 1 and Line 2 grain after twelve weeks exposure to 20µM AsIII or 40µM AsV. Data are from three independent experiments and values are means ±SEs.

2.3.4.4 Xylem As

The observed differences in shoot:root As between *CatB:ACR3* expressing and azygous rice may have been caused by alterations in loading of As into the xylem. To investigate this, the As concentration of xylem sap was collected from 3wo plants after exposure to 50µM AsV for three days. Sap from 5 individuals of each genotype was collected and bulked together to ensure detection of As using ICP-OES (Table 2.4). The As concentration of xylem sap in Line 1 *CatB:ACR3* plants was ~70% lower than the azygous controls while Line 2 *CatB:ACR3* expressing plants had a slightly higher concentration of As in the xylem.

Table 2.4: Xylem As concentration of 3wo plants after 3 days exposure to 50*µ*M AsV

Line	Genotype	Xylem As (*µ*g/ml)
1	Azygous	3.94
	CatB:ACR3	1.21
2	Azygous	2.96
	CatB:ACR3	3.42

The rate of water loss was measured alongside the xylem As concentration enabling calculation of the root to shoot flux of As through the xylem (Figure 2.27). The flux of As through the xylem of *CatB:ACR3* expressing Line 1 plants was significantly lower than

the azygous plants, while the flux through Line 2 *CatB:ACR3* expressing plants was not different than Line 2 azygous plants.

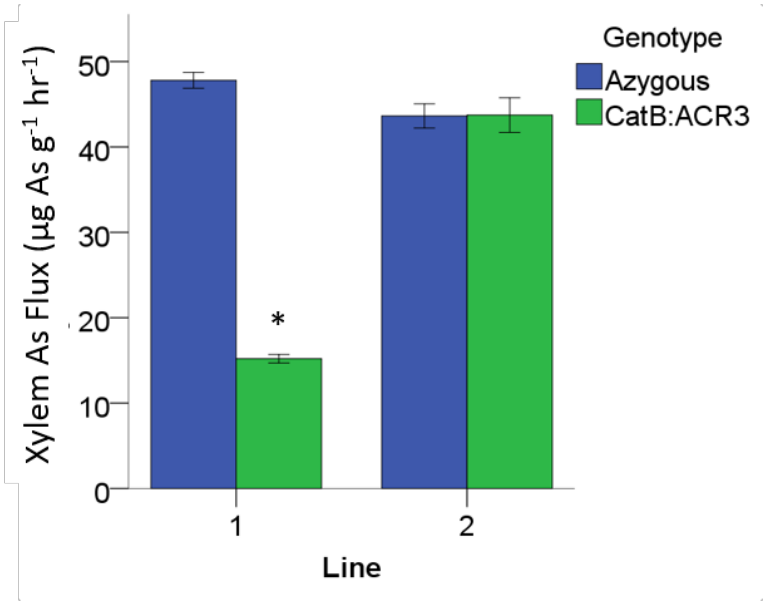

Figure 2.27 Xylem As flux
The graph shows the flux of As through the xylem of Line 1 and Line 2 transgenic and azygous plants. Flux is calculated as the rate of transpiration (water lost per gram of plant fresh weight per hour) multiplied by the concentration of As in the xylem sap. The values are means ±SEs of five individual plants of each genotype and the asterisk indicates a significant difference at $P<0.05$.

2.3.4.5 Efflux

The effect of *CatB:ACR3* expression on As efflux from the roots was investigated. Three week old seedlings were preloaded with 250µM AsV for 24hours in hydroponics. They were rinsed with dH_2O and returned to As free medium. The As concentration of the root, shoot and medium was analysed after 1, 3, 6 and 24 hours. Efflux from the roots was calculated as µg of As present in the medium relative to the As concentration in the plant (Figure 2.28).

There were no significant differences in the amount of As effluxed from the roots of Line 1 azygous and *CatB:ACR3* expressing plants as determined by two-way ANOVA. After one hour in As free medium, Line 2 *CatB:ACR3* expressing plants had effluxed significantly more As into the medium than the azygous controls. At the later time points tested, the difference between genotypes was no longer significant.

The amount of As effluxed from the roots into the medium initially increased over time and then decreased after 6 hours. This could be due to recycling of effluxed As back into the roots from the medium.

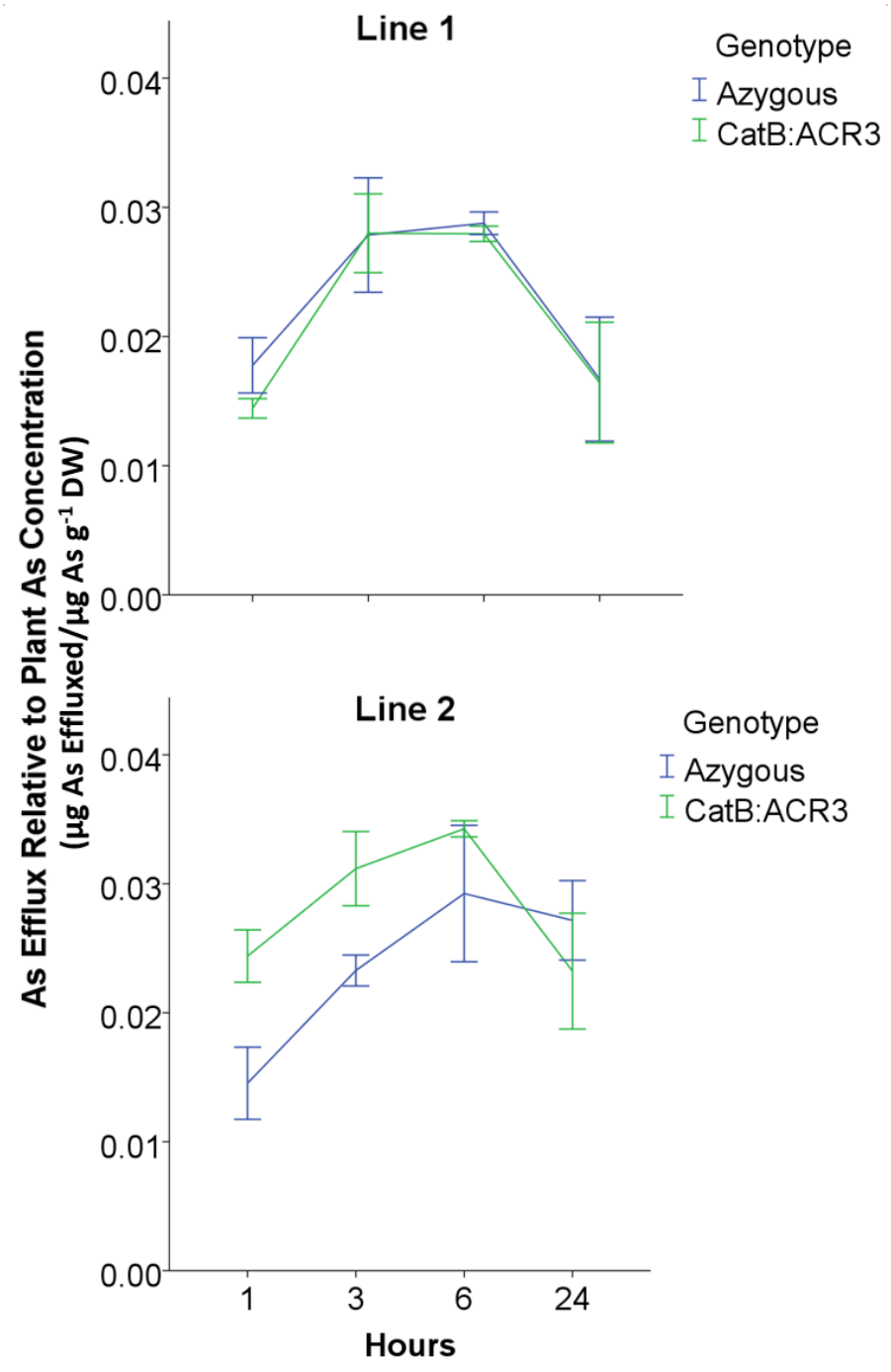

Figure 2.28 Arsenic effluxed from the roots of Line 1 and Line 2 plants
Graphs show the amount of As effluxed from the roots of 3wo Line 1 and Line 2 plants relative to the plant As concentration (µg As Effluxed/µg As g^{-1} DW plant). Plants were preloaded with As by exposure to 250µM AsV in hydroponics for 24hrs. Plants were rinsed and placed in As free medium, efflux was measured 1, 3, 6 and 24 hours after transfer. Data are from three independent experiments and values are means ±SEs.

To investigate differences in As loading between genotypes, the total plant As concentration and the shoot:root As ratio of *CatB:ACR3* and azygous plants used in the efflux experiment is shown in Figure 2.29. Transgenic plants exposed to 250µM AsV for 24 hours had reduced total As concentrations compared to the non-transgenic control plants and also had a reduced shoot:root As ratio, suggesting that after short

term exposure to As, *CatB:ACR3* expressing plants accumulate less As and translocate proportionally less As to the shoot.

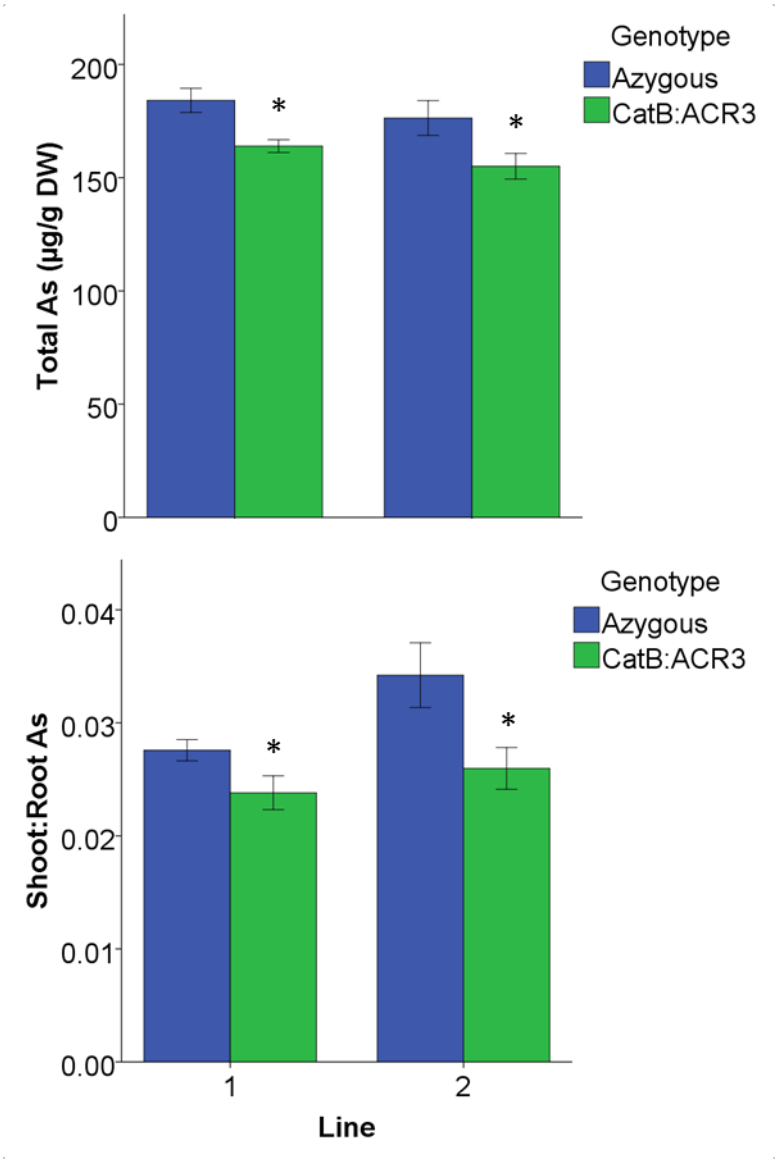

Figure 2.29 Arsenic loading of plants used in the efflux experiment
Graphs show the total As concentration (top graph) and shoot to root translocation (bottom graph) of As in 3wo Line 1 and Line 2 plants after 24 hours exposure to 250µM AsV. Data are from three independent experiments, values are means ±SEs and asterisks indicate significant differences between genotypes at $P<0.05$.

2.4 Discussion

Arsenic contamination of rice grain is a major problem worldwide, contributing to chronic As poisoning and posing a serious health risk to millions of people. In addition, the phytotoxic effects of As on rice growth impact on yield. Therefore, it is imperative that potential strategies to improve rice tolerance to As and reduce As accumulation in the grain are fully explored. In the current investigation, the yeast low affinity $AsIII/H^+$

efflux transporter *ScACR3* was heterologously expressed in rice under the control of tissue specific promoters to try and achieve those particular aims.

2.4.1 Expression of *Lsi1S:ACR3*

RT-PCR of *Lsi1S:ACR3* expressing plants revealed that the 226bp promoter was insufficient to drive root specific expression of *ACR3* as transcript was detected at similar levels in root, stem and leaf tissues. The full length *Lsi1* promoter was re-cloned and the vector pGreen-Lsi1F:ACR3 generated, however no *Lsi1F:ACR3* expressing rice plants were generated within the timeframe of this project. It would be interesting to explore the effect of strong root specific *ACR3* expression driven by the *Lsi1* promoter in rice, particularly since *CatB:ACR3* expression in Line 2 plants led to increased tolerance and reduced shoot:root translocation of As despite a relatively low level of expression in the root (compared to *CatalaseB* and *Actin*).

Ideally ACR3 would be engineered to have the same polar localisation pattern as Lsi1, however the mechanisms by which transporters such as Lsi1 show polar localisation are poorly understood [152-154]. It is likely that in *Lsi1:ACR3* expressing plants, ACR3 would be localised in a non-polar fashion and so contribute to AsIII flux in both directions from the endo- and exodermal cells. It is possible that proximity of ACR3 to Lsi1 (the site of AsIII influx) may lead to preferential efflux of AsIII through ACR3 on the distal side of the cell towards the external medium. This would be an interesting hypothesis for future investigations.

2.4.2 *ScACR3p* Expression Under the Control of the *OsCatB* Promoter

The *CatB* promoter fragment that was used to drive expression of *ACR3* in the transgenic rice lines described here (-221 to +115bp) encompasses the minimal core promoter identified by Mondal P. *et al.* [139] that was shown to drive strong expression in protoplasts. However, in roots, *ACR3* is not strongly expressed compared to the endogenous *CatB* in Line 2 plants. This suggests that although the minimal core promoter is sufficient to drive strong expression in protoplasts, it is not sufficient to drive strong expression in intact plants.

Previously, Iwamoto, M. *et al.* [134] stably transformed rice with the GUS reporter gene under the control of *CatB* promoter fragments similar in length to the fragment used in this study, namely *CatBΔ9:GUS* (-329 to +298bp) and *CatBΔ10:GUS* (-226 to +298bp). T_0 rice plants transformed with *CatBΔ9:GUS* showed strong root specific GUS expression in 13 out of 27 independently transformed lines, whereas only 3 out of 16

lines transformed with *CatBΔ10:GUS* showed preferential expression in the roots. The remaining 13 *CatBΔ10:GUS* expressing lines either showed no GUS activity or expression only in the leaf sheath and blade (3 and 9 plants respectively). The level of GUS staining in the roots of *CatBΔ10:GUS* plants was less intense than seen in the *CatBΔ9:GUS* plants [134]. Although Iwamoto, M. *et al*. [134] carried out RT-PCR on the transgenic lines, no comparison was made between the heterologous and endogenous *CatB* promoters so it is difficult to relate the levels of transgene expression in *CatBΔ9:GUS* and *CatBΔ10:GUS* expressing rice to those observed in this study for *CatB:ACR3* expressing rice. The tissue specificity of GUS expression in *CatBΔ9:GUS* and *CatBΔ10:GUS* plants (~50 and 20% root specific respectively) is consistent with what was observed for *CatB:ACR3* lines, with Line 2 showing root specific expression while in Line 1 *ACR3* is expressed mostly in the leaf blades and the stem. While it would be preferable to have more than one independently transformed line with the same tissue specific expression of *ACR3,* the different expression patterns observed in Line 1 and Line 2 present an interesting opportunity to compare the effects of *ACR3* expression in different tissues on As tolerance and accumulation.

Previous work [135, 136] showed that *OsCatB* expression is upregulated after short term (8-72 hours) salt and water stress treatment and is induced by the stress hormone ABA, suggesting that *CatB* induction is associated with oxidative stress and so could be upregulated in response to As treatment. Microarray gene expression studies have analysed the effect of As treatment on the rice genome and in these experiments *CatB* was not found to be differentially regulated by different AsIII and AsV treatments [110, 155, 156]. In the present study, the effect of long term (4 weeks) treatment with AsIII and AsV on *CatB* and *CatB:ACR3* expression was examined using semi-quantitative RT-PCR. The relative expression levels of *CatB* were comparable suggesting that *CatB* expression is not regulated by As. *CatB:ACR3* expression appeared to be slightly reduced in plants exposed to As, suggesting that the -221 to +115bp fragment of the *CatB* promoter used to drive expression of *ACR3* responds differently to As treatment than the full length endogenous promoter.

2.4.3 Arsenic Tolerance of *CatB:ACR3* Expressing Rice

In this chapter, the growth rate of azygous control and *CatB:ACR3* expressing rice plants was measured over a 12 week period of exposure to different concentrations of AsIII and AsV. The growth rate of all plants was fastest during the first four weeks of treatment, when plants were 3-7wo (Figures 2.10 & 2.17). During this period, exposure to AsIII and AsV significantly reduced the growth rate of transgenic and azygous control plants to a similar degree (Figures 2.11 & 2.18).

Differences in growth rate between transgenic and control plants were not observed until the following 8 weeks of treatment, when plants were 7-15wo. During this period, plants exposed to AsIII and AsV actually grew faster than plants in the As free control medium (Figures 2.12 & 2.19), suggesting that they are able to recover somewhat from the initial reduction in RGR caused by As induced phytotoxicity over long term exposure to As. In the lowest concentrations of AsIII and AsV tested, the increase in RGR during this recovery period was enough to compensate for the initial reduction in RGR; the final height and fresh weight of these plants was not different from plants grown in control conditions by the end of the experiment (Figures 2.8-9 & 2.14-15). The ability of rice plants to respond by altering their growth rate during this "recovery period" was affected by the expression of *CatB:ACR3*. Line 1 *CatB:ACR3* plants were more sensitive to As treatment and grew more slowly than the azygous controls during this period, while Line 2 *CatB:ACR3* expressing plants were less sensitive to As treatment and grew faster than the azygous control plants. This is also reflected in the tiller number and grain yield of plants exposed to As; Line 1 transgenic plants had fewer tillers and reduced yield while Line 2 transgenic plants had more tillers and increased yield compared to the non-transgenic controls. These result suggest that altering the AsIII efflux pathways in rice through heterologous expression of *ACR3* in different tissues can differentially affect As tolerance. In this study, two rice lines with different expression patterns of *ACR3* showed opposite responses to As treatment in terms of growth and grain yield, presumably caused by differences in As uptake, efflux and tissue distribution over long term As exposure.

2.4.4 Accumulation of Arsenic in *CatB:ACR3* Expressing Rice

One of the aims of this study was to target *ACR3* expression to the roots to enhance AsIII efflux to the external medium and reduce accumulation of As in the shoot. No difference in As efflux was observed from Line 1 *CatB:ACR3* expressing plants relative to the controls, however Line 2 transgenic plants effluxed significantly more As from the roots to the external medium after one hour (Figure 2.28). The total plant As concentration and shoot:root As was reduced in both Line 1 and Line 2 transgenic plants suggesting that during short term (24 hours) exposure, *CatB:ACR3* expressing plants accumulate less As and translocate proportionally less As to the shoot. Increased efflux of AsIII from the roots may result in reduced net As uptake in the transgenic lines.

An experiment investigating AsIII efflux from rice roots carried out by Zhao, F-J. *et al.* [103] revealed that up to 88% of AsV taken up was exuded from the roots as AsIII during the 24 hour period of exposure. When transferred to As free medium following

exposure, the amount of AsIII effluxed relative to AsV taken up was lower, falling to around 15% [103]. This may explain why reduced As uptake was observed in Line 1 transgenic plants without increased efflux; it may be that an increase in AsIII efflux from the roots of Line 1 transgenic plants would only be observed during the period of AsV exposure. The impact of *ACR3* expression on AsIII efflux from Line 2 transgenic plants is expected to be greater than in Line 1 due to the higher level of *ACR3* expression in the roots of Line 2 plants. This may explain why an increase in AsIII efflux from Line 2, but not Line 1 plants, was observed after transfer to As free medium. Future investigations into AsIII efflux from *ACR3* expressing rice would be improved by using As speciation analysis. This would enable AsIII efflux to be measured during exposure to AsV. It may also provide insight into the amount of AsIII recycled back into the roots, which may help explain the decrease observed in net As efflux after 24 hours (relative to 6 hours) in As free medium.

CatB:ACR3 expression altered the As uptake and tissue distribution patterns in Line 1 and Line 2 rice. After short term exposure to As, Line 1 *CatB:ACR3* expressing plants had accumulated less total As and had a reduced flux of As through the xylem resulting in a reduced shoot:root As compared to the azygous control plants (Figures 2.27 & 2.29). However, after long term exposure to As, Line 1 *CatB:ACR3* expressing plants had taken up more As in total and had translocated a higher proportion of As to the shoot compared to the azygous control plants (Figure 2.24). The increased uptake and root to shoot translocation of As in Line 1 transgenic plants explains the reduced tolerance of these plants to prolonged As exposure, the higher levels of As accumulation would result in increased phytotoxicity and so reduced growth rates.

It is surprising that Line 1 *CatB:ACR3* expressing plants had a higher root to shoot translocation of As after long term exposure when the As flux measured through the xylem was reduced compared to the azygous controls. It is possible that expression of *ACR3* in the stem tissues reduced As loading of the xylem by effluxing AsIII away from the stele. Expression of *ACR3* in the leaf tissue may increase unloading of As from the vasculature and so enhance As accumulation in the shoot. It would be interesting to compare the As concentration in the phloem of Line 1 transgenic and azygous plants, if *CatB:ACR3* expressing plants also have reduced flux of As through the phloem this may help explain the increase in shoot As accumulation over time. It is also possible that the As flux through the xylem changes over time, therefore it would be interesting to also determine the As concentration of xylem sap after long term As exposure.

In contrast to Line 1, Line 2 *CatB:ACR3* expressing plants had a reduced total As concentration and reduced shoot:root As after both short and long term exposure to As

(Figures 2.23, 2.25 & 2.29). Line 2 *CatB;ACR3* plants effluxed more As to the external medium than the azygous control plants (Figure 2.28) and there was no change in flux of As through the xylem after short term As exposure (Figure 2.26). This suggests that root specific expression of *ACR3* leads to increased AsIII efflux to the external medium without increasing efflux towards the stele for translocation to the shoot, resulting in reduced As uptake and translocation after long term As exposure. Lower As concentrations in the shoot and root tissues would limit the phytotoxic effects of As treatment on the transgenic plants, enabling them to grow faster than the azygous controls.

2.4.5 Accumulation of Arsenic in the Grain of *CatB:ACR3* Expressing Rice

By the end of the growth experiment, the majority of plants had reached the heading stage and were transferred to As free medium till maturity. Therefore the As present in the rice grain of these plants is probably due to reallocation of As from the shoot tissues during grain filling, as no further As was taken up from the medium. In a similar experiment carried out by Zheng, M-Z. *et al.* [157] rice plants grown in hydroponics and treated with 5μM AsV from seedling to the heading stage accumulated significantly less As in the grain compared to plants treated with As from heading to maturity. In addition, there was no significant difference between the grain As concentrations of rice plants exposed to As from heading to maturity and those exposed from seedling to maturity [157]. In plants exposed to As until heading, As was found to be redistributed from the root to the shoot in the period from heading to maturity. The concentration of As decreased in the root tissue and increased in the leaves, husk and to a lesser extent grain [157]. This suggests that As uptake during flowering is the most important growth stage in determining grain As concentration and that only a limited amount of As remobilisation occurs.

Expression of *CatB:ACR3* did not result in altered grain As levels in either Line 1 or Line 2 plants under the conditions tested here. In Line 1 plants *CatB:ACR3* expression in leaf and stem tissues increased the root to shoot translocation of As after long term treatment and led to increased shoot and total plant As concentrations but did not lead to an increase in grain As concentration. This suggests that *ACR3* expression may actually reduce the amount of As remobilised towards the panicle after flowering in these plants, as the shoot:grain As will be reduced in the transgenic compared to azygous plants.

When *ACR3* was expressed in rice under the control of the CaMV 35S promoter by Duan, G. *et al.* [128], treatment with 40μM AsIII from flowering to grain maturation

resulted in reduced grain As concentrations. Reduced grain As was also observed in *35S:ACR3* expressing rice by Waqar Ali (a previous PhD student in the Maathuis lab [133]) after treatment of 3wo plants with 10µM AsIII for four weeks before transfer to As free medium. The relatively high expression levels of *ACR3* in both studies may account for the reduced As grain concentration seen in *35S:ACR3* expressing plants which was not observed in *CatB:ACR3* expressing plants. The expression level of *ACR3* in this study was much lower than the level of expression of the endogenous *CatalaseB* gene (Figure 2.6) while CaMV 35S is regarded as a strong promoter. Perhaps increasing the level of *ACR3* expression in the transgenic rice plants used in this study would increase capacity for AsIII efflux and result in a reduced grain As concentration. Future investigations into the role of *ACR3* expression in different tissues would benefit from an elongated period of As treatment to determine the effect of *ACR3* on grain As concentration when treated till maturity.

2.5 Conclusions

Expression of *ACR3* in different rice tissues led to altered As tolerance and distribution after exposure to both AsIII and AsV. The main effects of *ACR3* expression were seen after long term rather than short term As exposure. Differences in As tolerance and distribution changed over time, which highlights the importance of carrying out long-term experiments when investigating strategies to improve crop plants.

Rice plants expressing *ACR3* most strongly in the stem and leaves had reduced tolerance to As and increased translocation to the shoot, whereas rice plants expressing *ACR3* most strongly in the roots were more tolerant to As and translocated less As to the shoot. These results provide support for the idea that tissue specific expression of As efflux transporters could be utilised to manipulate As accumulation and tolerance in rice plants, and warrants the future exploration of *ACR3* expression using different tissue and developmental stage specific promoters.

Chapter 3: Investigating the Role of NIPs in Arsenic Transport, Tolerance and Accumulation in *Arabidopsis*

3.1 Introduction

Aquaporins, or major intrinsic proteins (MIPs), were originally identified as water specific channels integral to the membrane, but have since been recognised as multifunctional transporters of water, glycerol and small uncharged solutes (such as urea, formamide and lactic acid) and metalloids (such as silicon, boron, and arsenic) [53, 54, 58]. Aquaporins in plants are highly diverse, with 33 isoforms found in rice and 35 in *Arabidopsis thaliana* [158, 159]. Plant aquaporins can be broadly separated into four subgroups based on sequence homology - plasma membrane intrinsic proteins (PIPs), tonoplast intrinsic proteins (TIPs), nodulin-26-like intrinsic proteins (NIPs) and the small and basic intrinsic proteins (SIPs).

The structural topology of aquaporins is conserved, with each functional unit arranged as a tetramer. Monomers consist of two tandem repeats of three transmembrane domains (TMD1-6) connected by five loops (A-E) with the amino- and carboxy- termini located in the cytoplasm (Figure 3.1) [160]. Loops B and E contain highly conserved Asn-Pro-Ala (NPA) motifs. The two loops dip into the membrane from opposite sides, where the NPA motifs interact to form part of the central core restriction. This is often referred to as the “hourglass” fold [161]. The main selectivity filter of aquaporins is a narrowing of the pore at the aromatic/arginine (Ar/R) constriction site located around 8 Å from the NPA motif towards the extracellular mouth of the pore [162]. The Ar/R domain is made up of two residues from loop E and one each from TMD2 and TMD5. The composition of the Ar/R domain determines the size and hydrophobicity of the pore, greatly influencing the substrate selectivity and function of aquaporins. The archetypal aquaporin has a constriction pore size of 3 Å [163], just wider than a water molecule (2.8 Å), however, several plant aquaporins (including NIPs) have wider constriction pores enabling transport of molecules larger than water.

Members of the NIP subfamily can be further divided into groups I, II and III based on the composition of their Ar/R domain. There are nine NIPs in *Arabidopsis*, of which six fall into group I and three into group II (Figure 3.2). The Ar/R domain of group I NIPs consists of a tryptophan in the TMD2 position, an isoleucine or valine in the TMD5 position, and alanine and arginine residues in loop E. Group II NIPs are predicted to have a wider pore aperture than group I NIPs, with an alanine replacing the tryptophan of group I NIPs in the TMD2 position [164]. This wider pore enables permeation of larger solutes such as urea, silicic acid, boric acid and arsenous acid but results in very low permeability for water.

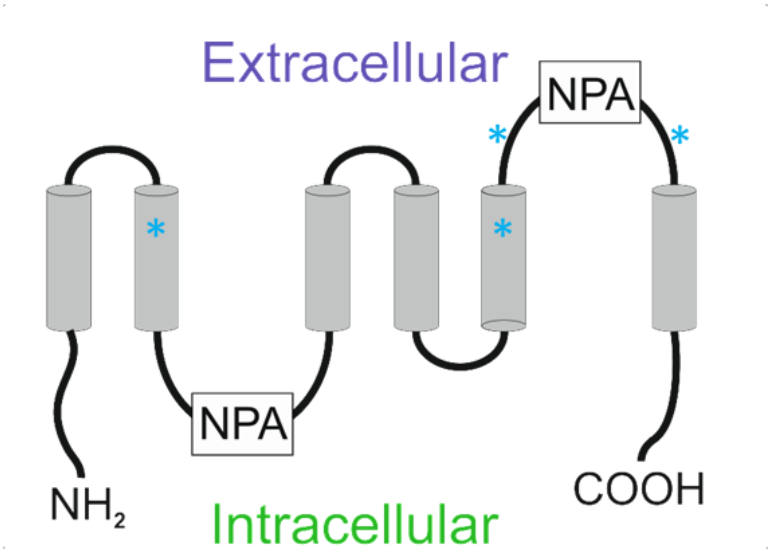

Figure 3.1: Predicted topology of aquaporin monomers
Structural topology of an aquaporin monomer showing six transmembrane domains and five interconnecting loops. The positions of the highly conserved NPA motifs are labelled in loop B and loop E. Blue asterisks denote the approximate location of the four residues which make up the Ar/R pore restriction site.

The activity of some NIPs has been shown to be regulated by phosphorylation of residues within the cytosolic regions. The archetypal NIP GmNOD26 is phosphorylated at Ser-246 in the cytosolic C terminal domain by a calcium dependent protein kinase (CDPK) [165] leading to enhanced water permeability in response to developmental cues and osmotic stress [166]. In *Arabidopsis*, NIP4;1 and NIP4;2 are phosphorylated at Ser-267 in the cytosolic C terminal domain by a pollen specific CDPK *in vitro* [167] while NIP7;1 can be phosphorylated at the C terminus by the mitogen activated protein kinase AtMPK4 in vitro [168]. NIP7;1 activity may also be regulated through gating of the pore; homology modelling revealed that the side chain containing Tyr81 can adopt one of two rotameric states. Tyr81 is located in the second transmembrane helix and faces the pore on the extracellular side of the Ar/R region. In the 'up' state, the Tyr81 containing side chain lies parallel to the pore while in the 'down' configuration the side chain lies across the pore. The 'down' state is predicted to be stabilised by hydrogen bonding with the Arg220 containing side chain, resulting in an occluded pore with a diameter less than 1 Å [169]. However, it is not known how the potential gating of NIP7;1 relates to its physiological role, nor how it is regulated *in planta*.

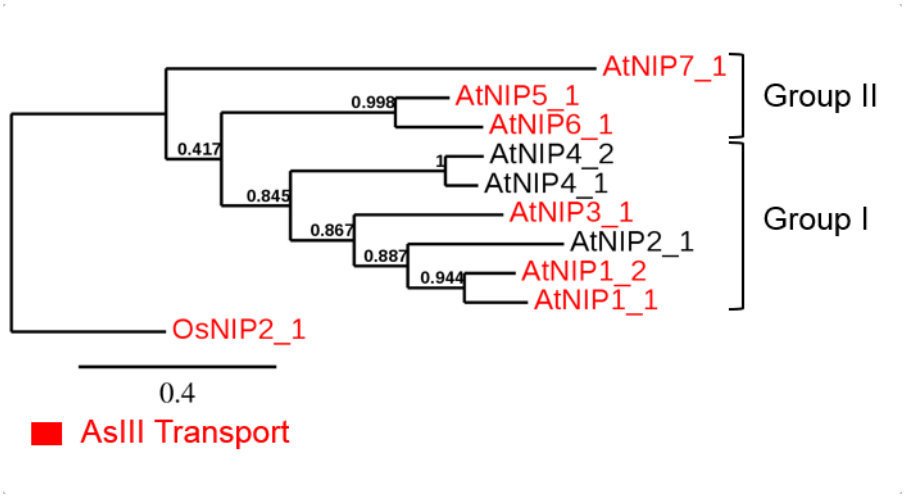

Figure 3.2: Phylogeny of *Arabidopsis* NIPs
Phylogenetic tree of *Arabidopsis* NIP family members constructed from amino acid sequences using the 'One Click' phylogeny analysis on the Phylogeny.fr website [170]. Red text denotes NIPs that have been shown to have AsIII transport capability. The tree is rooted to the rice NIP2;1 protein. Branch lengths are proportional to the number of substitutions per site and branch annotations are Confidence Indexes analogous to bootstrap values.

The physiological role of several plant NIPs has been determined, revealing a wide range of substrate specificities and functions. GmNOD26, after which the NIP subfamily is named, facilitates diffusion of ammonia across the symbiosome of soybean nodules [171]. The rice NIPs OsNIP2;1/Lsi1 and OsNIP2;2/Lsi6 are essential for the uptake and distribution of silicon [53, 63] and a NIP isoform in *Hydrangea* (HmPALT1) is involved in aluminium transport [172]. In *Arabidopsis*, NIP2;1 is a lactic acid transporter induced under anaerobic conditions [173] while NIP5;1, NIP6;1 and NIP7;1 are involved in the transport of boric acid [54, 169, 174]. NIP4;1 and NIP4;2 have recently been implicated in pollen development, pollination and fertilisation in *Arabidopsis*. While their precise physiological role in these processes is still unclear, heterologous expression in yeast and *Xenopus laevis* oocytes revealed permeability to water, glycerol, hydrogen peroxide, urea, boric acid and ammonia; suggesting possible roles in osmoregulation and/or boron (B) uptake during pollen tube growth [167].

Compared to other major intrinsic proteins, NIPs tend to be expressed at a relatively low level and several have been found to display cell, tissue and developmental stage specific expression patterns [175]. Among the Group II NIPs in *Arabidopsis*, *NIP5;1* is expressed predominantly in the root where it localises to the distal side of the plasma membrane in epidermal cells and is important for efficient B uptake [54, 154]. *NIP6;1* is expressed in the nodes, the base of the flower and in the petioles where it localises to the phloem. It has been proposed that *NIP6;1* is involved in source to sink redistribution of B via xylem to phloem transfer at the nodal regions [174]. *NIP7;1* is most highly expressed in developing anthers, where it is suggested to have a role in the delivery of

B to developing pollen, but is also present in many other tissues in both roots and shoots (Figure 3.3) [141, 169].

Several NIPs have been implicated in the transport of arsenite. In rice, OsNIP2;1/Lsi1 is the major route of AsIII uptake into the roots [56] while OsNIP1;1, OsNIP2;2, OsNIP3;1, OsNIP3;2 and OsNIP3;3 have been shown to have AsIII transport capability in heterologous expression systems (yeast and/or *X. laevis* oocytes) [56, 57, 61]. In *Arabidopsis*, T-DNA knockout insertions in NIP1;1, NIP1;2, NIP3;1, NIP5;1, and NIP7;1 resulted in reduced total plant As levels, and *nip1;1, nip3;1* and *nip7;1* plants were more tolerant to AsIII [58-60]. While a reduced total plant As level in NIP mutants suggests a possible role of these NIPs in As uptake, it does not rule out additional functions in translocation, distribution and compartmentalisation of As throughout the plant. To date, only NIP3;1 has been associated with root to shoot translocation of As, with shoot tissue of *nip3;1* plants accumulating significantly less As after exposure to AsIII than WT [59].

Several NIPs, including *NIP5;1, NIP6;1* and *NIP7;1* from *Arabidopsis*, confer increased resistance to AsV on yeast strains deficient in AsIII efflux transporters [57, 58]. This suggests that these NIPs are able to mediate transport of AsIII in both directions across the membrane, and so may be involved in both AsIII uptake and efflux. Indeed, AsIII efflux activity has been demonstrated for OsNIP2;1/Lsi1 from rice roots [103]. Bi-directional transport through NIPs could therefore contribute differentially to uptake, efflux, translocation and consequently accumulation, detoxification and tolerance of As in plants exposed to AsIII or AsV.

In order to improve tolerance to and reduce accumulation of As in plants, a more detailed understanding of the processes underlying As uptake, translocation and detoxification in different plant tissues is required. The potential contribution of different NIPs to these processes has yet to be revealed. The present study focuses on the role of group II NIPs in *Arabidopsis* in As uptake, efflux, translocation and tolerance on exposure to AsIII or AsV. Group II NIPs have previously been partially characterised for their response to As. When grown on plates containing AsIII or AsV, *nip5;1* and *nip6;1* T-DNA insertion mutants did not grow differently from WT plants but *nip7;1* plants grew better than WT, weighing significantly more after 14 days growth on plates containing 7 or 10μM AsIII [58]. In order to investigate further the role of group II NIPs in As transport and tolerance in *Arabidopsis*, crosses were performed between *nip5;1, nip6;1* and *nip7;1* T-DNA insertion mutants to obtain double and triple mutants. These plants were then exposed to AsIII or AsV and the effect of loss of function on As tolerance, uptake, translocation and efflux was explored.

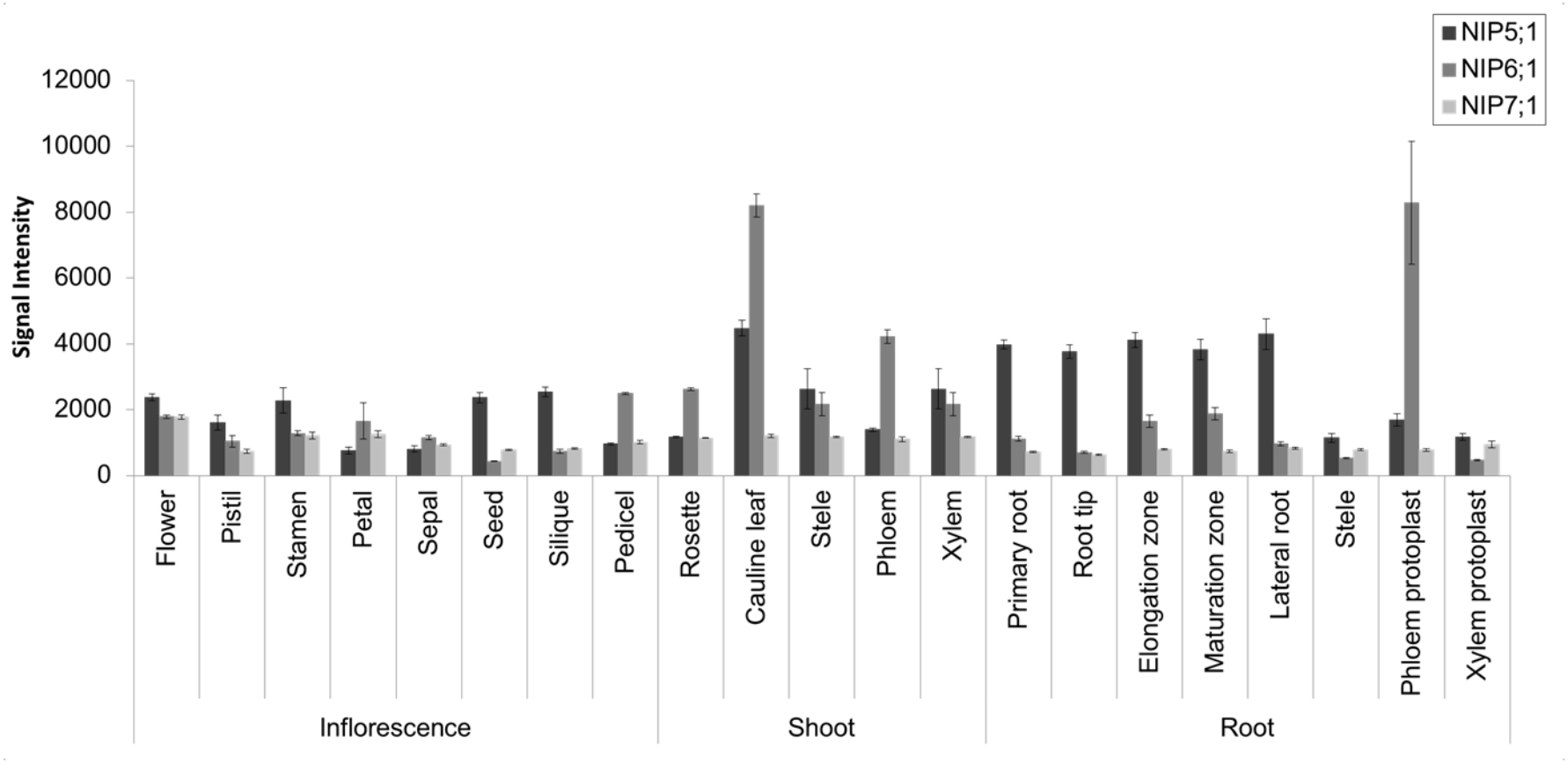

Figure 3.3: Expression patterns of Group II NIPs

Graph showing the relative expression level of *NIP5;1, NIP6;1* and *NIP7;1* in different *Arabidopsis* tissues. Data were obtained from the Genevestigator database [141]. Values are means ± SEs of signal intensities on the Affymetrix Rice Genome Array, plotted on a linear scale.

3.2 Materials and Methods

3.2.1 Plant Material and Characterisation of Mutants

T-DNA insertion lines were obtained for each of the group II NIPs in *Arabidopsis* Columbia (Col-0) background from the Nottingham Arabidopsis Stock Centre (NASC) [176] (SALK_012572, SALK_122287C, SALK_046323 and SALK_057023 relating to *nip5;1-1, nip5;1-2, nip6;1* and *nip7;1* respectively). These lines were previously characterised at the DNA and mRNA level and shown to be loss of function mutants [54, 58]. RT-PCR was performed on cDNA synthesised from the double and triple mutants as described in Section 2.2.3 using primers specific to *NIP5;1, NIP6;1, NIP7;1* and *Actin2* (Table 3.1).

Table 3.1: Primers used for RT-PCR on *nip* T-DNA insertion mutants

Primer Name	Sequence	Tm (°C)	Product Size (bp)
NIP5;1F	GGTAATGGTGATGGCTCCTC	51	801
NIP5;1R	ATGGCACCAAGTGTAGGAGC	51	
NIP6;1F	GATTCGAAGGGAAGAGGAATG	50	692
NIP6;1R	TGGACCCAGTGTTCTTACAGG	50	
NIP7;1F	CCTTCCATCACCATTGCTTT	49	337
NIP7;1R	GGTTCATCGATCCTCCTGAA	49	
ACTINF	ACGAGCAGGAGATGGAAACC	51	493
ACTINR	ACCCCAGCTTTTTAAGCCTTTG	51	

3.2.2 Crossing of *Arabidopsis* Plants

Unopened flowers of the plant used as female parent were emasculated by removal of the immature stamens using fine tweezers, leaving only the un-pollinated stigma. Mature pollen from the male parent was then used to pollinate the stigma and the stem of the female parent was labelled with a sticker. All unused inflorescences were removed from the female parent plant. When mature, seed was collected and F_1 plants grown on F2+S (Levington UK) soil. Homozygous plants were identified in the F_2 generation using PCR.

Homozygous *nip6;1* and *nip7;1* parents were crossed to generate *nip6;1nip7;1* double mutants. Subsequent crosses were performed by me. Homozygous *nip5;1-1* plants were used as female parents and *nip6;1, nip7;1* and *nip6;1nip7;1* plants used as pollen donors to generate *nip5;1nip6;1, nip5;1nip7;1* and *nip5;1nip6;1nip7;1* double and triple knockouts.

3.2.3 Genotyping of F_2 Plants

Homozygous knockout lines were identified using PCR. Three primers were used for each insertion, one complementary to the T-DNA insertion and two gene specific primers spanning the insertion (Table 3.2).

Table 3.2: Primers used for genotyping *nip* T-DNA insertion mutants

Primer Name	Sequence	Tm (°C)
NIP5;1-1LP	AATCGGTTTTGTTTTGCAATG	47
NIP5;1-1RP	GAGAGACTTACGGCACGAGTG	47
NIP5;1-2LP	TCCTAGCTCCATTTTCGTTTTC	47
NIP5;1-2RP	CTCCAAGTGTGACGTAAACCC	47
NIP6;1F	GATTCGAAGGGAAGAGGAATG	47
NIP6;1R	TGGACCCAGTGTTCTTACAGG	47
NIP7;1F	GCACGGTCAAGAGTAGTCGAC	47
NIP7;1R	CCGTCAAATTACCCAACTGCA	47
LBb1.3	ATTTTGCCGATTTCGGAAC	47

DNA extractions and PCR reactions were performed as described in Section 2.2.3. The example gel in Figure 3.4 shows the result obtained for plants containing 0, 1 or 2 copies of the T-DNA in each NIP.

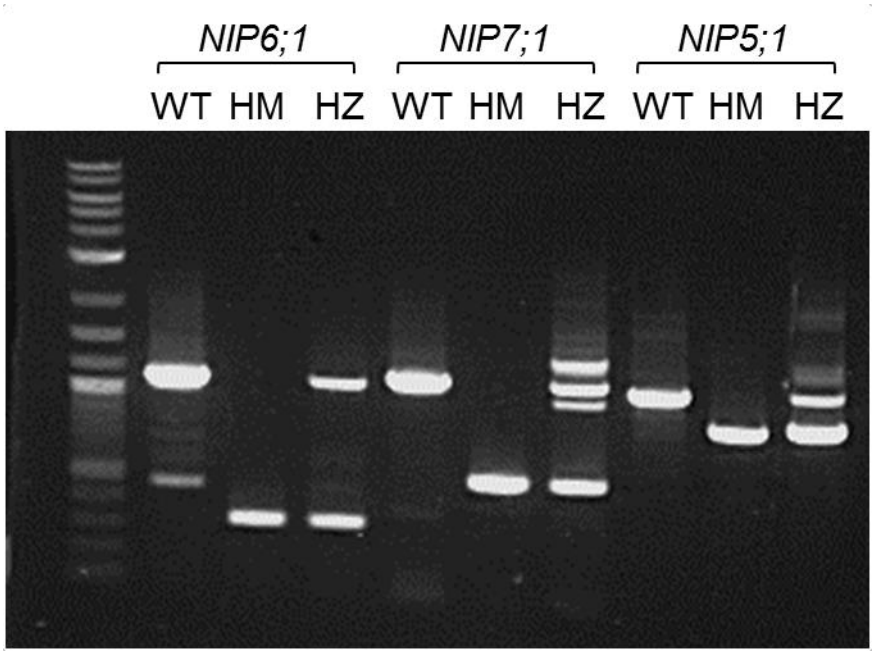

Figure 3.4 Agarose gel showing PCR products obtained from genotyping T-DNA mutants
PCR was performed on DNA from plants containing 0, 1 or 2 copies of the T-DNA insertion in *NIP5;1, NIP6;1* and *NIP7;1*. WT, HM and HZ refer to plants containing 0, 2 and 1 copy of the T-DNA respectively. A 2-Log DNA ladder was run in the first lane.

3.2.4 Growth Experiments on Plates

Arabidopsis WT and mutant seeds were surface sterilised with 70% ethanol containing 1µl Tween20 per 250ml for 20 minutes before being washed twice with 90% ethanol. Seeds were then spread on sterile filter paper to dry before being sprinkled onto plates containing half-strength Murashige and Skoog medium (half MS) solidified with 16g/L Agar. Plates were sealed with micropore tape and stratified at 4°C for 48hrs before transfer to the growth room. Plates were kept under 16hr light (~200 µmol m^{-2} sec^{-1}) /8hr dark conditions with night-day temperatures of 20-23°C for 7 days. Seedlings were then transferred to treatment plates using tweezers under sterile conditions. Treatment plates contained half MS with AsIII or AsV added as different concentrations of As_2O_3 and KH_2AsO_4 as indicated in the text. Plates were returned to the growth room in vertical racks. The root length of each seedling was marked on the plate 2 and 7 days after transfer to treatment. The growth rate of the roots was calculated as mm growth per day. The plant fresh weight was recorded after 14 days growth on treatment plates. The experiment was repeated six times. At least two plates of each treatment were included in each replicate, and each plate contained at least three individuals of each genotype.

3.2.5 Growth Experiments in Hydroponics

WT and mutant seeds were sown on F2+S (Levington UK) soil and stratified at 4°C for 48hrs before transfer to the growth room (conditions as above). Three week old plants were transferred to 1-litre hydroponics boxes containing half-strength MS medium and allowed to acclimatise for at least 24hrs before treatment. The fresh weight of the plants was recorded at the beginning of treatment, when AsIII and AsV were added to the medium at different concentrations as indicated in the text. The plants were returned to the growth room for two weeks, and the fresh weight recorded again after 7 and 14 days of treatment. The Relative Growth Rate was calculated as described by Poorter and Garnier (1996) [149]. At least three individuals of each genotype were grown in each condition, and the experiments were repeated at least six times.

3.2.6 Tissue Arsenic Concentration

The As concentration of different tissues was analysed from plants exposed to AsIII or AsV for 1, 7, 14 or 21 days in hydroponics. Plants were rinsed with dH_2O before immersion in ice-cold desorption buffer (1mM K_2HPO_4, 0.5mM $Ca(NO_3)_2$ and 5mM MES-pH 5.6) for 15 minutes to remove apoplastic As before rinsing in deionised water. Plant tissue was dried at 80°C for 48hrs and the dry weight recorded. Samples were digested in concentrated HNO_3 at 70°C for 24 hours before being made up to 5% HNO_3

with ultrapure water (18.2 MΩ cm^{-1}) and filtered through filter paper (equivalent Whatman Grade 1). The total As tissue concentration was determined using an ICP-OES (Thermo iCAP 7000 series). Tissue from three individuals was pooled for each sample, and the experiments were repeated at least four times

Seed samples were collected from plants that had been grown on F2+S soil in the glasshouse (16hr light/8hr dark and day time temperatures between 20-27°C). Plants were treated with tap water containing 150μM AsV twice a week from three weeks old to maturity. The total As concentration of seed tissue was analysed as described above.

3.2.7 Arsenic Concentration of Xylem Sap

Plants were grown on F2+S soil for five weeks before transfer to hydroponics. After a few days, 150μM AsV was added to the medium. After 24 hours exposure to AsV, the bolt was cut using a sharp razor around 5cm above the level of the rosette. Decapitated plants were then transferred to a pressure chamber (Digital Plant Water Potential Apparatus EL540-300) and around 20 kiloPascal pressure applied. Xylem sap was collected from the cut bolt for 20 minutes (~50μl). The volume was made up to 2.2ml using 5% HNO_3 and the total As concentration analysed as described above. The fresh weight of each plant was recorded, and the weight of the medium taken at the start and end of treatment to enable calculation of transpiration rate. The experiment was repeated three times, with samples collected from at least two individuals of each genotype per repeat. Xylem sap was also collected from plants which had been exposed to 150μM AsV in hydroponics for a period of three weeks (three individuals of each genotype).

3.2.8 Arsenic Concentration of Phloem Exudate

Three week old plants were exposed to 150μM AsV in hydroponics for a period of three weeks under short day conditions (8hr light/16hr dark) to encourage vegetative growth resulting in large leaves. Phloem exudates were collected as described by Tetyuk, O. *et al*. [177]. Briefly, EDTA was used to prevent plugging of the phloem following harvest of leaves using a sharp razor. After one hour in EDTA, the leaves were rinsed and the cut ends of the petioles submerged in 1.5ml deionised water. They were placed in humid conditions overnight and the As concentration of the leaves and exudate was determined as described above. Exudates were collected from 15 leaves (five from each of three plants) per sample, and the experiment was repeated four times.

3.2.9 Arsenic Efflux

For the As efflux experiment, three week old plants were exposed to 350μM AsV for 24 hours in hydroponics. The roots were rinsed in deionised water and placed into an Eppendorf containing 1.5ml liquid half MS medium for 6 and 24 hours. The total As concentration of the medium, root and shoot tissue was determined as described above. Tissue and medium from three individuals was pooled for each sample and the experiment was repeated at least four times.

3.2.10 Source to Sink Partitioning of Arsenic

Plants were grown on F2+S soil for three weeks before transfer to hydroponics where they were exposed to 50μM AsV for one week. The three youngest and oldest leaves were collected from six individuals for each genotype and the total As concentration determined as described above. The experiment was repeated five times.

Additionally, WT and *nip6;1* plants were transferred to hydroponics and exposed to 50μM AsV under short day growth conditions for four weeks. Shoot apices (1cm tip of shoot) and rosette leaves (3 from each plant) were collected and analysed for total As concentration from five individuals for each genotype. The experiment was repeated three times.

3.2.11 Statistical Analysis

Experiments were analysed in SPSS using a two-way ANOVA. The main effects and simple main effects were explored using Bonferroni adjusted pairwise comparisons. Alternatively, significant differences between genotypes were explored using unpaired *t*-tests or one-way ANOVA where appropriate and as indicated in the text. When a one-way ANOVA was used, significant differences between genotypes were explored using Tukey post-hoc analysis when there was homogeneity of variances (assessed by Levene's test of homogeneity of variances). When there was heterogeneity of variances, a one-way Welch ANOVA was used and the results interpreted using a Games-Howell post-hoc analysis.

3.3 Results

3.3.1 RT-PCR Analysis of T-DNA Insertion Lines

Homozygous *nip6;1nip7;1* plants were identified and confirmed to be loss of function double mutants at the mRNA level through RT-PCR using gene specific primers (Figure 3.5).

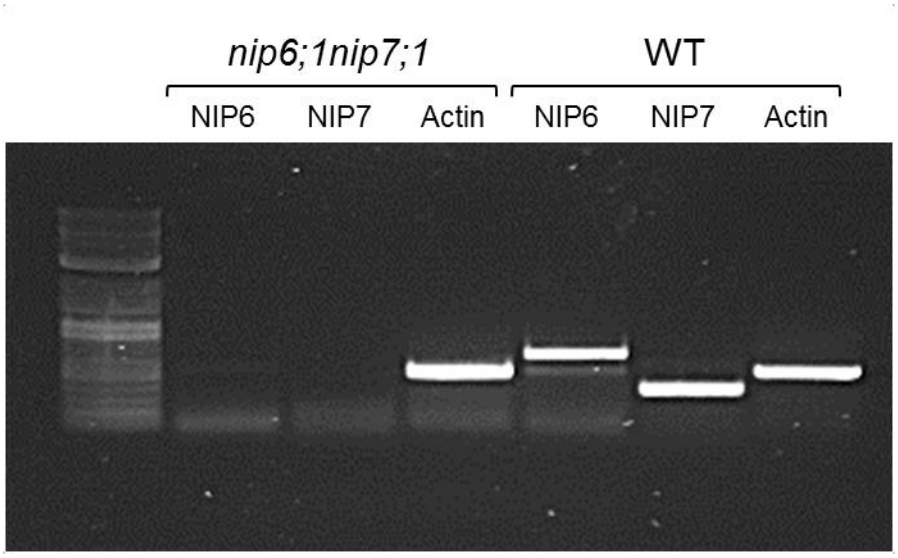

Figure 3.5 RT-PCR of *nip6;1nip7;1* mutant plants
RT-PCR was performed on *nip6;1nip7;1* and WT plants using primers specific to *NIP6;1, NIP7;1* and *Actin.* A 2-Log DNA ladder was run in the first lane. The double mutant plants showed no expression of *NIP6;1* or *NIP7;1* while bands of the expected size (692bp and 337bp) were observed for *NIP6;1* and *NIP7;1* in WT plants.

Homozygous triple knockout (*nip5;1-1nip6;1nip7;1*) plants were generated and RT-PCR performed (Figure 3.6). Expression of *NIP5;1* could be detected in the triple T-DNA insertion mutants, despite containing two copies of the T-DNA insertion in the gene as determined by PCR analysis. This was unexpected, as *nip5;1-1* has previously been characterised at the mRNA level and reported to be a true knockout [58]. In the same study a second allele, *nip5;1-2*, was found not to be a genuine loss of function mutant. However, *nip5;1-2* was characterised by Takano, J. *et al.* [54] using Q-PCR and found to be a loss of function mutant. It is possible that *nip5;1-1* and *nip5;1-2* were mislabelled by Isayenkov, S.V. [58], and it is *nip5;1-2* that is the true knockout. To investigate this, *nip5;1-1* and *nip5;1-2* homozygous plants were checked for expression of *NIP5;1* (Figure 3.6). No expression of *NIP5;1* could be detected in *nip5;1-2* plants, confirming that *nip5;1-2* is a true loss of function mutant whereas *nip5;1-1* is not. Crosses between *nip5;1-2, nip6;1, nip7;1* and *nip6;1nip7;1* plants were performed, however due to time limitations no further characterisation of the double or triple mutants was performed. Subsequent experiments focused on the other group II nips utilising the *nip6;1, nip7;1* and the *nip6;1nip7;1* loss of function mutants.

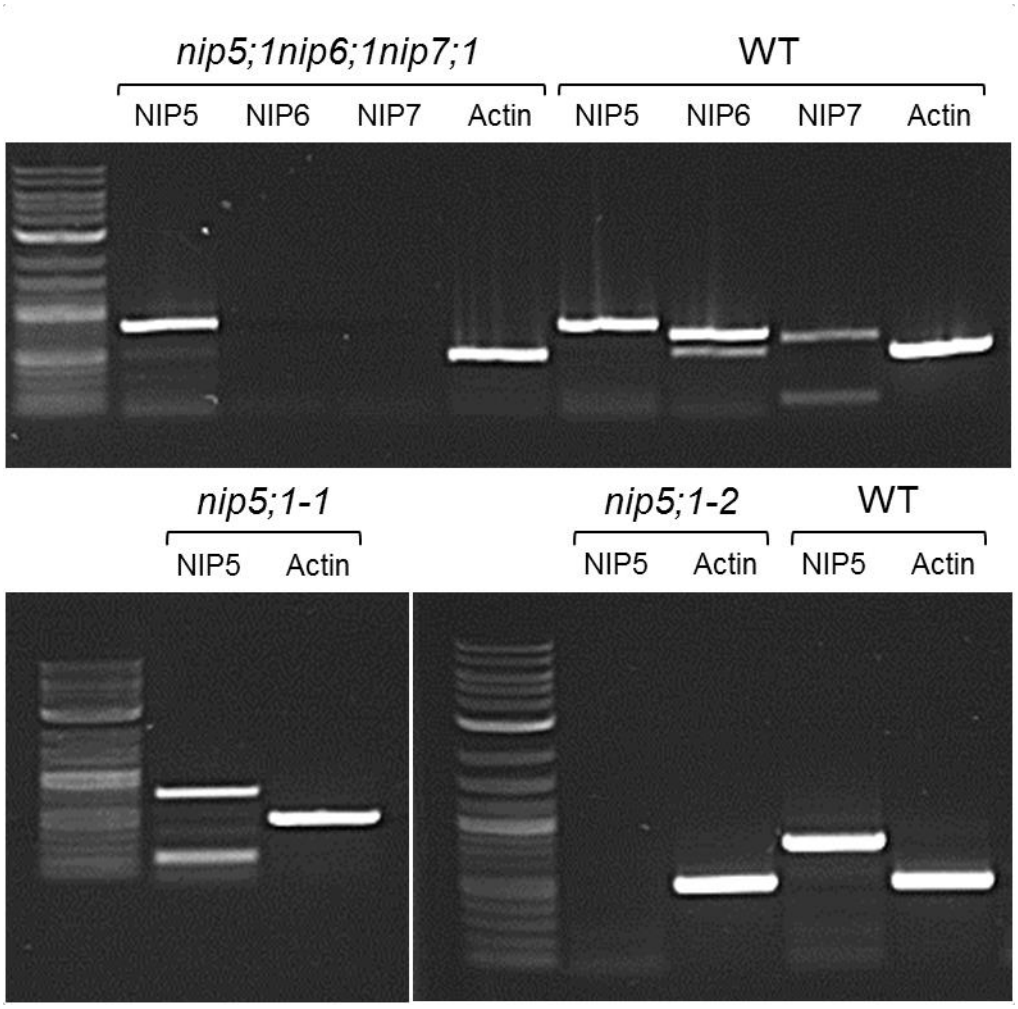

Figure 3.6 RT-PCR of *nip5;1nip6;1nip7;1* triple mutant and *nip5;1* T-DNA insertion lines
The top panel shows gel electrophoresis of RT-PCR performed on *nip5;1-1nip6;1nip7;1* and WT plants using primers specific to *NIP5;1, NIP6;1, NIP7;1* and *Actin*. The triple mutant plants showed no expression of *NIP6;1* or *NIP7;1* while bands of the expected size (801bp, 692bp and 337bp) were observed for *NIP5;1, NIP6;1* and *NIP7;1* in WT plants. The bottom panel depicts gel electrophoresis of RT-PCR performed on *nip5;1-1, nip5;1-2* and WT plants using primers specific to *NIP5;1* and *Actin*. Expression of *NIP5;1* was detected in WT and *nip5;1-1* plants while *nip65;1-2* plants showed no expression of *NIP5;1*. A 2-Log DNA ladder was run in the first lane of each gel.

3.3.2 Growth Experiments

3.3.2.1 Arsenic Tolerance of *nip6;1, nip7;1* and *nip6;1nip7;1* Plants Grown on Agar Plates

Homozygous knockout *nip6;1, nip7;1* and *nip6;1nip7;1* plants were grown alongside WT on agar plates. One week old seedlings were transferred to agar plates containing different concentrations of AsIII or AsV and plant fresh weight was recorded after a further two weeks growth. There were no significant differences in fresh weight between genotypes in any treatment as determined by two-way ANOVA (Figure 3.7).

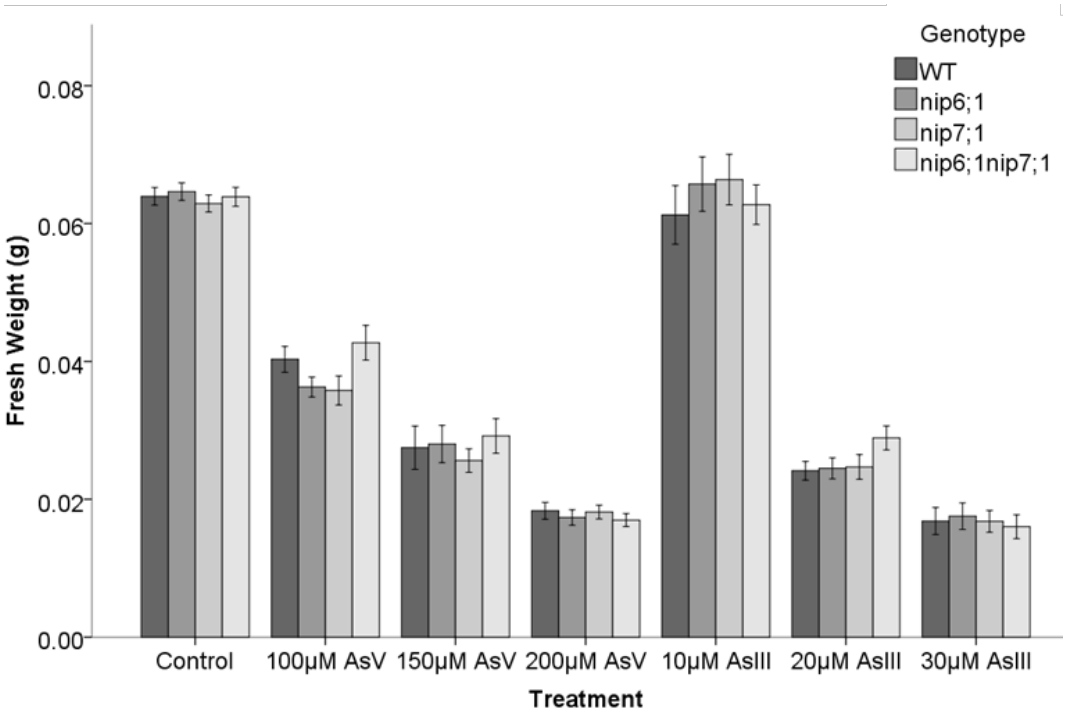

Figure 3.7: Fresh weight of WT and *nip* mutant plants grown on plates
WT, *nip6;1, nip7;1* and *nip6;1nip7;1* seedlings were grown on half MS plates for 7 days before transfer to plates containing different concentrations of AsIII or AsV. Fresh weights were measured after 2 weeks growth on treatment plates. Data are from 6 independent experiments and values are means ± SE.

The root length of the seedlings was marked on the plates after 2 and 7 days and root growth (as mm/day) was compared between genotypes (Figure 3.8). On control plates, the root growth of *nip6;1nip7;1* plants was significantly slower than WT and *nip7;1* plants. When root growth was calculated relative to control conditions, *nip6;1* and *nip6;1nip7;1* plant roots grew faster than WT when exposed to 200µM AsV. The double mutant plant roots also grew significantly faster than either of the single mutants under these conditions, suggesting that both *NIP6;1* and *NIP7;1* contribute to the enhanced root growth observed in response to AsV.

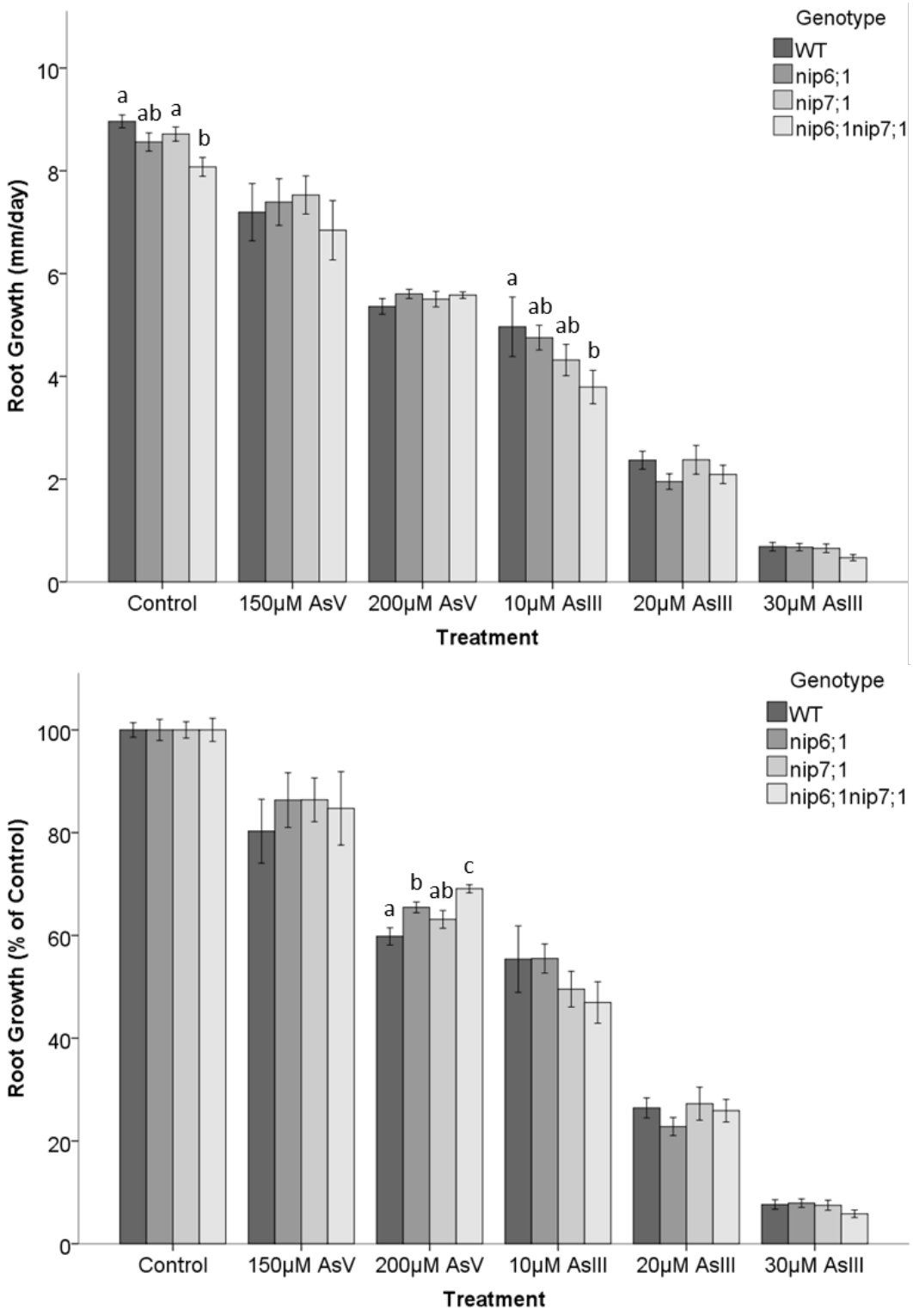

Figure 3.8: Root growth of WT and *nip* mutant plants grown on plates

The top panel displays the root growth of WT, *nip6;1, nip7;1* and *nip6;1nip7;1* plants grown on plates calculated as mm growth per day. The bottom panel shows the same data expressed relative to growth in control conditions. Data are from 6 independent experiments, values are means ± SE and letters indicate significant differences between genotypes at $P<0.05$.

3.3.2.2 Arsenic Tolerance of *nip6;1, nip7;1* and *nip6;1nip7;1* Plants Grown in Hydroponics

To measure plant growth under more physiological conditions, 3wo (week old) plants were exposed to different concentrations of AsIII and AsV in hydroponics and relative growth rates determined after one and two weeks in treatment. During the first week in treatment, plants grew more slowly in all concentrations of AsIII and AsV tested compared to control conditions (Figure 3.9). In the As free medium, the double mutant plants grew more slowly than the WT plants suggesting that *NIP6;1* and *NIP7;1* are required for normal plant growth. There were no differences between genotypes in the RGR of plants exposed to AsIII, however both *nip6;1* and *nip7;1* plants showed evidence of increased tolerance to AsV. In 50μM AsV *nip6;1* plants grew faster than WT while *nip7;1* plants grew faster than WT when exposed to 150μM AsV. The single knockout plants for *nip7;1* also grew faster than the double knockouts in 100, 150 and 200μM AsV.

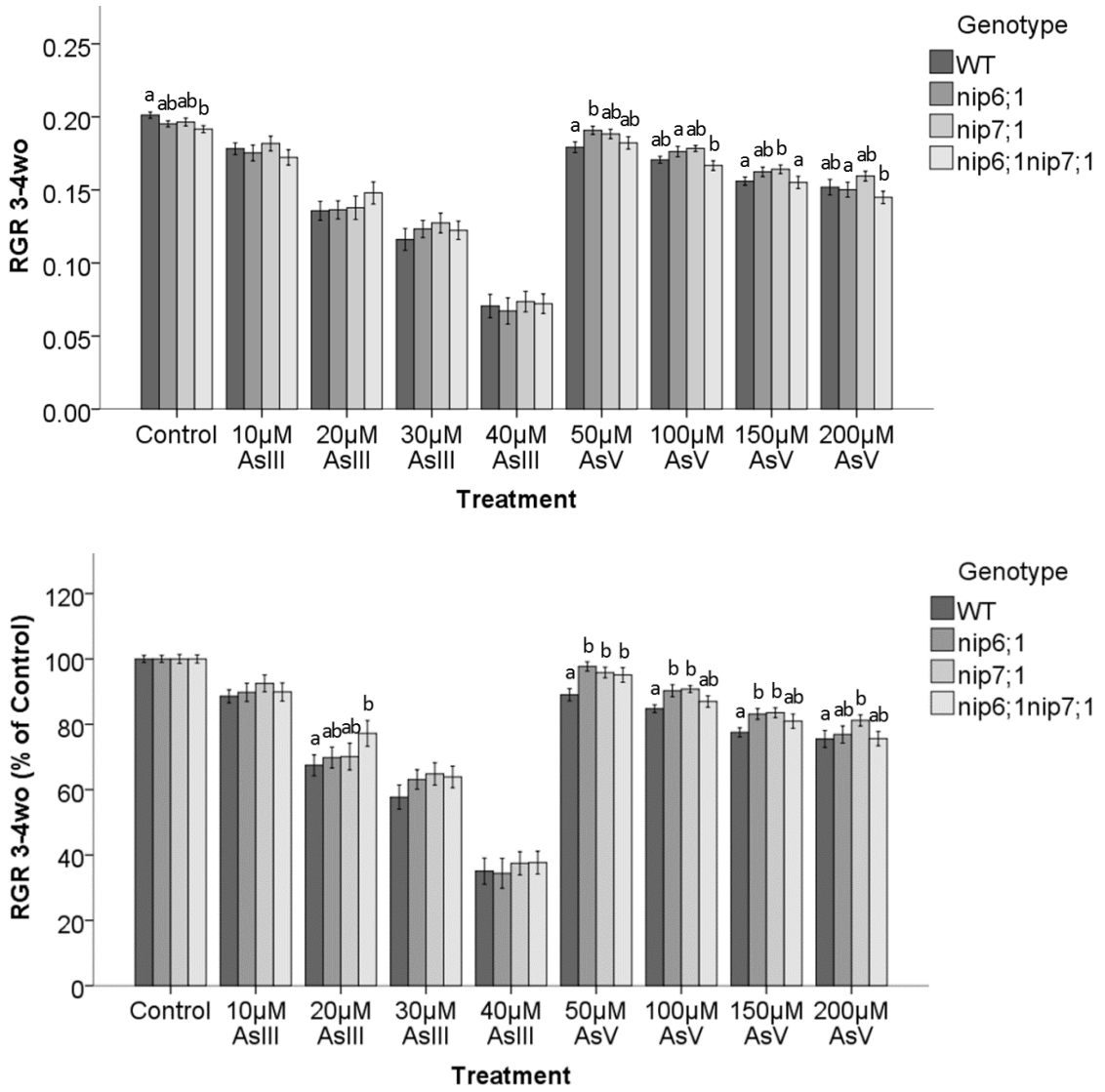

Figure 3.9: Relative growth rates of 3-4wo WT and *nip* mutant plants
The top panel displays the RGR of 3-4wo WT, *nip6;1*, *nip7;1* and *nip6;1nip7;1* plants grown in hydroponics and exposed to different concentrations of AsIII and AsV. The bottom panel shows the same data expressed relative to growth in control conditions. Data are from six independent experiments, values are means ± SE and letters indicate significant differences between genotypes at $P<0.05$.

When the RGR over the first week of As exposure was calculated relative to growth in control conditions (Figure 3.9) the reduction in RGR of *nip6;1nip7;1* plants exposed to 20μM AsIII was significantly lower than the reduction in RGR of WT plants. Neither of the single mutants performed better than WT in the same conditions, suggesting an interaction between *NIP6;1* and *NIP7;1* in the double mutant resulting in enhanced tolerance to AsIII. In response to 50μM AsV, *nip6;1, nip7;1* and *nip6;1nip7;1* plants all grew faster than WT, however, the double mutants did not grow differently than either of the single mutants. In the higher concentrations of 100 and 150μM AsV both single mutants grew faster than WT while in 200μM AsV only *nip7;1* plants showed increased tolerance. The double mutant plants had an intermediate phenotype in that they were

not more tolerant to the higher concentrations of AsV compared to WT and did not grow at a significantly different rate than either of the single mutants. This suggests that the loss of function of both *nip6;1* and *nip7;1* in the double mutant plants had an antagonistic effect on tolerance to the higher concentrations of AsV.

During the second week of the growth experiment, when plants were 4-5wo (Figure 3.10), the RGR of plants grown in control conditions was reduced compared to 3-4wo plants. This is probably due to the developmental stage of the plants, as they were beginning to flower when they reached 4wo. Following inflorescence emergence, rosette growth ceases and so the rate of biomass accumulation slows down. During this period of growth, there was no difference in RGR between the WT and mutant plants in the control conditions. This suggests that the role of *NIP6;1* and *NIP7;1* in plant growth is more important during the vegetative rather than the reproductive growth stage.

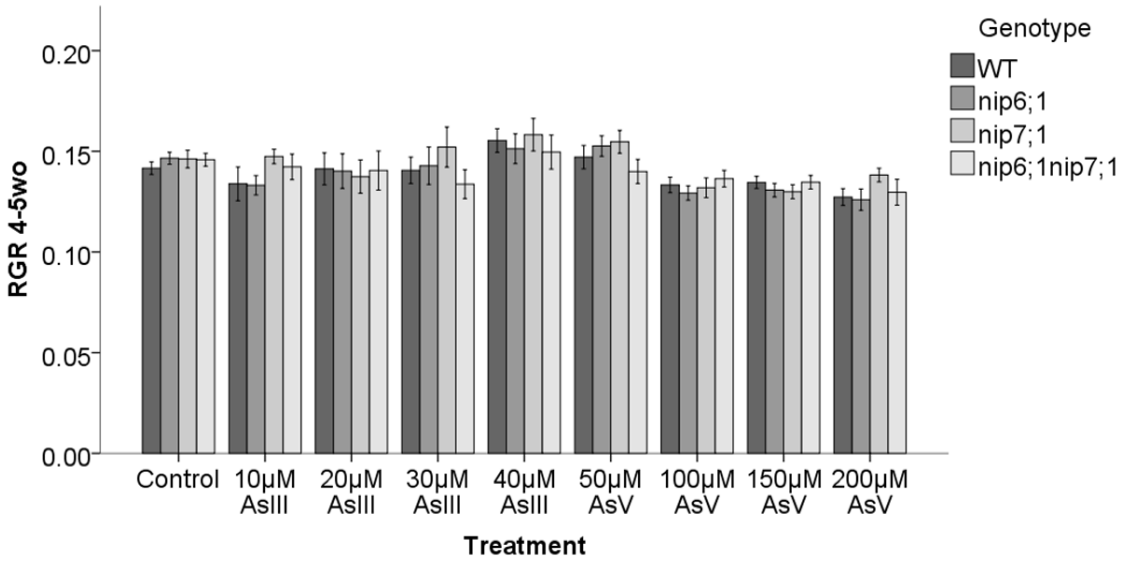

Figure 3.10: Relative growth rates of 4-5wo WT and *nip* mutant plants
RGR of 4-5wo WT, *nip6;1, nip7;1* and *nip6;1nip7;1* plants grown in hydroponics and exposed to different concentrations of AsIII and AsV. Data are from six independent experiments, values are means ± SE.

The RGRs were reduced by As treatment to a lesser extent during the second week of treatment compared to the first week. The average RGR of 4-5wo plants was significantly reduced compared to control conditions in plants exposed to 100,150 or 200µM AsV but there was no difference in average RGR between control conditions and treatment with AsIII or 50µM AsV. It may be that *Arabidopsis* plants are less sensitive to As treatment during flowering or it could be that larger, more mature 4-5wo plants are more tolerant compared to the relatively smaller 3-4wo plants. Alternatively the *Arabidopsis* plants may be able to adapt to As exposure over time in a similar

manner to the rice plants described in Chapter 2, although in this case the RGR was not increased upon exposure to As compared to control conditions during the 'recovery period'.

There were no differences in RGR between genotypes of 4-5wo plants in any As treatment. This suggests that the role of *NIP6;1* and *NIP7;1* in As tolerance may be more important during the period following initial As exposure rather than during adaptation to longer-term As exposure. Alternatively, this could be explained by the relatively low level of stress observed in the 4-5wo plants exposed to As which would make it more difficult to detect differences in tolerance between genotypes. In 200μM AsV, the average RGR was just 10% lower than the average RGR in control conditions.

The average RGR over the whole two weeks of treatment (3-5wo plants) was significantly reduced compared to control conditions in all concentrations of As tested except for the lower concentrations of 10μM AsIII and 50μM AsV (Figure 3.11). There were no significant differences between genotypes. When calculated relative to growth in control conditions, the RGR of *nip7;1* plants was significantly higher than WT in 50, 100 and 150μM AsV (Figure 3.11). Increased tolerance to AsV was not observed for *nip6;1nip7;1* plants. This suggests that loss of function in *nip6;1* in addition to *nip7;1* in the double mutants in some way counteracts the AsV tolerance conferred on *nip7;1* single knockout plants. In addition, the double mutants grew significantly slower than WT plants in 40μM AsIII although the RGR was not different from either of the single mutants. This indicates an interaction effect between *NIP6;1* and *NIP7;1* over long term As exposure resulting in a decrease in As tolerance in the double knockout plants. This is the reverse of what was observed in the growth experiments on plates and during the first week of growth in hydroponics (Figures 3.7-9), suggesting that the function of *NIP6;1* and *NIP7;1* in response to As may change with length of exposure, concentration of As and/or plant developmental stage.

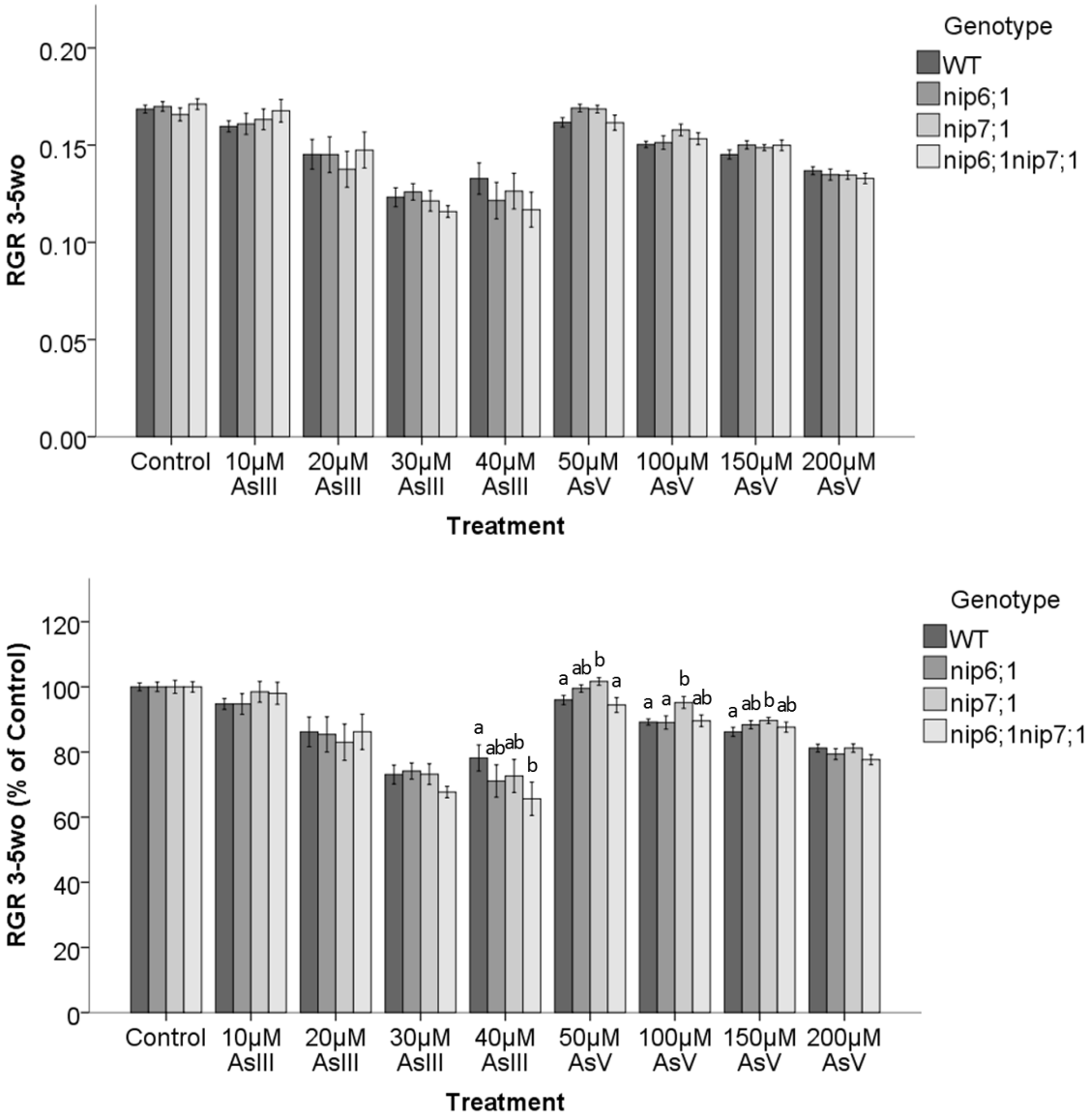

Figure 3.11: Relative growth rates of 3-5wo WT and *nip* mutant plants
The top panel displays the RGR of 3-5wo WT, *nip6;1, nip7;1* and *nip6;1nip7;1* plants grown in hydroponics and exposed to different concentrations of AsIII and AsV. The bottom panel shows the same data expressed relative to growth in control conditions. Data are from six independent experiments, values are means ± SE and letters indicate significant differences between genotypes at $P<0.05$.

3.3.3 Arsenic Concentration of *nip6;1, nip7;1* and *nip6;1nip7;1* Knockout Lines

NIP6;1 and *NIP7;1* may be involved in facilitating As influx, efflux or long-distance transport throughout the plant, resulting in altered tissue As concentrations in the mutant plants compared to WT. Any of these processes may lead to altered As tolerance and could help explain the increased tolerance to AsV observed in both *nip6;1* and *nip7;1* plants. To explore further how *NIP6;1* and *NIP7;1* contribute to As

transport and accumulation in *Arabidopsis*, the As efflux capacity and tissue As concentration was compared between the T-DNA insertion mutants and WT plants.

3.3.3.1 Arsenic Efflux of *nip6;1, nip7;1* and *nip6;1nip7;1* Knockout Lines

In order to determine if NIP6;1 or NIP7;1 have a role in AsIII efflux from the roots WT, *nip6;1, nip7;1* and *nip6;1nip7;1* plants were exposed to 350µM AsV for 24hrs. They were then rinsed and returned to As free medium. After 6 and 24 hours, the As concentration of the medium, root and shoot tissues was determined. Efflux was calculated as µg As in the medium relative to the As concentration of the plant.

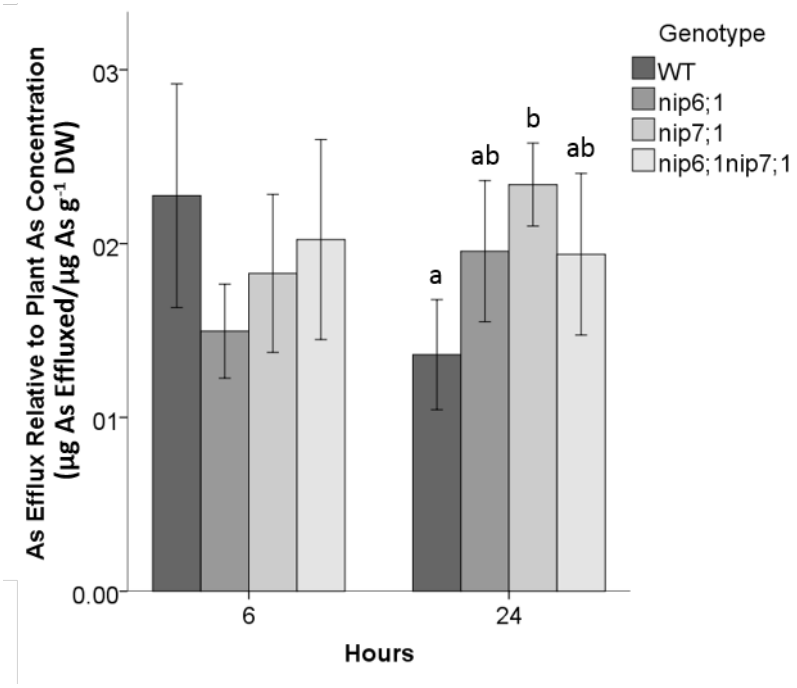

Figure 3.12 Efflux of As from WT and *nip* mutant plants
The graph shows the amount of As effluxed from the roots of 3wo *Arabidopsis* plants relative to the plant As concentration (µg As Effluxed/µg As g^{-1} DW plant). Plants were preloaded with As by exposure to 350µM AsV in hydroponics for 24hrs. Roots were rinsed and placed in As free medium. As efflux was measured 6 and 24 hours after transfer. Data are from at least four independent experiments and values are means ±SEs. Letters indicate significant differences between genotypes at $P<0.05$ using a one-way ANOVA.

There were no significant differences between genotypes in the proportion of As effluxed to the medium after 6 hours. After 24 hours, *nip7;1* plants had effluxed a higher proportion of As from the roots compared to WT plants (Figure 3.12). If *NIP7;1* was involved in efflux of As from the roots, we would expect the loss of function mutants to efflux less As than WT plants. The enhanced efflux observed in the knockout plants suggests an alternative role of *NIP7;1*. If *NIP7;1* is involved in root to shoot translocation of As, reduced translocation in the loss of function mutants may result in an increased local As concentration in the root. This would lead to a larger As

concentration gradient between the root and external medium thereby promoting efflux to the medium. However, when comparing the As loading between genotypes, there were no significant differences in shoot:root As, total plant As concentration (Figure 3.13) or in the root or shoot As tissue concentrations (data not shown) in the plants used for the efflux experiment. This does not rule out an increased local As concentration in specific parts of the root tissue in *nip7;1* plants which could drive greater efflux.

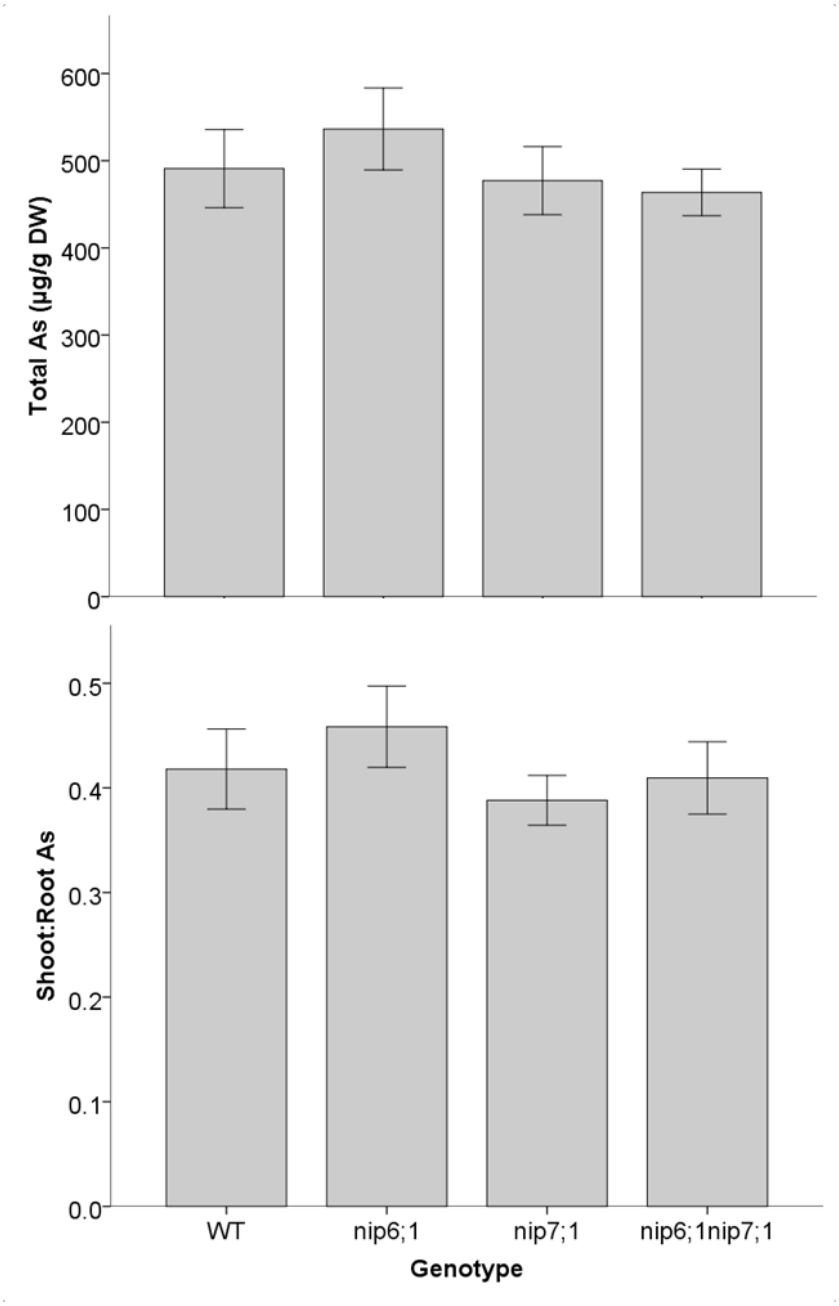

Figure 3.13 Arsenic loading of plants used in the efflux experiment
Graphs show the total As concentration (top graph) and shoot to root translocation (bottom graph) of As in 3wo plants after exposure to 350µM AsV for 24 hours. Data are from four independent experiments and values are means ±SEs.

3.3.3.2 Arsenic Distribution Between Root and Shoot Tissues

The total As concentration of root and shoot tissue was compared between genotypes after exposure to 30μM AsIII or 150μM AsV for 1, 7 and 14 days. After 1 day in 30μM AsIII, *nip7;1* plants had a higher concentration of As in the shoot compared to WT, although there was no significant difference in the shoot:root As or the total plant As concentration (Figures 3.14-15). The total As concentration increased in all genotypes after 7 and 14 days exposure to 30μM AsIII. The shoot As concentration and shoot:root As of WT plants also increased after 7 days exposure to AsIII while the root As concentration remained the same. Between 7 and 14 days, the shoot As concentration and shoot:root As of WT plants remained constant while the root As concentration increased. This suggests that *Arabidopsis* plants may respond differently to As exposure over time, with an initial increase in root to shoot translocation which then remains stable. The increase in root to shoot As translocation correlates with the observed reduction in RGR; after one week exposure to 30μM AsIII WT plants had significantly reduced RGR compared to control conditions (Figure 3.9) whereas during the second week of exposure there was no reduction in RGR (Figure 3.10).

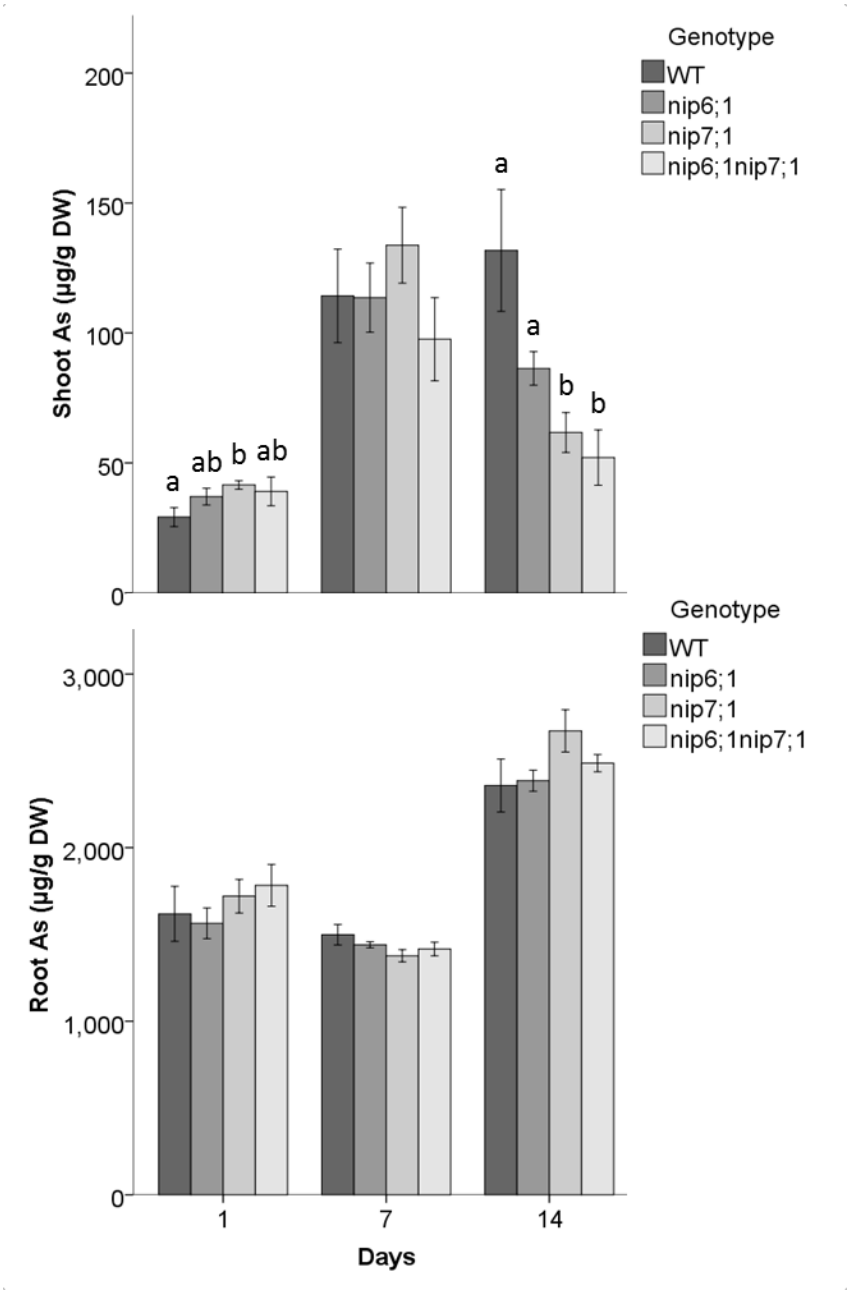

Figure 3.14 Arsenic concentration of WT and *nip* mutant plants exposed to 30*µ*M AsIII
Graphs show the shoot (top panel) and root (bottom panel) As concentration of WT and *nip* mutant plants after 1, 7 and 14 days exposure to 30µM AsIII. Data are from six independent experiments, values are means ± SEs and different letters indicate significant differences between genotypes at $P<0.05$.

The shoot As concentrations and the shoot:root As of *nip7;1* and *nip6;1nip7;1* plants were reduced compared to WT plants after 14 days of AsIII treatment. This suggests that *nip7;1* may be involved in root to shoot translocation of As after long term exposure. There were no differences between the double mutant and the *nip7;1* single mutant plants after 14 days, nor between *nip6;1* single mutants and WT plants suggesting that *NIP6;1* does not have a significant role in the uptake or long distance transport of As.

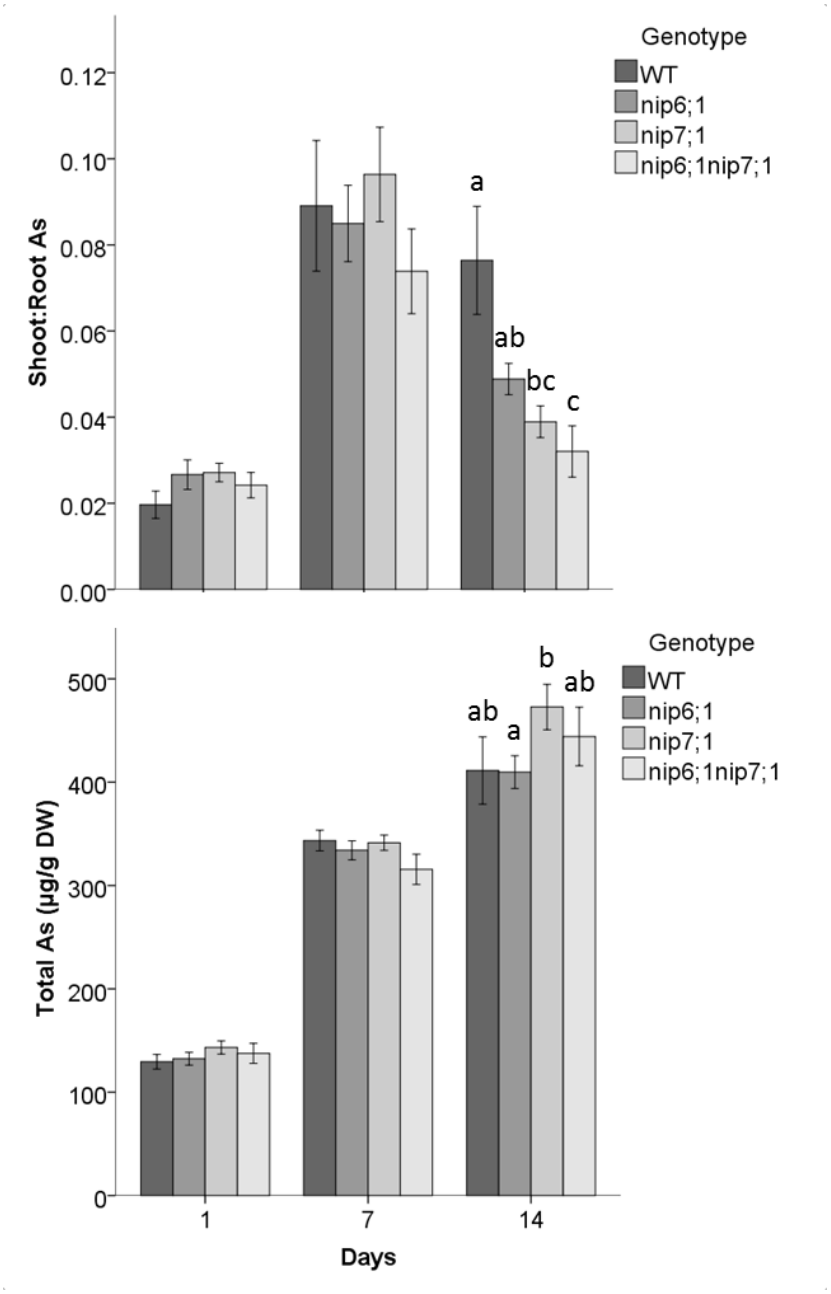

Figure 3.15 Arsenic concentration of WT and *nip* mutant plants exposed to 30*µ*M AsIII
Graphs show the shoot:root As (top panel) and total plant As concentration (bottom panel) of WT and *nip* mutant plants after 1, 7 and 14 days exposure to 30µM AsIII. Data are from six independent experiments, values are means ± SEs and different letters indicate significant differences between genotypes at $P<0.05$.

After 1 day in 150µM AsV treatment, *nip7;1* plants had a lower concentration of As in the shoot and a lower shoot:root As compared to WT plants (Figures 3.16-17). After 7 days, the As concentration of shoot and root tissues was higher than after 1 day in all genotypes. At this time point *nip6;1nip7;1* plants had a lower concentration of As in the shoot compared to WT but *nip7;1* plants did not. After 14 days exposure to AsV, tissue As concentrations had increased further compared to the shorter treatments. At this time point the As concentration in the shoots, the shoot:root As and total plant As

concentration of *nip7;1* plants was significantly higher than WT. There were no differences in As tissue concentration or distribution between WT and *nip6;1* plants exposed to AsV. This suggests that *NIP6;1* has little or no impact on As uptake or tissue distribution whereas *NIP7;1* affects both. Loss of function of *nip7;1* results in altered distribution of As between root and shoot tissues and the impact on the shoot:root As changes with length of As exposure.

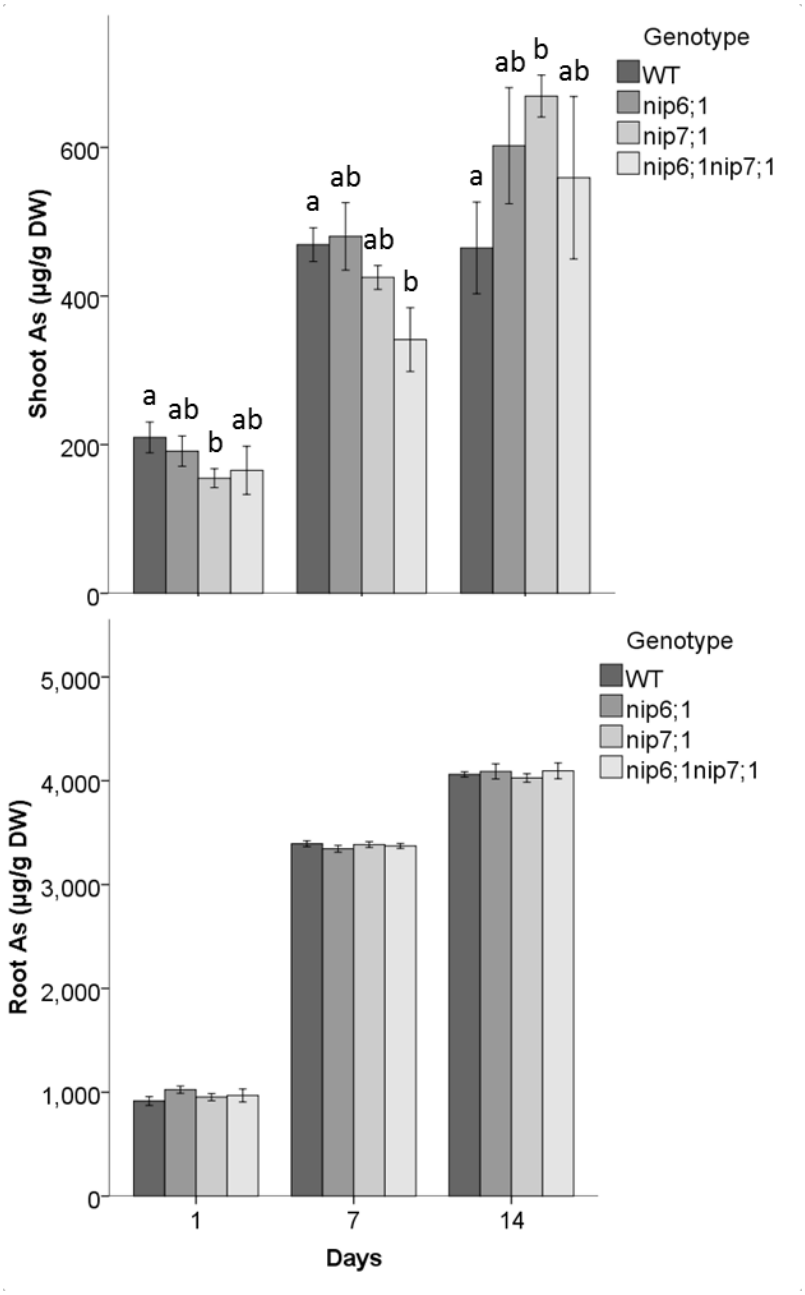

Figure 3.16 Arsenic concentration of WT and *nip* mutant plants exposed to 150*µ*M AsV
Graphs show the shoot (top panel) and root (bottom panel) As concentration of WT and *nip* mutant plants after 1, 7 and 14 days exposure to 150µM AsV. Data are from six independent experiments, values are means ± SEs and different letters indicate significant differences between genotypes at $P<0.05$.

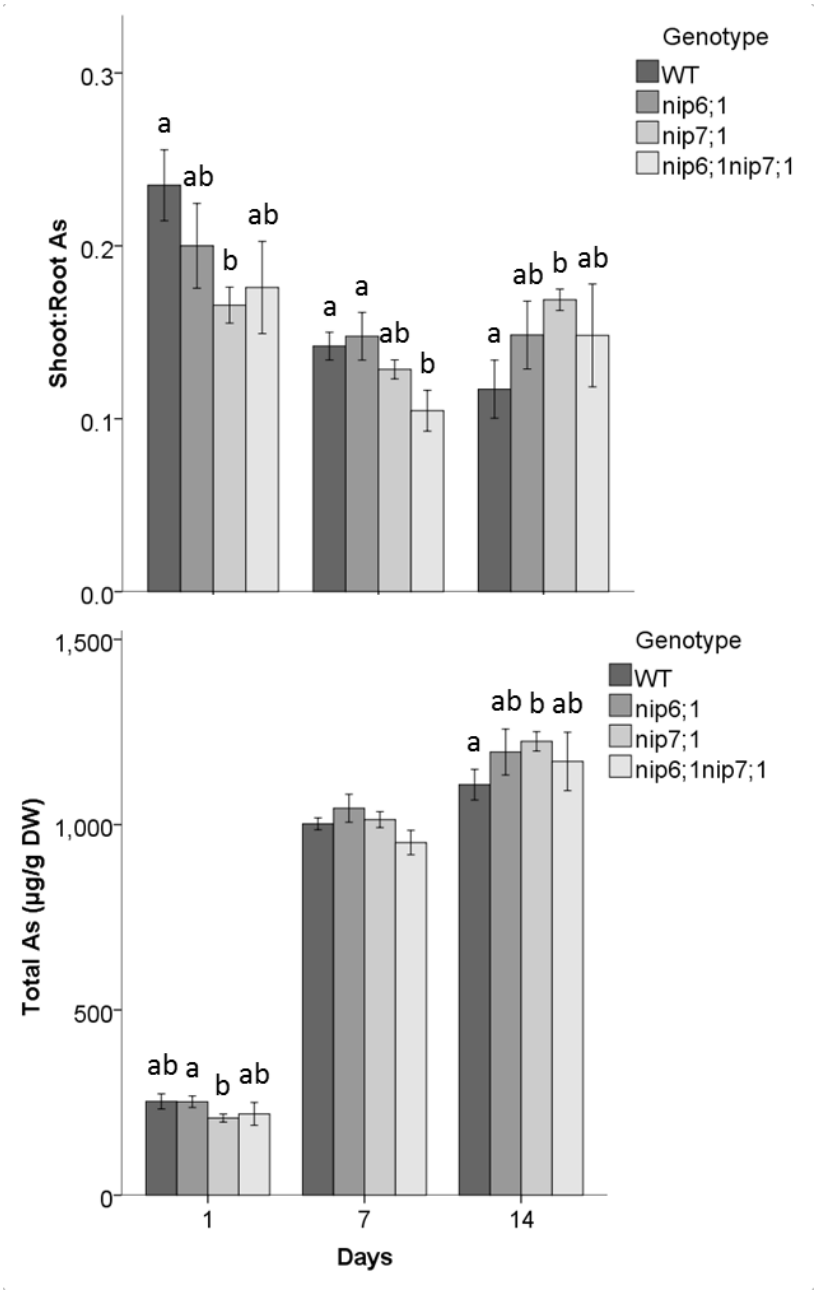

Figure 3.17 Arsenic concentration of WT and *nip* mutant plants exposed to 150*µ*M AsV
Graphs show the shoot:root As (top panel) and total plant As concentration (bottom panel) of WT and *nip* mutant plants after 1, 7 and 14 days exposure to 150µM AsV. Data are from six independent experiments, values are means ± SEs and different letters indicate significant differences between genotypes at $P<0.05$.

After 14 days treatment with AsIII and AsV *nip7;1* plants had significantly reduced and increased root to shoot translocation respectively as compared to WT plants. This suggests that loss of function of *NIP7;1* may affect long distance As transport in the plant differently depending on the speciation of As the plant is exposed to. Alternatively, the different phenotypes observed may be due to the difference in concentration of the As treatments. To explore this further, *nip7;1* and WT plants were

exposed to 30μM AsV for 14 days in hydroponics and the root and shoot As concentration determined (Figure 3.18).

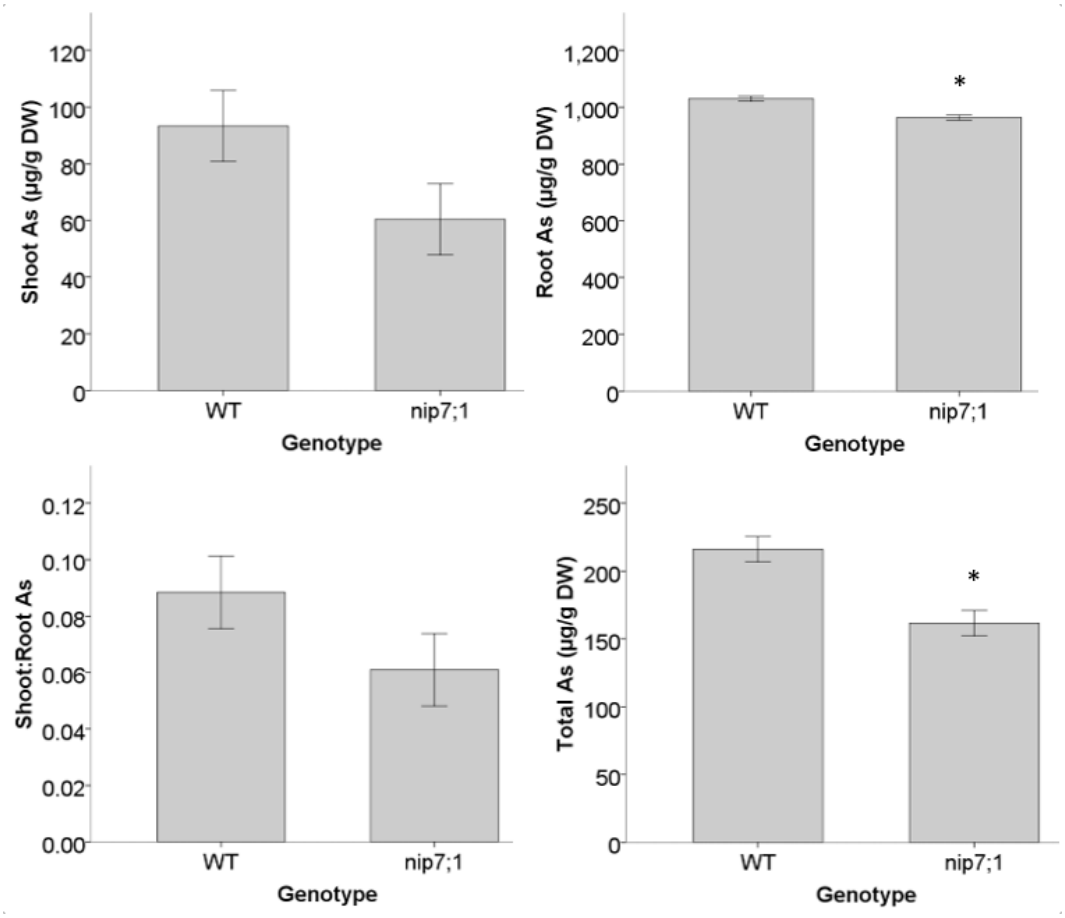

Figure 3.18 Arsenic concentration of WT and *nip7;1* plants exposed to 30μM AsV
Graphs show the total As concentration of WT and *nip7;1* plants after two weeks exposure to 30μM AsV in hydroponics. The top left and right panels show the average shoot and root As concentrations respectively. The bottom left panel shows the shoot:root As ratio and the bottom right panel shows the total plant As concentration. Data are from four independent experiments, values are means ±SEs and asterisks indicate significant differences between genotypes at $P<0.05$ using an unpaired *t*-test.

Plants exposed to 30μM AsIII accumulated higher levels of As, particularly in the root tissue, compared to plants exposed to 30μM AsV, indicating that Arabidopsis plants respond differently to AsIII and AsV treatment. It appears that AsIII is more readily taken up into the root but the proportion of As translocated to the shoot was actually lower in plants exposed to AsIII compared to plants exposed to AsV (Figure 3.15 & 3.18).

After exposure to the lower concentration of 30μM AsV for two weeks, *nip7;1* mutant plants had a reduced As concentration in the roots and a reduced total plant As concentration, but there was no significant difference in the concentration of As in the shoot or in the shoot:root As compared with WT plants (Figure 3.18). This suggests

that the effect of *nip7;1* loss of function on tissue distribution of As depends on both the speciation and concentration of As the plants are exposed to.

3.3.3.3 Arsenic Distribution Between Tissues After Long Term Exposure to AsV

Because *NIP7;1* is relatively highly expressed in reproductive tissues and the As tissue distribution of *nip7;1* plants altered over time, the As concentration of roots, rosette leaves, pedicels and green siliques of WT and *nip7;1* plants exposed to 150μM AsV for three weeks was compared (Figure 3.19). The As concentration of rosette leaves, pedicels and green siliques was significantly higher in *nip7;1* plants compared to WT. This is consistent with the increased shoot:root As ratio observed in *nip7;1* plants after two weeks exposure to 150μM AsV (Figure 3.17).

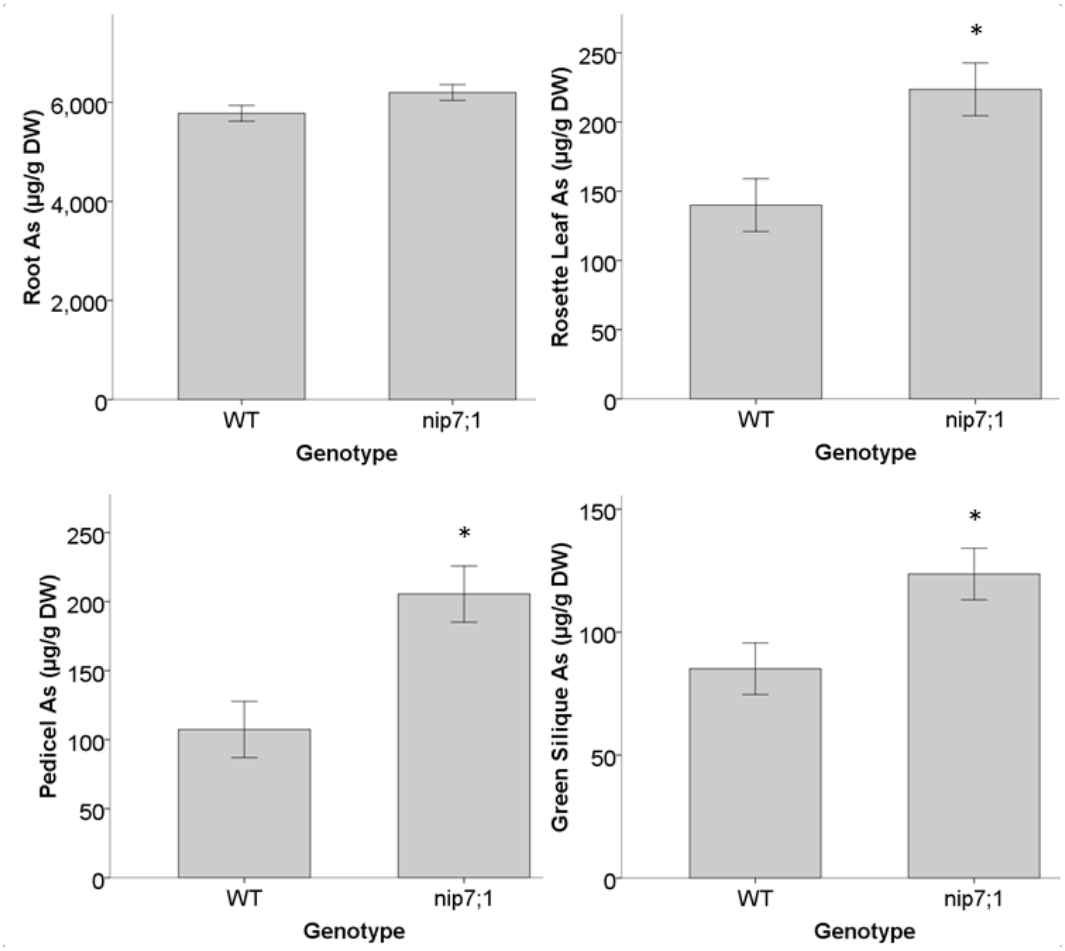

Figure 3.19 Arsenic concentration of WT and *nip7;1* plant tissues after long term AsV exposure

Graphs show the As concentration of WT and *nip7;1* plant tissues after three weeks exposure to 150μM AsV in hydroponics. The top left and right panels show the average root and rosette leaf As concentrations respectively. The bottom left panel shows the average As concentration of pedicels and the bottom right panel shows the As concentration of green siliques (siliques were collected at growth stage 17 [178]). Data are from four independent experiments, values are means ±SEs and asterisks indicate significant differences between genotypes at $P<0.05$ using an unpaired *t*-test.

In addition, WT and *NIP* T-DNA insertion mutants were grown on soil and watered with 150μM AsV from 3wo till maturity. Upon senescence, seeds were collected and the As concentration was compared between genotypes (Figure 3.20). Despite having an increased shoot:root As and a higher concentration of As in rosette leaves, pedicels and green siliques after long term exposure to AsV, seeds from *nip7;1* plants contained significantly less As than WT. Seeds from *nip6;1* and *nip6;1nip7;1* plants also contained significantly less As than WT, suggesting that group II NIPs may have an important role in As loading of the seed in *Arabidopsis*.

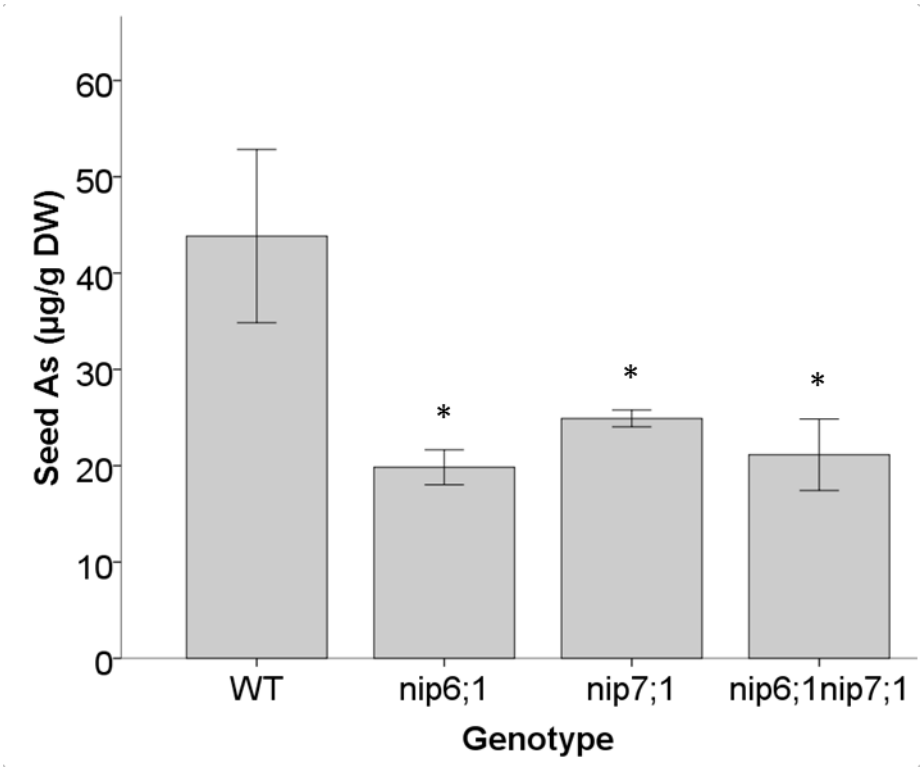

Figure 3.20 Arsenic concentration of WT and *nip* mutant plant seeds
The graph shows the As concentration of seeds collected from plants grown on soil and exposed to 150μM AsV from 3wo to maturity. Data are from four independent experiments, values are means ±SEs and asterisks indicate significant differences between genotypes at $P<0.05$ using a one-way ANOVA.

3.3.4 Long Distance Arsenic Transport in *nip6;1, nip7;1* and *nip6;1nip7;1* Knockout Lines

The altered distribution of As between tissues observed in loss of function *NIP* mutants could be caused by differences in the long distance transport of As throughout the plant. To explore this further, the As concentration of the xylem and phloem was compared between WT and knockout plants.

3.3.4.1 Xylem Arsenic Concentration

The As concentration of xylem sap collected from 5wo plants exposed to 150µM AsV for 24 hours was compared between WT, *nip6;1, nip7;1* and *nip6;1nip7;1* plants (Figure 3.21). The rate of water loss was measured over the period of As treatment and used to calculate the flux of As from root to shoot (Figure 3.21). The concentration of As in the xylem sap and the flux of As through the xylem was significantly lower in *nip7;1* plants compared to WT while no difference was observed in xylem As flux between WT and either *nip6;1* or *nip6;1nip7;1* plants.

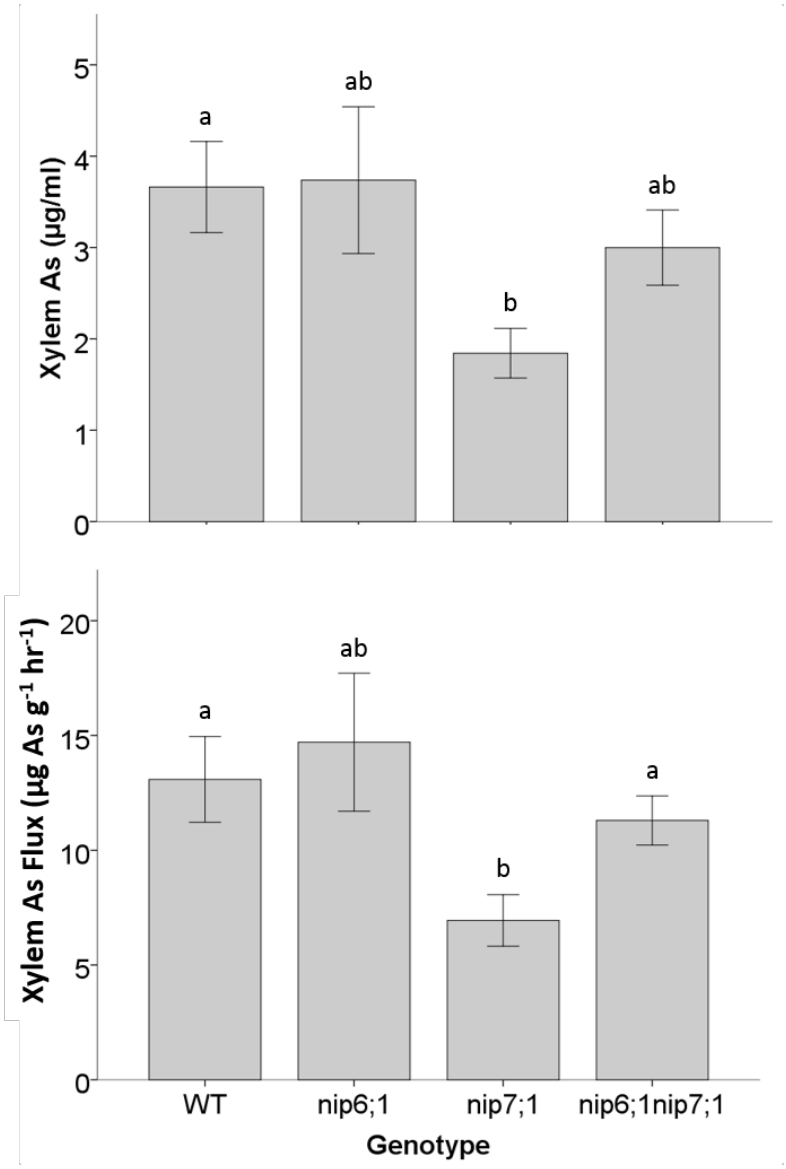

Figure 3.21 Arsenic concentration of xylem sap after 24 hours exposure to AsV
The top panel shows the total As concentration in the xylem sap of plants exposed to 150µM AsV for 24 hours. The bottom panel shows the flux of As through the xylem of the same plants. Flux is calculated as the rate of transpiration (water loss per gram of plant fresh weight) multiplied by xylem sap As concentration. The experiment was repeated three times, with samples collected from at least two individuals of each genotype per repeat. Values are means ±SEs and different letters indicate significant differences between genotypes at $P<0.05$ using a one-way ANOVA.

Xylem sap was also collected from WT, *nip6;1, nip7;1* and *nip6;1nip7;1* plants after long term (3 weeks) exposure to 150μM AsV to determine if the difference in As flux through the xylem between WT and *nip7;1* plants changes with length of exposure. Both the concentration of As in the xylem sap and the As flux had increased around 4 fold after 3 weeks exposure to AsV compared with 24 hours exposure for all genotypes except the double mutant, which had increased around 2 fold (Figure 3.22). The concentration of As in xylem sap in *nip7;1* plants was significantly lower than WT plants after long term exposure to AsV. The flux of As through the xylem in *nip7;1* plants was also reduced compared to WT although the difference was not statistically significant (P=0.051). The As concentration of xylem sap and As flux of double mutant plants was significantly less than both WT and *nip7;1* single mutants after long term AsV exposure.

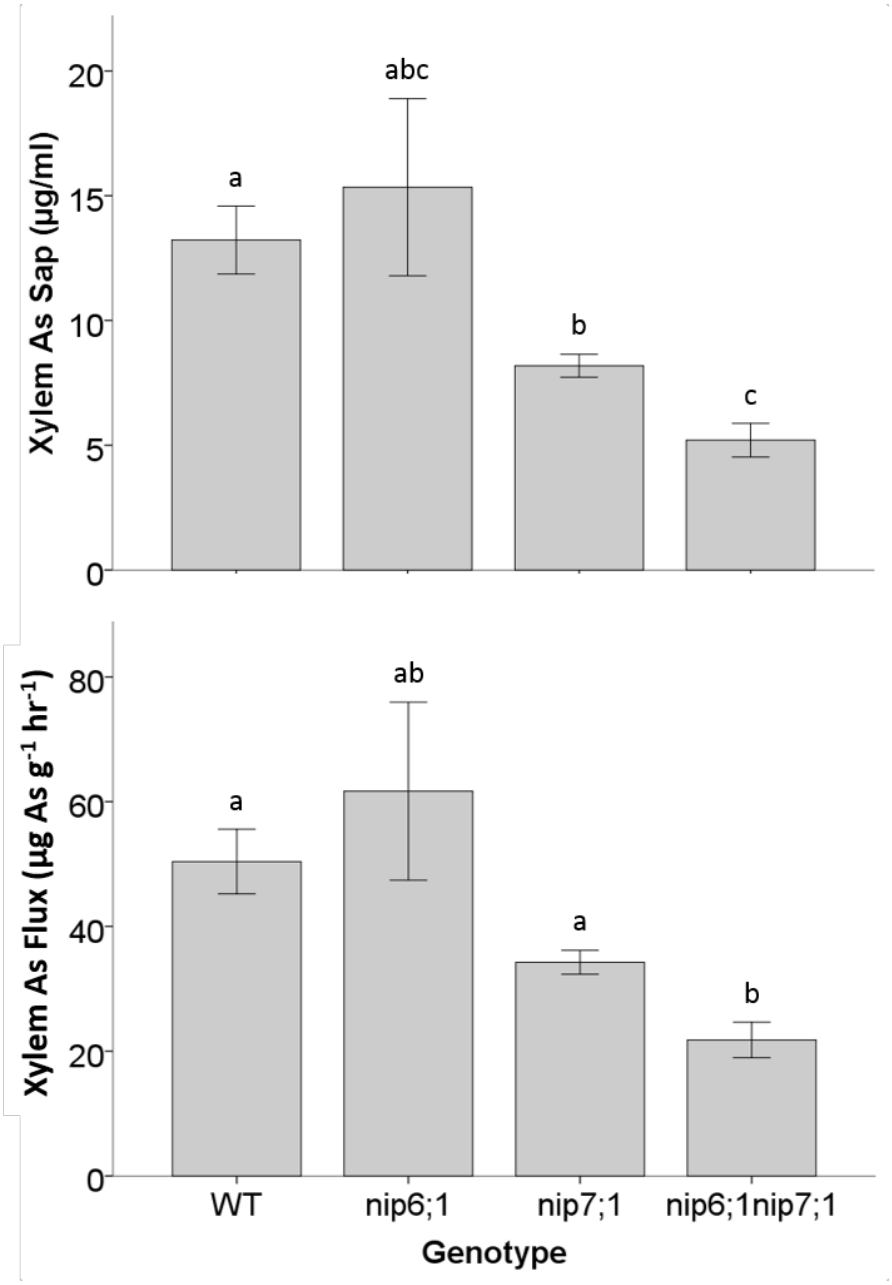

Figure 3.22 Arsenic concentration of xylem sap after 3 weeks exposure to AsV
The top panel shows the total As concentration in the xylem sap of plants exposed to 150µM AsV for 3 weeks. The bottom panel shows the flux of As through the xylem of the same plants. Flux is calculated as the rate of transpiration (water loss per gram of plant fresh weight) multiplied by xylem sap As concentration. Samples were collected from four individuals of each genotype. Values are means ±SEs and different letters indicate significant differences between genotypes at $P<0.05$ using a one-way ANOVA.

3.3.4.2 Phloem Arsenic Concentration

The As concentration of phloem exudate was measured from the cut petioles of WT, *nip6;1, nip7;1* and *nip6;1nip7;1* plants after exposure to 150µM AsV for three weeks in hydroponics. Phloem As concentration was calculated as µg As exuded relative to the As concentration of the leaves (Figure 3.23). Both *nip6;1* and *nip7;1* plants released a smaller proportion of As into the phloem compared to WT. The leaves of *nip7;1* plants

also had a significantly higher As concentration than WT after exposure to 150μM AsV, which is consistent with the increased shoot As concentration and shoot:root As observed after 2 and 3 weeks exposure to 150μM AsV (Figures 3.16-17 & 3.19).

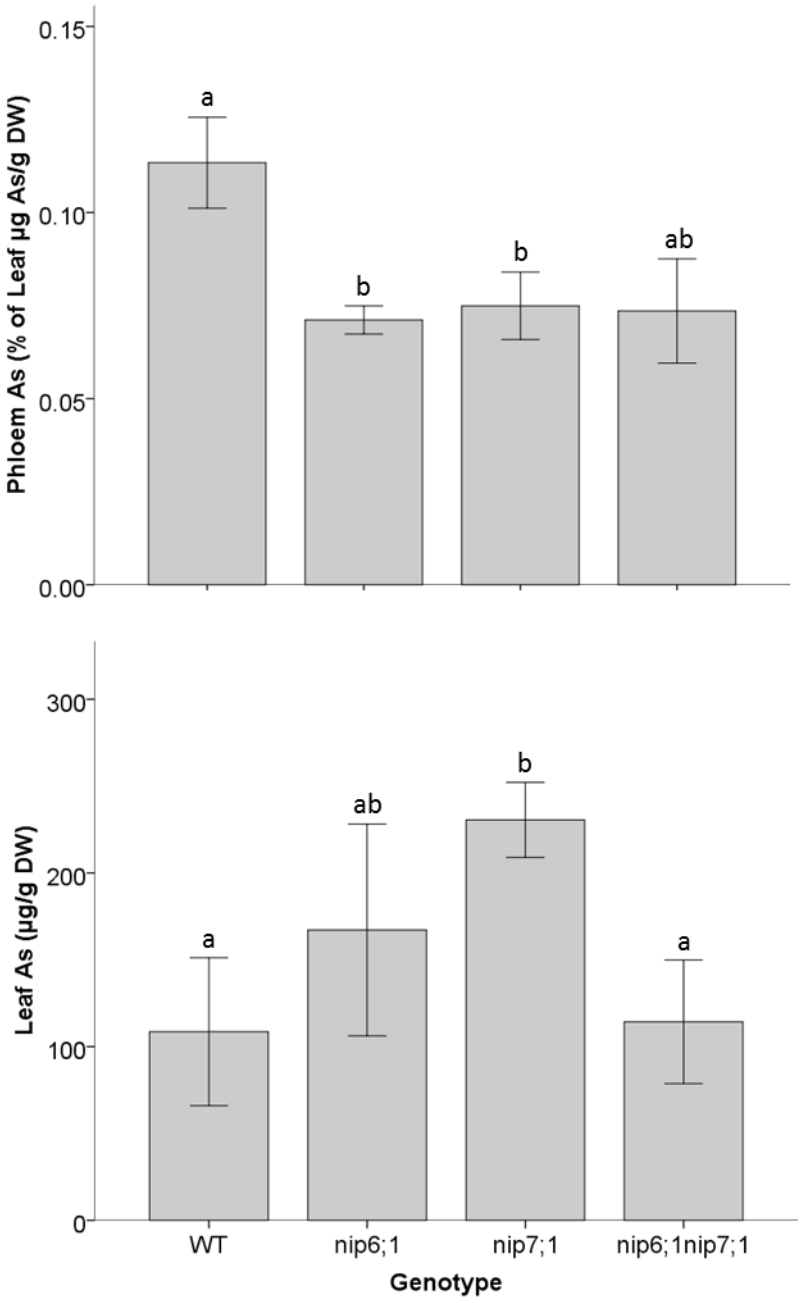

Figure 3.23 Arsenic concentration of phloem exudate from WT and *nip* mutant plants
Graphs show the phloem As concentrations (top panel) of plants exposed to 150μM AsV. The As in the phloem exudate is expressed relative to the As concentration in the leaves (bottom panel). Data are from four independent assays. Values are means ± SEs and different letters indicate significant differences between genotypes at $P>0.05$ using a one-way ANOVA.

3.3.4.3 Source to Sink Partitioning of Arsenic

NIP6;1 has been implicated in the source to sink partitioning of B and is required for the preferential transport of B to young, growing tissues in B limiting conditions [174]. The

phloem As concentration of *nip6;1* plants was reduced compared to WT plants which is consistent with the proposed role of *NIP6;1* in xylem to phloem transfer of B and suggests that *NIP6;1* may also be involved in the source to sink partitioning of As. To investigate this, WT and *nip6;1* plants were exposed to 50µM AsV for four weeks and the As concentration of rosette leaves and shoot apices determined. There were no differences in the As concentration of rosette leaves or shoot apices between WT and *nip6;1* plants (Figure 3.24). There was also no difference in the source to sink partitioning of As calculated as As concentration in shoot apices relative to As concentration in rosette leaves.

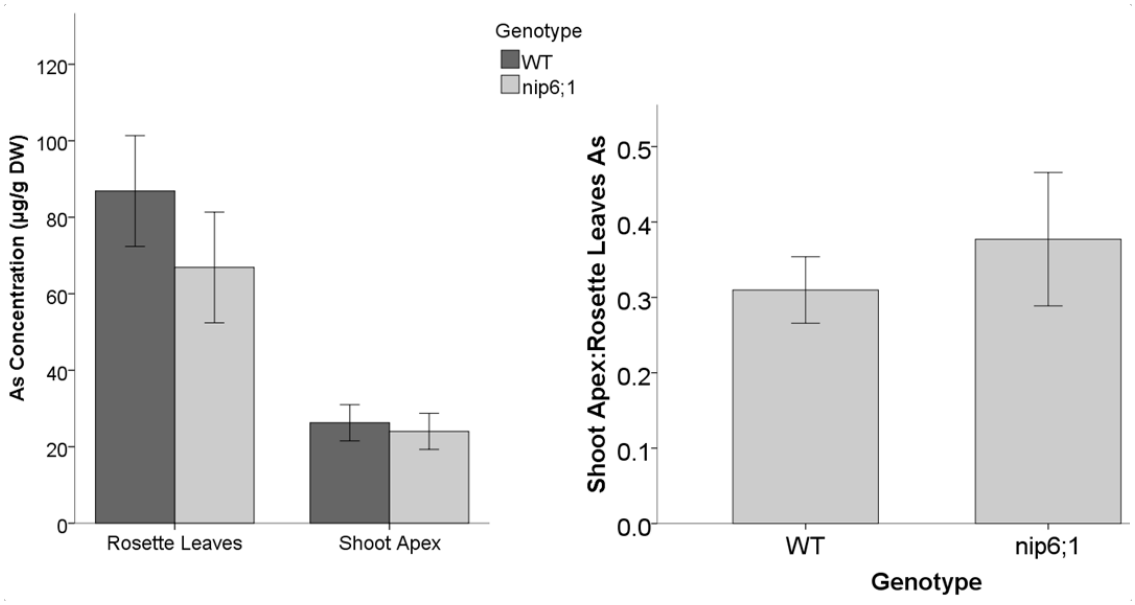

Figure 3.24 Arsenic concentration of source and sink tissues of WT and *nip6;1* plants
The left panel shows the As concentration of rosette leaves and shoot apices of WT and *nip6;1* plants after four weeks exposure to 50µM AsV. The right panel shows the ratio of As concentration between shoot apices and rosette leaves. Data are from three individual assays, values are means ± SEs.

The source to sink partitioning of As between old and young leaves in WT, *nip6;1, nip7;1* and *nip6;1nip7;1* plants was also investigated (Figure 3.25). There were no differences between genotypes in the As concentration of old or young leaves, however *nip6;1* plants had a significantly reduced ratio of As between young and old leaves indicating that loss of function in *nip6;1* results in proportionally less As transported to sink tissues. This is consistent with the reduced As concentration of the phloem observed in *nip6;1* plants (Figure 3.23). The ratio of As between young and old leaves of *nip7;1* and *nip6;1nip7;1* plants was also reduced compare to WT, although the differences were not statistically significant.

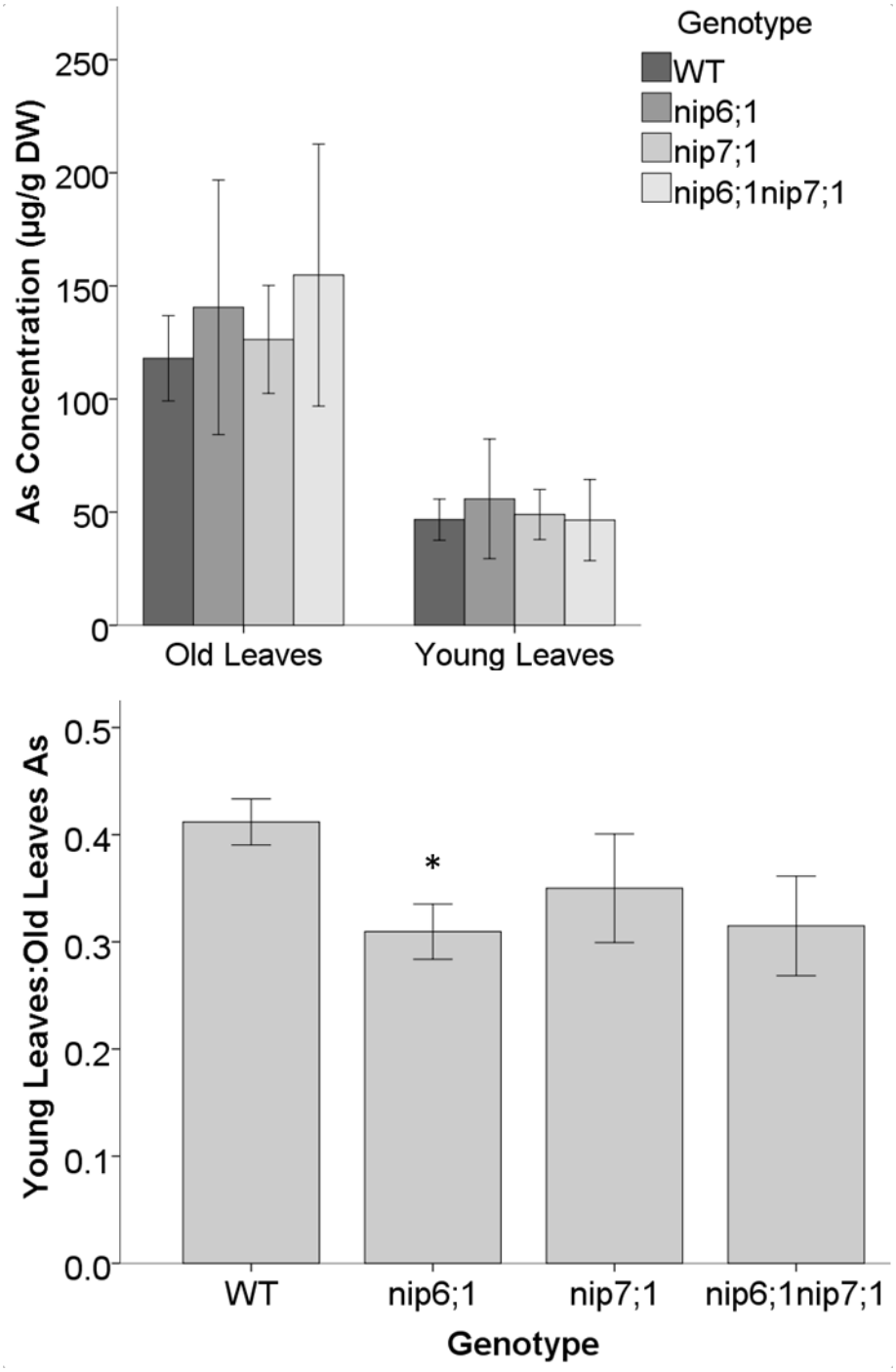

Figure 3.25 Arsenic concentration of source and sink tissue of WT and *nip* mutant plants
The top panel shows the total As concentration of old and young leaves of WT, *nip6;1, nip7;1* and *nip6;1nip7;1* plants exposed to 50µM AsV for one week in hydroponics. The three youngest and oldest leaves were collected from six individuals for each genotype. The experiment was repeated five times. The bottom panel shows the ratio of As concentration between young and old leaves. Values are means ± SEs and asterisks indicate a significant difference with WT at $P<0.05$ using a one-way ANOVA.

3.4 Discussion

Previous studies on NIPs in *Arabidopsis* have focused on the response to AsIII and have implicated *NIP1;1, NIP3;1* and *NIP7;1* in As uptake and tolerance. So far, only

NIP3;1 has been shown to be involved in root to shoot translocation of As. The potential roles of these bi-directional channels in As efflux and in the response to AsV has yet to be explored. In this chapter the role of group II NIPs in As uptake, efflux translocation and tissue distribution in response to both AsIII and AsV has been investigated and diverse roles of *NIP6;1* and *NIP7;1* have been revealed.

3.4.1 Role of *NIP6;1* in Source to Sink As Transport

NIP6;1 has previously been characterised for its role in B transport in *Arabidopsis*. *NIP6;1* transcript accumulates at the nodal regions of shoots where it is localised to the phloem region of vascular tissues. It is thought to be important for the xylem to phloem transfer of B at nodes, and is essential for delivering B to developing shoot tissues, including young leaves and shoot apices, under B limiting conditions [174]. Heterologous expression of *NIP6;1* in yeast conferred increased sensitivity to AsIII and increased tolerance to AsV indicating bi-directional AsIII transport activity [57], however the role of *NIP6;1* in As transport in plants has not been defined.

Loss of function *nip6;1* plants have been studied for altered tolerance to As by growth of seedlings on agar plates containing AsIII or AsV [58, 59] and no significant differences were observed in the growth of *nip6;1* and WT plants. In this study, *nip6;1* plants were exposed to different concentrations of AsIII or AsV on plates and in hydroponics. Compared to WT plants, *nip6;1* displayed a small but significant increase in tolerance to AsV in terms of root growth (Figure 3.8) and whole plant growth rate (Figure 3.9). No difference in growth was observed in response to AsIII.

Loss of function mutation in *nip6;1* did not significantly impact on total plant As uptake, efflux or root to shoot translocation. There was also no change in xylem As concentration or flux, however the amount of As released into the phloem of mature petioles was significantly reduced compared to WT (Figure 3.23). This is consistent with a role in xylem to phloem transfer of As and explains the reduced sink:source As ratio observed between young and old leaves of *nip6;1* plants (Figure 3.25). It may also explain the increase in AsV tolerance observed in *nip6;1* plants; reduced As partitioning to the young, growing regions of the shoot could lead to reduced As toxicity in these tissues and increased plant growth rates.

Reduced source to sink partitioning of As in *nip6;1* plants extends to the ultimate sink tissue of the seed. In *nip6;1* plants exposed to AsV from 3wo to maturity, seed As concentration was reduced >2 fold compared to WT plants. This highlights the importance of phloem mediated As transport in As loading of the seed. A similar mechanism for As loading of *Arabidopsis* seed was recently reported for loss of

function inositol transporter mutants [70]. Knockout mutation of *INT2* and *INT4* resulted in reduced As loading of the phloem which corresponded with reduced seed As concentrations following exposure to AsIII.

3.4.2 Role of NIP7;1 in Tissue Arsenic Distribution and Tolerance

Previous studies have shown that loss of function of *nip7;1* improves tolerance to AsIII and results in reduced total plant As concentrations [58]. In this study increased tolerance to AsIII was not observed for *nip7;1* plants grown on agar plates or in hydroponics, probably due to differences in experimental set-up. The reported tolerance of *nip7;1* plants was observed under low levels of AsIII stress [58], whereas in this and other studies [59, 179] which did not detect improved tolerance, *nip7;1* plants were exposed to higher concentrations of AsIII. Future studies would benefit from the calculation of a dose-response curve of As on growth of WT plants to enable an appropriate range of As treatment concentrations to be chosen.

Loss of function *nip7;1* plants showed increased tolerance to AsV, growing faster than WT plants exposed to different concentrations of AsV in hydroponics (Figures 3.9 & 3.11). Detailed As tissue distribution analysis revealed *NIP7;1* is involved in As efflux and long distance transport in the plant. Loss of function *nip7;1* mutants effluxed significantly more As to the external medium compared to WT plants, in agreement with previous studies [127]. The increased efflux from *nip7;1* roots may be an indirect effect of the reduced translocation of As from the root to the shoot through the xylem. Although the shoot:root As of *nip7;1* plants used for the efflux experiment did not differ from WT (Figure 3.13), increased concentrations of As in specific parts of the root may be the driving force for greater efflux to the external medium. This could occur through other NIP proteins located at the epidermis of the roots such as NIP3;1 or NIP5;1 [59, 154]. Alternatively, loss of function of *nip7;1* may result in increased net efflux due to reduced uptake of AsIII from the medium. The bulk of the AsV taken up into the plant will rapidly be reduced to AsIII before being effluxed from the root [82, 88]; knockout of *nip7;1* may reduce recycling of effluxed AsIII back into the root.

Increased As efflux may contribute to the increased AsV tolerance of *nip7;1* plants, as may the reduced flux of As through the xylem and phloem. The effect of loss of function of *nip7;1* on tissue As distribution depended on the As concentration, speciation and length of exposure. After short term exposure to AsV and long term exposure to AsIII, *nip7;1* plants had a reduced shoot As concentration and a reduced shoot:root As compared to WT plants (Figures 3.14-17) indicating that the reduced xylem As flux had a more significant impact than the reduced phloem As flux on tissue As distribution in the mutant plants. This is not entirely unexpected as phloem flux is generally around 3

to 4 fold lower than xylem flux [180]. However, after longer term exposure to AsV, *nip7;1* plants accumulated higher levels of As in the shoot compared to WT despite showing increased tolerance. It could be that as shoot As concentrations increase with length of exposure, reduced As flux through the phloem becomes relatively more important leading to increased shoot:root As in *nip7;1* plants relative to WT.

Increased As accumulation in AsV tolerant plants has been reported before; Caterecha, P. *et al.* [181] identified an allele of the high affinity phosphate transporter *PHT1;1* with a reduced rate of AsV uptake which nevertheless resulted in increased tolerance and accumulation. The reduced uptake rate was suggested to allow more efficient detoxification of AsV resulting in enhanced AsV reduction, complexation and vacuolar sequestration, leading to greater As accumulation without greater phytotoxicity. There may be more efficient detoxification and sequestration of As in the shoots of *nip7;1* knockout plants as a result of reduced As flux through the xylem and phloem. This could help explain the improved tolerance and increased accumulation over time.

Increased shoot:root As was observed only in *nip7;1* plants after long term exposure to 150μM AsV. Long term treatment with the lower concentration of 30μM AsV lead to reduced root and total plant As concentrations in *nip7;1* plants compared to WT and no significant difference in shoot or shoot:root As (Figure 3.18) while treatment with an equimolar concentration of AsIII resulted in reduced shoot and shoot:root As in the mutants (Figures 3.14-5). This highlights the dynamic effect that knockout of *nip7;1* has on tissue As distribution, which alters with length of exposure and is dependent on the concentration and speciation of As.

As NIPs are permeable to AsIII and not AsV, it is reasonable to conclude that the role of *NIP7;1* in As transport in the plant would be the same regardless of the speciation of As the plant is exposed to. However, the differences in tolerance and As tissue distribution observed in this study suggest that both WT and *nip7;1* plants respond differently to AsIII and AsV treatment. It would therefore be interesting for future studies to investigate differences in As speciation between WT and *nip* mutant plants exposed to AsIII and AsV, as in the present study only total As concentration was measured.

Previous studies [57] on AsIII transport through NIP proteins heterologously expressed in yeast suggested that aquaporin channels may have different preferences regarding direction of AsIII transport. Yeast transformed with NIP5;1 and NIP6;1 grew better than yeast transformed with rAQP9 (Aquaporin 9 from rat), while growth of rAQP9 expressing yeast was more severely inhibited by AsIII than the NIP5;1 or NIP6;1 expressing yeast [57]. This mechanism could impact on the role of individual NIPs in

response to different As species, and could be particularly interesting for NIP7;1 whose function may also be regulated through gating of the pore [169]. Future studies characterising the regulation and function of NIPs in AsIII influx and efflux *in planta* may help explain the different responses to AsIII and AsV in terms of tissue As distribution and tolerance.

Despite increased As concentrations in the shoot, rosette leaves, pedicels and green siliques after long term AsV exposure, *nip7;1* knockout plants had significantly reduced As concentration in the seed (Figure 3.20). This may be a result of the reduced As flux through the phloem in *nip7;1* plants (Figure 3.23). However, a direct effect of *NIP7;1* on As loading into the seed is more likely because a lower phloem flux would also reduce the As concentration of other non-transpiring tissues such as the pedicel and siliques. *NIP7;1* is expressed at a relatively low level in many tissues throughout the plant but is most highly expressed in the reproductive tissues (Figure 3.3). A transcriptomic study of maternal seed tissues [182] revealed upregulation of *NIP7;1* in the seed coat and funiculus of seeds at the mature green stage of development. Interestingly, *NIP6;1* was identified as uniquely expressed in the funiculus where it was >5 fold upregulated compared to other tissues tested, while *NIP5;1* was also highly upregulated in the funiculus at the mature green stage of seed development. The funiculus represents the primary source of water and nutrients for seed growth and development as it is the only tissue physically connecting the seed to the maternal plant. Expression of group II NIPs in the funiculus suggests they may be directly involved in As loading of the seed, which could help explain the mechanism by which *nip7;1* knockout plants accumulate increased As concentrations in the pedicel and green siliques whilst excluding As from the mature seed. It would be interesting to analyse the As concentration of triple mutant seeds, to determine if knocking out all three group II NIPs would reduce As accumulation in the seed even further.

3.4.3 Effect of Double Loss of Function in *nip6;1nip7;1* Plants

Loss of function T-DNA insertions in *nip6;1* and *nip7;1* resulted in increased tolerance to AsV. However, with the exception of root growth rate on agar plates, combining both insertions into a double mutant did not have the additive effect of further increasing tolerance to As. Similarly, the efflux, uptake, distribution and long distance transport of As in *nip6;1nip7;1* plants was intermediate to the single mutants. This suggests that *NIP6;1* and *NIP7;1* may have epistatic roles in As transport. Both *NIP6;1* and *NIP7;1* are required for normal plant growth (Figures 3.8-9) and have been implicated in B transport and nutrition [169, 174] suggesting that they may form part of the same transport pathway mediating long distance B and As distribution between plant tissues.

3.5 Conclusions

Group II NIPs are important in the response to As; loss of function mutations in *nip6;1* and *nip7;1* led to increased AsV tolerance and differential spatiotemporal distribution of As, most likely through altered As loading of the phloem and xylem. The role of *NIP6;1* in As transport appears to be similar to its role in B transport from source to sink tissues through phloem loading. *NIP7;1* is important in As efflux, uptake and long distance transport through the xylem and phloem. Interestingly, the initial response to As exposure was not indicative of the long term pattern of tissue distribution and As tolerance was not correlated with As concentrations or shoot:root translocation. Loss of function mutation in both *nip6;1* and *nip7;1* significantly affected seed As concentration, making them prime targets for the development of crops with a lower dietary As impact.

In conclusion, NIPs may be very relevant targets for engineering As tolerance and reducing seed/grain As accumulation in crops grown both in anaerobic conditions where AsIII predominates in addition to those grown in aerobic soils where AsV is the predominant species. On the other hand, increased As accumulation in above ground tissues coupled with improved tolerance (as observed in *nip7;1* plants) would be beneficial for phytoremediation attempts.

Chapter 4: Identification of Novel Genes Involved in Arsenic Tolerance in *Arabidopsis*

4.1 Introduction

While significant progress has been made over the past decade or so in our understanding of the As transport, metabolism and detoxification mechanisms in plants, there are still many gaps in our knowledge of how plants respond to As. One way to identify novel components of the plant As response is through genetic screens. In this chapter both forward and reverse genetic approaches have been employed to try and identify novel genes involved in As tolerance in *Arabidopsis*.

A collection of 6868 confirmed homozygous T-DNA insertion lines (CS27941) was obtained from NASC [176]. Each line in the collection contains a T-DNA insertion at a unique location in or near a gene, representing coverage of approximately 25% of the *Arabidopsis* genome. The approximate location of each insertion is known and can be visualised using the T-DNA Express: Arabidopsis Gene Mapping Tool (http://signal.salk.edu/cgi-bin/tdnaexpress) making this a useful tool for carrying out forward genetic screens.

This collection was used for both forward and reverse genetic screens. A reverse genetics approach was taken by identifying insertions in genes already characterised as important in the response to As in other species. A search for arsenic in a FOX (full-length cDNA over expressed) *Arabidopsis* mutant database [183] revealed two *Arabidopsis* orthologues of As associated rice genes. The first of these, Os02g0745000, is one of 6 rice proteins that show homology to the bacterial arsenical pump ATPase (ArsA). The closest orthologue of Os02g0745000 in *Arabidopsis* is At3g10350. The other As associated rice genes were Os10g0447900/Lsi3 and Os02g0822100. These are two out of five rice homologues of the AsIII efflux transporter *OsLsi2* (Figure 4.1).

OsLsi2 has been characterised as a Si and AsIII efflux transporter in rice which belongs to an uncharacterised family of anion transporters predicted to have 11 transmembrane domains [56, 65]. Unlike transport through Lsi1, efflux through Lsi2 is an active process, assumed to depend on the proton gradient across the membrane [65]. Orthologues of *Lsi2* can be found in other Si accumulating plants such as barley and maize (*ZmLsi2* and *HvLsi2*) [184] and also in non-accumulators including tomato (Solyc06g036100) and *Arabidopsis* (At1g02260). Similar to OsLsi2, the maize and barley orthologues localise to the plasma membrane where they have Si efflux activity [184]. The physiological role of Lsi2 in tomato and *Arabidopsis* is less clear, as these plants do not accumulate Si [185] suggesting an alternative role of Lsi2 in these species.

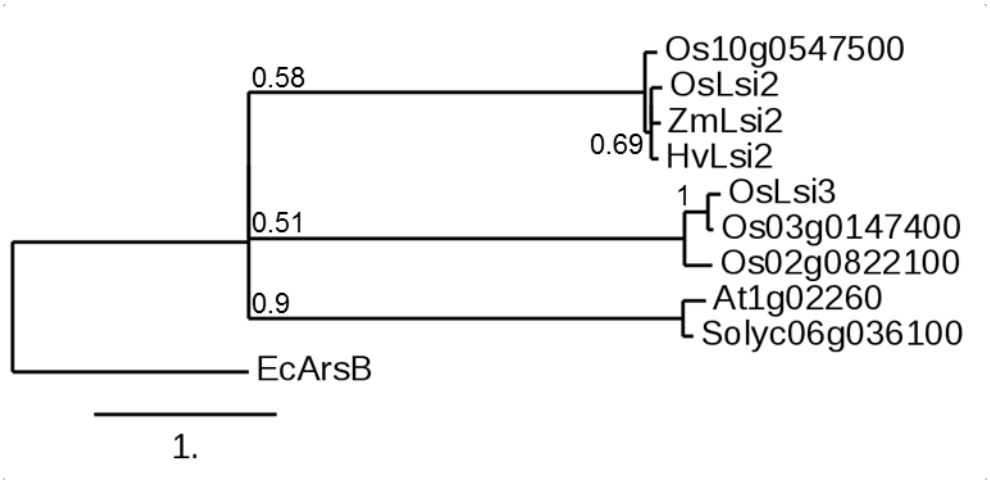

Figure 4.1 Phylogeny of Lsi2 orthologues
Phylogenetic tree of Lsi2 orthologues in rice, maize, barley, tomato and *Arabidopsis* constructed from amino acid sequences using the 'One Click' phylogeny analysis on the Phylogeny.fr website [170]. The tree is rooted to the *E.coli* ArsB protein. Branch lengths are proportional to the number of substitutions per site and branch annotations are Confidence Indexes analogous to bootstrap values.

A forward genetic screen was carried out with the aim of identifying novel genes involved in As tolerance in *Arabidopsis*. The screen generated a list of potential candidates, one of which was chosen for further characterisation. At2g21900 encodes a member of the WRKY transcription factor superfamily (WRKY59) which has 74 members in *Arabidopsis*.

WRKYs are plant specific transcription factors (TFs) characterised by the presence of at least one highly conserved WRKY domain. The WRKY domain is ~60 amino acids in length with the residues WRKYGQK at the N terminus and an atypical zinc finger structure at the C terminus [186]. The WRKY domain folds into a four stranded β-sheet which enters into the major groove of DNA, the WRKYGQK residues partly protrude from the surface of the protein and make contact with the DNA [187]. All WRKY TFs recognise and bind to the DNA sequence motif TTGACC/T known as the W box [186]. The W box is the minimal consensus sequence required for DNA binding of WRKY TFs although adjacent DNA sequences also partly determine binding site preference, which allows for specificity between targets [188]. WRKY TFs can both repress and activate gene expression, and individual TFs can regulate seemingly unrelated and distinct processes [188]. They have a major role in response to biotic stress but have also been shown to respond to abiotic stresses such as drought, cold and nutrient deficiency, and have roles in germination, senescence and development [188, 189]. WRKY TFs are highly regulated, and have been shown to interact with map kinases, calcium dependent protein kinases, 14-3-3 proteins, calmodulin, histone deacetylases and can also form complexes with other WRKY TFs [188, 189]. The expression of

WRKY TFs can be moderated by proteasome-mediated degradation and many WRKYs are regulated by W boxes in their own promoter sequences [188, 189]. Therefore, WRKY TFs are members of diverse signalling webs whose expression and function are highly regulated at the transcriptional and post-transcriptional and translational levels.

An arsenic responsive WRKY TF has previously been described in *Arabidopsis; WRKY6* is rapidly upregulated upon exposure to AsV and negatively regulates the expression of the phosphate transporter *PHT1;1* leading to a reduction in AsV uptake [104]. The expression of *AtWRKY33, WRKY40* and *WRKY53* was downregulated in response to AsV [190] however their role in the As response has yet to be further explored. Two other *Arabidopsis* WRKY TFs have been indirectly associated with the AsV response through their roles in maintaining phosphate homeostasis. *AtWRKY45* expression is induced by low phosphate levels and positively regulates *PHT1;1* expression [191]. In conditions with sufficient phosphate, *AtWRKY42* positively regulates *PHT1;1* expression but negatively regulates *PHO1* expression [192]. Overexpression of both *WRKY45* and *WRKY42* resulted in enhanced sensitivity to AsV presumably caused by enhanced uptake through *PHT1;1* [191, 192].

In this chapter, T-DNA insertion mutants of candidate genes identified through forward and reverse genetics were investigated to determine their role in As tolerance. Growth experiments were carried out on both agar plates and in hydroponics to determine the effect of loss of function mutations in *LSI2* and *WRKY59* on tolerance to both AsIII and AsV. The As uptake, translocation, accumulation and efflux ability of *lsi2* and *wrky59* plants was also investigated to ascertain the mechanism of As tolerance in these lines.

4.2 Materials and Methods

4.2.1 Forward Genetics T-DNA Screen

For the initial screen, *Arabidopsis* T-DNA insertion line seeds were sown in individual wells of p60 inserts filled with sand and saturated with tap-water. Seeds were stratified at 4°C in the dark for 3 days before transfer to the glasshouse. Growth conditions in the glasshouse were maintained at around 22°C during the day and 17°C at night, with a minimum of a 16hr day. Plants were watered with Yoshida medium [148] for 2 weeks, thereafter they were watered with 1 litre of Yoshida medium containing 350μM AsV once a week and topped up with tap water in between as required. Photos were taken of the trays once a week to help facilitate identification of individual lines with particularly slow or vigorous growth. After four weeks of AsV treatment, plants were assessed by eye and particularly large or small plants were taken forward.

To narrow down the list of candidates, the Arabidopsis Information Resource (TAIR) bulk data retrieval tool was utilised to download gene descriptions and lines with insertions in genes with unknown function were discarded. The remaining candidates were re-sown on sand as described above except each line was sown in 6 individual wells and WT plants were included in each tray. Alternatively, around half of the lines were screened in 24-well tissue culture plates as this method was quicker and required less space. Around 10 seeds were sown into the wells containing 2ml half MS medium and stratified for 2 days at 4°C. Plates were lifted out and placed in the growth room (conditions as in Section 3.2.4). After 24hours to allow germination, 400μM AsV or 50μM AsIII was added to the medium. Seedlings were observed under a dissecting microscope and scored visually for growth compared to WT at 24 hour intervals for 3 days. Scoring was based on the size and colour (pale vs green) of seedlings.

The second round of screening resulted in a shortlist of 48 candidates (Table 6.1 in the Appendix) which was subsequently further narrowed down to 11 (Table 4.1) using the tissue culture plate screen and bioinformatics to search for the most interesting candidates. Second alleles were ordered from NASC for each of the 11 candidate genes. One candidate (At2g21900) was chosen for further characterisation based on the consistency and strength of the phenotype throughout the rounds of screening.

Table 4.1 Shortlist of candidate genes identified through a forward genetics screen for altered response to As

Gene ID	T-DNA Insertion Lines	As Tolerance	Gene Description
At3g55090	SALK_119868C SALK_005006C	>WT	ABC-2 type transporter family protein
At2g21900	SALK_039436C SALK_113059C	>WT	WRKY transcription factor
At2g27240	SALK_082322C SALK_141513C	>WT	Aluminium activated malate transporter family protein
At5g04260	SALK_045620C SALK_036628C	>WT	thioredoxin
At4g14030	SALK_058073C SALK_147322	>WT	Selenium binding protein
At5g17830	SALK_133704C SALK_096870	>WT	choline transporter family protein
At2g36950	SALK_151770C SALK_069207C	<WT	Heavy metal transport/detoxification superfamily protein
At1g77990	SALK_111268C SALK_076328C	<WT	Sulphate transporter
At2g02380	SALK_058977C SALK_036296	<WT	Glutathione S-transferase (zeta class)
At3g53510	SALK_031147C SALK_081053C	<WT	ABC-2 type transporter family protein
At3g07600	SALK_028592C SALK_123210C	<WT	Heavy metal transport/detoxification superfamily protein

4.2.2 Characterisation of T-DNA Insertion Mutants

T-DNA insertion mutants were characterised at the DNA and mRNA level using PCR and RT-PCR as described in Sections 3.2.1 and 3.2.3. Primers specific to *Lsi2* and *WRKY59* are listed in Table 4.2. The Salk ID of *lsi2-1* and *lsi2-2* is SALK_025230C and SALK_138220C respectively.

Table 4.2: Primers used for characterisation of *lsi2* and *wrky59* T-DNA insertion mutants

Primer Name	Sequence	Tm (°C)
Lsi2-1LP	GAAAATTGGAAAAGGGCTGA	48
Lsi2-1RP	CCATCTCTTGGTCTGGAACAT	48
Lsi2-2LP	TCCGCAGAATCTTGTTATTGC	51
Lsi2-2RP	GAAGAGACCAATCGCAGTGAC	51
Lsi2F	CCAGCTACATTTTCGCCAGT	53
WRKY59-1LP	GCACGAAAGTAGCCATGAAAG	47
WRKY59-1RP	TGATTTCTGCAATGAATAAATGTG	47
WRKY59-2LP	ATCGATCAATTTTAAACCGGC	48
WRKY59-2RP	TAGCTAGGCTTGTTTGAAGCG	48
WRKY59F	CGTATTTGCCGTCTGAAAGG	52
WRKY59R	TCGTCACCGACTTTGAGTTG	52

4.2.2.1 Growth Experiments

Growth experiments on plates and in hydroponics were carried out as described in Sections 3.2.4 and 3.2.5 for WT and *lsi2-1* T-DNA insertion mutant plants. For experiments with different B concentrations, H_3BO_3 was added to the medium at the concentrations indicated in the text. In B free medium, the micronutrient solution was made up without B and Phytagel (3g/L) was used as a gelling agent rather than Agar. For low S treatments, $MgSO_4$ was replaced in the medium with equimolar amounts of $MgCl_2$.

For *wrky59* T-DNA insertion mutants, growth experiments in hydroponics were carried out as described in Section 3.2.5. Growth experiments on plates were carried out as described in Section 3.2.4 except that sterilised seeds were sown directly onto treatment plates. Root lengths were marked 5 and 10 days after sowing and fresh weights were measured after 21 days. The experiment was repeated four times with each plate containing four individuals of each genotype. At least two plates of each treatment were included in each replicate.

4.2.2.2 Arsenic Concentration Analysis

The As concentration of root and shoot tissues was analysed as described in Section 3.2.6. Plants were grown in hydroponics and exposed to AsIII or AsV for 2 weeks at the concentrations indicated in the text.

The As efflux ability of the knockout and WT plants was determined as described in Section 3.2.9.

4.2.2.3 Statistical Analysis

As in Section 3.2.11

4.3 Results

4.3.1 Reverse Genetic Screen of T-DNA Insertion Mutants

4.3.1.1 Bioinformatics Analysis of *Lsi2*

A reverse genetic screen of the T-DNA insertion mutant collection identified two potential As associated *Arabidopsis* genes; At3g10350 and At1g02260. At3g10350 is the closest orthologue to the bacterial arsenical pump ATPase (*arsA)* in *Arabidopsis*. It is predicted to be localised to the plastid (using the SUBA3 database [193]) and is most highly expressed in seed tissue (using the Arabidopsis electronic fluorescent pictographic or eFP browser [194]). At3g10350 is one of three genes encoding uncharacterised anion transporting ATPase proteins. They have also been described as putative orthologues of yeast GET3 proteins, which are ATPases involved in the targeting of tail anchored proteins into the endoplasmic reticulum membrane [195]. This suggests that At3g10350 may be involved in protein targeting to the plastid membrane. At3g10350 and Os02g0745000 share ~75% identity in amino acid sequence with each other, but only ~30% identity with both ArsA and GET3 [196]. So far, no orthologues of ArsA have been shown to be involved in As extrusion in any plant species and so further investigations focused on the other As associated rice genes, Os10g0447900 and Os02g0822100.

The closest *Arabidopsis* orthologue to Os10g0447900 and Os02g0822100 is At1g02260, hereafter referred to as *Lsi2. Lsi2* is expressed in different tissues of the root, shoot and inflorescence. In root tissues, *Lsi2* is more strongly expressed in the outer cell layers (epidermis and cortex) compared to the endodermis and stele while in the shoot; *Lsi2* expression is particularly high in senescing leaves (Figure 4.2). Running the Genevestigator perturbations tool (filtered for conditions with ≥ 2 fold change in expression and a *P* value ≤ 0.05) revealed upregulation of *Lsi2* by biotic stress and low pH and downregulation by abiotic stresses including cold, drought and salinity stress [141]. Genevestigator was also used to search for genes with similar expression patterns to *Lsi2.* Co-expression with other genes may provide clues as to the function of Lsi2, as genes that are highly co-expressed may be involved in similar biological processes. The top scoring gene (with a Pearson's correlation co-efficient of 0.48) for co-expression with *Lsi2* using the perturbations option was *Mitogen Activated Protein Kinase 1* (*MPK1*) which is a component of signalling cascades that is activated by ABA,

JA and H_2O_2 [197]. Signalling through *MPK1* has been linked to abiotic stress responses and leaf senescence [198, 199].This suggests that *Lsi2* may be involved in leaf senescence and the response to abiotic stress and could potentially be regulated by a map kinase signalling cascade.

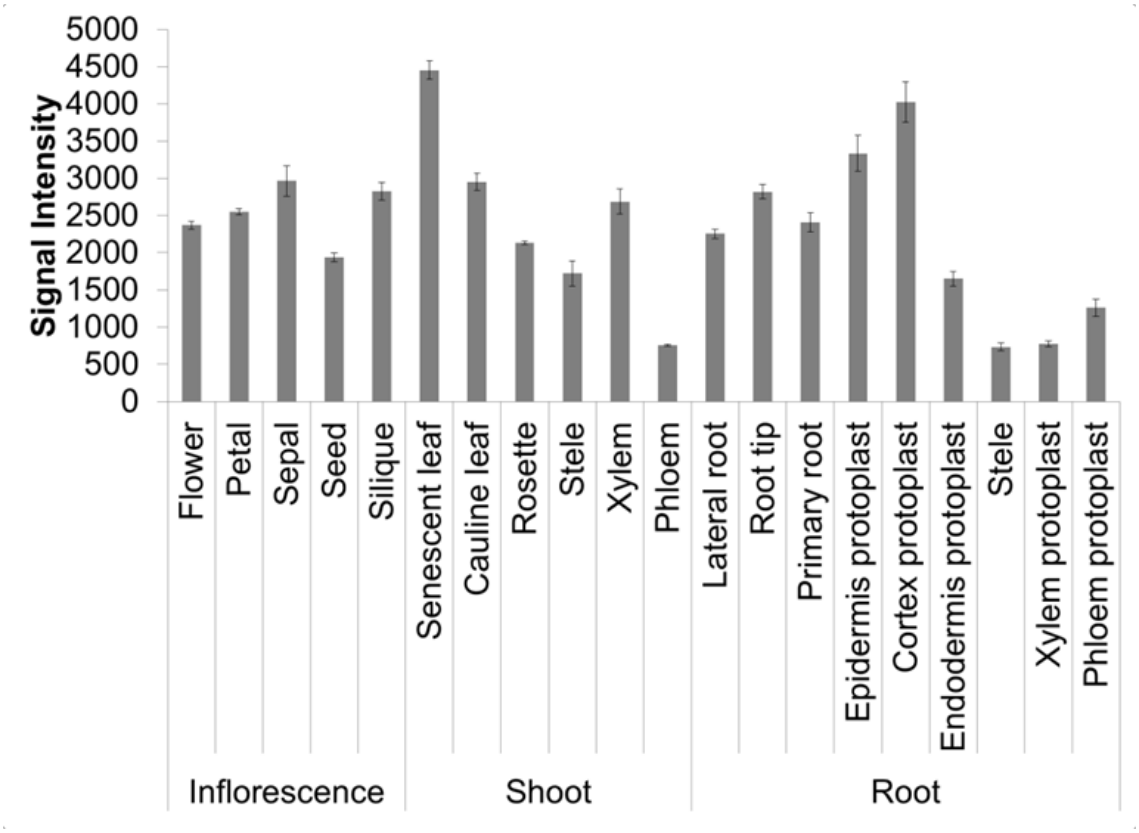

Figure 4.2 Expression pattern of *AtLsi2*
Graph showing the relative expression level of *Lsi2* in different *Arabidopsis* tissues. Data were obtained from the Genevestigator database [141]. Values are means ± SEs of signal intensities on the Affymetrix Rice Genome Array, plotted on a linear scale.

AtLsi2 encodes a gene with three exons and an open reading frame of 2437bp long. The deduced protein consists of 502 amino acids, has a molecular weight of 54.7 kDa and shares between 60 and 74% identity with the other Lsi2 plant homologues [196]. Using the SUBA3 database, AtLsi2 is predicted to be localised to either the tonoplast or plasma membrane [193], although all other Lsi2 homologues previously characterised have been localised exclusively to the plasma membrane [65, 66, 184, 200]. Entering the AtLsi2 protein sequence into the HMMER web service [201] revealed matches to two Pfam domain families, CitMHS and ArsB. The CitMHS domain is found in proteins related to two characterised citrate uptake permeases from *Bacillus subtilis*. The first of these is CitM which is a $citrate^{2-}Mg^{2+}/H^{+}$ symporter while CitH is thought to transport $citrate^{2-}Ca^{2+}$ complexes in symport with H^{+} [202]. The CitMHS domain is also found in the other plant orthologues of Lsi2 although none have been shown to have citrate transport capability so far. ArsB proteins are integral membrane proteins with arsenite

and antimonite efflux activity first identified in bacteria [203]. The presence of an ArsB domain in both OsLsi2 and AtLsi2 suggests that the *Arabidopsis* homologue may also have AsIII efflux activity and so could contribute to As tolerance, a hypothesis that is explored in this chapter using T-DNA insertion mutants of *AtLsi2*.

4.3.2 Characterisation of *lsi2* T-DNA Insertion Mutants

Two homozygous T-DNA insertion mutants in *Lsi2* were characterised at the mRNA level to confirm that they are true knockouts. The approximate position of T-DNA insertion in *lsi2-1* and *lsi2-2* is shown in Figure 4.4. The first allele is a true knockout, with no *Lsi2* transcript detected in *lsi2-1* plants. In the second allele, the T-DNA is inserted in the second exon resulting in truncation of the mRNA. No transcript was detected from *lsi2-2* using primers located in the first and third exon however transcript was detected when the primers used were both located in the first exon (Figure 4.3).

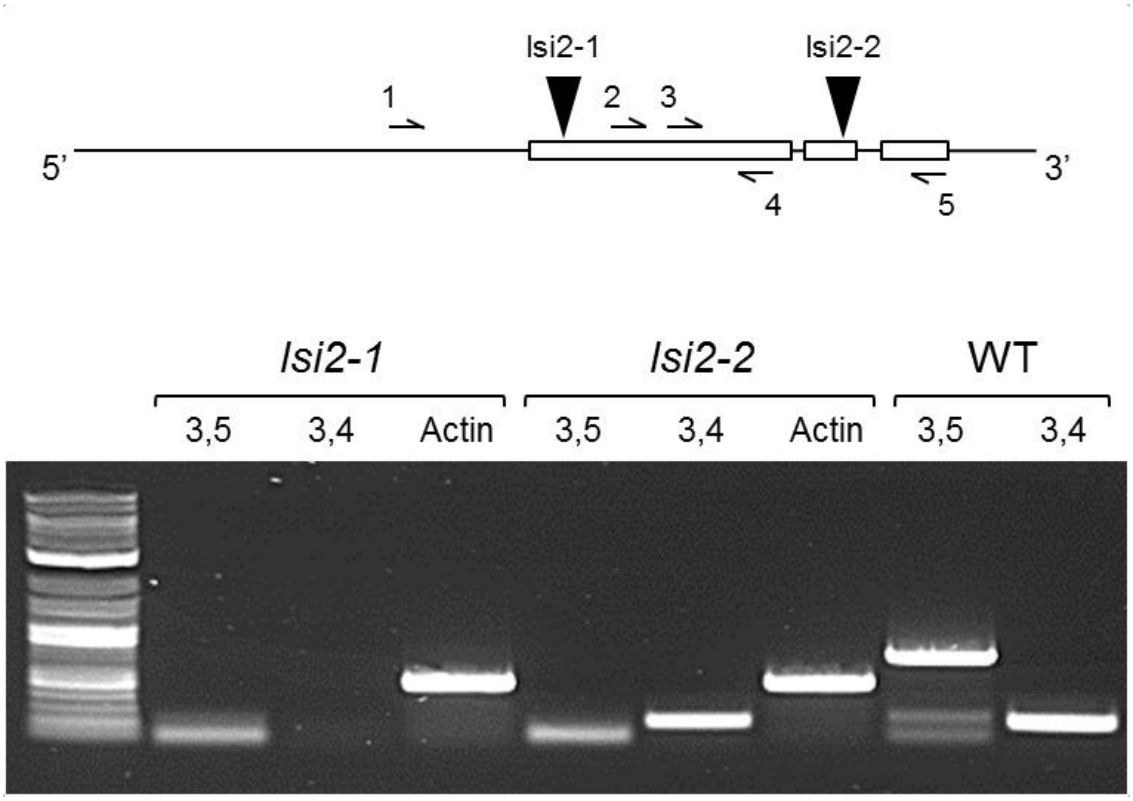

Figure 4.3 RT-PCR of *lsi2* T-DNA insertion lines
RT-PCR was performed on *lsi2-1, lsi2-2* and WT plants using primers specific to *Lsi2* and *Actin*. The top panel shows the approximate position of the T-DNA insertion in each line, with numbers 1-5 indicating the position of primers Lsi2-1LP, Lsi2-2LP, Lsi2F, Lsi2-1RP and Lsi2-2 RP respectively. The whole length of the genomic DNA is represented, with the position of the exons indicated by the rectangles. The bottom panel displays RT-PCR carried out on WT, *lsi2-1* and *lsi2-2* cDNA. A 2-Log DNA ladder was run in the first lane. Using primers 3 and 5, no band was observed for either T-DNA insertion line while a band of the expected size (789bp) was observed in WT plants. No band was observed using primers 3 and 4 in *lsi2-1* plants however bands of the expected size (201bp) were observed in *lsi2-2* and WT plants.

4.3.2.1 Growth Experiments on Agar Plates

WT and *lsi2-1* plants were grown on Agar plates containing different concentrations of AsIII or AsV. One week old seedlings were transferred to treatment plates and plant fresh weight was recorded after two weeks. In addition, root growth was monitored. When grown on control plates, *lsi2* knockout plants weighed significantly less than WT and their roots grew more slowly (Figures 4.4-5). When compared with growth on control plates *lsi2* plants were more sensitive to AsIII treatment than WT, with a significantly smaller fresh weight on plates containing 20μM AsIII (Figure 4.4). When grown on agar plates containing different concentrations of AsV, *lsi2* knockout plants weighed significantly more than WT and their roots grew significantly faster (Figure 4.6). These results suggest that *Lsi2* is important for normal plant and root growth, and that it is involved in the response to As.

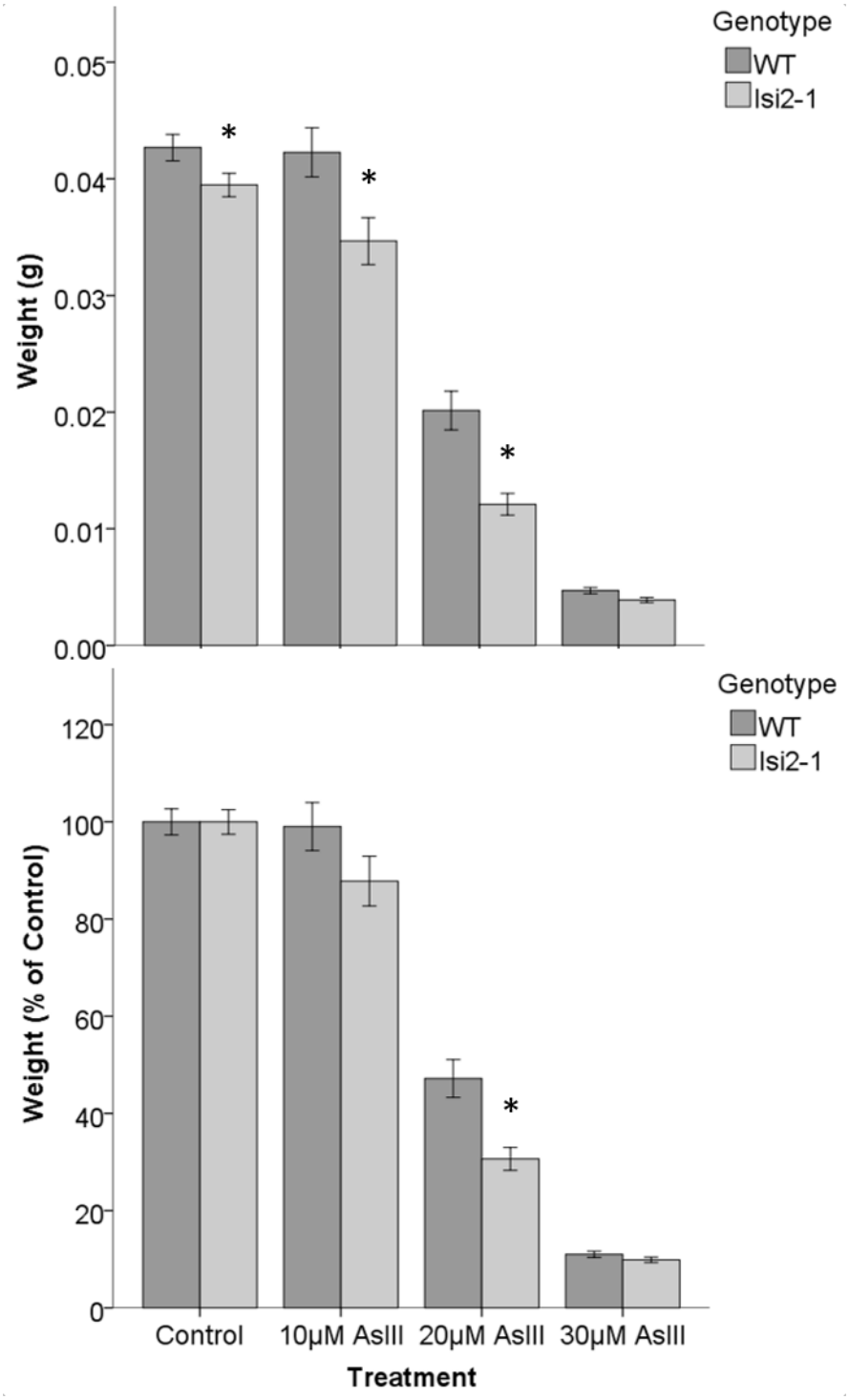

Figure 4.4 Fresh weight of WT and *lsi2-1* plants grown on plates containing AsIII
WT and *lsi2-1* seedlings were grown on agar plates for 7 days before transfer to plates containing different concentrations of AsIII. Fresh weights per plant were measured after 2 weeks on treatment plates. The top panel shows plant average fresh weight and the bottom panel shows the same data plotted relative to growth in control conditions. Data are from six independent experiments, values are means ± SE and asterisks indicate significant differences between genotypes at $P<0.05$.

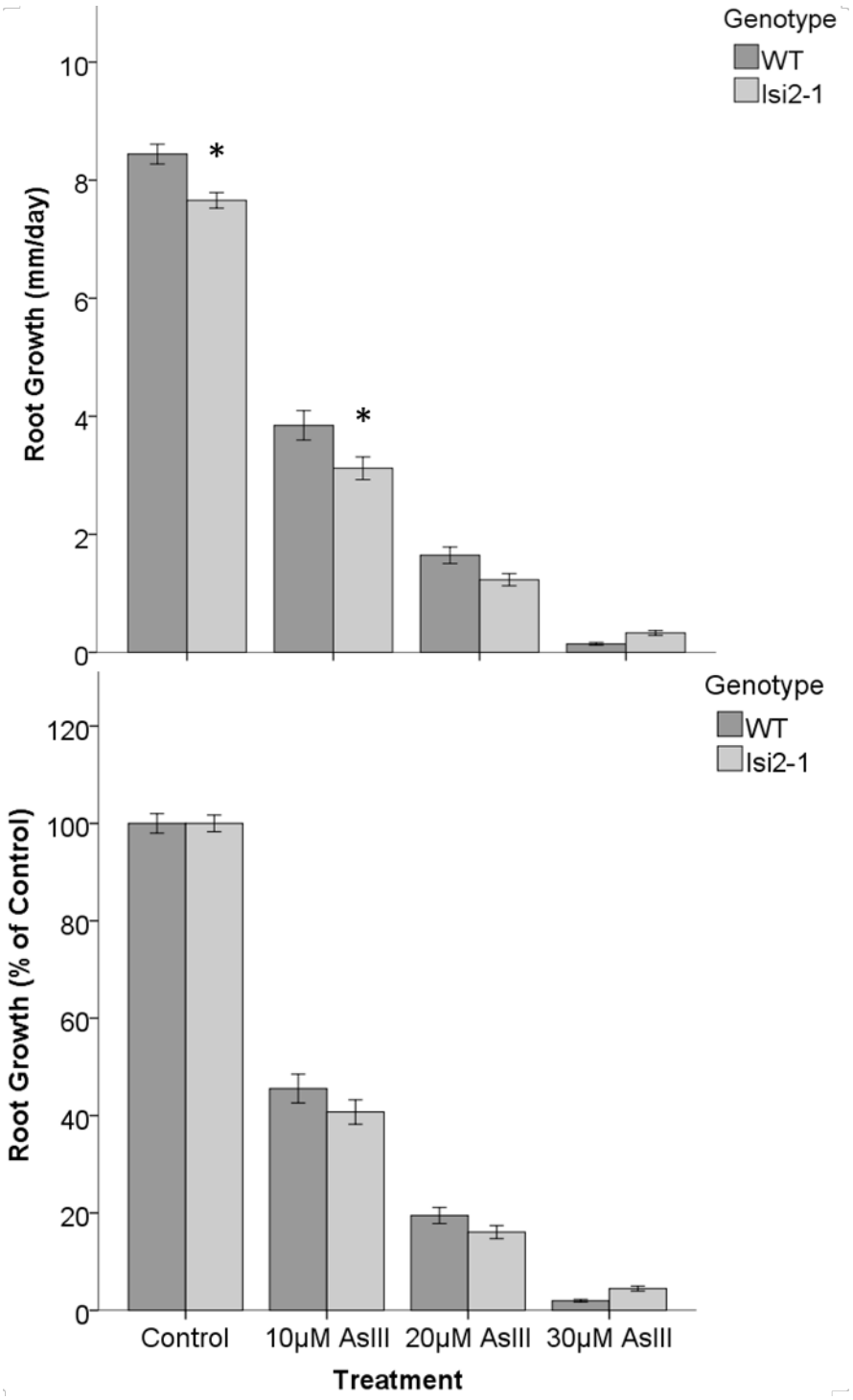

Figure 4.5 Root growth of WT and *Isi2-1* plants grown on plates containing AsIII
The top panel displays the root growth of WT and *Isi2-1* plants grown on plates containing different concentrations of AsIII. Root growth is calculated as mm growth per day. The bottom panel shows the same data expressed relative to growth in control conditions. Data are from six independent experiments, values are means ± SE and asterisks indicate significant differences between genotypes at $P<0.05$.

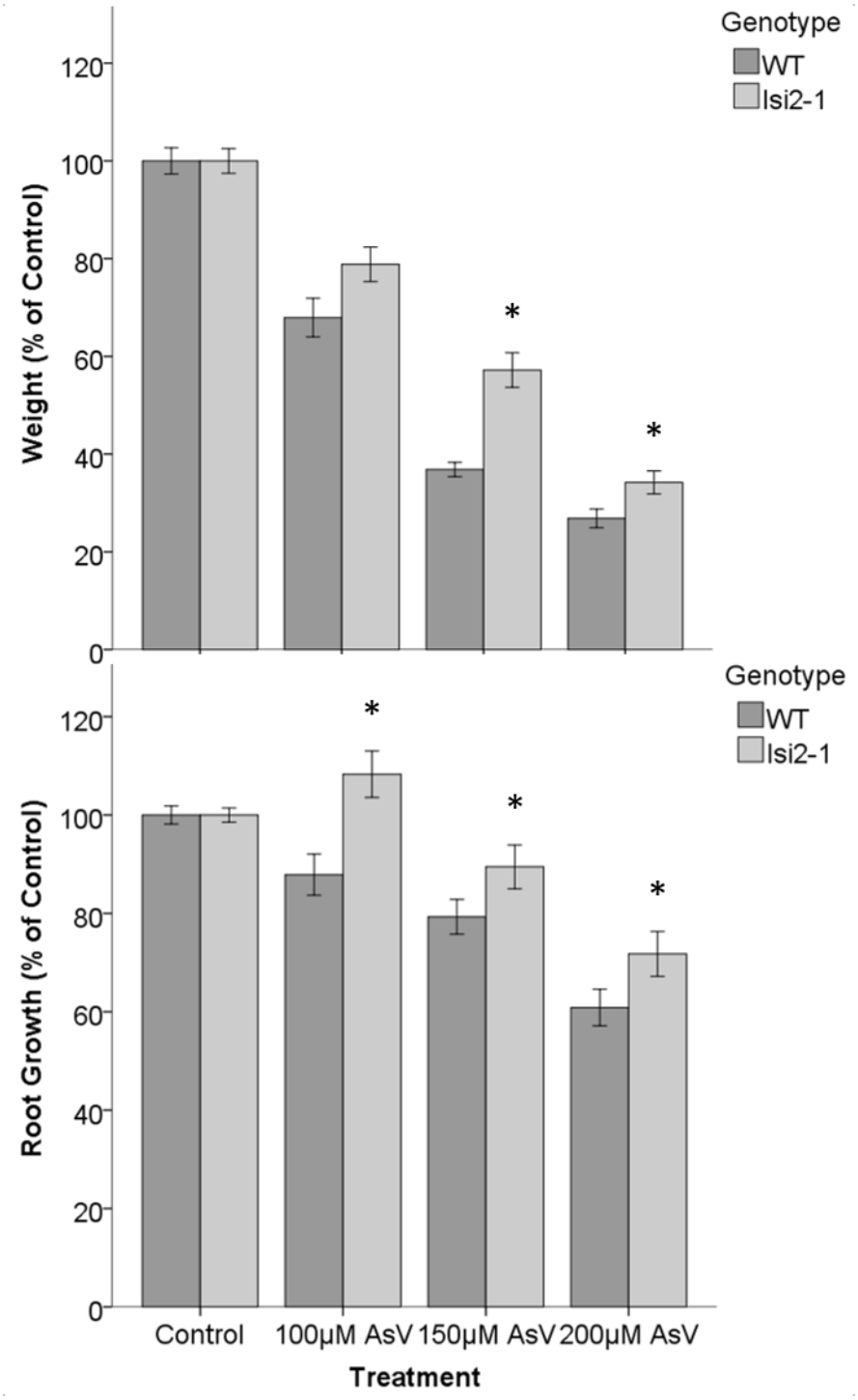

Figure 4.6 Growth of WT and *Isi2-1* plants grown on plates containing AsV
The top panel shows the average fresh weight of WT and *Isi2-1* plants grown on plates with different concentrations of AsV plotted relative to growth in control conditions. The bottom panel shows the root growth of the same plants calculated as mm growth per day and expressed relative to growth in control conditions. Data are from six independent experiments, values are means ± SE and asterisks indicate significant differences between genotypes at $P<0.05$.

In order to investigate the physiological role of *Lsi2*, WT and *Isi2* mutant plants were grown on plates with different concentrations of boron. It is plausible that *Lsi2* may be able to transport B as it is an analogue of AsIII and Silicic acid. Loss of function of *Isi2* led to increased sensitivity to both toxic levels of B and conditions of B deficiency

(Figure 4.7). Relative to growth on control plates, *lsi2* plants weighed significantly less than WT on plates containing 2mM B while *lsi2* root growth was significantly reduced on plates with no added B compared with WT root growth.

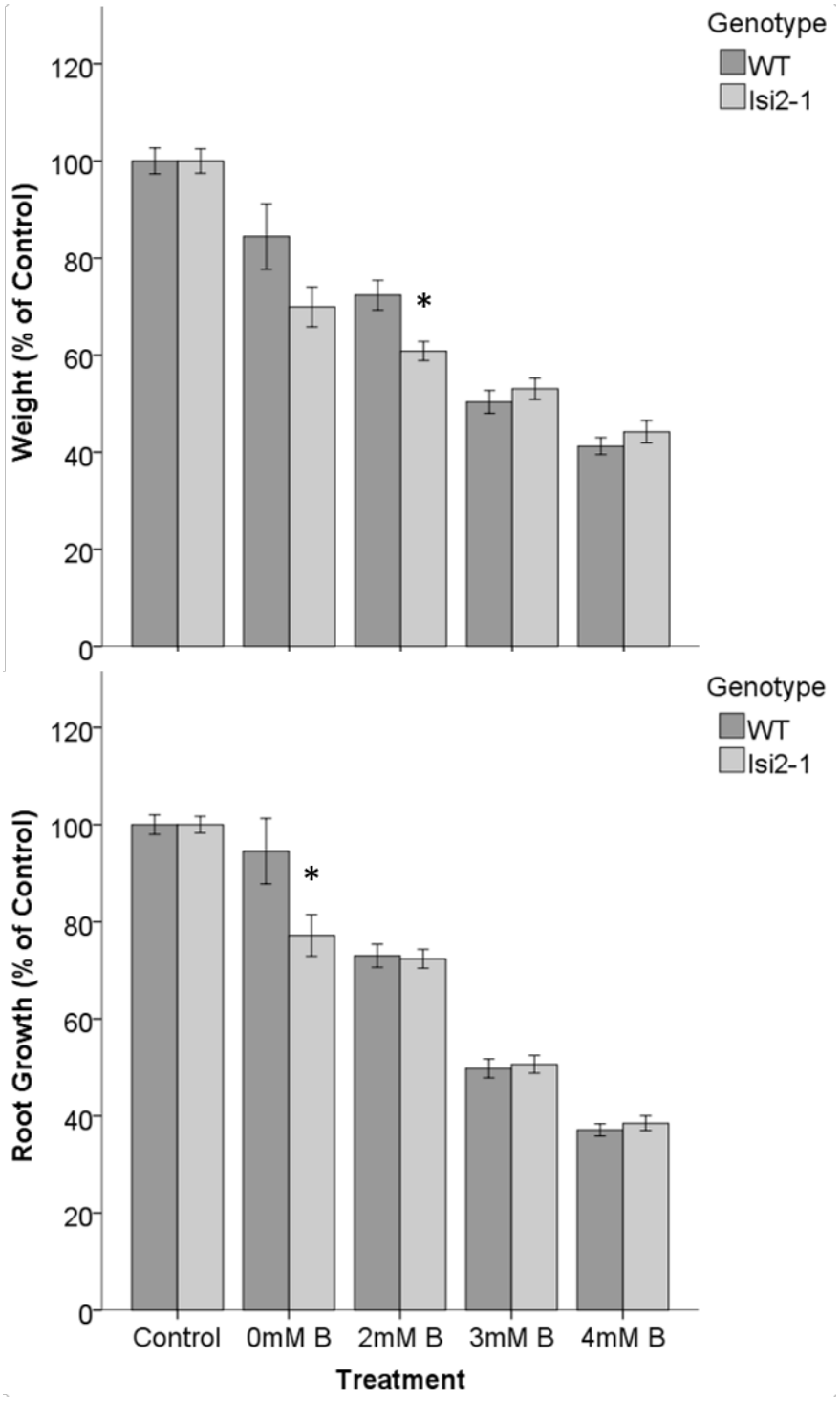

Figure 4.7 Growth of WT and *lsi2-1* plants grown on plates containing B
The top panel shows the average fresh weight of WT and *lsi2-1* plants grown on plates with different concentrations of AsV plotted relative to growth in control conditions. The bottom panel shows the root growth of the same plants calculated as mm growth per day and expressed relative to growth in control conditions. Data are from at least four independent experiments, values are means ± SE and asterisks indicate significant differences between genotypes at $P<0.05$.

4.3.2.2 Growth Experiments in Hydroponics

To measure growth under more physiological conditions, 3wo WT and *lsi2* plants were exposed to different concentrations of AsIII and AsV in hydroponics and relative growth rates determined. Similar to growth on plates, *lsi2* plants grew more slowly than WT in control conditions (Figure 4.8). After one (Figure 4.8) and two weeks of treatment (Figure 4.9), *lsi2* knockout plants showed more tolerance to growth in 200µM AsV than WT plants. There was no significant difference in RGR of WT and *lsi2* plants grown in AsIII.

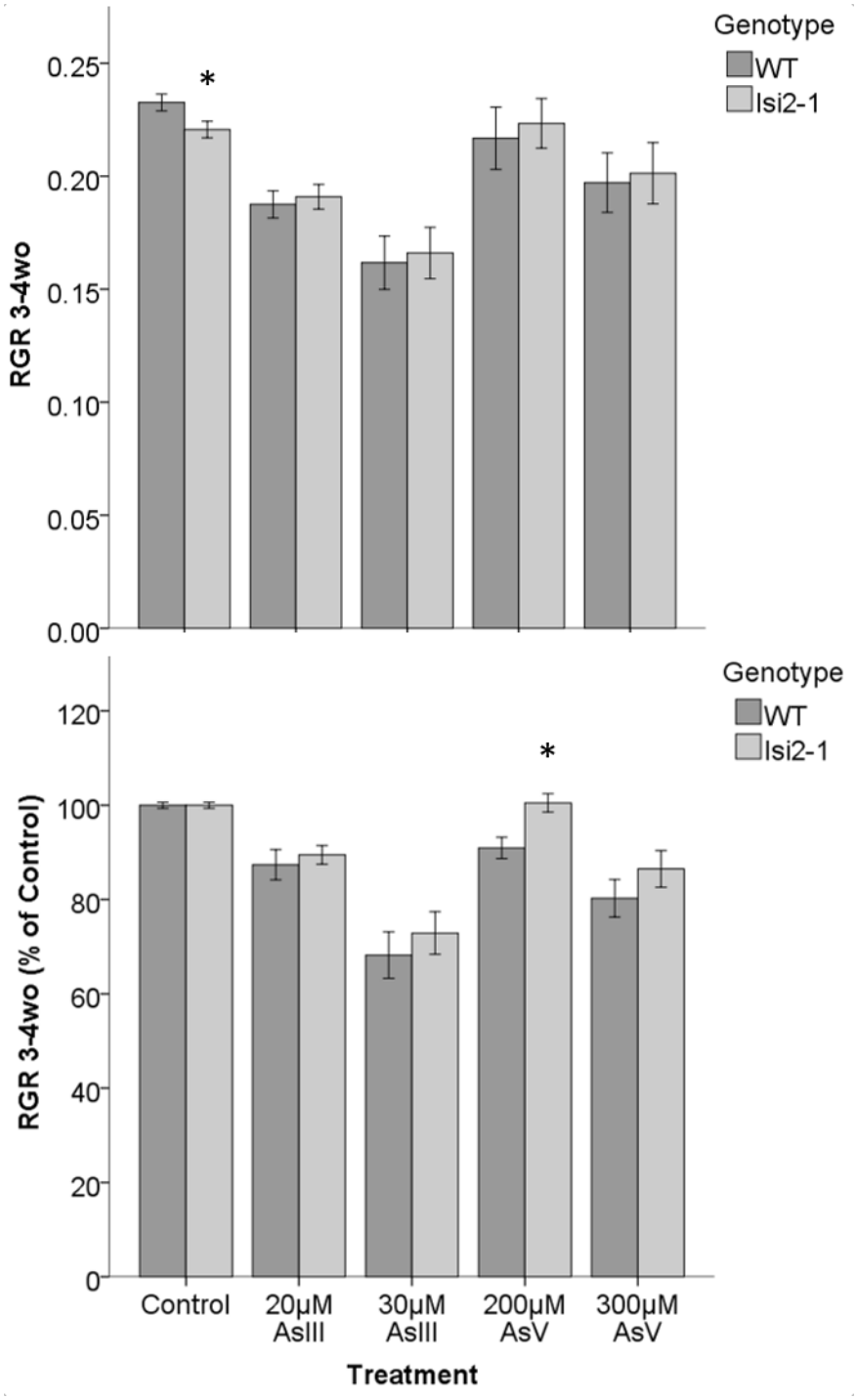

Figure 4.8 Relative growth rates of 3-4wo WT and *Isi2-1* plants exposed to As
The top panel displays the relative growth rate (RGR) of 3-4wo WT and *Isi2-1* plants grown in hydroponics and exposed to different concentrations of AsIII and AsV. The bottom panel shows the same data expressed relative to growth in control conditions. Data are from at least four independent experiments, values are means ± SE and asterisks indicate significant differences between genotypes at $P<0.05$.

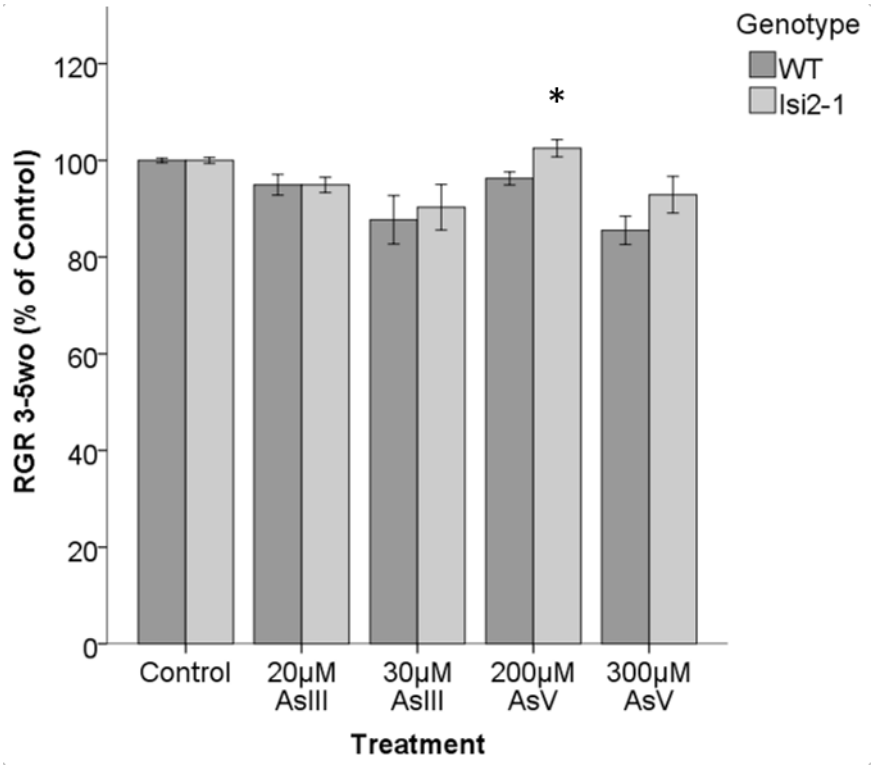

Figure 4.9 Relative growth rates of 3-5wo WT and *lsi2-1* plants exposed to As
The graph displays the relative growth rate of 3-5wo WT and *lsi2-1* plants exposed to different concentrations of AsIII and AsV for two weeks in hydroponics. Data are expressed relative to growth in control conditions. Data are from at least four independent experiments, values are means ± SE and asterisks indicate significant differences between genotypes at $P<0.05$.

The physiological role of *Lsi2* was further investigated by exposure of WT and *lsi2* knockout plants to different concentrations of B. There was no difference in RGR between WT and *lsi2* plants grown in B free medium but in medium containing high levels of B, *lsi2* plants grew significantly more slowly than WT (Figure 4.10). Loss of function in *Lsi2* therefore leads to enhanced sensitivity to B toxicity in terms of whole plant growth, while in conditions of B deficiency *Lsi2* is important for root growth but loss of function does not affect whole plant growth.

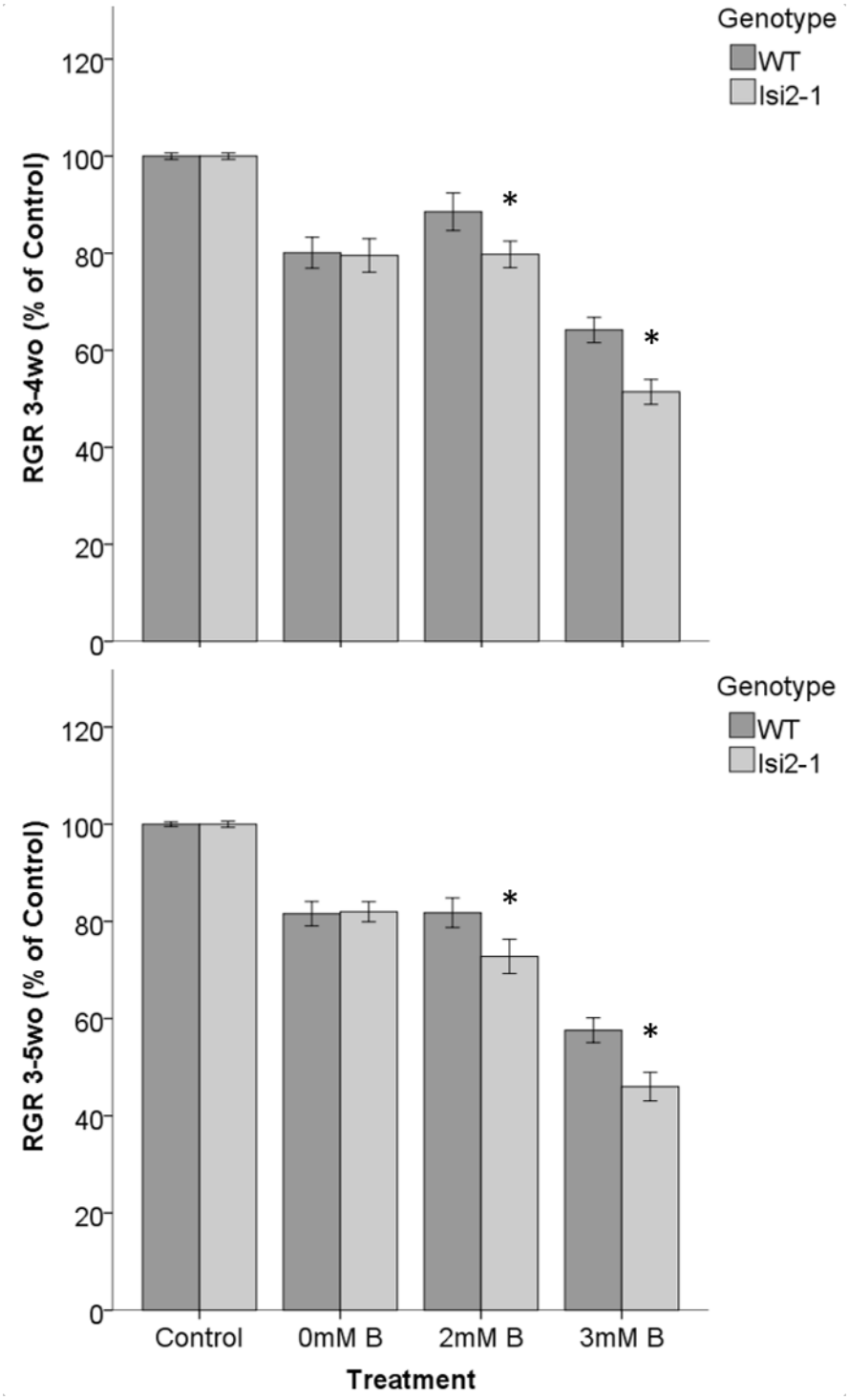

Figure 4.10 Relative growth rates of WT and *lsi2-1* plants exposed to B
The top panel shows the relative growth rates of 3-4wo WT and *lsi2-1* plants exposed to different concentrations of B in hydroponics for one week. The bottom panel shows the relative growth rates of 3-5wo WT and *lsi2-1* plants exposed to different concentrations of B in hydroponics for two weeks. All data are displayed relative to growth in control conditions. Data are from at least five independent experiments, values are means ± SE and asterisks indicate significant differences between genotypes at $P<0.05$.

Lsi2 contains a CitMHS domain which is found in proteins with similarity to bacterial citrate uptake permeases [202]. To investigate if *Lsi2* is involved in citrate transport in *Arabidopsis, lsi2* knockout mutants were grown alongside WT plants in medium

containing 1mM citric acid. No significant difference was observed between the RGR of WT and *lsi2* plants (Figure 4.11).

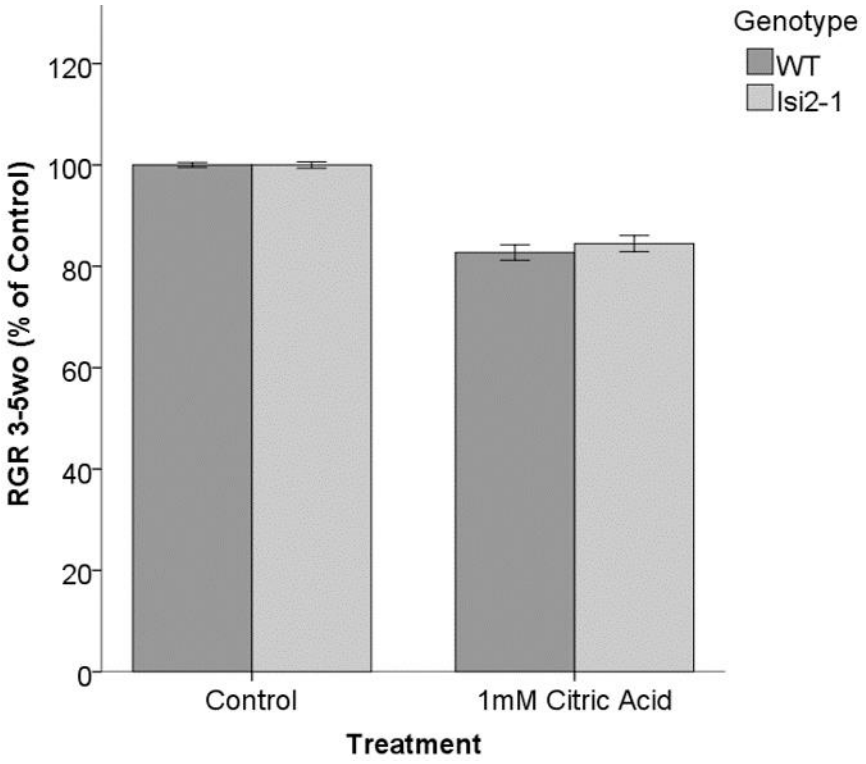

Figure 4.11 Relative growth rates of WT and *lsi2-1* plants exposed to citric acid
The graph shows the relative growth rates of 3-5wo WT and *lsi2-1* plants exposed to 1mM citric acid for two weeks in hydroponics. Data are displayed relative to growth in control conditions. Data are from four independent experiments and values are means ± SE.

CitMHS domains are also found in proteins belonging to the Na^+/sulphate symporter family including the SLT1 sulphate transporter in *Chlamydomonas reinhardtii* [204]. According to the Arabidopsis eFP browser, expression levels of *Lsi2* are downregulated in the epidermis and cortex and upregulated in the endodermis and stele of the root in sulphur (S) deficient compared to S sufficient conditions [194]. It is possible that *Lsi2* may be able to transport sulphate, and so *lsi2* mutant plants were grown alongside WT in S deficient conditions with and without As to investigate the potential role of *Lsi2* in S homeostasis. There was no significant difference in RGR between WT and *lsi2* plants grown in S deficient medium (Figure 4.12). In S sufficient medium, *lsi2* plants were more tolerant to AsV (Figures 4.8-9) while in S deficient medium *lsi2* were more sensitive to AsV (Figure 4.12). When As was added to the low S medium, *lsi2* plants had a significantly reduced RGR compared to WT plants, indicating that S is required for the As tolerance observed in *lsi2* knockout plants.

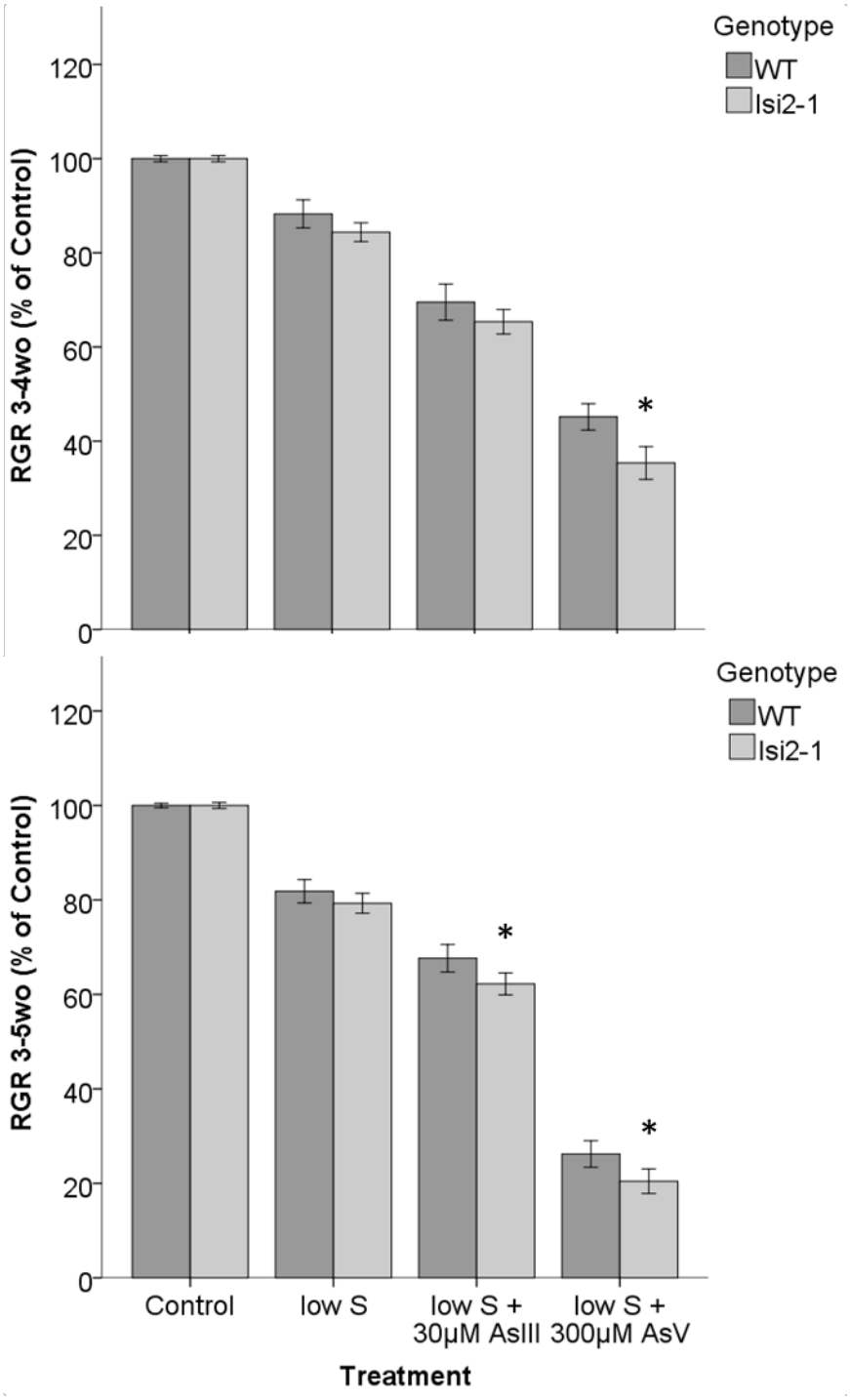

Figure 4.12 Relative growth rates of WT and *lsi2-1* plants exposed to low S and As
The top panel shows the relative growth rates of 3-4wo WT and *lsi2-1* plants exposed to S deficient medium with and without As in hydroponics for one week. The bottom panel shows the relative growth rates of 3-5wo WT and *lsi2-1* plants exposed to S deficient medium with and without As in hydroponics for two weeks. All data are displayed relative to growth in control conditions. Data are from at five independent experiments, values are means ± SE and asterisks indicate significant differences between genotypes at $P<0.05$.

4.3.2.3 Arsenic Concentration of *lsi2* Plants

WT and *lsi2* T-DNA insertion mutants were exposed to 20µM AsIII and 200µM AsV for two weeks and the tissue As concentrations compared between genotypes. There

were no significant differences between WT and *lsi2* plants in root, shoot, shoot:root As or total plant As concentrations after exposure to AsIII (Figure 4.13).

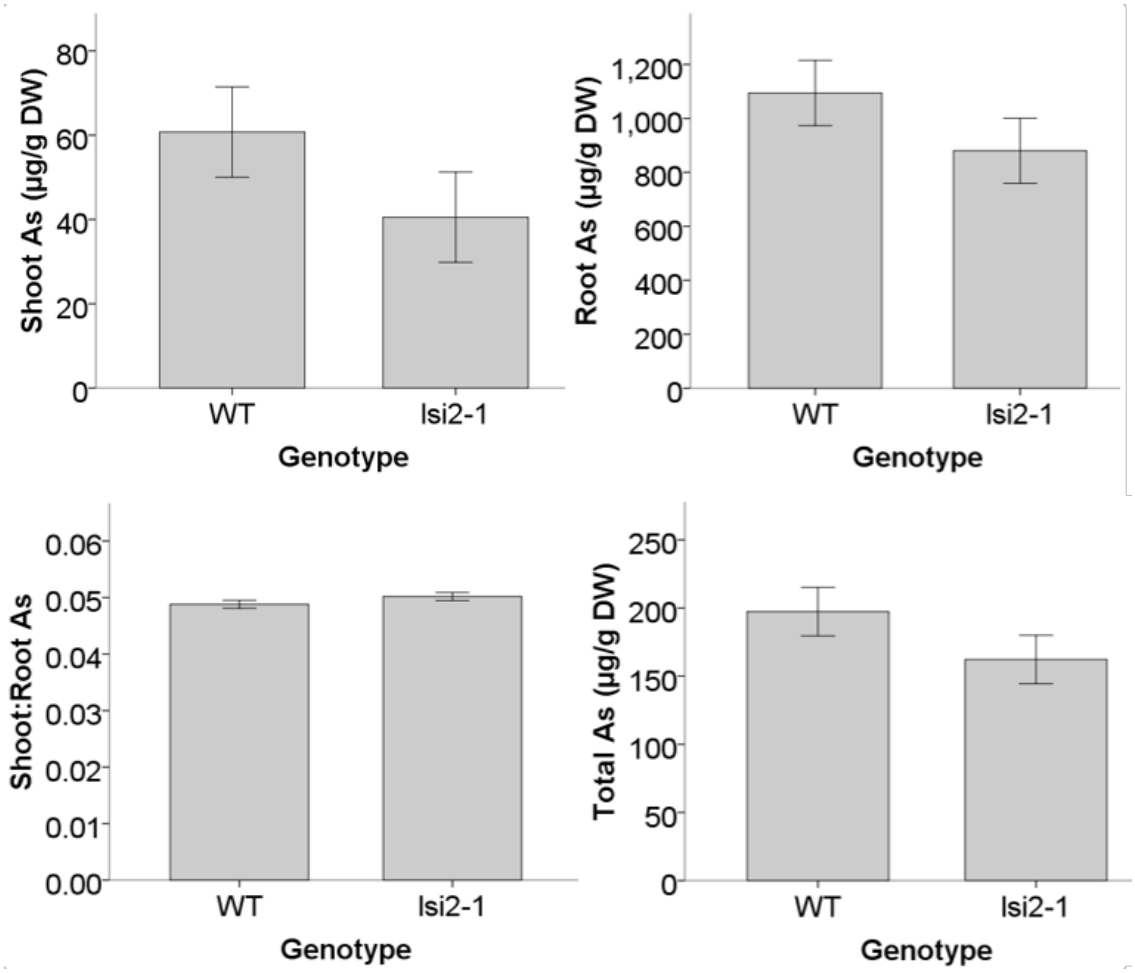

Figure 4.13 Arsenic concentration of WT and *lsi2-1* plants exposed to 20*µ*M AsIII
Graphs show the As concentration of WT and *lsi2-1* plant tissues after two weeks exposure to 20µM AsIII in hydroponics. The top left and right panels show the average shoot and root As concentrations respectively. The bottom left panel shows the shoot:root As and the bottom right panel shows the total plant As concentration. Data are from three independent experiments, values are means ±SEs and asterisks indicate significant differences between genotypes at $P<0.05$ using an unpaired *t*-test.

After two weeks treatment with AsV, *lsi2* loss of function mutants had a significantly increased shoot:root As compared with WT plants (Figure 4.14). There was no difference in the total plant As concentration of WT and *lsi2* mutants, however *lsi2* plants had a reduced root As concentration and increased shoot As concentration compared to WT although the difference was only statistically significant for *lsi2-1* (Figure 4.15). This suggests that *Lsi2* is involved in reducing the root to shoot translocation of As in response to AsV but not AsIII.

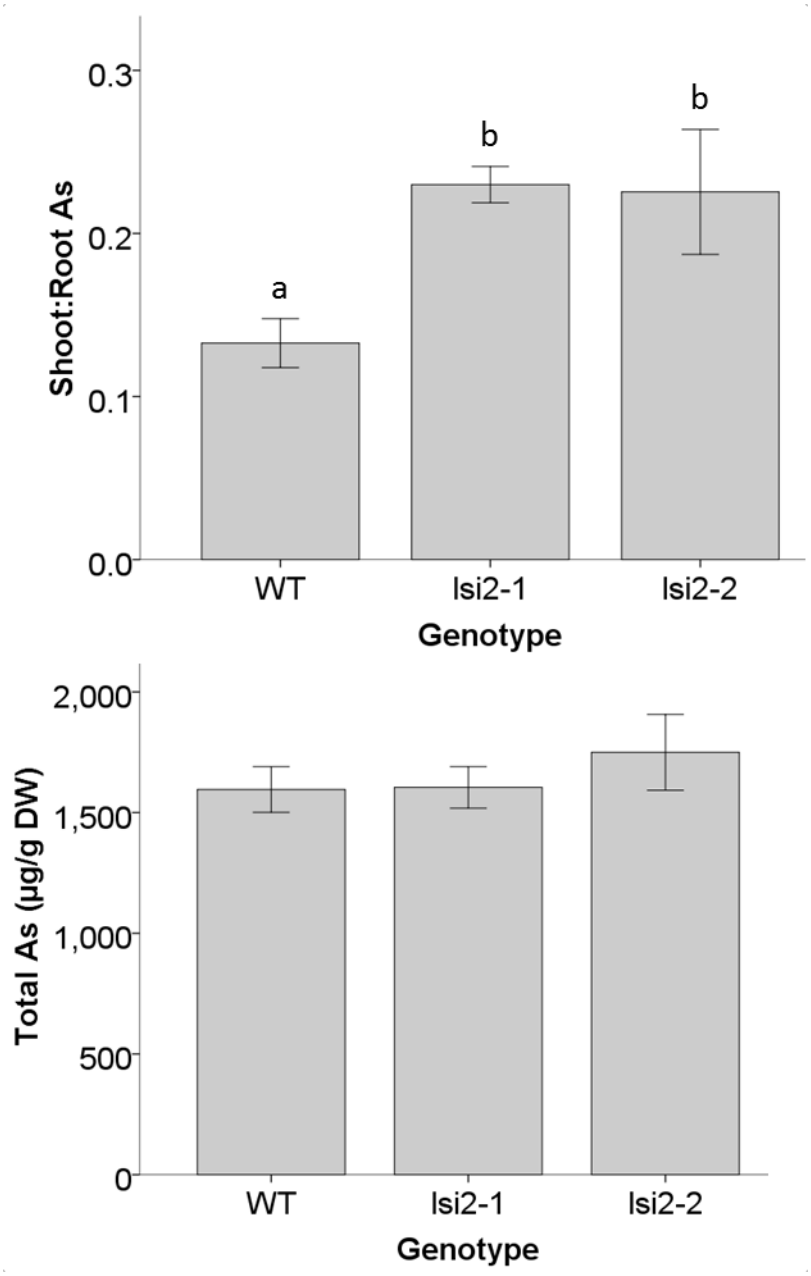

Figure 4.14 Arsenic concentration of WT and *lsi2-1* plants exposed to 200*µ*M AsV
Graphs show the shoot:root As (top panel) and total plant As concentration (bottom panel) of WT, *lsi2-1* and *lsi2-2* plants after 2 weeks exposure to 200µM AsV in hydroponics. Data are from at least three independent experiments, values are means ±SEs and letters indicate significant differences between genotypes at $P<0.05$ using unpaired *t*-tests.

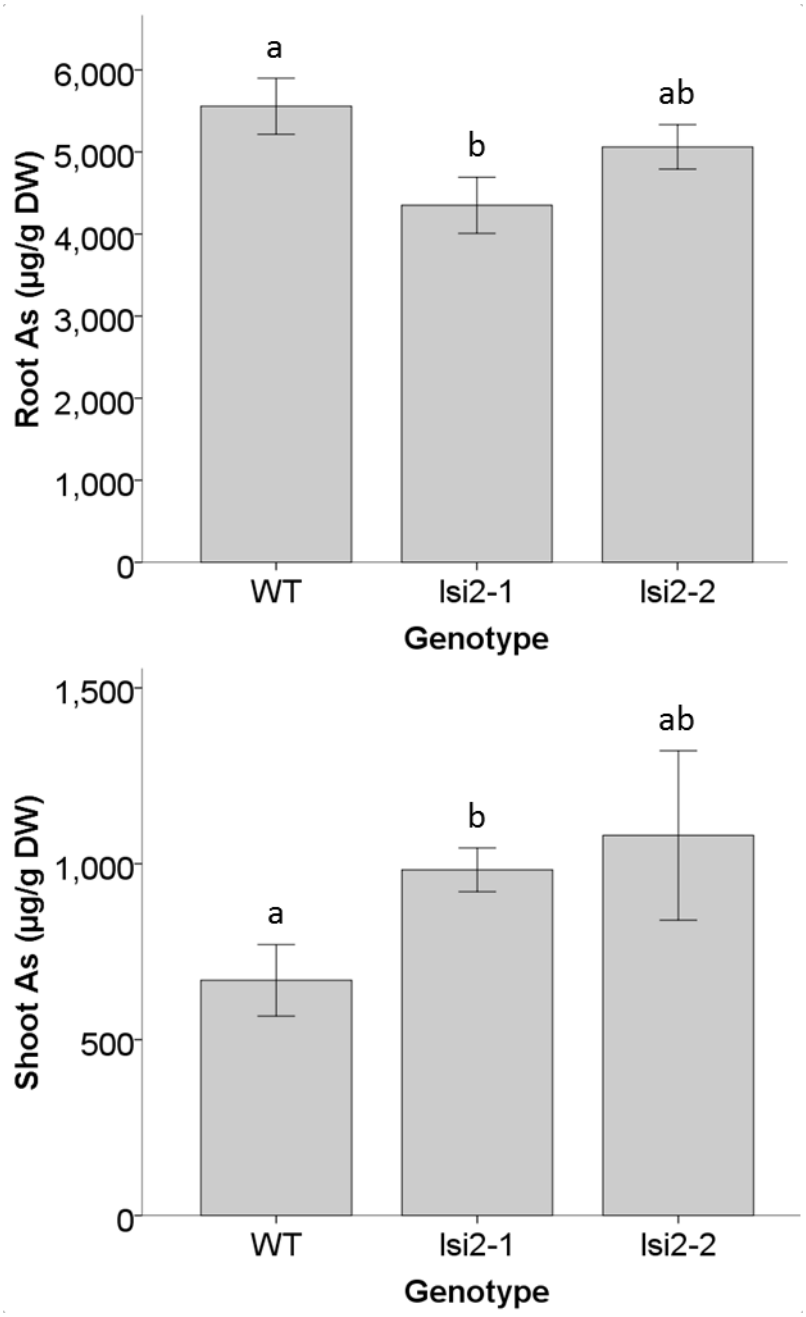

Figure 4.15 Arsenic concentration of WT and *lsi2-1* plants exposed to 200µM AsV
Graphs show the root As concentration (top panel) and shoot As concentration (bottom panel) of WT, *lsi2-1* and *lsi2-2* plants after 2 weeks exposure to 200µM AsV in hydroponics. Data are from at least three independent experiments, values are means ±SEs and letters indicate significant differences between genotypes at $P<0.05$ using unpaired *t*-tests.

4.3.2.4 Arsenic Efflux of *lsi2* Plants

The role of *Lsi2* in As efflux was investigated by exposing WT, *lsi2-1* and *lsi2-2* plants to 350µM AsV for 24hrs as described in Section 3.2.9. There were no significant differences in As efflux between genotypes after 6 or 24 hours (Figure 4.16).

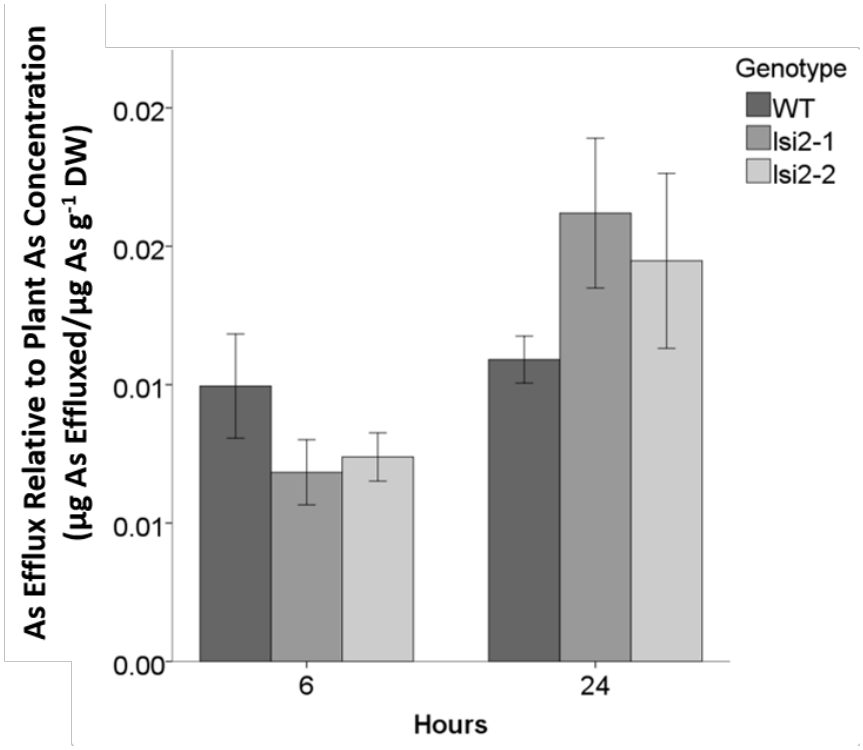

Figure 4.16 Efflux of As from WT and *Isi2* mutant plants
The graph shows the amount of As effluxed from the roots of 3wo *Arabidopsis* plants relative to the plant As concentration (As Effluxed/µg As g^{-1} DW plant). Plants were preloaded with As by exposure to 350µM AsV in hydroponics for 24hrs. Roots were rinsed and placed in As free medium. As efflux was measured 6 and 24 hours after transfer. Data are from three independent experiments and values are means ±SEs.

To investigate differences in As loading between genotypes, the total plant As concentration and the shoot:root As ratio of plants used in the efflux experiment was determined (Figure 4.17) . There was no difference in total plant As concentrations but *Isi2-1* plants had a significantly increased shoot:root As compared to WT. The second allele, *Isi2-2,* also had increased shoot:root As although the difference was not significantly different from WT.

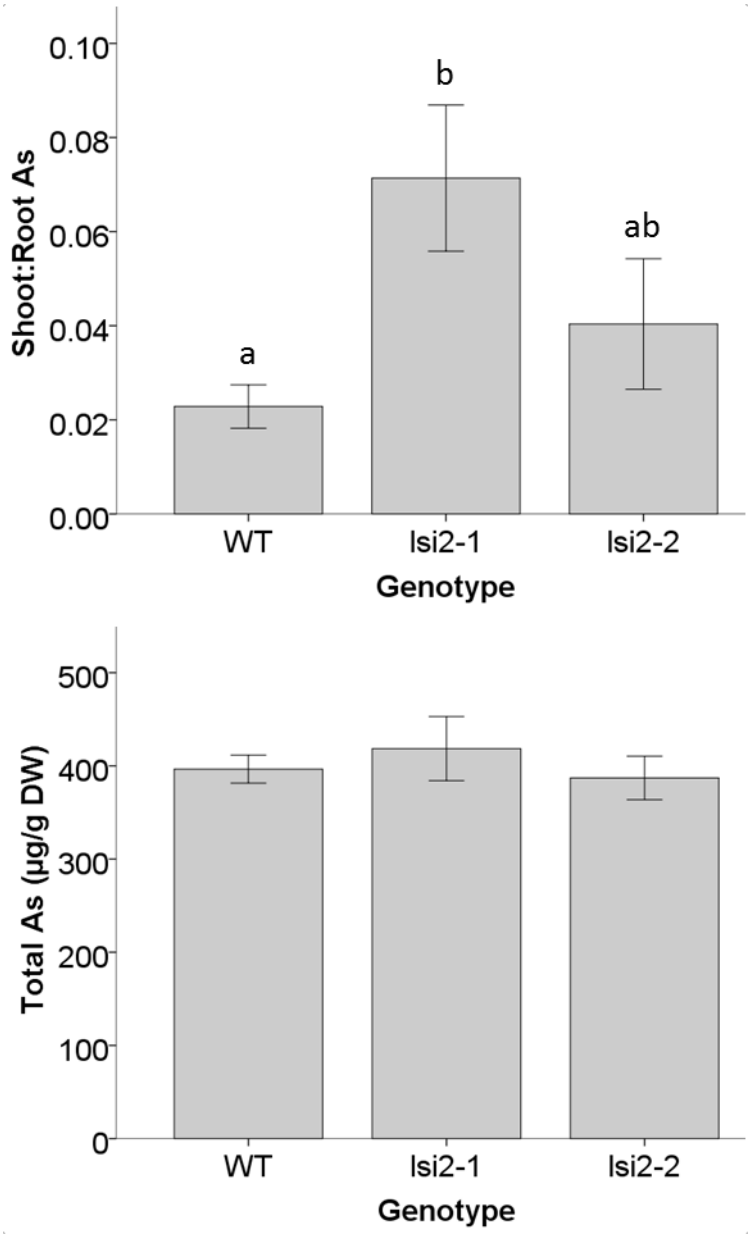

Figure 4.17 Arsenic loading of WT and *Isi2* mutant plants used in the efflux experiment
Graphs show the shoot:root As (top graph) and total plant As concentration (bottom graph) of As in 3wo plants after exposure to 350µM AsV for 24 hours. Data are from three independent experiments, values are means ±SEs, and letters indicate significant differences between genotypes at $P<0.05$ using unpaired *t*-tests.

4.3.3 Characterisation of *wrky59* T-DNA Insertion Mutants

A forward genetics screen was carried out on a collection of 6868 confirmed homozygous T-DNA insertion lines. One of the most promising candidates for improved tolerance to As was chosen for further characterisation. SALK_039436C contains a T-DNA insertion in the gene At2g21900 which encodes the transcription factor WRKY59. After four weeks of exposure to 350µM AsV on sand, SALK_039436C (*wrky59-1*) plants were larger and more green than WT plants (Figure 4.18).

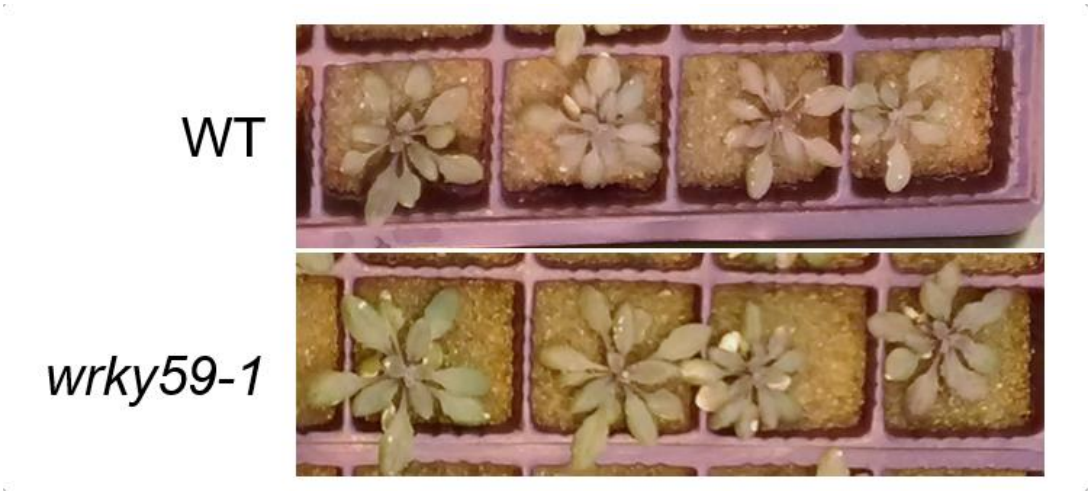

Figure 4.18 Arsenic tolerance of *wrky59-1* plants
The pictures show the appearance of WT and *wrky59-1* plants after exposure to 350μM AsV on sand for four weeks. The plants were grown on the same tray, and the pictures are cropped from the same photo.

A second allele was ordered and the two homozygous T-DNA insertion mutants (confirmed by PCR) in *WRKY59* were characterised at the mRNA level to confirm that they are true knockouts. The approximate position of T-DNA insertion in *wrky59-1* and *wrky59-2* is shown in Figure 4.19. The T-DNA insertion in the first allele is located in the second exon, which appears to be spliced out in the *wrky59-1* line. Using RT-PCR, primers specific for the first and third exon generate a smaller band from *wrky59-1* cDNA compared to WT (Figure 4.19). The *wrky59-1* specific band is ~300bp rather than 459bp. The second exon is 162bp long and is the site of T-DNA insertion in *wrky59-1*. This suggests that in this line, rather than T-DNA insertion resulting in truncation of the transcript, the second exon containing the insertion is alternatively spliced. The second exon contains the highly conserved WRKY domain, which is required for DNA binding [187] implying that the alternatively spliced mRNA in *wrky59-1* will give rise to a non-functional protein.

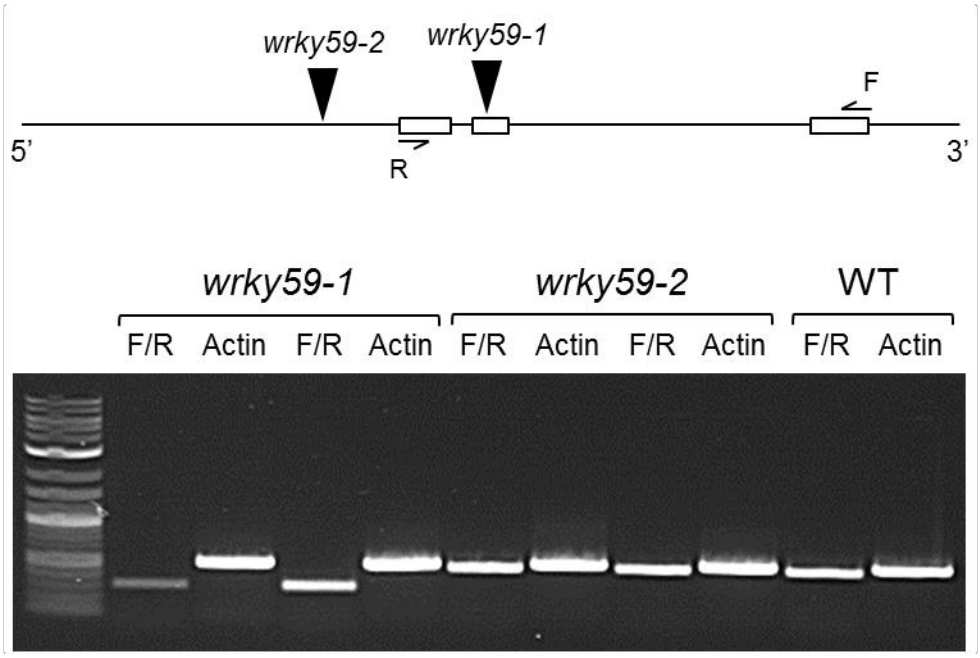

Figure 4.19 RT-PCR of *wrky59* T-DNA insertion lines

RT-PCR was performed on *wrky59-1, wrky59-2* and WT plants using primers specific to *WRKY59* and *Actin*. The top panel shows the approximate position of the T-DNA insertion in each line and the position of the WRKY59F (F) and WRKY59R (R) primers used for RT-PCR. The full length genomic DNA is represented and the positions of the exons is indicated by the rectangles. The bottom panel displays RT-PCR carried out on WT, *wrky59-1* and *wrky59-2* cDNA. For each T-DNA insertion line, cDNA was synthesised from two independent RNA extractions. A 2-Log DNA ladder was run in the first lane. Using primers specific to *WRKY59* (F/R), a band of the expected size (459bp) was observed in WT and *wrky59-2* plants while a smaller band (~300bp) was observed for *wrky59-1* plants. This size is consistent with alternative splicing of the second exon, which would result in amplification of a band 297bp long. A band of the expected size was observed using *Actin* specific primers in all samples.

In the second line, the T-DNA insertion is located approximately 500bp upstream of the first exon in the promoter region. Expression of *WRKY59* can still be detected in *wrky59-2* plants, although the presence of the T-DNA in the promoter may disrupt transcriptional regulation of the gene. When RT-PCR was performed with a lower cycle number, it seems that in *wrky59-2* the TF may be more highly expressed than in WT (Figure 4.20). As RT-PCR is only semi-quantitative, Q-PCR should be carried out in order to confirm this. It would also be interesting to determine the effect of T-DNA insertion on *WRKY59* expression in response to As stress.

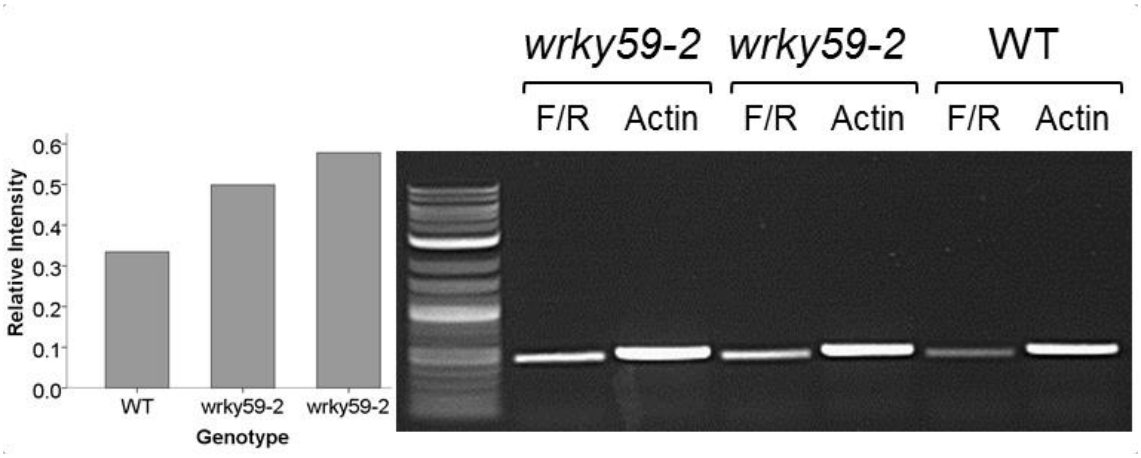

Figure 4.20 RT-PCR of WT and *wrky59-2* T-DNA insertion lines
RT-PCR was performed on two individual *wrky59-2* plants and WT using primers specific to *WRKY59* (F/R) and *Actin.* RT-PCR conditions were the same as in Figure 4.20 above except PCR cycle number was 27 rather than 37. The graph shows the intensity of the *WRKY59* bands from WT and *wrky59-2* plants relative to the intensity of the respective *Actin* band calculated using ImageJ [205].

4.3.3.1 Bioinformatics Analysis of *WRKY59*

WRKY TFs can be divided into different phylogenetic groups based on the number and structure of the WRKY domains they contain [186]. *WRKY59* falls into the group IIc subfamily whose members contain one WRKY domain preceded by a possible nuclear localisation signal KAKKxxQK and the sequence [K/R]EPRVAV[Q/K]T[K/V]SEVD[I/V]L [186]. *WRKY59* encodes a gene with three exons and an open reading frame of 2074bp. The deduced protein consists of 202 amino acids, has a molecular weight of 23.3kDa and is predicted to localise to the nucleus [193]. *WRKY59* is expressed most highly in the epidermis of the roots and the vascular tissues of the shoot, in particular the phloem (Figure 4.21).

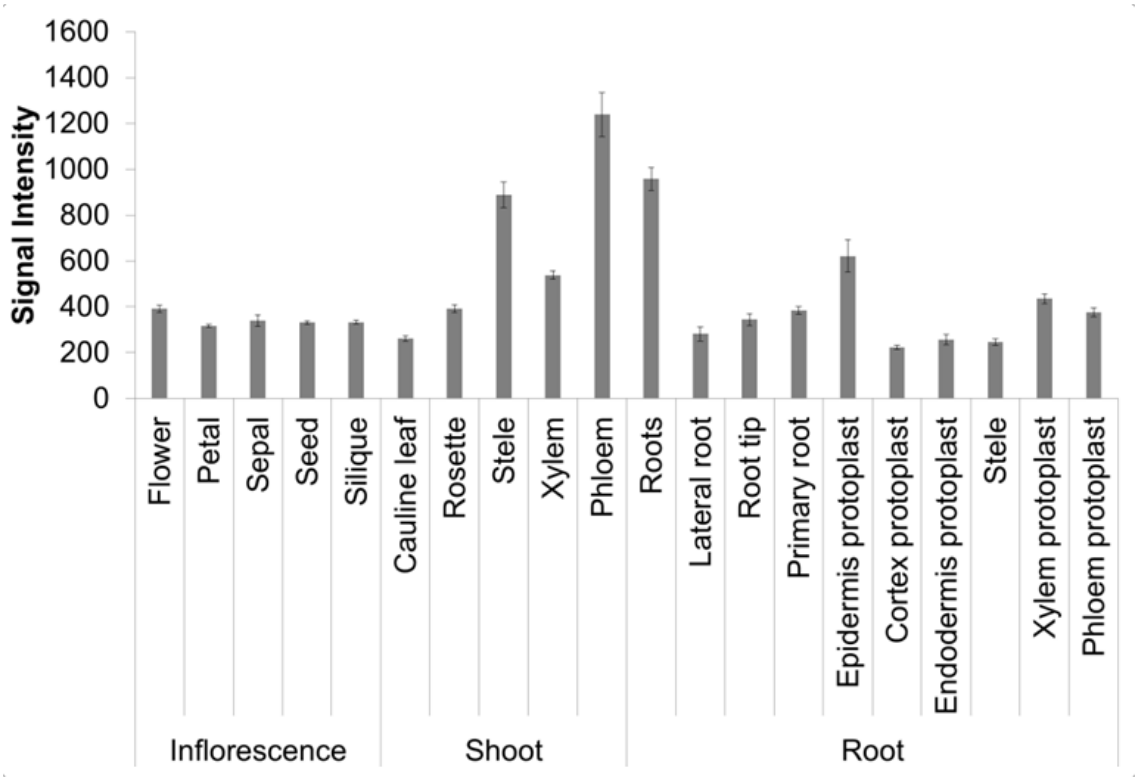

Figure 4.21 Expression pattern of *WRKY59*
Graph showing the relative expression level of *WRKY59* in different *Arabidopsis* tissues. Data were obtained from the Genevestigator database [141]. Values are means ± SEs of signal intensities on the Affymetrix Rice Genome Array, plotted on a linear scale.

WRKY59 is differentially regulated in response to heavy metals; transcript levels are reduced >3 fold in root tissues following exposure to gold [206] and upregulated in roots exposed to excess zinc and cadmium [207]. Expression of *WRKY59* is also altered in mutant backgrounds deficient in the response to biotic stress, levels are upregulated in *edr1* (*enhanced disease resistance* 1) mutant plants and markedly reduced in *npr1* (*nonexpresser of PR genes 1*) [208, 209].). Running the Genevestigator perturbations tool (filtered for conditions with ≥ 2 fold change in expression and a *P* value ≤ 0.05) revealed that *WRKY59* is strongly upregulated by salicylic acid and treatment with DFPM (an inhibitor of ABA induced expression of genes) [141]. *WRKY59* expression is also upregulated by biotic stress and abiotic stresses including salt and cold. Interestingly, *WRKY59* is downregulated (>10 fold) by brassinolide/boric acid treatment, which induces xylogenesis and tracheary element differentiation in *Arabidopsis* suspension culture cells [141], indicating a possible role of *WRKY59* in negatively regulating these processes in the stele of the shoot. Like many other members of the WRKY TF family, *WRKY59* appears likely to be involved in several disparate processes including the response to both abiotic and biotic stress [188]. The potential role of *WRKY59* in response to As was investigated in this chapter.

4.3.3.2 Arsenic Tolerance of *wrky59* Plants Grown on Agar Plates

WT, *wrky59-1* and *wrky59-2* seeds were sown on agar plates containing different concentrations of AsIII or AsV. Root lengths were marked 5 and 10 days after sowing and fresh weights were measured after 21 days. On control plates, *wrky59-2* plants weighed significantly less than WT and their roots grew more slowly (Figures 4.22-3). Relative to growth on control plates, both *wrky59-1* and *wrky59-2* plants were more tolerant to AsIII and AsV. Compared to WT, *wrky59-1* plants had a significantly higher fresh weight on plates containing 20μM AsIII and 100μM AsV and *wrky59-2* plants were larger on plates containing 200μM AsV (Figure 4.22). The root growth of *wrky59-1* plants was faster than WT on plates containing 100μM AsV while the roots of *wrky59-2* plants grew faster than WT on plates containing 10 and 20μM AsIII and 200μM AsV (Figure 4.23). This suggests that *WRKY59* affects normal plant and root growth and is involved in the response to both AsIII and AsV.

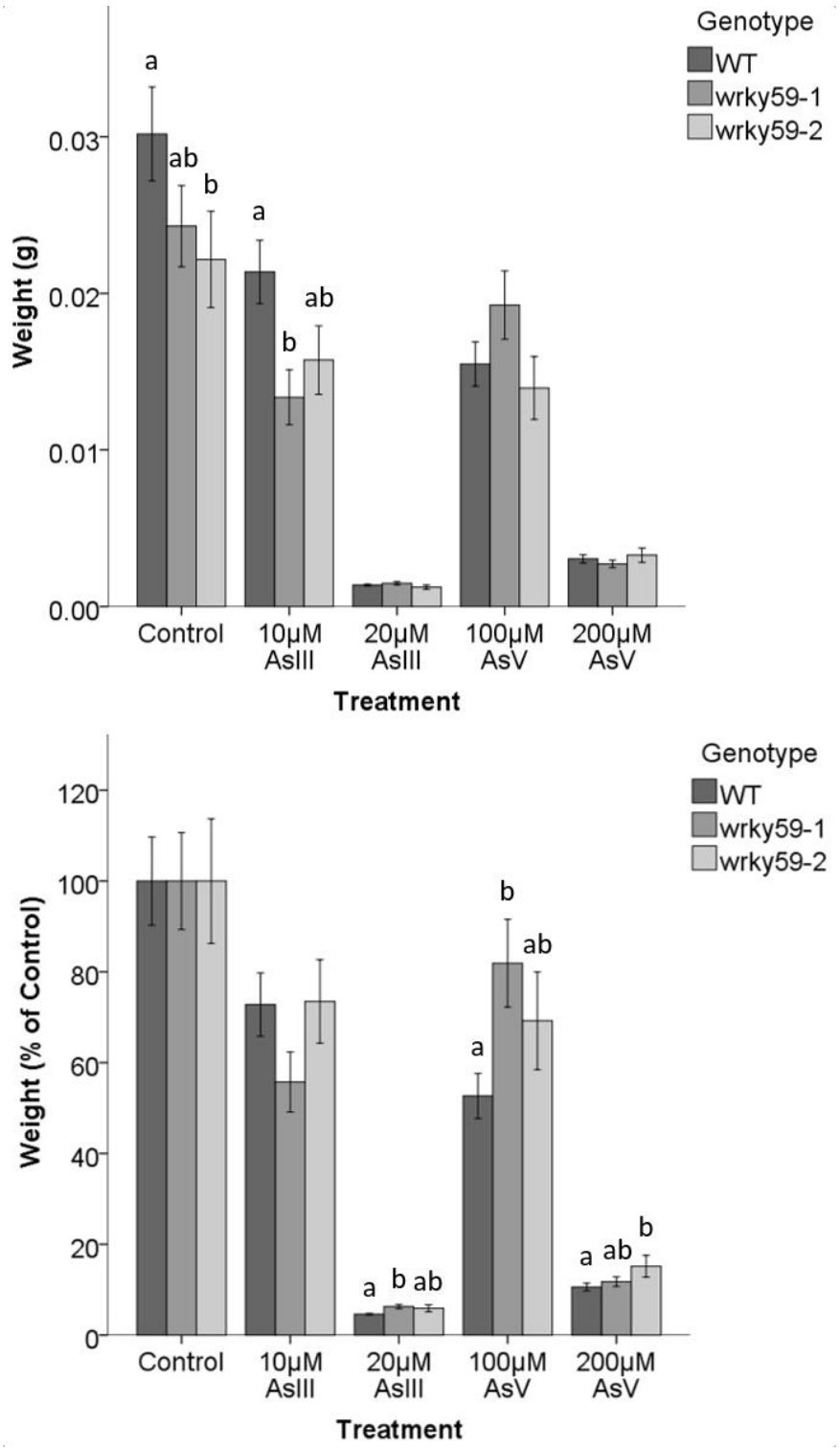

Figure 4.22 Fresh weight of WT and *wrky59* T-DNA insertion lines on plates
WT, *wrky59-1* and *wrky59-2* seeds were sown on agar plates containing different concentrations of AsIII and AsV. Fresh weights were measured after three weeks on treatment plates. The top panel shows plant average fresh weight and the bottom panel shows the same data plotted relative to growth in control conditions. Data are from four independent experiments, values are means ± SE and letters indicate significant differences between genotypes at $P<0.05$.

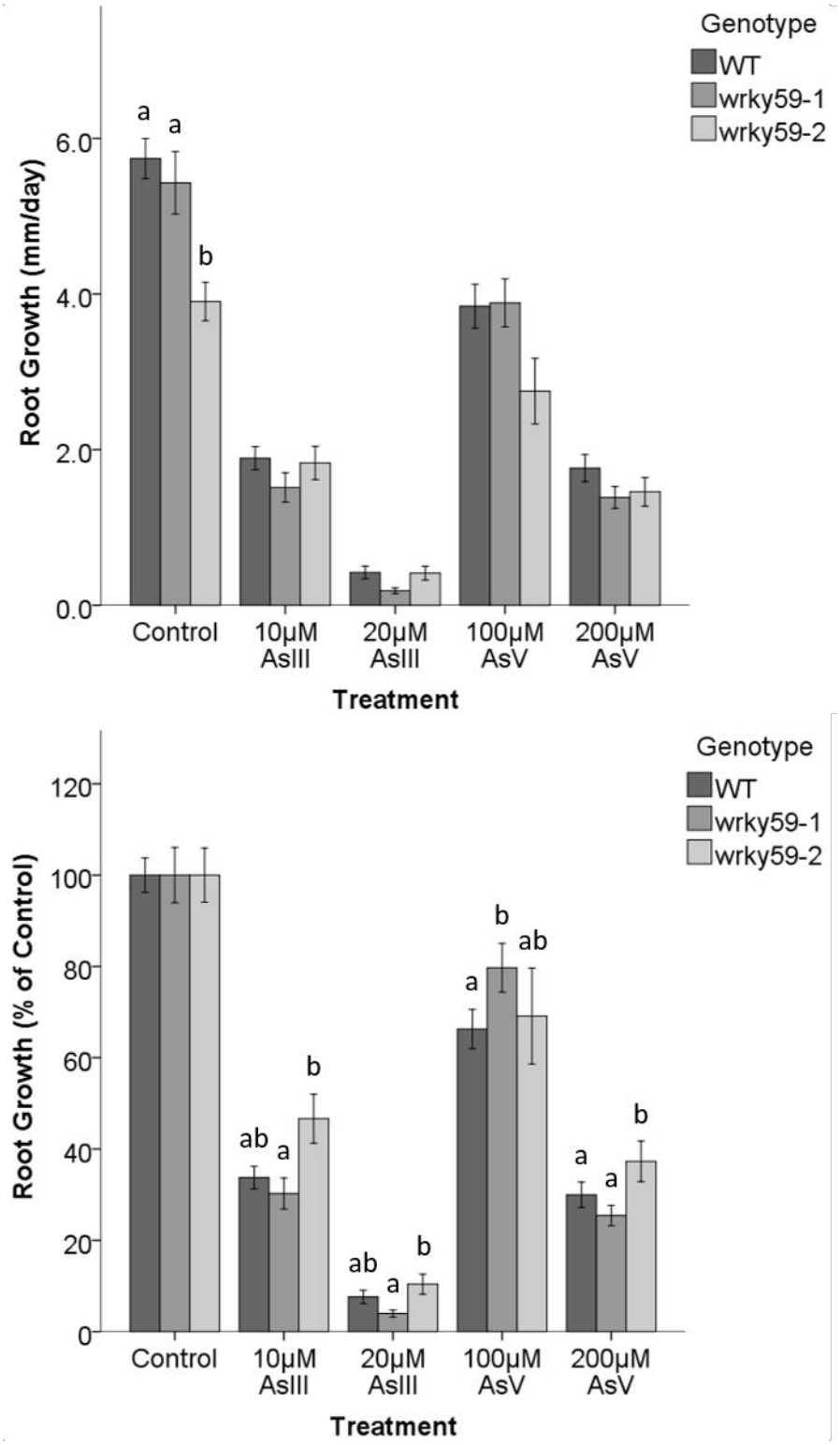

Figure 4.23 Root growth of WT and *wrky59* T-DNA insertion lines on plates
WT, *wrky59-1* and *wrky59-2* seeds were sown on agar plates containing different concentrations of AsIII and AsV. The top panel shows root growth calculated as mm growth per day and the bottom panel shows the same data plotted relative to growth in control conditions. Data are from four independent experiments, values are means ± SE and letters indicate significant differences between genotypes at $P<0.05$.

4.3.3.3 Arsenic Tolerance of *wrky59* Plants Grown in Hydroponics

In hydroponics, *wrky59* plants grew more slowly than WT in control conditions, however the difference was only significant for *wrky59-1* (Figures 2.24-5). Similar to growth on plates, both *wrky59-1* and *wrky59-2* plants were more tolerant to AsIII and AsV. Over the course of one and two weeks of exposure to 30μM AsIII and 300μM AsV, *wrky59* plants grew significantly faster than WT relative to growth in control conditions (Figures 4.24-5). Plants containing a T-DNA insertion upstream of *WRKY59* (*wrky59-2*) were also more tolerant to the higher concentrations of 40μM AsIII after two weeks of exposure (Figure 4.25) and 400μM AsV during the first week of exposure (Figure 4.24), while *wrky59-1* plants were more tolerant to 40μM AsIII after one week (Figure 4.24).

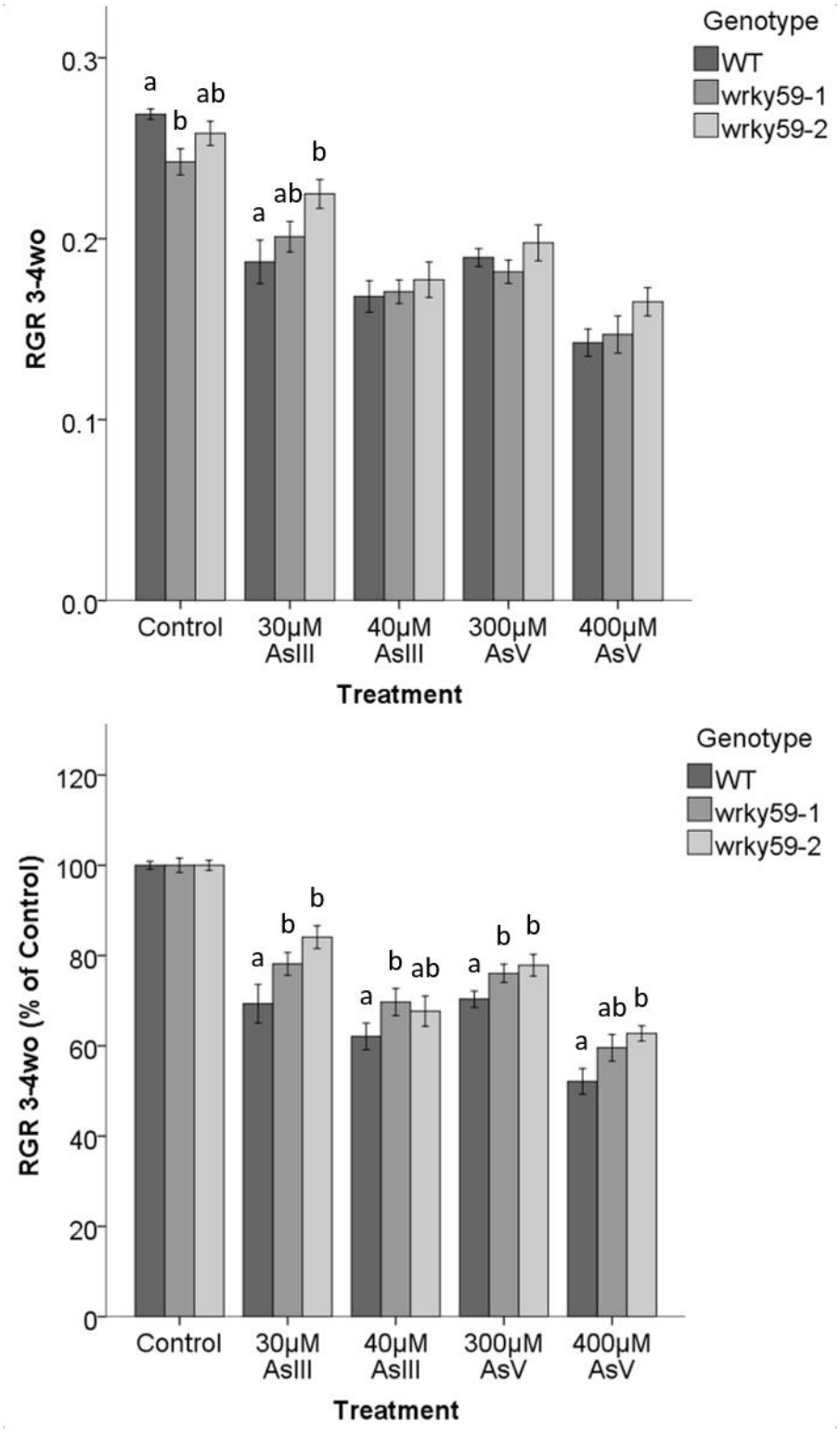

Figure 4.24 Relative growth rates of 3-4wo WT and *wrky59* plants exposed to As
The top panel displays the relative growth rate of 3-4wo WT, *wrky59-1* and *wrky59-2* plants grown in hydroponics and exposed to different concentrations of AsIII and AsV. The bottom panel shows the same data expressed relative to growth in control conditions. Data are from at least four independent experiments, values are means ± SE and letters indicate significant differences between genotypes at $P<0.05$.

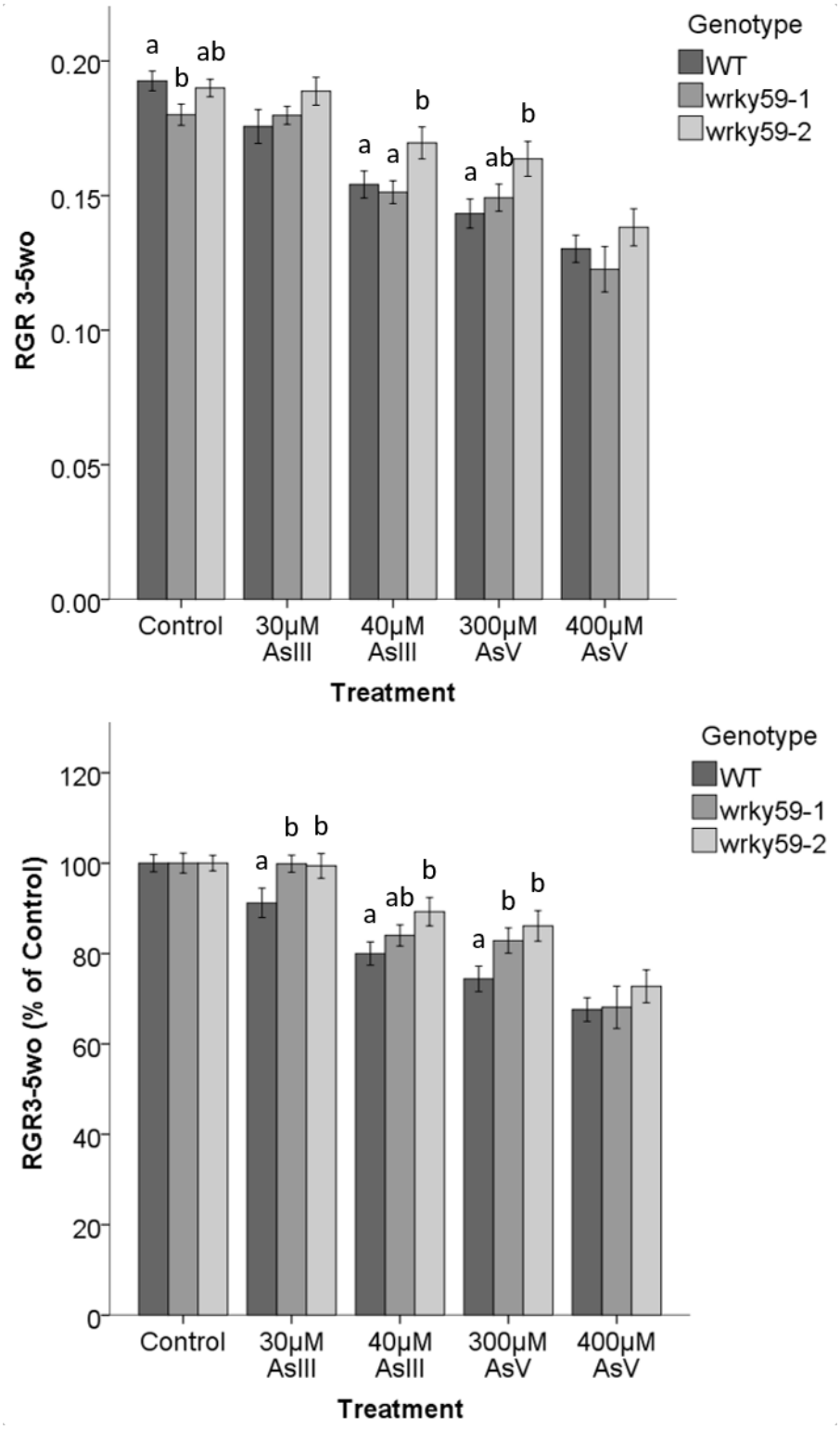

Figure 4.25 Relative growth rates of 3-5wo WT and *wrky59* plants exposed to As
The top panel displays the relative growth rate of 3-5wo WT, *wrky59-1* and *wrky59-2* plants grown in hydroponics and exposed to different concentrations of AsIII and AsV. The bottom panel shows the same data expressed relative to growth in control conditions. Data are from at least four independent experiments, values are means ± SE and letters indicate significant differences between genotypes at $P<0.05$.

4.3.3.4 Arsenic Concentration of *wrky59* Plants

WT, *wrky59-1* and *wrky59-2* plants were exposed to 30μM AsIII or 300μM AsV in hydroponics for two weeks and the tissue As concentrations compared between genotypes. There were no significant differences between genotypes in root, shoot, shoot:root As or total plant As concentrations after exposure to AsIII (Figure 4.26).

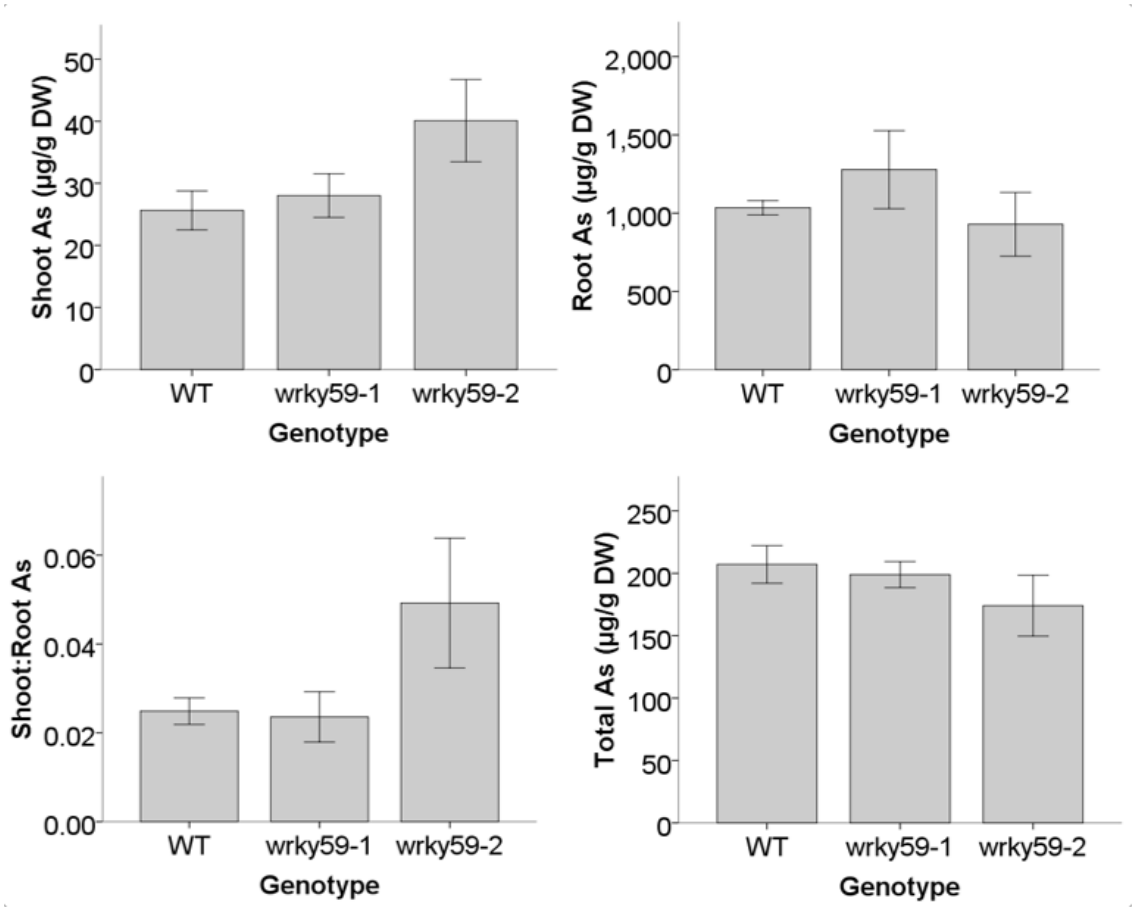

Figure 4.26 Arsenic concentration of WT, *wrky59-1* and *wrky59-2* plants exposed to 30μM AsIII

Graphs show the As concentration of WT, *wrky59-1* and *wrky59-2* plant tissues after two weeks exposure to 30μM AsIII in hydroponics. The top left and right panels show the average shoot and root As concentrations respectively. The bottom left panel shows the shoot:root As and the bottom right panel shows the total plant As concentration. Data are from three independent experiments, values are means ±SEs and letters indicate significant differences between genotypes at $P<0.05$ using unpaired *t*-tests.

After two weeks of exposure to 300μM AsV, *wrky59* plants had accumulated less As in the roots compared to WT although the difference was significant only for *wrky59-1* (Figure 4.27). There was no difference in the shoot As concentration or the root to shoot partitioning of WT and *wrky59* plants, but both *wrky59-1* and *wrky59-2* plants had a significantly lower total plant As concentration compared to WT (Figure 4.27). This suggests that *WRKY59* has a role in As uptake and/or efflux, but is not involved in the root to shoot translocation of As.

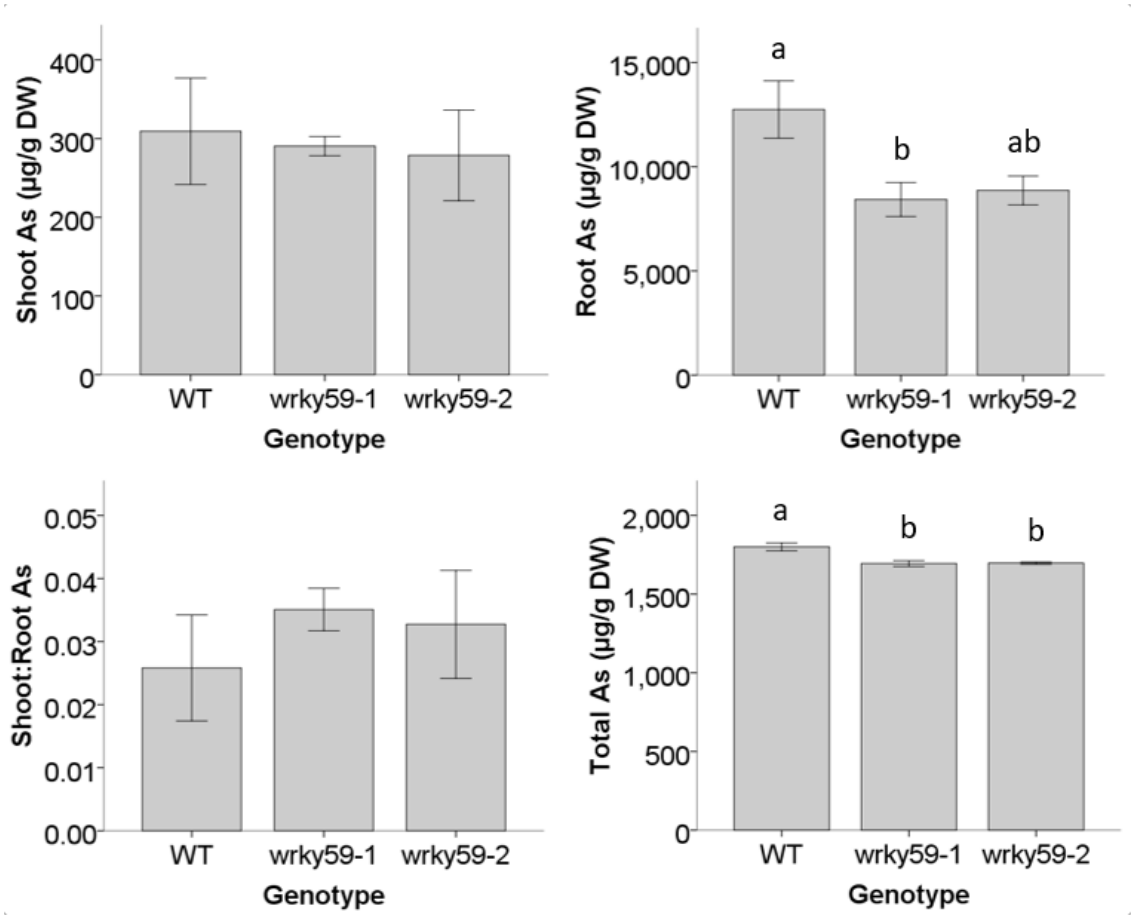

Figure 4.27 Arsenic concentration of WT, *wrky59-1* and *wrky59-2* plants exposed to 300µM AsV

Graphs show the As concentration of WT, *wrky59-1* and *wrky59-2* plant tissues after two weeks exposure to 300µM AsV in hydroponics. The top left and right panels show the average shoot and root As concentrations respectively. The bottom left panel shows the shoot:root As and the bottom right panel shows the total plant As concentration. Data are from three independent experiments, values are means ±SEs and letters indicate significant differences between genotypes at $P<0.05$ using unpaired *t*-tests.

4.3.3.5 Arsenic Efflux of *wrky59* Plants

The role of *WRKY59* in As efflux was investigated by exposing WT, *wrky59-1* and *wrky59-2* plants to 350µM AsV for 24hrs. There were no significant differences in As efflux between WT and *wrky59-1* plants after 6 or 24 hours (Figure 4.28). After 6 hours, *wrky59-2* plants had effluxed significantly less As than WT while there was no difference after 24 hours. The *wrky59-2* plants used for the 6 hour efflux experiment were significantly smaller than WT and *wrky59-1*, which may help explain the markedly reduced efflux observed (probably due to reduced root surface area for efflux). When efflux was calculated relative to root dry weight rather than plant As concentration, there was no difference in efflux between genotypes after 6 or 24 hours (Figure 4.28).

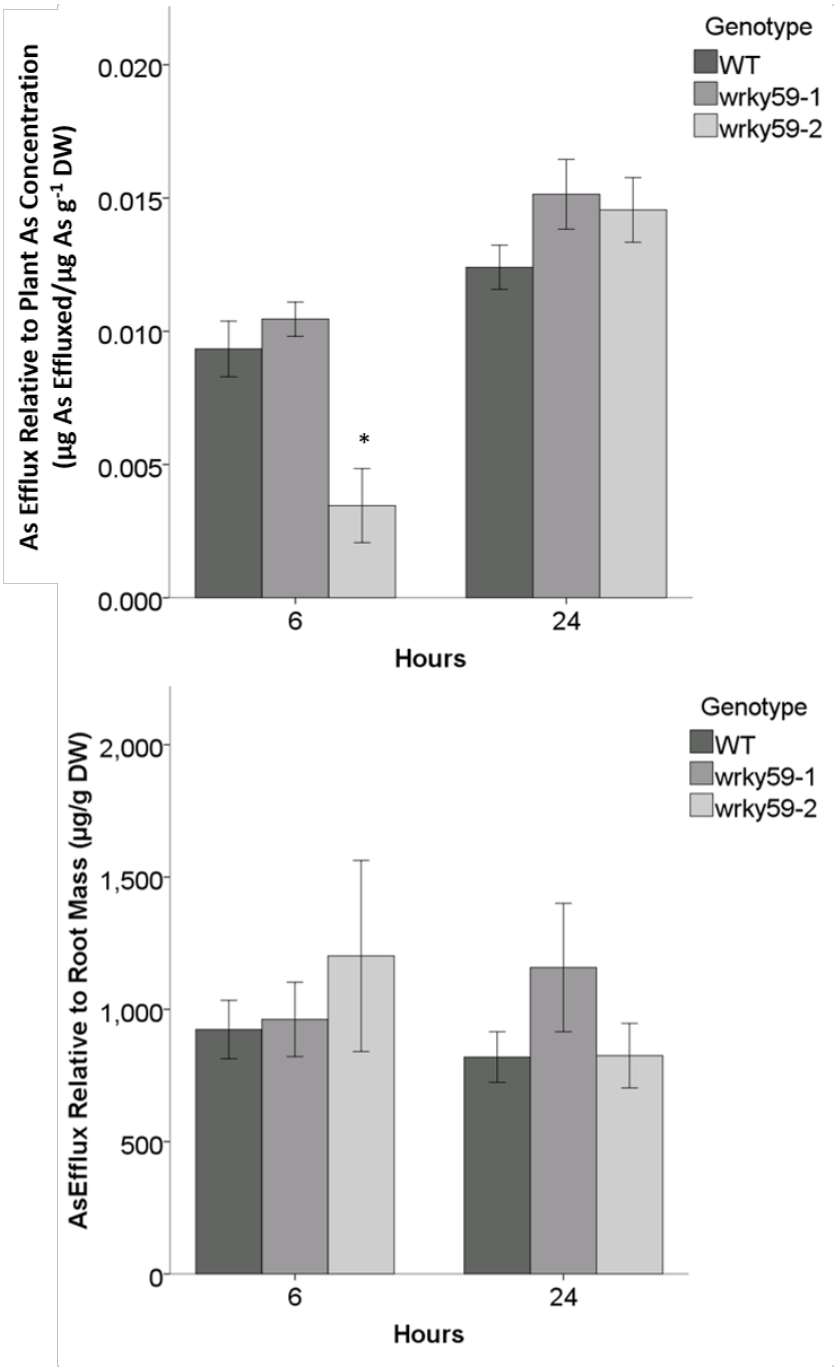

Figure 4.28 17 Efflux of As from WT and *wrky59* mutant plants
The top panel shows the amount of As effluxed from the roots of 3wo *Arabidopsis* plants relative to the plant As concentration (As Effluxed/µg As g^{-1} DW plant). The bottom panel shows the amount of As effluxed relative to the root mass (µg As effluxed/g root DW). Plants were preloaded with As by exposure to 350µM AsV in hydroponics for 24hrs. Roots were rinsed and placed in As free medium. As efflux was measured 6 and 24 hours after transfer. Data are from three independent experiments, values are means ±SEs and asterisks indicate a significant difference from WT at $P<0.05$ using an unpaired t-test.

To investigate differences in As loading between genotypes, the total plant As concentration and the shoot:root As ratio of plants used in the efflux experiment was determined. There was no significant difference in shoot:root As ratio (Figure 4.29), but

wrky59-2 plants had a small but significant increase in total plant As concentration compared to WT.

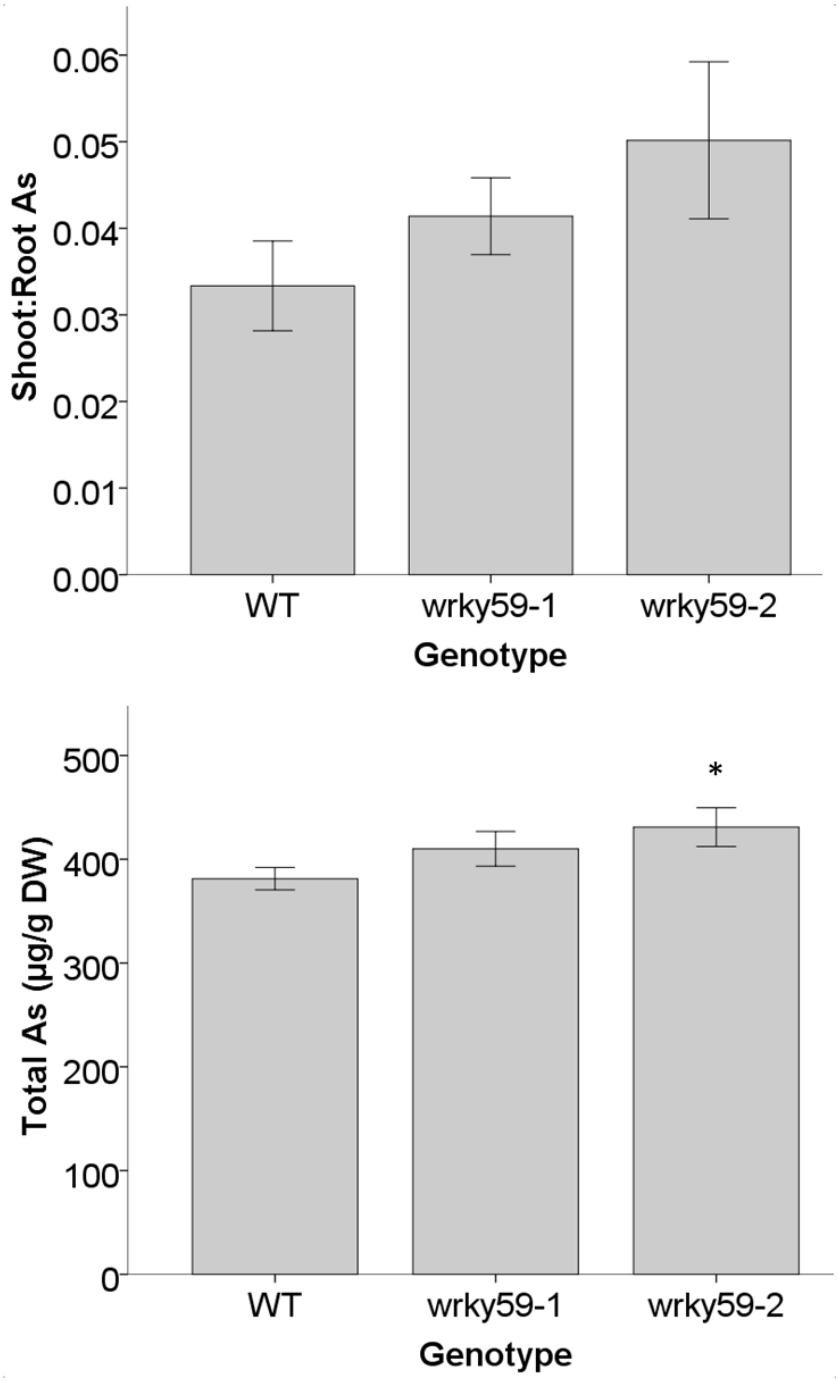

Figure 4.29 Arsenic loading of WT and *wrky59* plants used in the efflux experiment
Graphs show the shoot:root As (top graph) and total plant As concentration (bottom graph) of As in 3wo plants after exposure to 350µM AsV for 24 hours. Data are from three independent experiments, values are means ±SEs, and asterisks indicate a significant difference from WT at $P<0.05$ using an unpaired *t*-test.

4.4 Discussion

In this chapter, a combination of forward and reverse genetic screening of a T-DNA insertion library has led to the identification and characterisation of novel components of the As response in *Arabidopsis*.

4.4.1 Role of *AtLsi2* in Response to As

AtLsi2 is an orthologue of the rice AsIII efflux transporter *OsLsi2*. Two T-DNA insertion mutants in *AtLsi2* were characterised in order to determine the role of *Lsi2* in response to As. Growth experiments on agar plates and in hydroponics were carried out with WT and *lsi2-1* plants and revealed increased tolerance to AsV in the knockout plants in terms of fresh weight and root growth on plates in addition to growth rate in hydroponics (Figures 4.6,8 & 9). Loss of function *lsi2-1* plants were not more tolerant than WT to AsIII when exposed in hydroponics, and were actually more sensitive to AsIII treatment on agar plates (Figures 4.4-5 & 8-9).

Both long and short term treatment with AsV resulted in reduced Root As, increased Shoot As and subsequently higher shoot:root As in *lsi2-1* and *lsi2-2* plants compared to WT (Figures 4.14-15). There was no difference in the total plant As concentration, nor in As efflux between WT and the *lsi2* T-DNA insertion mutants, suggesting that *Lsi2* is not involved in As uptake or efflux, but instead has a role in controlling the root to shoot translocation of As. The increased shoot and reduced root concentrations of As in *lsi2* knockout plants suggest Lsi2 may have a role in As sequestration and/or accumulation in the roots.

Lsi2 is expressed most highly in the epidermis and cortex of the roots (Figure 4.2), where it could be involved in efflux of As towards the external medium or towards the stele. If this were the case, we might expect there to be reduced As efflux to the external medium or reduced root to shoot As translocation in *lsi2* loss of function mutants, neither of which were observed under the conditions tested in this study. Alternatively, Lsi2 may be localised to the tonoplast rather than the plasma membrane where it may have a role in vacuolar sequestration of As in the root. This could explain the reduced root As concentration and increased root to shoot translocation observed in the *lsi2* loss of function mutants. Future experiments to determine the subcellular and tissue specific localisation of Lsi2, such as expression of Lsi2-GFP fusion proteins and promoter:GUS studies, would help determine the precise role of Lsi2 in response to As in *Arabidopsis* roots.

It is unclear how increased shoot:root As correlates with increased tolerance to AsV in *lsi2* plants. If *Lsi2* is involved in vacuolar sequestration of As in the roots, we might expect loss of function to result in increased sensitivity to As rather than increased tolerance. The growth experiments carried out with minimal sulphur levels in the medium suggest that S is required for the increased AsV tolerance observed in *lsi2* plants. When WT and *lsi2-1* plants were exposed to AsV in minimal S medium, *lsi2* plants were more sensitive than WT (Figure 4.12). Sulphur has previously been described as an important component of the As detoxification and sequestration pathway in plants; it is incorporated in GSH and PC synthesis and so is essential for As detoxification through complexation of AsIII prior to sequestration in the vacuole [51]. It also has a role in GSH mediated AsV reduction [90]. In *Arabidopsis* mutants defective in GSH and PC synthesis (*cad2-1* and *cad1-3* respectively), reduced complexation of AsIII in the roots was correlated with increased As mobility resulting in increased efflux from the roots and a markedly increased root to shoot translocation of As [93] which is reminiscent of the increased shoot:root As in *lsi2* mutants. However, *cad2-1* and *cad1-3* plants were also dramatically more sensitive to AsV than WT while *lsi2* plants were more tolerant except under S deficient conditions. This, coupled with the knowledge that *lsi2* mutant plants did not grow differently than WT in S deficient medium (Figure 4.12), suggests that *Lsi2* is probably not involved in S homeostasis. Under conditions of S deprivation and exposure to AsV, WT plants translocated a higher proportion of As to the shoot compared to plants exposed to sufficient S [93]. It may be that in *lsi2* plants exposed to As in S deficient medium, a further increase in root to shoot As translocation negated the tolerance conferred by loss of function in *lsi2* in sufficient S. It would therefore be interesting and informative to determine the tissue distribution and speciation of As in WT and *lsi2* plants exposed to As in S deficient medium compared to S sufficient medium.

Alternatively, the increased sensitivity to As observed in *lsi2* plants under low S conditions could be explained by the altered tissue expression pattern of *Lsi2* under conditions of S deficiency. According to the Arabidopsis eFP browser, *Lsi2* expression is downregulated in the epidermis and cortex of the roots and upregulated in the endodermis and stele under low S conditions [194]. It would be interesting to study the tissue specific expression of *Lsi2* under low S conditions in the presence of As. This may give some clues as to the function of *Lsi2* and may help explain the relative tolerance of WT plants under these conditions compared to the *lsi2* loss of function mutants.

In order to fully understand the role of Lsi2 in response to As in *Arabidopsis* it will be necessary to determine the substrate specificity and transport activity of the protein.

Orthologues of Lsi2 in other species have so far been shown to have Si and AsIII efflux activity [56, 65, 184]. Heterologous expression of *AtLsi2* and *OsLsi2* in yeast had no effect on growth in the presence of AsIII or AsV [57] despite *OsLsi2* having been characterised as an AsIII transporter in plants, suggesting that the protein is not functional in yeast. Expression in an alternative heterologous system, such as *Xenopus* oocytes, or transport studies using plant protoplasts expressing *AtLsi2* could be used to provide evidence of Lsi2 function in *Arabidopsis.*

4.4.2 Physiological Role of *Lsi2* in *Arabidopsis*

Lsi2 has been characterised as a plasma membrane localised Si efflux transporter involved in Si accumulation in rice, maize and barley [65, 184]. Orthologues of *Lsi2* can also be found in non-Si accumulators including tomato and *Arabidopsis* [185], suggesting an alternative physiological role of *Lsi2* in these species. The growth of *lsi2* loss of function mutants was impaired under control, non-stressed conditions in terms of root growth and fresh weight on agar plates (Figures 4.4-5) and whole plant growth rate in hydroponics (Figure 4.8). This suggests that *Lsi2* has an important role in normal plant growth. Growth experiments carried out on agar plates and in hydroponics suggested a putative role of *Lsi2* in B homeostasis in *Arabidopsis*. Loss of function mutants in *lsi2* were more sensitive to B deficiency in terms of root growth, while whole plant growth was more sensitive to B toxicity compared to WT plants (Figures 4.7 & 4.10).

If we assume a similar pattern of B tissue distribution in *lsi2* knockout plants as observed with As, an increased shoot:root B could explain the observed sensitivity to excess B supply in *lsi2* plants and the increased sensitivity to B deficiency in the roots of *lsi2* plants. Increased shoot B concentrations in the *lsi2* mutants could render them more sensitive to excess B in these tissues, while reduced root B concentrations would increase sensitivity of root tissues to B deprivation. It would be interesting to investigate the B transport capability of Lsi2 and to compare B tissue distribution patterns between WT and *lsi2* loss of function plants in future studies.

Lsi2 is highly expressed in senescing leaves, where it could also be involved in B homeostasis. B may be remobilised along with other phloem mobile nutrients from senescing leaves during flower/seed development [210]. *Arabidopsis* is known to have phloem mobile B, as the role of *NIP6;1* in xylem to phloem B transfer at nodal tissues demonstrates [174]. It would be interesting to explore the role of *Lsi2* in senescing leaves in future studies, as if it is involved in B remobilisation this could have important implications for reproductive development and could potentially affect seed As concentration.

Two types of membrane transporter have been implicated in B transport in plants so far; members of the aquaporin family including NIPs [54, 174, 211], PIPs [212] and TIPs [213] and BOR-type efflux transporters [214]. *AtLsi2* may represent a novel type of B transporter in plants whose putative role in B homeostasis would be interesting to study further in the future, and may provide an explanation for the presence of this orthologue of Si transporters in non-Si accumulating species.

4.4.3 Forward Genetic Screen for As Tolerance in *Arabidopsis*

In this chapter, a forward genetic screen was carried out on *Arabidopsis* T-DNA insertion lines with the aim of identifying novel genes involved in As tolerance. The screen generated a list of candidate genes which may be more sensitive or tolerant to AsV and which would be interesting to investigate further in the future. One of the most promising candidates, a line containing a T-DNA insertion in the TF *WRKY59*, was chosen for further characterisation and found to be more tolerant to both AsIII and AsV stress. This indicates that the screen was successful in identifying novel genes involved in As tolerance in *Arabidopsis.* A list of 48 candidate genes (Table 6.1 in the Appendix) was compiled out of 6868 tested T-DNA insertion lines. Of these, only one has been confirmed as having an As responsive phenotype so far (*WRKY59*).

Included within the 6868 lines tested was a line with a T-DNA insertion in *NIP1;1*, a line which has previously been associated with increased tolerance to As [60]. This line was not picked out under the screening conditions used in this study, indicating that the screen while useful is not a perfect tool, there may be other genes involved in As tolerance which were also not picked up. The screening conditions could be improved upon, the criteria used to pick out As tolerant/sensitive lines was subjective rather than quantitative. The initial screening did not include WT plants as a comparison, and the germination and growth of individual lines was often very variable. Taking photos of the plants over the course of the screen was time consuming but helpful in distinguishing between As sensitive plants and those which had germinated more slowly. The length of the initial screen (4 weeks of AsV treatment) while perhaps more physiologically relevant than screens undertaken on agar plates with short term As treatments, meant that the screening process was quite time consuming and took up a lot of space in the glasshouse. A more efficient (preferably at least semi-quantitative) screening method would enable more replicates and probably result in a higher reward to effort ratio, as it would be easier to correctly and successfully identify additional As responsive mutants.

4.4.3.1 Role of *WRKY59* in As Tolerance

Two lines containing T-DNA insertions in *WRKY59* were characterised at the mRNA level to confirm loss of function. In the first allele, the T-DNA insertion is located in the second exon, presumably causing alternative splicing of the transcript (Figure 4.19). The second exon contains the WRKY domain which is required for DNA binding [186, 187], which implies that the alternatively spliced protein in *wrky59-1* is non-functional. In the second allele, the T-DNA is inserted upstream of the coding region in the promoter of *WRKY59.* Transcript was still detected in *wrky59-2*, and in fact seemed to be present at higher concentrations than WT plants (Figure 4.20). The effect of T-DNA insertion in the promoter region of *wrky59-2* plants requires further characterisation using a quantitative approach. The expression of *WRKY59* in WT and *wrky59-2* plants in response to As should also be investigated.

Considering the contrasting effect of T-DNA insertion in the two alleles, it is surprising that both lines respond similarly to As treatment. Both *wrky59-1* and *wrky59-2* were more tolerant to AsIII and AsV treatment on agar plates and in hydroponics compared to WT (Figures 4.22-25). There were no differences in As uptake or root to shoot translocation after two weeks exposure to AsIII however after two weeks exposure to AsV, both lines had accumulated less As in total than WT plants. There was no significant difference in the amount of As effluxed from the roots of WT, *wrky59-1* or *wrky59-2* plants, suggesting that the increased As tolerance in the T-DNA insertion lines is a result of reduced As uptake.

Increased As tolerance of *wrky59* T-DNA insertion lines was observed after exposure to both AsIII and AsV, while reduced uptake was only seen after exposure to AsV. This suggest that *WRKY59* may have an additional role in As detoxification which could explain the tolerance phenotype observed in plants exposed to AsIII. In order to determine the precise role of *WRKY59* in the As response, further studies will be required. Transcriptomic studies comparing WT and *wrky59* T-DNA insertion plants would reveal targets of the *WRKY59* TF, giving insight to the mechanism of As tolerance in these lines and may reveal additional novel components of the As response in plants.

4.5 Conclusions

In this chapter, both forward and reverse genetics approaches were used to successfully identify novel components of the As response in *Arabidopsis*. Lsi2 was found to be involved in the root to shoot translocation of As and may be involved in B homeostasis. WRKY59 was identified as a potential regulator of the As response,

disruption of the *WRKY59* gene resulted in increased As tolerance and reduced As uptake. Further characterisation of *Lsi2* and *WRKY59,* as well as the other potential candidates identified through the screen, will further our understanding of how plants respond to As and could eventually lead to the development of crop plants with improved tolerance to As and reduced accumulation of As in the edible parts.

Chapter 5: Final Discussion

Chronic arsenic poisoning poses a major public health risk worldwide. One of the routes by which people are exposed to As is through its uptake and accumulation in crop plants. There is no known cure for As poisoning, so it is imperative that exposure to As is limited and prevented where possible [8]. Therefore, it is important that research is undertaken to reduce As accumulation in crops. To achieve this aim, a more complete understanding of the As transport and detoxification mechanisms in plants will be required. Nevertheless, significant advances in our knowledge of plant As responses have been made in the past decade or so. This knowledge has been utilised to improve As tolerance in both model and crop species using a biotechnological approach as discussed in detail in Chapter 1.

5.1 A Transgenic Approach to Improving As Tolerance in Plants

Previously, a plasma membrane localised AsIII efflux transporter from yeast (*ACR3*) was heterologously expressed in rice under the control of the 35S promoter. This successfully increased AsIII efflux from the roots to the external medium, and reduced accumulation of As in the grain by up to 30% [128]. However, there was no concurrent increase in As tolerance and in some cases there was an increase in root to shoot As translocation [133]. As described in the Chapter 2, *ACR3* was expressed in rice under the control of the *CatB* promoter to investigate if tissue specific expression of *ACR3* could improve upon the reported lines constitutively expressing *ACR3.*

Expression of *ACR3* in different tissues had differential effects on As tolerance and transport in rice. Root specific expression increased As efflux to the external medium without increasing the root to shoot translocation of As, leading to reduced As accumulation and increased tolerance to As over long term exposure. On the other hand, expression of *ACR3* in stem and leaf tissue resulted in increased sensitivity to long term As treatment and increased accumulation of As. These results confirm that expression of an As permeable transporter in different tissues can alter As tolerance and accumulation over long term exposure to As, even when expressed at relatively low levels. It suggests that heterologously expressing As transporters under the control of different tissue specific promoters could have startlingly different effects on As tissue distribution. Therefore, this is a promising strategy for the future development of As accumulating (for phytoremediation purposes) and As excluding (for human consumption) plants.

In addition to exploring the effect of expressing *ACR3* under the control of alternative tissue specific promoters, it may be beneficial to combine *ACR3* expression with increased As detoxification mechanisms to further enhance As tolerance in plants. For example, increasing AsV reductase, GSH/PC synthesis and sequestration capabilities

in specific tissues (e.g. roots) could restrict the majority of As accumulation to that particular tissue, enabling more efficient phytoremediation or exclusion of As from the shoot and/or grain. Stacking of multiple As resistance genes has successfully enhanced As tolerance to a greater extent than expression of single genes in the model plant *Arabidopsis* [83, 117] and root specific expression of *SpHMT1* (tonoplast localised PC-As transporter) in *Arabidopsis* restricted the majority of As accumulation to the roots [118]. Therefore, stacking multiple As resistance genes in crop plants such as rice may be a viable strategy for developing super-tolerant varieties with reduced As accumulation in the future.

5.2 The Role of NIPs in Arsenic Transport, Tolerance and Accumulation in *Arabidopsis*

Efforts to improve As tolerance and reduce As accumulation in crops will benefit from enhanced knowledge and understanding of As uptake and detoxification pathways in plants. Chapters 3 and 4 of this thesis focused on increasing our knowledge of these processes in the model plant *Arabidopsis*.

In Chapter 3, group II NIPs were identified as having an important role in controlling the tissue distribution of As, particularly in the As loading of the seeds. Both *nip6;1* and *nip7;1* loss of function mutants had significantly reduced concentrations of As in the seed compared to WT. For *nip6;1* loss of function plants, it seems likely that this is due to reduced loading of As into the phloem whereas *NIP7;1* may be involved in loading As into the seed directly. It would be beneficial to determine the precise mechanism by which *nip7;1* loss of function mutants accumulate higher concentrations of As in the rosette leaves, pedicels and green siliques compared to WT plants whilst excluding As from the mature seed. To this end, it would be very interesting to compare the cellular and subcellular distribution of As in the reproductive tissues of WT and *nip* loss of function mutants. This could be achieved using synchrotron X-Ray fluorescence and/or high resolution secondary ion mass spectrometry, and may offer clues as to the function of *NIP7;1* in As loading of the seed. These techniques were successfully utilised by Moore, K.L. *et al.* [215, 216] to reveal the subcellular localisation of As in the shoot vascular system and grain of rice. In the shoot vascular tissues, As co-localised with S to the vacuole which is consistent with As-thiol chelation and sequestration [216]. It would be interesting to determine if the excess As accumulated in shoot tissues of *nip7;1* plants after long term AsV exposure localised similarly with S to the vacuole. This would lend support to the hypothesis that increased detoxification and sequestration efficiency of As in *nip7;1* plants confers increased tolerance to AsV alongside increased As accumulation. It would also be interesting to compare the

speciation of As in different tissues of WT and *nip7;1* insertion mutants. This could help determine if AsV detoxification mechanisms are more efficient in *nip7;1* mutant plants, by comparing the abundance of AsV, AsIII and As-thiol complexes in *nip7;1* tissues compared to WT. This can be done using techniques such as ion exchange chromatography or reversed-phase-HPLC coupled to ICP-MS [217] . A more complete understanding of the mechanism of AsV tolerance and seed As exclusion in *nip* loss of function mutants could prove invaluable for informing future strategies to improve As tolerance in crops.

Knocking out the function of multiple As permeable channels did not have an additive effect; loss of function in *nip6;1nip7;1* double mutants resulted in impaired plant growth under control conditions and no enhanced tolerance or reduced As uptake or seed As concentrations compared to the single mutants. Rather than knocking out the function of As transporters in crops completely, it would be beneficial to find or create variants of these transporters with reduced As affinity. This would allow uptake and translocation of beneficial nutrients such as Si, B and P to continue unimpeded while restricting AsIII and AsV accumulation.

It would be interesting to determine the relative selectivity of different transporters for P/Si/B over AsV/AsIII, and to examine allelic variation in substrate specificity between As tolerant and sensitive plant varieties. There is evidence that different Pht1 transporters have different transport rates for AsV. For example, PvPht1;3 had a higher affinity for AsV relative to AtPht1;5 and AtPht1;7 when competitive uptake assays were performed in yeast [48]. In addition, analysis of P and AsV uptake rates of different wheat cultivars revealed differences in the P:AsV uptake ratios [218] which suggests that there is allelic variation in AsV binding affinity of P transporters in wheat. Another possibility for discovering As excluding transporters could be to study organisms living in extreme As-rich environments. For example, phosphate binding proteins (PBPs) belonging to the ABC-type transport family have been described in bacterial strains isolated from the arsenate-rich Mono Lake environment which are capable of discriminating P transport over AsV up to 4500 fold [219]. If similar variation in AsIII permeability of NIPs could be discovered and exploited, it could help dramatically reduce As accumulation in the edible portions of crops grown in both aerobic and anaerobic conditions.

5.3 Identification of Novel Components of the Arsenic Response in *Arabidopsis*

Forward and reverse genetic screening of *Arabidopsis* T-DNA insertion mutants identified novel genes involved in As tolerance. *AtLsi2* is an orthologue of the Si/AsIII efflux transporter *OsLsi2*. This family of efflux transporters has not been extensively studied in plants and their physiological role in non-Si accumulating species is unclear. In rice, *OsLsi2* is essential for efficient Si/AsIII uptake and translocation to the shoot and loss of function mutations result in improved AsIII tolerance and markedly reduced grain As concentrations [56]. However, loss of function mutations in *Lsi2* in *Arabidopsis* do not increase tolerance to AsIII but rather improved tolerance to AsV. Also in contrast to rice *lsi2* mutants, *Arabidopsis lsi2* loss of function mutants translocated a higher proportion of As to the shoot. This indicates divergent roles for Lsi2 transporters in Si and non-Si accumulating plants and suggests they could also be relevant targets for improving As tolerance in crops other than cereals, such as vegetables grown in aerobic soils. While vegetables typically accumulate lower concentrations of inorganic As than rice, they can still contribute significantly to dietary As intake particularly when grown in As contaminated regions [220-223].

In the present study, the transcription factor *WRKY59* was identified as a novel gene involved in As tolerance in *Arabidopsis*. There are several examples of *WRKY* transcription factors whose expression has been modified for crop improvement purposes, as recently reviewed by Phukan, U.J. *et al.* [189]. Transcription factors are attractive targets for genetic engineering of novel crop traits as they enable manipulation of multiple components of stress responses through the modification of one regulatory gene. T-DNA insertion mutants in *WRKY59* were more tolerant to both AsIII and AsV and accumulated significantly less As when exposed to AsV. The reduction in As uptake following exposure to AsV in the *WRKY59* T-DNA insertion mutants suggests that *WRKY59* may affect As uptake similarly to *WRKY6, WRKY42* and *WRKY45* through the regulation of P transporters. However, the increased tolerance observed following exposure to AsIII suggests an alternative or additional effect of *wrky59* T-DNA insertion on As detoxification mechanisms. It would be interesting to determine which genes are transcriptionally regulated by *WRKY59* in response to As, as this could help determine the mechanism of As tolerance in these lines and may identify further novel components of the As response.

Appendix

gtcttatctcctcgtgatccctttttttggatcgatccatgttcgtagtacgtgacaa
gcacgcgcaccaaccgaagcaggtacctgtgtcgctgcctgtgggcccca
cacaccccaagacggccattaataaacaaacacgacgtggacgaagag
aagggaggccggcaagaagcatactagcacgctacgaaacccccttctc
ttcgtccccaaattGCACTACAAAAAAGGCCGCCCCTTTCT
TCTCTCCTCGTCCTTATCACCACCAATCCGATCCTCT
TCTCTTCTCTTCTCTTCTTCCCCACATCCAGTTCGAT
TCTCATCTCTCCCACAACA

Figure 6.1 Sequence of *CatB* promoter
Figure shows the 340bp sequence of the *CatB* promoter region used to drive expression of *ACR3* in *CatB:ACR3* expressing rice. Uppercase letters indicate the start of the 5' UTR of *CatB* cDNA.

GCCTGCCTAATCAAAAGGCAGTGAGGACTGTAACTA
CTAGTACCTGCCACCTCCCAGTTGCTCAGGCTTCTC
AACCTTAGCTAGCTCGATCTCCCTATAAATACTCCTG
CTCATTACCACAACGAGCAAGCGATCGACGGAGCG
AGCGAGCTAGCCAGCCAGTGTTAGAGCTTGAGCTG
CTTGTTCTTCTTCTACCTCCTGCACTCGCGTGCTGC
ACAAGTAGCTC

Figure 6.2 Sequence of *Lsi1S* promoter
Figure shows the 226bp fragment of the *OsLsi1* promoter region that was used to drive expression of *ACR3* in *Lsi1S:ACR3* expressing rice.

Table 6.1 Shortlist of candidate genes identified through a forward genetic screen for altered response to As

Gene ID	Response to As
AT1G05300	<WT
AT1G19450	<WT
AT1G61720	<WT
AT1G63450	<WT
AT1G77990	<WT
AT2G02380	<WT
AT2G21410	<WT
AT2G23970	<WT
AT2G28090	<WT
AT2G36950	<WT
AT2G39010	<WT
AT2G40460	<WT
AT3G07600	<WT
AT3G17650	<WT
AT3G26590	<WT
AT3G53510	<WT
AT4G19690	<WT
AT4G28580	<WT
AT5G17220	<WT
AT5G20500	<WT
AT5G20650	<WT
AT5G41220	<WT
AT5G41240	<WT
AT5G44000	<WT
AT5G57350	<WT
AT1G06925	>WT
AT1G48070	>WT
AT1G65310	>WT
AT2G21900	>WT
AT2G22460	>WT
AT2G25520	>WT
AT2G27240	>WT
AT3G09640	>WT

AT3G11280	>WT
AT3G13080	>WT
AT3G55090	>WT
AT4G01440	>WT
AT4G04700	>WT
AT4G09000	>WT
AT4G14030	>WT
AT4G31170	>WT
AT5G04260	>WT
AT5G07000	>WT
AT5G17830	>WT
AT5G48850	>WT
AT5G49450	>WT
AT5G58050	>WT
AT5G65687	>WT

Abbreviations

ABA	Abscisic Acid
ABC	ATP-binding cassette
ACR	Arsenic compounds resistance
ADP	Adenosine diphosphate
AQP	Aquaporin
Ar/R	Aromatic/arginine
Ars	Arsenic resistance system
arsM	S-adenosylmethyltransferase
As	Arsenic
AsIII	Arsenite
AsV	Arsenate
ATQ1/HAC1	Arsenate tolerance QTL1/High arsenic content1
B	Boron
BOR	Boron transporter
CaMV 35S	Cauliflower mosaic virus 35S promoter
CatB	CatalaseB
CCCP	Carbonyl cyanide m-chlorophenylhydrazone
Cd	Cadmium
CDC25	Cell cycle dual-specificity phosphatase 25
CitMHS	Citrate Magnesium/Calcium Symporter
CO2	Carbon Dioxide
CDPK	Calcium dependent protein kinase
DFPM	[5-(3,4-Dichlorophenyl)Furan-2-yl]-Piperidin-1-ylMethanethione
DMA	Dimethylarsinic acid
DNA	Deoxyribonucleic acid
EDR1	Enhanced disease resistance 1
FOX	Full length cDNA over-expressed
Grx	Glutaredoxin
GSH	Glutathione
GSSG	Glutathione disulphide
GUS	β-Glucuronidase
ICP-OES	Inductively Coupled Plasma-Optical Emission Spectrometry
INT	Inositol transporter
JA	Jasmonic acid
Lsi	Low silicon rice

MIP	Membrane intrinsic protein
MMA	Monomethylarsonic acid
MPK	Mitogen activated protein kinase
NASC	Nottingham Arabidopsis Stock Centre
NIP	Nodulin-26-like intrinsic protein
NPA	Asn-Pro-Ala motif
NPR1	Nonexpressor of PR genes 1
NRAMP	Natural resistance-associated macrophage protein
P	Phosphate
PAF	Proteasome α subunit F
PC	Phytochelatin
PCS	Phytochelatin synthase
PHO	Phosphate permease
Pht	Phosphate transporter
PIP	Plasma membrane instrinsic protein
RGR	Relative growth rate
RNA	Ribonucleic acid
ROS	Reactive oxygen species
RT-PCR	Reverse transcriptase-polymerase chain reaction
S	Sulphur
Si	Silicon
SIP	Small and basin intrinsic protein
T-DNA	Transfer-DNA
TF	Transcription factor
TIP	Tonoplast intrinsic protein
TMD	Transmembrane Domain
WHO	World health organisation
wo	week old
WT	Wild type
YCF	Yeast cadmium factor
γ-ECS	γ-glutamylcysteine synthetase

References

1. Zhao, F.-J., McGrath, S. P. & Meharg, A. A. (2010) Arsenic as a Food Chain Contaminant: Mechanisms of Plant Uptake and Metabolism and Mitigation Strategies, *Annual Review of Plant Biology.* **61**, 535-559.

2. Garg, N. & Singla, P. (2011) Arsenic toxicity in crop plants: physiological effects and tolerance mechanisms, *Environmental Chemistry Letters.* **9**, 303-321.

3. Mandal, B. K. & Suzuki, K. T. (2002) Arsenic round the world: a review, *Talanta.* **58**, 201-235.

4. Hartley, T. N., Macdonald, A. J., McGrath, S. P. & Zhao, F.-J. (2013) Historical arsenic contamination of soil due to long-term phosphate fertiliser applications, *Environmental Pollution.* **180**, 259-264.

5. Singh, R., Singh, S., Parihar, P., Singh, V. P. & Prasad, S. M. (2015) Arsenic contamination, consequences and remediation techniques: A review, *Ecotoxicology and Environmental Safety.* **112**, 247-270.

6. Waxman, S. & Anderson, K. C. (2001) History of the Development of Arsenic Derivatives in Cancer Therapy, *The Oncologist.* **6**, 3-10.

7. IARC (2004) *Some Drinking-water disenfectants and Contaminants, including Arsenic*, Lyon, France.

8. Ratnaike, R. N. (2003) Acute and chronic arsenic toxicity, *Postgrad Med J.* **79**, 391-396.

9. ICPS (2001) *Arsenic and arsenic compounds*, 2nd edn, WHO, Geneva.

10. Meharg, A. A. & Hartley-Whitaker, J. (2002) Arsenic uptake and metabolism in arsenic resistant and nonresistant plant species, *New Phytologist.* **154**, 29-43.

11. Turpeinen, R., Pantsar-Kallio, M., Häggblom, M. & Kairesalo, T. (1999) Influence of microbes on the mobilization, toxicity and biomethylation of arsenic in soil, *Science of The Total Environment.* **236**, 173-180.

12. Ernst, W. H. O. (1996) Bioavailability of heavy metals and decontamination of soils by plants, *Applied Geochemistry.* **11**, 163-167.

13. Marin, A. R., Masscheleyn, P. H. & Patrick, W. H. (1993) Soil redox-pH stability of arsenic species and its influence on arsenic uptake by rice, *Plant and Soil.* **152**, 245-253.

14. Smith, A. H., Lingas, E. O. & Rahman, M. (2000) Contamination of drinking-water by arsenic in Bangladesh: a public health emergency, *Bulletin of the World Health Organization.* **78**, 1093-1103.

15. Ravenscroft, P., Brammer, H. & Richards, K. (2009) Health Effects of Arsenic in Drinking Water and Food in *Arsenic Pollution* pp. 157-212, Wiley-Blackwell.

16. Meharg, A. A., Williams, P. N., Adomako, E., Lawgali, Y. Y., Deacon, C., Villada, A., Cambell, R. C. J., Sun, G., Zhu, Y.-G., Feldmann, J., Raab, A., Zhao, F.-J., Islam, R., Hossain, S. & Yanai, J. (2009) Geographical Variation in Total and Inorganic

Arsenic Content of Polished (White) Rice, *Environmental Science & Technology.* **43**, 1612-1617.

17. (CONTAM), E. P. o. C. i. t. F. C. (2009) Scientific Opinion on Arsenic in Food., *EFSA Journal.* **7**, 1351-1550.

18. Williams, P. N., Villada, A., Deacon, C., Raab, A., Figuerola, J., Green, A. J., Feldmann, J. & Meharg, A. A. (2007) Greatly Enhanced Arsenic Shoot Assimilation in Rice Leads to Elevated Grain Levels Compared to Wheat and Barley, *Environmental Science & Technology.* **41**, 6854-6859.

19. Huq, S. M. I., Joardar, J. C., Parvin, S., Correll, R. & Naidu, R. (2006) Arsenic Contamination in Food-chain: Transfer of Arsenic into Food Materials through Groundwater Irrigation, *J Health Popul Nutr.* **24**, 305-316.

20. Xu, X. Y., McGrath, S. P., Meharg, A. A. & Zhao, F. J. (2008) Growing Rice Aerobically Markedly Decreases Arsenic Accumulation, *Environmental Science & Technology.* **42**, 5574-5579.

21. Khan, M. A., Stroud, J. L., Zhu, Y.-G., McGrath, S. P. & Zhao, F.-J. (2010) Arsenic Bioavailability to Rice Is Elevated in Bangladeshi Paddy Soils, *Environmental Science & Technology.* **44**, 8515-8521.

22. Panaullah, G., Alam, T., Hossain, M., Loeppert, R., Lauren, J., Meisner, C., Ahmed, Z. & Duxbury, J. (2009) Arsenic toxicity to rice (Oryza sativa L.) in Bangladesh, *Plant and Soil.* **317**, 31-39.

23. Stroud, J. L., Norton, G. J., Islam, M. R., Dasgupta, T., White, R. P., Price, A. H., Meharg, A. A., McGrath, S. P. & Zhao, F.-J. (2011) The dynamics of arsenic in four paddy fields in the Bengal delta, *Environmental Pollution.* **159**, 947-953.

24. Garnier, J. M., Travassac, F., Lenoble, V., Rose, J., Zheng, Y., Hossain, M. S., Chowdhury, S. H., Biswas, A. K., Ahmed, K. M., Cheng, Z. & van Geen, A. (2010) Temporal variations in arsenic uptake by rice plants in Bangladesh: The role of iron plaque in paddy fields irrigated with groundwater, *Science of The Total Environment.* **408**, 4185-4193.

25. Zavala, Y. J. & Duxbury, J. M. (2008) Arsenic in Rice: I. Estimating Normal Levels of Total Arsenic in Rice Grain, *Environmental Science & Technology.* **42**, 3856-3860.

26. Commission, E. (2015) Commission Regulation (EU) 2015/1006 of 25 June 2015 amending Regulation (EC) No 1881/2006 as regards maximum levels of inorganic arsenic in foodstuffs, *Official Journal of the European Union.* **58**, 14-16.

27. Shao, Y., Wang, J., Chen, X. & Wu, Y. (2014) The consolidation of food contaminants standards in China, *Food Control.* **43**, 213-216.

28. Meharg, A. A. & Rahman, M. M. (2003) Arsenic Contamination of Bangladesh Paddy Field Soils: Implications for Rice Contribution to Arsenic Consumption, *Environmental Science & Technology.* **37**, 229-234.

29. Carbonell-Barrachina, A. A., Aarabi, M. A., DeLaune, R. D., Gambrell, R. P. & Patrick, W. H. (1998) The influence of arsenic chemical form and concentration on Spartina patens and Spartina alterniflora growth and tissue arsenic concentration, *Plant and Soil.* **198**, 33-43.

30. Marin, A. R., Masscheleyn, P. H. & Patrick, W. H. (1992) The influence of chemical form and concentration of arsenic on rice growth and tissue arsenic concentration, *Plant and Soil.* **139**, 175-183.

31. Abbas, M. H. H. & Meharg, A. A. (2008) Arsenate, arsenite and dimethyl arsinic acid (DMA) uptake and tolerance in maize (Zea mays L.), *Plant and Soil.* **304**, 277-289.

32. Tang, Z., Kang, Y., Wang, P. & Zhao, F.-J. (2016) Phytotoxicity and detoxification mechanism differ among inorganic and methylated arsenic species in Arabidopsis thaliana, *Plant and Soil.* **401**, 243-257.

33. Tang, Z., Lv, Y., Chen, F., Zhang, W., Rosen, B. P. & Zhao, F.-J. (2016) Arsenic Methylation in Arabidopsis thaliana Expressing an Algal Arsenite Methyltransferase Gene Increases Arsenic Phytotoxicity, *J Agric Food Chem.* **64**, 2674-2681.

34. Finnegan, P. M. & Chen, W. (2012) Arsenic Toxicity: The Effects on Plant Metabolism, *Front Physiol.* **3**, 182.

35. Ter Welle, H. F. & Slater, E. C. (1967) Uncoupling of respiratory-chain phosphorylation by arsenate, *Biochimica et Biophysica Acta (BBA) - Bioenergetics.* **143**, 1-17.

36. Requejo, R. & Tena, M. (2005) Proteome analysis of maize roots reveals that oxidative stress is a main contributing factor to plant arsenic toxicity, *Phytochemistry.* **66**, 1519-1528.

37. Shin, H., Shin, H.-S., Dewbre, G. R. & Harrison, M. J. (2004) Phosphate transport in Arabidopsis: Pht1;1 and Pht1;4 play a major role in phosphate acquisition from both low- and high-phosphate environments, *The Plant Journal.* **39**, 629-642.

38. Remy, E., Cabrito, T. R., Batista, R. A., Teixeira, M. C., Sá-Correia, I. & Duque, P. (2012) The Pht1;9 and Pht1;8 transporters mediate inorganic phosphate acquisition by the Arabidopsis thaliana root during phosphorus starvation, *New Phytologist.* **195**, 356-371.

39. Nagarajan, V. K., Jain, A., Poling, M. D., Lewis, A. J., Raghothama, K. G. & Smith, A. P. (2011) Arabidopsis Pht1;5 Mobilizes Phosphate between Source and Sink Organs and Influences the Interaction between Phosphate Homeostasis and Ethylene Signaling, *Plant Physiology.* **156**, 1149-1163.

40. LeBlanc, M. S., McKinney, E. C., Meagher, R. B. & Smith, A. P. (2013) Hijacking membrane transporters for arsenic phytoextraction, *Journal of Biotechnology.* **163**, 1-9.

41. Hamburger, D., Rezzonico, E., MacDonald-Comber Petétot, J., Somerville, C. & Poirier, Y. (2002) Identification and Characterization of the Arabidopsis PHO1 Gene Involved in Phosphate Loading to the Xylem, *Plant Cell.* **14**, 889-902.

42. Stefanovic, A., Arpat, A. B., Bligny, R., Gout, E., Vidoudez, C., Bensimon, M. & Poirier, Y. (2011) Over-expression of PHO1 in Arabidopsis leaves reveals its role in mediating phosphate efflux, *The Plant Journal.* **66**, 689-699.

43. Quaghebeur, M. & Rengel, Z. (2004) Arsenic uptake, translocation and speciation in pho1 and pho2 mutants of Arabidopsis thaliana, *Physiologia Plantarum.* **120**, 280-286.

44. Liu, T.-Y., Huang, T.-K., Tseng, C.-Y., Lai, Y.-S., Lin, S.-I., Lin, W.-Y., Chen, J.-W. & Chiou, T.-J. (2012) PHO2-Dependent Degradation of PHO1 Modulates Phosphate Homeostasis in Arabidopsis, *Plant Cell.* **24**, 2168-2183.

45. Wang, Y., Ribot, C., Rezzonico, E. & Poirier, Y. (2004) Structure and Expression Profile of the Arabidopsis PHO1 Gene Family Indicates a Broad Role in Inorganic Phosphate Homeostasis, *Plant Physiology.* **135**, 400-411.

46. Wu, Z., Ren, H., McGrath, S. P., Wu, P. & Zhao, F.-J. (2011) Investigating the Contribution of the Phosphate Transport Pathway to Arsenic Accumulation in Rice, *Plant Physiology.* **157**, 498-508.

47. Kamiya, T., Islam, R., Duan, G., Uraguchi, S. & Fujiwara, T. (2013) Phosphate deficiency signaling pathway is a target of arsenate and phosphate transporter OsPT1 is involved in As accumulation in shoots of rice, *Soil Science and Plant Nutrition.* **59**, 580-590.

48. DiTusa, S. F., Fontenot, E. B., Wallace, R. W., Silvers, M. A., Steele, T. N., Elnagar, A. H., Dearman, K. M. & Smith, A. P. (2016) A member of the Phosphate transporter 1 (Pht1) family from the arsenic-hyperaccumulating fern Pteris vittata is a high-affinity arsenate transporter, *New Phytologist.* **209**, 762-772.

49. Meharg, A. A. & Macnair, M. R. (1990) An Altered Phosphate Uptake System in Arsenate-Tolerant Holcus lanatus L, *The New Phytologist.* **116**, 29-35.

50. Poynton, C. Y., Huang, J. W., Blaylock, M. J., Kochian, L. V. & Elless, M. P. (2004) Mechanisms of arsenic hyperaccumulation in Pteris species: root As influx and translocation, *Planta.* **219**, 1080-1088.

51. Zhao, F. J., Ma, J. F., Meharg, A. A. & McGrath, S. P. (2009) Arsenic uptake and metabolism in plants, *New Phytologist.* **181**, 777-794.

52. Bhattacharjee, H. & Rosen, B. P. (2007) Arsenic Metabolism in Prokaryotic and Eukaryotic Microbes in *Molecular Microbiology of Heavy Metals* (Nies, D. H. & Silver, S., eds) pp. 371-406, Springer Berlin Heidelberg.

53. Ma, J. F., Tamai, K., Yamaji, N., Mitani, N., Konishi, S., Katsuhara, M., Ishiguro, M., Murata, Y. & Yano, M. (2006) A silicon transporter in rice, *Nature.* **440**, 688-691.

54. Takano, J., Wada, M., Ludewig, U., Schaaf, G., Wirén, N. v. & Fujiwara, T. (2006) The Arabidopsis Major Intrinsic Protein NIP5;1 Is Essential for Efficient Boron Uptake and Plant Development under Boron Limitation, *The Plant Cell Online.* **18**, 1498-1509.

55. Mosa, K. A., Kumar, K., Chhikara, S., Mcdermott, J., Liu, Z., Musante, C., White, J. C. & Dhankher, O. P. (2012) Members of rice plasma membrane intrinsic proteins subfamily are involved in arsenite permeability and tolerance in plants, *Transgenic Research.* **21**, 1265-1277.

56. Ma, J. F., Yamaji, N., Mitani, N., Xu, X.-Y., Su, Y.-H., McGrath, S. P. & Zhao, F.-J. (2008) Transporters of arsenite in rice and their role in arsenic accumulation in rice grain, *Proceedings of the National Academy of Sciences.* **105**, 9931-9935.

57. Bienert, G., Thorsen, M., Schussler, M., Nilsson, H., Wagner, A., Tamas, M. & Jahn, T. (2008) A subgroup of plant aquaporins facilitate the bi-directional diffusion of As(OH)3 and Sb(OH)3 across membranes, *BMC Biology.* **6**, 26.

58. Isayenkov, S. V. & Maathuis, F. J. M. (2008) The Arabidopsis thaliana aquaglyceroporin AtNIP7;1 is a pathway for arsenite uptake, *FEBS Letters.* **582**, 1625-1628.

59. Xu, W., Dai, W., Yan, H., Li, S., Shen, H., Chen, Y., Xu, H., Sun, Y., He, Z. & Ma, M. (2015) Arabidopsis NIP3;1 Plays an Important Role in Arsenic Uptake and Root-to-Shoot Translocation under Arsenite Stress Conditions, *Molecular Plant.* **8**, 722-733.

60. Kamiya, T., Tanaka, M., Mitani, N., Ma, J. F., Maeshima, M. & Fujiwara, T. (2009) NIP1;1, an Aquaporin Homolog, Determines the Arsenite Sensitivity of Arabidopsis thaliana, *Journal of Biological Chemistry.* **284**, 2114-2120.

61. Katsuhara, M., Sasano, S., Horie, T., Matsumoto, T., Rhee, J. & Shibasaka, M. (2014) Functional and molecular characteristics of rice and barley NIP aquaporins transporting water, hydrogen peroxide and arsenite, *Plant Biotechnology.* **31**, 213-219.

62. Liu, Q., Wang, H., Zhang, Z., Wu, J., Feng, Y. & Zhu, Z. (2009) Divergence in function and expression of the NOD26-like intrinsic proteins in plants, *BMC Genomics.* **10**, 313.

63. Yamaji, N., Mitatni, N. & Ma, J. F. (2008) A Transporter Regulating Silicon Distribution in Rice Shoots, *Plant Cell.* **20**, 1381-1389.

64. King, L. S., Kozono, D. & Agre, P. (2004) From structure to disease: the evolving tale of aquaporin biology, *Nat Rev Mol Cell Biol.* **5**, 687-698.

65. Ma, J. F., Yamaji, N., Mitani, N., Tamai, K., Konishi, S., Fujiwara, T., Katsuhara, M. & Yano, M. (2007) An efflux transporter of silicon in rice, *Nature.* **448**, 209-212.

66. Yamaji, N., Sakurai, G., Mitani-Ueno, N. & Ma, J. F. (2015) Orchestration of three transporters and distinct vascular structures in node for intervascular transfer of silicon in rice, *Proceedings of the National Academy of Sciences.* **112**, 11401-11406.

67. Chen, Y., Moore, K. L., Miller, A. J., McGrath, S. P., Ma, J. F. & Zhao, F.-J. (2015) The role of nodes in arsenic storage and distribution in rice, *Journal of Experimental Botany.* **66**, 3717-3724.

68. Yamaji, N. & Ma, J. F. (2009) A Transporter at the Node Responsible for Intervascular Transfer of Silicon in Rice, *Plant Cell.* **21**, 2878-2883.

69. Tiwari, M., Sharma, D., Dwivedi, S., Singh, M., Tripathi, R. D. & Trivedi, P. K. (2013) Expression in Arabidopsis and cellular localization reveal involvement of rice NRAMP, OsNRAMP1, in arsenic transport and tolerance, *Plant, Cell & Environment.* **37**, 140-152.

70. Duan, G.-L., Hu, Y., Schneider, S., McDermott, J., Chen, J., Sauer, N., Rosen, B. P., Daus, B., Liu, Z. & Zhu, Y.-G. (2015) Inositol transporters AtINT2 and AtINT4 regulate arsenic accumulation in Arabidopsis seeds, *Nature Plants.* **2**, 15202.

71. Raab, A., Williams, P. N., Meharg, A. & Feldmann, J. (2007) Uptake and translocation of inorganic and methylated arsenic species by plants, *Environ Chem.* **4**, 197-203.

72. Li, R.-Y., Ago, Y., Liu, W.-J., Mitani, N., Feldmann, J., McGrath, S. P., Ma, J. F. & Zhao, F.-J. (2009) The Rice Aquaporin Lsi1 Mediates Uptake of Methylated Arsenic Species, *Plant Physiology.* **150**, 2071-2080.

73. Wang, J., Zhao, F.-J., Meharg, A. A., Raab, A., Feldmann, J. & McGrath, S. P. (2002) Mechanisms of Arsenic Hyperaccumulation in Pteris vittata. Uptake Kinetics, Interactions with Phosphate, and Arsenic Speciation, *Plant Physiology.* **130**, 1552-1561.

74. Carey, A.-M., Scheckel, K. G., Lombi, E., Newville, M., Choi, Y., Norton, G. J., Charnock, J. M., Feldmann, J., Price, A. H. & Meharg, A. A. (2010) Grain Unloading of Arsenic Species in Rice, *Plant Physiology.* **152**, 309-319.

75. Zheng, M.-Z., Cai, C., Hu, Y., Sun, G.-X., Williams, P. N., Cui, H.-J., Li, G., Zhao, F.-J. & Zhu, Y.-G. (2011) Spatial distribution of arsenic and temporal variation of its concentration in rice, *New Phytologist.* **189**, 200-209.

76. Carey, A.-M., Norton, G. J., Deacon, C., Scheckel, K. G., Lombi, E., Punshon, T., Guerinot, M. L., Lanzirotti, A., Newville, M., Choi, Y., Price, A. H. & Meharg, A. A. (2011) Phloem transport of arsenic species from flag leaf to grain during grain filling, *New Phytologist.* **192**, 87-98.

77. Rosen, B. P. (2002) Biochemistry of arsenic detoxification, *FEBS Letters.* **529**, 86-92.

78. Mukhopadhyay, R. & Rosen, B. P. (2002) Arsenate Reductases in Prokaryotes and Eukaryotes, *Environmental Health Perspectives.* **110**, 745-748.

79. Wysocki, R., Bobrowicz, P. & Ul/aszewski, S. a. (1997) The *Saccharomyces cerevisiae ACR3* Gene Encodes a Putative Membrane Protein Involved in Arsenite Transport, *Journal of Biological Chemistry.* **272**, 30061-30066.

80. Ghosh, M., Shen, J. & Rosen, B. P. (1999) Pathways of As(III) detoxification in Saccharomyces cerevisiae, *Proceedings of the National Academy of Sciences.* **96**, 5001-5006.

81. Pickering, I. J., Prince, R. C., George, M. J., Smith, R. D., George, G. N. & Salt, D. E. (2000) Reduction and Coordination of Arsenic in Indian Mustard, *Plant Physiology.* **122**, 1171-1178.

82. Xu, X. Y., McGrath, S. P. & Zhao, F. J. (2007) Rapid reduction of arsenate in the medium mediated by plant roots, *The New phytologist.* **176**, 590-599.

83. Dhankher, O. P., Li, Y., Rosen, B. P., Shi, J., Salt, D., Senecoff, J. F., Sashti, N. A. & Meagher, R. B. (2002) Engineering tolerance and hyperaccumulation of arsenic in plants by combining arsenate reductase and γ-glutamylcysteine synthetase expression, *Nature Biotechnology.* **20**, 1140-1145.

84. Delnomdedieu, M., Basti, M. M., Otvos, J. D. & Thomas, D. J. (1994) Reduction and binding of arsenate and dimethylarsinate by glutathione: a magnetic resonance study, *Chemico-Biological Interactions.* **90**, 139-155.

85. Bleeker, P. M., Hakvoort, H. W. J., Bliek, M., Souer, E. & Schat, H. (2006) Enhanced arsenate reduction by a CDC25-like tyrosine phosphatase explains increased phytochelatin accumulation in arsenate-tolerant Holcus lanatus, *The Plant Journal.* **45**, 917-929.

86. Dhankher, O. P., Rosen, B. P., McKinney, E. C. & Meagher, R. B. (2006) Hyperaccumulation of arsenic in the shoots of Arabidopsis silenced for arsenate reductase (ACR2), *Proceedings of the National Academy of Sciences.* **103**, 5413-5418.

87. Sánchez-Bermejo, E., Castrillo, G., del Llano, B., Navarro, C., Zarco-Fernández, S., Martinez-Herrera, D. J., Leo-del Puerto, Y., Muñoz, R., Cámara, C., Paz-Ares, J., Alonso-Blanco, C. & Leyva, A. (2014) Natural variation in arsenate tolerance identifies an arsenate reductase in Arabidopsis thaliana, *Nat Commun.* **5**.

88. Chao, D.-Y., Chen, Y., Chen, J., Shi, S., Chen, Z., Wang, C., Danku, J. M., Zhao, F.-J. & Salt, D. E. (2014) Genome-wide Association Mapping Identifies a New Arsenate Reductase Enzyme Critical for Limiting Arsenic Accumulation in Plants, *PLoS Biol.* **12**, e1002009.

89. Ellis, D. R., Gumaelius, L., Indriolo, E., Pickering, I. J., Banks, J. A. & Salt, D. E. (2006) A Novel Arsenate Reductase from the Arsenic Hyperaccumulating Fern Pteris vittata, *Plant Physiology.* **141**, 1544-1554.

90. Duan, G.-L., Zhou, Y., Tong, Y.-P., Mukhopadhyay, R., Rosen, B. P. & Zhu, Y.-G. (2007) A CDC25 homologue from rice functions as an arsenate reductase, *New Phytologist.* **174**, 311-321.

91. Landrieu, I., da Costa, M., De Veylder, L., Dewitte, F., Vandepoele, K., Hassan, S., Wieruszeski, J.-M., Faure, J.-D., Van Montagu, M., Inzé, D. & Lippens, G. (2004) A small CDC25 dual-specificity tyrosine-phosphatase isoform in Arabidopsis thaliana, *Proceedings of the National Academy of Sciences of the United States of America.* **101**, 13380-13385.

92. Liu, W., Schat, H., Bliek, M., Chen, Y., McGrath, S. P., George, G., Salt, D. E. & Zhao, F.-J. (2012) Knocking Out ACR2 Does Not Affect Arsenic Redox Status in Arabidopsis thaliana: Implications for As Detoxification and Accumulation in Plants, *PLoS ONE.* **7**, e42408.

93. Liu, W.-J., Wood, B. A., Raab, A., McGrath, S. P., Zhao, F.-J. & Feldmann, J. (2010) Complexation of Arsenite with Phytochelatins Reduces Arsenite Efflux and Translocation from Roots to Shoots in Arabidopsis, *Plant Physiology.* **152**, 2211-2221.

94. Cobbett, C. S. (2000) Phytochelatins and Their Roles in Heavy Metal Detoxification, *Plant Physiology.* **123**, 825-832.

95. Norton, G. J., Nigar, M., Williams, P. N., Dasgupta, T., Meharg, A. A. & Price, A. H. (2008) Rice–arsenate interactions in hydroponics: a three-gene model for tolerance, *Journal of Experimental Botany.* **59**, 2277-2284.

96. Raab, A., Schat, H., Meharg, A. A. & Feldmann, J. (2005) Uptake, translocation and transformation of arsenate and arsenite in sunflower (Helianthus annuus): formation of arsenic–phytochelatin complexes during exposure to high arsenic concentrations, *New Phytologist.* **168**, 551-558.

97. Raab, A., Feldmann, J. & Meharg, A. A. (2004) The Nature of Arsenic-Phytochelatin Complexes in Holcus lanatus and Pteris cretica, *Plant Physiology.* **134**, 1113-1122.

98. Batista, B. L., Nigar, M., Mestrot, A., Rocha, B. A., Júnior, F. B., Price, A. H., Raab, A. & Feldmann, J. (2014) Identification and quantification of phytochelatins in roots of rice to long-term exposure: evidence of individual role on arsenic accumulation and translocation, *Journal of Experimental Botany.* **65**, 1467-1479.

99. Song, W.-Y., Park, J., Mendoza-Cózatl, D. G., Suter-Grotemeyer, M., Shim, D., Hörtensteiner, S., Geisler, M., Weder, B., Rea, P. A., Rentsch, D., Schroeder, J. I., Lee, Y. & Martinoia, E. (2010) Arsenic tolerance in Arabidopsis is mediated by two ABCC-

type phytochelatin transporters, *Proceedings of the National Academy of Sciences.* **107**, 21187-21192.

100. Song, W.-Y., Yamaki, T., Yamaji, N., Ko, D., Jung, K.-H., Fujii-Kashino, M., An, G., Martinoia, E., Lee, Y. & Ma, J. F. (2014) A rice ABC transporter, OsABCC1, reduces arsenic accumulation in the grain, *Proceedings of the National Academy of Sciences.* **111**, 15699-15704.

101. Zhao, F. J., Wang, J. R., Barker, J. H. A., Schat, H., Bleeker, P. M. & McGrath, S. P. (2003) The role of phytochelatins in arsenic tolerance in the hyperaccumulator Pteris vittata, *New Phytologist.* **159**, 403-410.

102. Indriolo, E., Na, G., Ellis, D., Salt, D. E. & Banks, J. A. (2010) A vacuolar arsenite transporter necessary for arsenic tolerance in the arsenic hyperaccumulating fern *Pteris vittata* is missing in flowering plants, *Plant Cell.* **22**, 2045-2057.

103. Zhao, F.-J., Ago, Y., Mitani, N., Li, R.-Y., Su, Y.-H., Yamaji, N., McGrath, S. P. & Ma, J. F. (2010) The role of the rice aquaporin Lsi1 in arsenite efflux from roots, *New Phytologist.* **186**, 392-399.

104. Castrillo, G., Sánchez-Bermejo, E., Lorenzo, L. d., Crevillén, P., Fraile-Escanciano, A., Tc, M., Mouriz, A., Catarecha, P., Sobrino-Plata, J., Olsson, S., Puerto, Y. L. d., Mateos, I., Rojo, E., Hernández, L. E., Jarillo, J. A., Piñeiro, M., Paz-Ares, J. & Leyva, A. (2013) WRKY6 Transcription Factor Restricts Arsenate Uptake and Transposon Activation in Arabidopsis, *The Plant Cell Online.* **25**, 2944-2957.

105. Sung, D.-Y., Kim, T.-H., Komives, E. A., Mendoza-Cózatl, D. G. & Schroeder, J. I. (2009) ARS5 is a component of the 26S proteasome complex, and negatively regulates thiol biosynthesis and arsenic tolerance in Arabidopsis, *The Plant Journal.* **59**, 802-813.

106. Kurepa, J., Toh-e, A. & Smalle, J. A. (2008) 26S proteasome regulatory particle mutants have increased oxidative stress tolerance, *The Plant Journal.* **53**, 102-114.

107. Mohan, T. C., Castrillo, G., Navarro, C., Zarco-Fernández, S., Ramireddy, E., Mateo, C., Zamarreño, A. M., Paz-Ares, J., Muñoz, R., García-Mina, J. M., Hernández, L. E., Schmülling, T. & Leyva, A. (2016) Cytokinin Determines Thiol-Mediated Arsenic Tolerance and Accumulation, *Plant Physiology.* **171**, 1418-1426.

108. Yu, L.-j., Luo, Y.-f., Liao, B., Xie, L.-j., Chen, L., Xiao, S., Li, J.-t., Hu, S.-n. & Shu, W.-s. (2012) Comparative transcriptome analysis of transporters, phytohormone and lipid metabolism pathways in response to arsenic stress in rice (Oryza sativa), *New Phytologist.* **195**, 97-112.

109. Fu, S.-F., Chen, P.-Y., Nguyen, Q. T. T., Huang, L.-Y., Zeng, G.-R., Huang, T.-L., Lin, C.-Y. & Huang, H.-J. (2014) Transcriptome profiling of genes and pathways associated with arsenic toxicity and tolerance in Arabidopsis, *BMC Plant Biology.* **14**, 94.

110. Chakrabarty, D., Trivedi, P. K., Misra, P., Tiwari, M., Shri, M., Shukla, D., Kumar, S., Rai, A., Pandey, A., Nigam, D., Tripathi, R. D. & Tuli, R. (2009) Comparative transcriptome analysis of arsenate and arsenite stresses in rice seedlings, *Chemosphere.* **74**, 688-702.

111. Li, R. Y., Stroud, J. L., Ma, J. F., McGrath, S. P. & Zhao, F. J. (2009) Mitigation of Arsenic Accumulation in Rice with Water Management and Silicon Fertilization, *Environmental Science & Technology.* **43**, 3778-3783.

112. Raab, A., Baskaran, C., Feldmann, J. & Meharg, A. A. (2009) Cooking rice in a high water to rice ratio reduces inorganic arsenic content, *Journal of Environmental Monitoring.* **11**, 41-44.

113. Li, Y., Dhankher, O. P., Carreira, L., Lee, D., Chen, A., Schroeder, J. I., Balish, R. S. & Meagher, R. B. (2004) Overexpression of Phytochelatin Synthase in Arabidopsis Leads to Enhanced Arsenic Tolerance and Cadmium Hypersensitivity, *Plant and Cell Physiology.* **45**, 1787-1797.

114. Gasic, K. & Korban, S. S. (2007) Transgenic Indian mustard (Brassica juncea) plants expressing an Arabidopsis phytochelatin synthase (AtPCS1) exhibit enhanced As and Cd tolerance, *Plant Molecular Biology.* **64**, 361-369.

115. Li, Y., Dhankher, O. P., Carreira, L., Balish, R. S. & Meagher, R. B. (2005) Arsenic and mercury tolerance and cadmium sensitivity in Arabidopsis plants expressing bacterial γ-glutamylcysteine synthetase, *Environmental Toxicology and Chemistry.* **24**, 1376-1386.

116. Reisinger, S., Schiavon, M., Terry, N. & Pilon-Smits, E. A. H. (2008) Heavy Metal Tolerance and Accumulation in Indian Mustard (Brassica Juncea L.) Expressing Bacterial γ-Glutamylcysteine Synthetase or Glutathione Synthetase, *International Journal of Phytoremediation.* **10**, 440-454.

117. Guo, J., Dai, X., Xu, W. & Ma, M. (2008) Overexpressing GSH1 and AsPCS1 simultaneously increases the tolerance and accumulation of cadmium and arsenic in Arabidopsis thaliana, *Chemosphere.* **72**, 1020-1026.

118. Huang, J., Zhang, Y., Peng, J.-S., Zhong, C., Yi, H.-Y., Ow, D. W. & Gong, J.-M. (2012) Fission Yeast HMT1 Lowers Seed Cadmium through Phytochelatin-Dependent Vacuolar Sequestration in Arabidopsis, *Plant Physiology.* **158**, 1779-1788.

119. Sundaram, S., Wu, S., Ma, L. Q. & Rathinasabapathi, B. (2009) Expression of a Pteris vittata glutaredoxin PvGRX5 in transgenic Arabidopsis thaliana increases plant arsenic tolerance and decreases arsenic accumulation in the leaves, *Plant, Cell & Environment.* **32**, 851-858.

120. Verma, P. K., Verma, S., Pande, V., Mallick, S., Deo Tripathi, R., Dhankher, O. P. & Chakrabarty, D. (2016) Overexpression of Rice Glutaredoxin OsGrx_C7 and OsGrx_C2.1 Reduces Intracellular Arsenic Accumulation and Increases Tolerance in Arabidopsis thaliana, *Frontiers in Plant Science.* **7**, 740.

121. Lillig, C. H., Berndt, C. & Holmgren, A. (2008) Glutaredoxin systems, *Biochimica et Biophysica Acta (BBA) - General Subjects.* **1780**, 1304-1317.

122. Verma, P. K., Verma, S., Meher, A. K., Pande, V., Mallick, S., Bansiwal, A. K., Tripathi, R. D., Dhankher, O. P. & Chakrabarty, D. (2016) Overexpression of rice glutaredoxins (OsGrxs) significantly reduces arsenite accumulation by maintaining glutathione pool and modulating aquaporins in yeast, *Plant Physiology and Biochemistry.* **106**, 208-217.

123. Meng, X.-Y., Qin, J., Wang, L.-H., Duan, G.-L., Sun, G.-X., Wu, H.-L., Chu, C.-C., Ling, H.-Q., Rosen, B. P. & Zhu, Y.-G. (2011) Arsenic biotransformation and volatilization in transgenic rice, *New Phytologist.* **191**, 49-56.

124. Verma, S., Verma, P. K., Pande, V., Tripathi, R. D. & Chakrabarty, D. (2016) Transgenic Arabidopsis thaliana expressing fungal arsenic methyltransferase gene

(WaarsM) showed enhanced arsenic tolerance via volatilization, *Environmental and Experimental Botany.* **132**, 113-120.

125. Rosen, B. P., Bhattacharjee, H., Zhou, T. & Walmsley, A. R. (1999) Mechanism of the ArsA ATPase, *Biochimica et Biophysica Acta (BBA) - Biomembranes.* **1461**, 207-215.

126. Maciaszczyk-Dziubinska, E., Migocka, M. & Wysocki, R. (2011) Acr3p is a plasma membrane antiporter that catalyzes As(III)/H^+ and Sb(III)/H^+ exchange in *Saccharomyces cerevisiae*, *Biochim Biophys Acta.* **1808**, 1855-1859.

127. Ali, W., Isner, J.-C., Isayenkov, S. V., Liu, W., Zhao, F.-J. & Maathuis, F. J. M. (2012) Heterologous expression of the yeast arsenite efflux system ACR3 improves *Arabidopsis thaliana* tolerance to arsenic stress, *New Phytologist.* **194**, 716-723.

128. Duan, G., Kamiya, T., Ishikawa, S., Arao, T. & Fujiwara, T. (2012) Expressing *ScACR3* in Rice Enhanced Arsenite Efflux and Reduced Arsenic Accumulation in Rice Grains, *Plant and Cell Physiology.* **53**, 154-163.

129. Chen, Y., Xu, W., Shen, H., Yan, H., Xu, W., He, Z. & Ma, M. (2013) Engineering Arsenic Tolerance and Hyperaccumulation in Plants for Phytoremediation by a PvACR3 Transgenic Approach, *Environmental Science & Technology.* **47**, 9355-9362.

130. Maciaszczyk-Dziubinska, E., Wawrzycka, D., Sloma, E., Migocka, M. & Wysocki, R. (2010) The yeast permease Acr3p is a dual arsenite and antimonite plasma membrane transporter, *Biochimica et Biophysica Acta (BBA) - Biomembranes.* **1798**, 2170-2175.

131. Markowska, K., Maciaszczyk-Dziubinska, E., Migocka, M., Wawrzycka, D. & Wysocki, R. (2015) Identification of critical residues for transport activity of Acr3p, the *Saccharomyces cerevisiae* As(III)/H^+ antiporter, *Molecular Microbiology.* **98**, 162-174.

132. Maciaszczyk-Dziubinska, E., Migocka, M., Wawrzycka, D., Markowska, K. & Wysocki, R. (2014) Multiple cysteine residues are necessary for sorting and transport activity of the arsenite permease Acr3p from *Saccharomyces cerevisiae*, *Biochimica et Biophysica Acta (BBA) - Biomembranes.* **1838**, 747-755.

133. Ali, W. (2012) *Arsenic Transport in Plants*, University of York.

134. Iwamoto, M., Higo, H. & Higo, K. (2004) Strong expression of the rice catalase gene *CatB* promoter in protoplasts and roots of both a monocot and dicots, *Plant Physiology and Biochemistry.* **42**, 241-249.

135. Ye, N., Zhu, G., Liu, Y., Li, Y. & Zhang, J. (2011) ABA Controls H_2O_2 Accumulation Through the Induction of *OsCATB* in Rice Leaves Under Water Stress, *Plant and Cell Physiology.* **52**, 689-698.

136. Menezes-Benavente, L., Teixeira, F. K., Alvim Kamei, C. L. & Margis-Pinheiro, M. (2004) Salt stress induces altered expression of genes encoding antioxidant enzymes in seedlings of a Brazilian indica rice (*Oryza sativa L.*), *Plant Science.* **166**, 323-331.

137. Yamane, K., Mitsuya, S., Taniguchi, M. & Miyake, H. (2010) Transcription Profiles of Genes Encoding Catalase and Ascorbate Peroxidase in the Rice Leaf Tissues under Salinity, *Plant Production Science.* **13**, 164-168.

138. Ahsan, N., Lee, D.-G., Alam, I., Kim, P. J., Lee, J. J., Ahn, Y.-O., Kwak, S.-S., Lee, I.-J., Bahk, J. D., Kang, K. Y., Renaut, J., Komatsu, S. & Lee, B.-H. (2008)

Comparative proteomic study of arsenic-induced differentially expressed proteins in rice roots reveals glutathione plays a central role during As stress, *PROTEOMICS.* **8**, 3561-3576.

139. Mondal, P., Dey, N., Dash, A., Chatterjee, A., Sahu, B., Panda, B., Maiti, I. & Sabat, S. (2007) Structural and Functional Analysis of Rice *Catalase-B* Gene Promoter: Presence of Dof and CAAT Binding Site, *Plant Molecular Biology Reporter.* **25**, 71-82.

140. Iwamoto, M., Higo, H. & Higo, K. (2000) Differential diurnal expression of rice catalase genes: the 5′-flanking region of *CatA* is not sufficient for circadian control, *Plant Science.* **151**, 39-46.

141. Hruz, T., Laule, O., Szabo, G., Wessendorp, F., Bleuler, S., Oertle, L., Widmayer, P., Gruissem, W. & Zimmermann, P. (2008) Genevestigator V3: A Reference Expression Database for the Meta-Analysis of Transcriptomes, *Advances in Bioinformatics.* **2008**, e420747.

142. Yamaji, N. & Ma, J. F. (2007) Spatial Distribution and Temporal Variation of the Rice Silicon Transporter Lsi1, *Plant Physiology.* **143**, 1306-1313.

143. Dixit, G., Singh, A. P., Kumar, A., Singh, P. K., Kumar, S., Dwivedi, S., Trivedi, P. K., Pandey, V., Norton, G. J., Dhankher, O. P. & Tripathi, R. D. (2015) Sulfur mediated reduction of arsenic toxicity involves efficient thiol metabolism and the antioxidant defense system in rice, *Journal of Hazardous Materials.* **298**, 241-251.

144. Chiba, Y., Mitani, N., Yamaji, N. & Ma, J. F. (2009) HvLsi1 is a silicon influx transporter in barley, *The Plant Journal.* **57**, 810-818.

145. Hellens, R. P., Edwards, E. A., Leyland, N. R., Bean, S. & Mullineaux, P. M. (2000) pGreen: a versatile and flexible binary Ti vector for *Agrobacterium*-mediated plant transformation, *Plant Molecular Biology.* **42**, 819-832.

146. Nishimura, A., Aichi, I. & Matsuoka, M. (2007) A protocol for *Agrobacterium*-mediated transformation in rice, *Nat Protocols.* **1**, 2796-2802.

147. Edwards, K., Johnstone, C. & Thompson, C. (1991) A simple and rapid method for the preparation of plant genomic DNA for PCR analysis, *Nucl Acids Res.* **19**, 1349.

148. Yoshida, S., Forno, D. A. & Cock, J. *Laboratory Manual for Physiological Studies of Rice*, Int. Rice Res. Inst.

149. Poorter, H. & Garnier, E. (1996) Plant growth analysis: an evaluation of experimental design and computational methods, *Journal of Experimental Botany.* **47**, 1343-1351.

150. Chen, Z., Iyer, S., Caplan, A., Klessig, D. F. & Fan, B. (1997) Differential Accumulation of Salicylic Acid and Salicylic Acid-Sensitive Catalase in Different Rice Tissues, *Plant Physiology.* **114**, 193-201.

151. Jay Maclean, B. H., Gene Hettel (2013) *Rice Almanac*, Fourth edn, International Rice Research Institute.

152. Luu, D.-T. & Maurel, C. (2013) Aquaporin Trafficking in Plant Cells: An Emerging Membrane-Protein Model, *Traffic.* **14**, 629-635.

153. Łangowski, Ł., Wabnik, K., Li, H., Vanneste, S., Naramoto, S., Tanaka, H. & Friml, J. (2016) Cellular mechanisms for cargo delivery and polarity maintenance at different polar domains in plant cells, *Cell Discovery.* **2**, 16018.

154. Takano, J., Tanaka, M., Toyoda, A., Miwa, K., Kasai, K., Fuji, K., Onouchi, H., Naito, S. & Fujiwara, T. (2010) Polar localization and degradation of Arabidopsis boron transporters through distinct trafficking pathways, *Proceedings of the National Academy of Sciences.* **107**, 5220-5225.

155. Norton, G. J., Lou-Hing, D. E., Meharg, A. A. & Price, A. H. (2008) Rice–arsenate interactions in hydroponics: whole genome transcriptional analysis, *Journal of Experimental Botany.* **59**, 2267-2276.

156. Huang, T.-L., Nguyen, Q. T. T., Fu, S.-F., Lin, C.-Y., Chen, Y.-C. & Huang, H.-J. (2012) Transcriptomic changes and signalling pathways induced by arsenic stress in rice roots, *Plant Molecular Biology.* **80**, 587-608.

157. Zheng, M.-Z., Li, G., Sun, G.-X., Shim, H. & Cai, C. (2013) Differential toxicity and accumulation of inorganic and methylated arsenic in rice, *Plant and Soil.* **365**, 227-238.

158. Sakurai, J., Ishikawa, F., Yamaguchi, T., Uemura, M. & Maeshima, M. (2005) Identification of 33 Rice Aquaporin Genes and Analysis of Their Expression and Function, *Plant and Cell Physiology.* **46**, 1568-1577.

159. Johanson, U., Karlsson, M., Johansson, I., Gustavsson, S., Sjövall, S., Fraysse, L., Weig, A. R. & Kjellbom, P. (2001) The Complete Set of Genes Encoding Major Intrinsic Proteins in Arabidopsis Provides a Framework for a New Nomenclature for Major Intrinsic Proteins in Plants, *Plant Physiology.* **126**, 1358-1369.

160. Preston, G. M., Jung, J. S., Guggino, W. B. & Agre, P. (1994) Membrane topology of aquaporin CHIP. Analysis of functional epitope-scanning mutants by vectorial proteolysis, *Journal of Biological Chemistry.* **269**, 1668-1673.

161. Jung, J. S., Preston, G. M., Smith, B. L., Guggino, W. B. & Agre, P. (1994) Molecular structure of the water channel through aquaporin CHIP. The hourglass model, *Journal of Biological Chemistry.* **269**, 14648-14654.

162. Sui, H., Han, B.-G., Lee, J. K., Walian, P. & Jap, B. K. (2001) Structural basis of water-specific transport through the AQP1 water channel, *Nature.* **414**, 872-878.

163. Murata, K., Mitsuoka, K., Hirai, T., Walz, T., Agre, P., Heymann, J. B., Engel, A. & Fujiyoshi, Y. (2000) Structural determinants of water permeation through aquaporin-1, *Nature.* **407**, 599-605.

164. Wallace, I. S. & Roberts, D. M. (2005) Distinct Transport Selectivity of Two Structural Subclasses of the Nodulin-like Intrinsic Protein Family of Plant Aquaglyceroporin Channels†, *Biochemistry.* **44**, 16826-16834.

165. Weaver, C. D., Crombie, B., Stacey, G. & Roberts, D. M. (1991) Calcium-Dependent Phosphorylation of Symbiosome Membrane Proteins from Nitrogen-Fixing Soybean Nodules: Evidence for Phosphorylation of Nodulin-26, *Plant Physiology.* **95**, 222-227.

166. Guenther, J. F., Chanmanivone, N., Galetovic, M. P., Wallace, I. S., Cobb, J. A. & Roberts, D. M. (2003) Phosphorylation of Soybean Nodulin 26 on Serine 262 Enhances Water Permeability and Is Regulated Developmentally and by Osmotic Signals, *Plant Cell.* **15**, 981-991.

167. Pérez Di Giorgio, J., Bienert, G. P., Ayub, N., Yaneff, A., Barberini, M. L., Mecchia, M. A., Amodeo, G., Soto, G. & Muschietti, J. P. (2016) Pollen-specific aquaporins NIP4;1 and NIP4;2 are required for pollen development and pollination in *Arabidopsis thaliana*, *Plant Cell.* **28**, 1053-1077.

168. Wallace, I. S., Choi, W.-G. & Roberts, D. M. (2006) The structure, function and regulation of the nodulin 26-like intrinsic protein family of plant aquaglyceroporins, *Biochimica et Biophysica Acta (BBA) - Biomembranes.* **1758**, 1165-1175.

169. Li, T., Choi, W.-G., Wallace, I. S., Baudry, J. & Roberts, D. M. (2011) Arabidopsis thaliana NIP7;1: An Anther-Specific Boric Acid Transporter of the Aquaporin Superfamily Regulated by an Unusual Tyrosine in Helix 2 of the Transport Pore, *Biochemistry.* **50**, 6633-6641.

170. Dereeper, A., Guignon, V., Blanc, G., Audic, S., Buffet, S., Chevenet, F., Dufayard, J. F., Guindon, S., Lefort, V., Lescot, M., Claverie, J. M. & Gascuel, O. (2008) Phylogeny.fr: robust phylogenetic analysis for the non-specialist, *Nucl Acids Res.* **36**, W465-W469.

171. Hwang, J. H., Ellingson, S. R. & Roberts, D. M. (2010) Ammonia permeability of the soybean nodulin 26 channel, *FEBS Letters.* **584**, 4339-4343.

172. Negishi, T., Oshima, K., Hattori, M., Kanai, M., Mano, S., Nishimura, M. & Yoshida, K. (2012) Tonoplast- and Plasma Membrane-Localized Aquaporin-Family Transporters in Blue Hydrangea Sepals of Aluminum Hyperaccumulating Plant, *PLoS ONE.* **7**, e43189.

173. Choi, W.-G. & Roberts, D. M. (2007) Arabidopsis NIP2;1, a Major Intrinsic Protein Transporter of Lactic Acid Induced by Anoxic Stress, *Journal of Biological Chemistry.* **282**, 24209-24218.

174. Tanaka, M., Wallace, I. S., Takano, J., Roberts, D. M. & Fujiwara, T. (2008) NIP6;1 Is a Boric Acid Channel for Preferential Transport of Boron to Growing Shoot Tissues in Arabidopsis, *The Plant Cell Online.* **20**, 2860-2875.

175. Alexandersson, E., Fraysse, L., Sjövall-Larsen, S., Gustavsson, S., Fellert, M., Karlsson, M., Johanson, U. & Kjellbom, P. (2005) Whole Gene Family Expression and Drought Stress Regulation of Aquaporins, *Plant Molecular Biology.* **59**, 469-484.

176. Alonso, J. M., Stepanova, A. N., Leisse, T. J., Kim, C. J., Chen, H., Shinn, P., Stevenson, D. K., Zimmerman, J., Barajas, P., Cheuk, R., Gadrinab, C., Heller, C., Jeske, A., Koesema, E., Meyers, C. C., Parker, H., Prednis, L., Ansari, Y., Choy, N., Deen, H., Geralt, M., Hazari, N., Hom, E., Karnes, M., Mulholland, C., Ndubaku, R., Schmidt, I., Guzman, P., Aguilar-Henonin, L., Schmid, M., Weigel, D., Carter, D. E., Marchand, T., Risseeuw, E., Brogden, D., Zeko, A., Crosby, W. L., Berry, C. C. & Ecker, J. R. (2003) Genome-Wide Insertional Mutagenesis of *Arabidopsis thaliana*, *Science.* **301**, 653-657.

177. Tetyuk, O., Benning, U. F. & Hoffmann-Benning, S. (2013) Collection and Analysis of Arabidopsis Phloem Exudates Using the EDTA-facilitated Method, *J Vis Exp*, 51111.

178. Smyth, D. R., Bowman, J. L. & Meyerowitz, E. M. (1990) Early flower development in Arabidopsis, *Plant Cell.* **2**, 755-67.

179. Kamiya, T. & Fujiwara, T. (2009) Arabidopsis NIP1;1 Transports Antimonite and Determines Antimonite Sensitivity, *Plant and Cell Physiology.* **50**, 1977-1981.

180. Maathuis, F. J. M., Ahmad, I. & Patishtan, J. (2014) Regulation of Na+ fluxes in plants, *Plant Physiology.* **5**, 467.

181. Catarecha, P., Segura, M. D., Franco-Zorrilla, J. M., García-Ponce, B., Lanza, M., Solano, R., Paz-Ares, J. & Leyva, A. (2007) A Mutant of the Arabidopsis Phosphate Transporter PHT1;1 Displays Enhanced Arsenic Accumulation, *The Plant Cell Online.* **19**, 1123-1133.

182. Khan, D., Millar, J. L., Girard, I. J., Chan, A., Kirkbride, R. C., Pelletier, J. M., Kost, S., Becker, M. G., Yeung, E. C., Stasolla, C., Goldberg, R. B., Harada, J. J. & Belmonte, M. F. (2015) Transcriptome atlas of the Arabidopsis funiculus – a study of maternal seed subregions, *The Plant Journal.* **82**, 41-53.

183. Sakurai, T., Kondou, Y., Akiyama, K., Kurotani, A., Higuchi, M., Ichikawa, T., Kuroda, H., Kusano, M., Mori, M., Saitou, T., Sakakibara, H., Sugano, S., Suzuki, M., Takahashi, H., Takahashi, S., Takatsuji, H., Yokotani, N., Yoshizumi, T., Saito, K., Shinozaki, K., Oda, K., Hirochika, H. & Matsui, M. (2011) RiceFOX: A Database of *Arabidopsis* Mutant Lines Overexpressing Rice Full-Length cDNA that Contains a Wide Range of Trait Information to Facilitate Analysis of Gene Function, *Plant and Cell Physiology.* **52**, 265-273.

184. Mitani, N., Chiba, Y., Yamaji, N. & Ma, J. F. (2009) Identification and Characterization of Maize and Barley Lsi2-Like Silicon Efflux Transporters Reveals a Distinct Silicon Uptake System from That in Rice, *The Plant Cell Online.* **21**, 2133-2142.

185. Mitani, N. & Ma, J. F. (2005) Uptake system of silicon in different plant species, *Journal of Experimental Botany.* **56**, 1255-1261.

186. Eulgem, T., Rushton, P. J., Robatzek, S. & Somssich, I. E. (2000) The WRKY superfamily of plant transcription factors, *Trends in Plant Science.* **5**, 199-206.

187. Yamasaki, K., Kigawa, T., Watanabe, S., Inoue, M., Yamasaki, T., Seki, M., Shinozaki, K. & Yokoyama, S. (2012) Structural Basis for Sequence-specific DNA Recognition by an Arabidopsis WRKY Transcription Factor, *Journal of Biological Chemistry.* **287**, 7683-7691.

188. Rushton, P. J., Somssich, I. E., Ringler, P. & Shen, Q. J. (2010) WRKY transcription factors, *Trends in Plant Science.* **15**, 247-258.

189. Phukan, U. J., Jeena, G. S. & Shukla, R. K. (2016) WRKY Transcription Factors: Molecular Regulation and Stress Responses in Plants, *Frontiers in Plant Science.* **7**, 760.

190. Abercrombie, J., Halfhill, M., Ranjan, P., Rao, M., Saxton, A., Yuan, J. & Stewart, C. N. (2008) Transcriptional responses of Arabidopsis thaliana plants to As (V) stress, *BMC Plant Biology.* **8**, 87.

191. Wang, H., Xu, Q., Kong, Y.-H., Chen, Y., Duan, J.-Y., Wu, W.-H. & Chen, Y.-F. (2014) Arabidopsis WRKY45 Transcription Factor Activates PHOSPHATE TRANSPORTER1;1 Expression in Response to Phosphate Starvation, *Plant Physiology.* **164**, 2020-2029.

192. Su, T., Xu, Q., Zhang, F.-C., Chen, Y., Li, L.-Q., Wu, W.-H. & Chen, Y.-F. (2015) WRKY42 Modulates Phosphate Homeostasis through Regulating Phosphate Translocation and Acquisition in Arabidopsis, *Plant Physiology.* **167**, 1579-1591.

193. Heazlewood, J. L., Verboom, R. E., Tonti-Filippini, J., Small, I. & Millar, A. H. (2007) SUBA: the Arabidopsis Subcellular Database, *Nucl Acids Res.* **35**, D213-D218.

194. Winter, D., Vinegar, B., Nahal, H., Ammar, R., Wilson, G. V. & Provart, N. J. (2007) An "Electronic Fluorescent Pictograph" Browser for Exploring and Analyzing Large-Scale Biological Data Sets, *PLoS ONE.* **2**, e718.

195. Duncan, O., van der Merwe, M. J., Daley, D. O. & Whelan, J. (2013) The outer mitochondrial membrane in higher plants, *Trends in Plant Science.* **18**, 207-217.

196. Sievers, F., Wilm, A., Dineen, D., Gibson, T. J., Karplus, K., Li, W., Lopez, R., McWilliam, H., Remmert, M., Söding, J., Thompson, J. D. & Higgins, D. G. (2011) Fast, scalable generation of high-quality protein multiple sequence alignments using Clustal Omega, *Molecular Systems Biology.* **7**, 539.

197. Ortiz-Masia, D., Perez-Amador, M. A., Carbonell, J. & Marcote, M. J. (2007) Diverse stress signals activate the C1 subgroup MAP kinases of Arabidopsis, *FEBS Letters.* **581**, 1834-1840.

198. Matsuoka, D., Yasufuku, T., Furuya, T. & Nanmori, T. (2015) An abscisic acid inducible Arabidopsis MAPKKK, MAPKKK18 regulates leaf senescence via its kinase activity, *Plant Molecular Biology.* **87**, 565-575.

199. Danquah, A., de Zélicourt, A., Boudsocq, M., Neubauer, J., Frei dit Frey, N., Leonhardt, N., Pateyron, S., Gwinner, F., Tamby, J.-P., Ortiz-Masia, D., Marcote, M. J., Hirt, H. & Colcombet, J. (2015) Identification and characterization of an ABA-activated MAP kinase cascade in Arabidopsis thaliana, *The Plant Journal.* **82**, 232-244.

200. Vivancos, J., Deshmukh, R., Grégoire, C., Rémus-Borel, W., Belzile, F. & Bélanger, R. R. (2016) Identification and characterization of silicon efflux transporters in horsetail (Equisetum arvense), *Journal of Plant Physiology.* **200**, 82-89.

201. Finn, R. D., Clements, J., Arndt, W., Miller, B. L., Wheeler, T. J., Schreiber, F., Bateman, A. & Eddy, S. R. (2015) HMMER web server: 2015 update, *Nucl Acids Res.* **43**, W30-W38.

202. Boorsma, A., van der Rest, M. E., Lolkema, J. S. & Konings, W. N. (1996) Secondary transporters for citrate and the Mg(2+)-citrate complex in *Bacillus subtilis* are homologous proteins, *Journal of Bacteriology.* **178**, 6216-22.

203. Carlin, A., Shi, W., Dey, S. & Rosen, B. P. (1995) The ars operon of *Escherichia coli* confers arsenical and antimonial resistance, *Journal of Bacteriology.* **177**, 981-6.

204. Pootakham, W., Gonzalez-Ballester, D. & Grossman, A. R. (2010) Identification and Regulation of Plasma Membrane Sulfate Transporters in Chlamydomonas, *Plant Physiology.* **153**, 1653-1668.

205. Schneider, C. A., Rasband, W. S. & Eliceiri, K. W. (2012) NIH Image to ImageJ: 25 years of image analysis, *Nat Meth.* **9**, 671-675.

206. Tiwari, M., Krishnamurthy, S., Shukla, D., Kiiskila, J., Jain, A., Datta, R., Sharma, N. & Sahi, S. V. (2016) Comparative transcriptome and proteome analysis to reveal the biosynthesis of gold nanoparticles in *Arabidopsis*, *Sci Rep.* **6**, 21733.

207. Van De Mortel, J. E., Schat, H., Moerland, P. D., Van Themaat, E. V. L., Van Der Ent, S., Blankestijn, H., Ghandilyan, A., Tsiatsiani, S. & Aarts, M. G. M. (2008) Expression differences for genes involved in lignin, glutathione and sulphate

metabolism in response to cadmium in Arabidopsis thaliana and the related Zn/Cd-hyperaccumulator Thlaspi caerulescens, *Plant, Cell & Environment.* **31**, 301-324.

208. Wang, D., Amornsiripanitch, N. & Dong, X. (2006) A Genomic Approach to Identify Regulatory Nodes in the Transcriptional Network of Systemic Acquired Resistance in Plants, *PLoS Pathog.* **2**, e123.

209. Christiansen, K. M., Gu, Y., Rodibaugh, N. & Innes, R. W. (2011) Negative regulation of defence signalling pathways by the EDR1 protein kinase, *Molecular Plant Pathology.* **12**, 746-758.

210. Brown, P. H. & Shelp, B. J. (1997) Boron mobility in plants, *Plant and Soil.* **193**, 85-101.

211. Schnurbusch, T., Hayes, J., Hrmova, M., Baumann, U., Ramesh, S. A., Tyerman, S. D., Langridge, P. & Sutton, T. (2010) Boron Toxicity Tolerance in Barley through Reduced Expression of the Multifunctional Aquaporin HvNIP2;1, *Plant Physiology.* **153**, 1706-1715.

212. Kumar, K., Mosa, K. A., Chhikara, S., Musante, C., White, J. C. & Dhankher, O. P. (2014) Two rice plasma membrane intrinsic proteins, OsPIP2;4 and OsPIP2;7, are involved in transport and providing tolerance to boron toxicity, *Planta.* **239**, 187-198.

213. Pang, Y., Li, L., Ren, F., Lu, P., Wei, P., Cai, J., Xin, L., Zhang, J., Chen, J. & Wang, X. (2010) Overexpression of the tonoplast aquaporin AtTIP5;1 conferred tolerance to boron toxicity in Arabidopsis, *Journal of Genetics and Genomics.* **37**, 389-397.

214. Takano, J., Yamagami, M., Noguchi, K., Hayashi, H. & Fujiwara, T. (2001) Preferential translocation of boron to young leaves in Arabidopsis thaliana Regulated by the BOR1 Gene, *Soil Science and Plant Nutrition.* **47**, 345-357.

215. Moore, K. L., Schröder, M., Lombi, E., Zhao, F.-J., McGrath, S. P., Hawkesford, M. J., Shewry, P. R. & Grovenor, C. R. M. (2010) NanoSIMS analysis of arsenic and selenium in cereal grain, *New Phytologist.* **185**, 434-445.

216. Moore, K. L., Chen, Y., van de Meene, A. M. L., Hughes, L., Liu, W., Geraki, T., Mosselmans, F., McGrath, S. P., Grovenor, C. & Zhao, F.-J. (2014) Combined NanoSIMS and synchrotron X-ray fluorescence reveal distinct cellular and subcellular distribution patterns of trace elements in rice tissues, *New Phytologist.* **201**, 104-115.

217. Mishra, S., Mattusch, J. & Wennrich, R. (2017) Accumulation and transformation of inorganic and organic arsenic in rice and role of thiol-complexation to restrict their translocation to shoot, *Sci Rep.* **7**, 40522.

218. ZHU, Y.-G., GENG, C.-N., TONG, Y.-P., SMITH, S. E. & SMITH, F. A. (2006) Phosphate (Pi) and Arsenate Uptake by Two Wheat (Triticum aestivum) Cultivars and Their Doubled Haploid Lines, *Ann Bot.* **98**, 631-636.

219. Elias, M., Wellner, A., Goldin-Azulay, K., Chabriere, E., Vorholt, J. A., Erb, T. J. & Tawfik, D. S. (2012) The molecular basis of phosphate discrimination in arsenate-rich environments, *Nature.* **491**, 134-137.

220. Ciminelli, V. S. T., Gasparon, M., Ng, J. C., Silva, G. C. & Caldeira, C. L. (2017) Dietary arsenic exposure in Brazil: The contribution of rice and beans, *Chemosphere.* **168**, 996-1003.

221. Alam, M. G. M., Snow, E. T. & Tanaka, A. (2003) Arsenic and heavy metal contamination of vegetables grown in Samta village, Bangladesh, *Science of The Total Environment.* **308**, 83-96.

222. Das, H. K., Mitra, A. K., Sengupta, P. K., Hossain, A., Islam, F. & Rabbani, G. H. (2004) Arsenic concentrations in rice, vegetables, and fish in Bangladesh: a preliminary study, *Environment International.* **30**, 383-387.

223. Bhattacharya, P., Samal, A. C., Majumdar, J. & Santra, S. C. (2010) Arsenic Contamination in Rice, Wheat, Pulses, and Vegetables: A Study in an Arsenic Affected Area of West Bengal, India, *Water Air Soil Pollut.* **213**, 3-13.